SHRP-S-666

Concrete Bridge Protection and Rehabilitation: Chemical and Physical Techniques

Corrosion Inhibitors and Polymers

Imad L. Al-Qadi, Brian D. Prowell, Richard E. Weyers, Tapas Dutta, and Harinath Gouru
Virginia Polytechnic Institute and State University

Neal Berke
W.R. Grace Company

Strategic Highway Research Program
National Research Council
Washington, DC 1993

SHRP–S-666
Contract C-103

Program Manager: *Don M. Harriott*
Project Manager: *Joseph F. Lamond*
Production Editor: *Marsha Barrett*
Program Area Secretary: *Carina S. Hreib*

July 1993

key words:
corrosion inhibitors
polymer-impregnated concrete
resin-modified pavement
concrete bridges
reinforcement corrosion

Strategic Highway Research Program
National Academy of Sciences
2101 Constitution Avenue N.W.
Washington, DC 20418

(202) 334-3774

350/NAP/793

Acknowledgments

The research described herein was supported by the Strategic Highway Research Program (SHRP). SHRP is a unit of the National Research Council that was authorized by section 128 of the Surface Transportation and Uniform Relocation Assistance Act of 1987.

We wish to acknowledge the help of the Pennsylvania Department of Transportation and the Virginia Department of Transportation SHRP coordinators, District Bridge Engineers and maintenance personnel who graciously assisted us by providing access to and traffic control for bridge test sites and in the procurement of the polymer impregnated bridge deck test specimens.

CONTENTS

List of Figures

List of Tables

Abstract

The chloride-induced corrosion of concrete reinforcing steel has been recognized for the past 20 years as a primary factor contributing to concrete bridge component deterioration. This report deals with the improvement of existing non-electrochemical methods for protecting and rehabilitating chloride-contaminated concrete with and without concrete removal and with the development of new methods. Existing methods include deep impregnation of the concrete with a polymer or with calcium nitriteand the new methods include corrosion inhibitor application processes and a resin concrete asphalt composite material.

The effectiveness of polymer-impregnated concrete to abate corrosion was evaluated on two bridge decks in Pennsylvania. The field data suggested that deep polymer-impregnation can increase the service life of corrosion deteriorating decks by at least 30 years. Two methods of impregnating calcium nitrite were also examined in the field. One involved drying the concrete while the other used a grout.

In the laboratory, polymer-impregnated concrete was compared to other protection techniques. The study concluded that there was little difference between the five methods evaluated: LMC overlay, LSDC overlay, polymer-impregnated concrete, polymer-impregnated concrete with a LMC overlay, and polymer-impregnated concrete with a LSDC overlay. It was also found that the pre-impregnation drying temperature could be lowered to 180°F (82°C) at 1/2 in (13 mm) below top rebar level.

Five corrosion inhibitors were evaluated in the laboratory. A treatment matrix was established to evaluate the inhibitors' performance over three corrosion ranges as well as the effect of application time and drying. The effect of inhibitors on overlay bond strength and the durability of the inhibitor-modified concrete was also evaluated. Three inhibitor treatments were identified for large-scale testing; large specimens which were removed from a bridge deck were treated to evaluate the field application effectiveness of the corrosion inhibitor treatments. Service lives were estimated for the two most effective treatments.

Asphalt Portland Cement Concrete Composite (APCCC) material was designed and evaluated for physical properties and durability characteristics for different moist and dry curing periods. APCCC showed higher strength properties and resistance to freeze-thaw and stripping than hot-mix asphalts. It also was more resistance to chloride intrusion than

portland cement concrete. The study concluded that moist curing for one day was very effective. It is suggested that this material be used to rehabilitate existing bridge decks with hot-mix asphalt preformed membrane protection systems.

Executive Summary

Currently, several methods are accepted for preventing corrosion and for maintaining, repairing, and rehabilitating bridge deck components which deteriorate as a result of chloride-induced reinforcing steel corrosion. These techniques can be considered in three categories: methods which provide a protective coating for the reinforcement steel, methods which reduce the diffusion rate of chlorides and moisture into concrete and/or change the thermodynamics of the corrosion cell, and electrochemical methods. Techniques in the second category were used to meet the objective of this study, which is to develop new techniques and to improve existing corrosion-protection techniques for concrete bridge components.

This report is divided into two parts: Part One deals with improving existing techniques while Part Two deals with developing new techniques. Existing techniques evaluated included deep monomer impregnation, calcium nitrite impregnation, and a calcium nitrite grout. These techniques were evaluated in the laboratory and in the field. New promising techniques included inhibitor application processes and resin modified concrete.

To evaluate the deep polymer-impregnated concrete in the field, a post-treatment evaluation was conducted of 2 bridge decks, one in Boalsburg and one in Bethlehem, Pennsylvania which had been polymer-impregnated at an earlier time. Their corrosion activity was monitored periodically. The corrosion performance surveys included visual inspection, delamination survey, cover-depth survey, chloride content as a function of depth, corrosion potentials, corrosion current density measurements, and petrographic analysis of drilled concrete cores. The performance of the Boalsburg bridge deck was excellent 7 years after impregnation. The chloride content for polymer-impregnated deck was less than that of control section. However, the half-cell potentials were almost the same for polymer-impregnated and control sections. The corrosion current density for the control section, on the other hand, was almost twice that of the polymer-impregnated section using a 3LP device and a Gecor device. The impregnation process was also found to increase concrete resistivity.

A test section of the Bethlehem bridge deck was polymer-impregnated, using a pressure method, when it was 8 years old. The entire deck was replaced 15 years after the impregnation, and test sections were removed to the laboratory for continuing monitoring and experimentation. The bridge deck test sections were monitored periodically. The removed

sections, polymer-impregnated and adjoining control section, were placed in the outdoor exposure area at the Structures and Materials Research Laboratory of Virginia Polytechnic Institute and State University (VPI&SU). The slabs were inspected when they arrived at VPI&SU and repaired using LMC. A 60% reduction of chloride intrusion was noticed at 1.5 in (38 mm) deep and greater. It was interesting to notice that the polymer-impregnated area remained above the chloride content threshold level, 1.2 lb/yd^3 (0.7 kg/m^3) of concretes for 14 years without spalling or delamination. The polymer-impregnated and control slabs had the same half-cell potentials when removed and placed at VPI&SU. However, after repair, the mean potential in the repaired non-impregnated section decreased by 61% and the mean potential in the polymer-impregnated section (non-repaired) decreased by 39% from their arrival levels. The microscopic examination of polymer-impregnated cores showed that a deep monomer impregnation process would arrest steel corrosion in concrete. The corrosion current density of the polymer-impregnated section was 10 times less than that of the control, using 3LP and Geocor devices. Based on the Bethlehem trial section, deep polymer impregnation can increase the service life of a bridge deck by at least 30 years.

Calcium nitrite was introduced as an inhibitor to prevent and/or stop corrosion at the reinforcing steel in concrete in the 1980's. It was found, after trying many methods, that the most effective was drying concrete by heating it to above the boiling point of water. In 1985, calcium nitrite was successfully used to impregnate large-scale slabs at the University of Texas at Austin. A parking deck in a garage was repaired using this technique. No adverse structural effect to the concrete was noted. However, in the garage, severe surface contamination led to a minimal amount of calcium nitrite impregnation.

In this study, a section of a bridge deck which was undergoing corrosion due to chloride intrusion was treated with calcium nitrite. Grooves were cut to bypass surface contamination. The procedure and equipment are described in the report. The calcium nitrite impregnation was successful. Both the mean and standard deviation of the CSE corrosion potentials and the 3LP corrosion current density measurements after two years indicated a reduction in the corrosion activity. It was not possible to determine from the chloride content analyses whether the calcium nitrite performed well. For inhibition to take place, the chloride to nitrite ratio must be less than two at the rebar level; the ratio in the tested sample was high. Further surveys will be required to make an accurate assessment of calcium nitrite performance as an impregnate corrosion inhibitor.

A column undergoing severe spalling from corrosion was also treated using a grout containing 10% calcium nitrite by mass of cement. Holes were drilled to the reinforcement level and filled with the grout. The spalled area was patched with the same grout. The CSE corrosion potentials in the patched area showed a 31% decrease after treatment and remained constant for the two year evaluation period. The corrosion current density measurements also decreased slightly for the grout-filled hole section. The practicality of using grouts and concrete with high inhibitor contents was confirmed. This technology may be used in column repair where it is difficult to remove the column or apply other means of protection. It appears that the addition of calcium nitrite to concrete patches is promising and deserves

further investigation.

To further investigate the effectiveness of deep polymer-impregnated concrete in abating the corrosion of reinforcing steel in bridge decks, concrete laboratory specimens with rebars were cast and subjected to a chloride environment. The corrosion potential and current density were monitored. When active corrosion had been initiated, five rehabilitation treatment methods were applied to the corroding specimens: latex modified concrete (LMC) overlay, low slump dense concrete (LSDC) overlay, monomer impregnation followed in-situ polymerization, LMC overlay with monomer impregnation/polymerization, and LSDC with monomer impregnation/polymerization.

The monomer system used was 90% methyl methacrylate (MMA), 10% trimethylolpropane trimethacrylate (TMPTMA) and 0.5% of azobisiobutyronitrile (AZO) of the above monomer mixture (MMA and TMPTMA). The impregnated specimens were grooved and dried to 230°F (110°C) prior to impregnation and subsequent polymerization. The post-treatment corrosion current densities were used for analyzing the effectiveness of the different treatment methods. The treatment methods investigated reduced the corrosion current density dramatically compared to untreated specimens. However, the difference in effectiveness between the five methods was insignificant.

The optimum drying temperature of concrete prior to monomer impregnation was also investigated. Mortar cubes were cast, dried at different temperatures between room temperature and 600°F (316°C), and then impregnated with monomer and polymerized in-situ. The cubes were then vacuum saturated and their resistivities were measured. The cubes were cut, dried to 220°F (104°C) and the influence of drying temperature on the degree of impregnation was evaluated using a mercury porosimeter and a scanning electron microscope-energy dispersive spectroscope. Companion cubes were subjected to ponding-drying cycles in a sodium chloride solution and the ingress of chloride was determined from powdered mortar samples. The results demonstrated that monomer impregnation of concrete to a desired depth can be achieved at a lower temperature, 180°F (82°C), than the previously accepted, 230°F (110°C). The results were validated on 1 ft x 1 ft (0.3 m x 0.3 m) concrete specimens.

Seven corrosion inhibitors, surface applied liquids and concrete admixtures, were identified in this project (reported in Concrete Bridge Protection and Rehabilitation: Chemical and Physical Techniques, Feasibility of New Rehabilitation Techniques) as promising for the rehabilitation of reinforced concrete structures subject to chloride induced corrosion. Small scale 1 ft x 1 ft (0.3 m x 0.3 m) reinforced concrete specimens were cast. A treatment matrix was established to evaluate the inhibitors' performance over three ranges of corrosion activity and to evaluate the effect of application time and drying. Corrosion current density was used to monitor the inhibitor effectiveness.

The effect of the admixtures on concrete properties and the effect of the surface-applied inhibitors on the overlay bond strength were evaluated. Rapid freeze-thaw tests were

conducted to estimate the durability of the inhibitor-modified concrete. Three combinations of inhibitors were identified for large scale testing after 10 months of accelerated chloride exposure. The large scale specimens were removed from an actual bridge deck and treated to test the effectiveness of the select inhibitors and develop field application procedures.

The researchers concluded that removing chloride-contaminated concrete above the reinforcing steel and replacing it with fresh concrete was an effective method which facilitated the application of corrosion inhibitors. Among the evaluated corrosion inhibitors, Alox 901 was a very effective surface-applied corrosion inhibitor; it increased the overlay service life by twice, while Cortec 1307 and Cortec 1609 were effective inhibitors when applied as ponding agents and concrete admixtures, respectively. However, sand-blasting was needed when using Alox 901 and Cortec 1337 because they had a detrimental effect on bond strength. Calcium nitrite (DCI) was effective in reducing low corrosion current densities when applied at the 0.1 M concentration. Also, the nitrite:chloride ratio is important. Insignificant difference was found in samples' performance subjected to ponding for one or two days.

A model for service life prediction was developed. The model suggested that Alox 901 inhibitor would increase the service life of reinforced concrete by twice when ponded for one day while drying prior to ponding showed no additional increase in service. Ponding using Cortec 1337/1609 for one day after drying will increase the service life by at least 50%.

Another new technique was evaluated, Asphalt Portland Cement Concrete Composite (APCCC) material. APCCC is hot-mix asphalt with air voids in the range of 25 to 30% which are later filled with resin modified cement grout. The resin modified cement grout consists of portland cement, fly ash, sand, water, and Prosalvia (PL7) additive. In this part of the project, APCCC was evaluated under laboratory conditions and the results were compared to those of conventional highway materials: hot-mix asphalt and portland cement concrete. The mixture of resin modified cement grout was designed. Hot-mix asphalt specimens were prepared using the Marshall method at 25-30% air void and then filled with the grout.

APCCC specimens were evaluated for stability, indirect tensile strength, compressive strength, resilient modulus, water sensitivity, freeze-thaw effect and more importantly, for chloride intrusion. Specimens were moist cured for zero days, one day, or three days as part of total curing time, and tested after 1 day, 3 days, 7 days, and 28 days of curing (moist plus air).

All test results were compared with those of hot-mix asphalt, cast in accordance with Virginia surface mix SM-5; results of chloride intrusion resistance were compared to those of portland cement concrete specimens exposed to similar conditions. The investigation concluded that APCCC possesses greater strength properties and higher resistance to stripping and freeze-thaw effects than does hot-mix asphalt. Its resistance to chloride intrusion is found to be two to three times that of normal portland cement concrete. Also,

the study suggested that the optimum moist curing is one day.

The study concluded that APCCC could be an effective alternative technique to be used as an overlay on bridge decks along with preformed membranes due to its high strength, durability, and lower air void contentand may be used to rehabilitate existing bridge decks with an asphalt membrane system without removing the existing membrane.

1

Introduction

Background

Recently, a U. S. Department of Transportation report stated that 39% of the 576,665 bridges in the nation's federally aided highway system are structurally deficient or functionally obsolete (1). Approximately, 20% of the cost to rehabilitate these bridges is attributed to chloride-induced corrosion of reinforced concrete.

Premature deterioration of reinforced concrete bridge decks was first recognized by highway agencies in the late 1950's and early 1960's. An initial study suggested that the principal cause was spalling which resulted from steel reinforcing bar corrosion (2,3). The primary source of chlorides in the northern climates is deicing salts, while in marine environments it is sea water and spray. Damage in marine environments may occur within 5 years of exposure (4).

Prior to the initiation of corrosion, estimated to be 1.2 lbs Cl^-/yd^3 (0.72 kg/m^3), the pH of the concrete (greater than 12.5) is sufficiently high to prevent the corrosion of unprotected reinforcement steel (5). The ingress of chlorides disrupts the protective layer of ferric oxide on the reinforcement steel. This breakdown, along with sufficient moisture and free oxygen create a spontaneous corrosion environment.

Corrosion of the reinforcement steel results in cracking, delamination, and spalling of the concrete cover. The damage is not usually sufficient to jeopardize the structural load capacity (6). However, the bridge rideability is affected by bridge deck damage and creates poor travel conditions. Bridge decks are usually rehabilitated when 20 to 40% of the riding surface is spalled and/or delaminated (7).

By the 1970's, highway agencies had begun to identify the enormous cost involved in the repair and rehabilitation of deficient bridge components. In 1986, the cost of repairing bridges damaged by corrosion alone was estimated at $20 billion with an annual increase of

$0.5 billion (8).

A first response to bridge deck deterioration was to modify the design parameters. The cover depth was increased from 2 in (51 mm) to 3 in (76 mm) which prolonged the time needed for the chloride to reach the top steel mat. The water to cement ratio was reduced to 0.4 - 0.45 which would decrease the permeability of the concrete as well as reduce the rate of chloride diffusion. These methods did not abate or stop corrosion; however, they did extend the time required to initiate it.

Currently, several methods are used to prevent, repair, and rehabilitate bridge components deterioration by chloride-induced corrosion. These methods can be divided into three categories:

1. protect the reinforcing steel,
2. reduce the concrete permeability and thus rate of diffusion, and
3. electrochemical protection

In new structures, reinforcing steel may be protected by coating the steel prior to placing the concrete or by using a corrosion inhibitor admixture. Epoxy-coated rebars have been widely used in bridge construction after the advent of a bridge deck protection policy in 1972 (9). Although thermal cure of applied dry powdered epoxy is considered the best coating, the coating reliability in general is still debatable due to shipping and handling damage. The dielectric properties of the coating prevent the electrical coupling of the mats when only the top mat is coated, thus preventing macro-cell corrosion. However, imperfections can lead to accelerated corrosion (10). Galvanized reinforcing steel has also been used. A galvanic couple is produced by the zinc which protects the steel even if the coating is damaged.

Concrete coatings and sealers have been used on new bridge components where chloride contamination is not yet critical. These materials are considered low initial cost protection methods. Another common corrosion prevention practice is the use of organic and inorganic corrosion inhibiting admixtures. Although the performance of inhibitors depends on the chemical composition of the inhibitor and the factors causing corrosion, inhibitors generally form a stable film on the rebar surface.

The most common repair techniques (chloride contaminated concrete left-in-place) used on bridge decks are overlay systems: latex modified concrete, low slump dense concrete, thin polymer, and hot-mix asphalt in conjunction with a membrane. These overlay systems attempt to reduce the ingress of chlorides and moisture and thus reduce the corrosion of reinforcing steel.

Prior to overlay, the unsound concrete is normally removed to or below the bar level and the exposed rebar is sandblasted to near white metal. This process is extremely expensive and does not guarantee the removal of all of the corrosion products from the bar. The preparation described above does not address the areas where the corrosion has not advanced

to a state where the concrete has cracked or delaminated, even though these areas may be critically chloride contaminated. If this is the case, then the corrosion process will continue, if the necessary moisture and free oxygen are available. Thus, the anticipated improvement in service life using these repair techniques may be significantly reduced because the steel continues to corrode in the critically chloride contaminated areas.

Two electrochemical rehabilitation methods have been developed, cathodic protection and chloride migration. Cathodic protection supplies an external source of current to the reinforcing steel, reversing the corrosion reaction. The current is applied through an external anode added to the structure using a power of approximately 0.015 watts/m^2 of concrete (11); this power is minimal and can be supplied by a solar panel. This method can only be applied to structures with electrically continuous reinforcing steel. In the chloride removal method, a DC potential is applied to the concrete which causes the chloride ions to migrate to a surface anode where they are captured by an electrolyte solution (12).

In this report, an evaluation of some of the existing techniques used to reduce or abate corrosion of steel reinforcement is presented. In addition, new inhibitors and overlay systems were evaluated in the laboratory.

Scope and Objectives

The main objectives of this project are two: to improve the existing non-electrochemical corrosion rehabitation techniques and to develop new non-electrochemical methods for rehabilitating chloride contaminated concrete bridge components. To satisfy the objectives of this study, existing techniques for rehabilitating chloride- contaminated concrete bridge components were identified. The identified techniques were investigated to determine their success and possible improvement. Two bridge decks treated by monomer impregnation in Pennsylvania in the last decade were evaluated to determine the corrosion reduction effectiveness of deep polymer-impregnated concrete. Calcium nitrite impregnation of a bridge deck and a calcium nitrite column repair in Virginia were conducted and the techniques were evaluated.

To improve the deep polymer-impregnation technique, scaled down concrete bridge deck specimens were cast and evaluated in the laboratory in a controlled environment. Five different methods were used: Latex-Modified Concrete (LMC) overlay, Low Slump Dense Concrete (LSDC) overlay, polymer impregnation, impregnation of specimens overlaid by LMC and impregnation of specimens overlaid by LSDC. The optimum drying temperature prior to monomer impregnation was investigated using mortar cubes and concrete specimens. The nature and distribution of impregnated polymer molecules in concrete was evaluated using a Scanning Electron Microscope (SEM). The effect of monomer impregnation on resistivity was also examined for normal mortar as well as chloride-contaminated mortar.

This study also evaluated the effectiveness of the inhibitors, identified in Task 2 (13) of the

project, when applied in a manner practical for field construction and determined the procedure which should be employed to ensure their successful application. This part of the project was performed in three phases: evaluation of corrosion inhibitors, development of field technique, and estimation of the service life of the developed techniques.

Asphalt Portland Cement Concrete Composite (APCCC) was also evaluated as a bridge deck overlay material to replace the hot-mix asphalt on decks with preformed membranes. The investigation included the design of APCCC mixtures and the evaluation of APCCC for mechanical properties and durability characteristics.

Research Approach

The research approach employed in the pursuit of the objectives of the research consisted of the following steps:

- Identification of existing and promising rehabilitation techniques
- Evaluation of existing rehabilitation techniques in the field
- Improving existing rehabilitation techniques
- Development of new promising rehabilitation techniques
- Laboratory evaluation of feasible rehabilitation techniques for decks with a hot-mix asphalt (HMA) overlay-membrane protection system
- Recommendation of feasible rehabilitation techniques for field validation

Part I: Improving Existing Rehabilitation Techniques

2

Polymer Impregnated Deck Installations

Introduction

In 1972, the National Cooperative Highway Research Program (NCHRP) sponsored a research project with an objective of developing a monomer impregnation process for bridge decks. The process involves drying the concrete, monomer impregnation to a depth of 4 in (102 mm) to encapsulate the upper rebar mat, and then polymerizing the monomer in situ. The deep impregnation process should abate or arrest the reinforcing steel corrosion by replacing the corrosion cell electrolyte (concrete pore water) with a dielectric polymer, immobilizing the existing chloride and reducing the ingress of further chlorides, water and oxygen. The research project culminated in the impregnation of a test section 3.5 ft by 11.5 ft (1.1 m by 3.5 m) of a bridge deck in Bethlehem, Pennsylvania.

In 1985, the Pennsylvania Department of Transportation (Penn Dot) sponsored a research project to demonstrate the technical and economical feasibility of full scale impregnation of bridge decks. Approximately one-half, 60 ft by 44 ft (18 m by 13.4 m), of a 131 ft (39.9 m) long center span of a bridge deck in Boalsburg, Pennsylvania was impregnated to a design depth of 4 in (102 mm) using the grooving technique (14,15).

Field corrosion performance investigations were conducted on both bridge decks in 1989. In March of 1990, the Bethlehem bridge deck was replaced. Prior to replacement, the impregnated section and an adjoining untreated control section were removed for further study. These decks sections are maintained in the outdoor exposure area at the Virginia Polytechnic Institute and State University, Civil Engineering, Structures and Materials Research Laboratory (S&M Lab). Since then, the corrosion activity has been periodically monitored. A second post-treatment corrosion assessment was carried out on the Boalsburg bridge in May 1992. The results of the corrosion performance surveys are presented, including: visual inspection, delamination survey, cover-depth survey, chloride contents as a function of depth, corrosion potentials, petrographic analysis of drilled concrete cores, and corrosion current density measurements.

Performance of Boalsburg Bridge Deck

Background

The Boalsburg bridge is a three-span multi-girder bridge, simply supported with steel plate girders. The end spans are 42 ft (12.8 m) and 38 ft (11.6 m) and the center span is 131 ft (40 m). The deck width, curb to curb, is 44 ft (13.4 m), consisting of two 12 ft (3.7 m) traffic lanes and two 10 ft (3.5 m) aprons. The concrete deck was placed in April 1972 using permanent steel forms; it is composite design. The main reinforcement consists of No. 5 bars on 6 in (15.2 cm) centers in the transverse direction, top and bottom. The longitudinal steel consists of No. 4 bars at 12 in (30.4 cm) in the top and No. 5 bars at 9 in (22.9 cm) in the bottom. The design deck thickness is 8 in (20.3 cm), with a 2 in (51 mm) minimum concrete cover depth.

Physical Damage Survey

In March 1983, a visual inspection of the deck indicated that the deck was in excellent condition. The only deterioration observed was a series of shallow spalls about 0.5 in (12.7 mm) deep immediately adjacent to the expansion joint cover plate at the east end of the center span. A cover depth survey showed the mean cover depth to be 2.9 in (72.6 mm) with a range of 2.3 to 3.3 (58.4 to 83.8 mm) and a standard deviation of 0.22 in (5.6 mm).

The mean value of the Copper-Copper Sulfate (CSE) half-cell measurements performed in March 1983, was -176 mV with a standard deviation of -28 mV. Therefore, the probability was less than 10% that active corrosion cells existed in about 80% of the deck, and the remaining 20% of the area showed potentials in the questionable zone. Chloride sampling and analyses, obtained at the same time demonstrated that less than 0.005% of the reinforcing steel had a chance of being above the chloride corrosion threshold level (1.2 lbs/yd^3, 0.71 Kg/m^3). No delaminations associated with reinforcing steel corrosion were discovered in March, 1983. It must be noted that all of these measurements were taken more than two years prior to impregnation which took place in June 1985.

A section, approximately one-half the center span, 60 ft (18.3 m) long by 44 ft (14.6 m) wide was monomer (methyl methacrylate) impregnated using the grooving technique and polymerized in situ in June, 1985 (16). The grooves were backfilled with latex modified mortar. The impregnation depth was approximately 3.5 in (89 mm).

Immediately after impregnation, drying shrinkage cracking was observed in both the impregnated and control section cores. The observed cracks were fine and generally shallow, less than 0.5 in (12 mm). The cracking frequency was almost the same for the control and impregnated section. However, the cracks in the impregnated section were generally deeper.

In May 1992, a visual inspection and delamination survey showed that the deck was in excellent condition after approximately 7 years of impregnation and 9 years after the pre-impregnation condition survey. The only visual evidence of concrete deterioration was a few delaminated areas along the east expansion joint in the control section. These delaminations were in the same locale as the previously noted spalls which had been repaired at an earlier date, which supports the suggestion that they were probably the result of poor construction practices. No additional delaminations were detected in the impregnated or control sections.

A cover depth survey was conducted on the entire center span. The mean cover depth was 2.6 in (66 mm) with a range of 2.1 to 3.1 in (54 to 79 mm) and a standard deviation of 0.19 in (5 mm) for 80 observations.

Chloride Contamination Levels

In March 1983, powdered concrete samples for chloride analyses were taken at mean depths of 0.25, 0.75, 1.50, and 2.5 in (6.4, 19.1, 38.1, and 63.5 mm) in the aprons, right wheel path, and the center of wheel path locations in both the to-be-impregnated and control areas on the eastbound side of the bridge. Six years later, five powdered concrete samples were taken from the outer wheel path in both the impregnated and control sections. The mean depths for these samples were 0.5, 1.0, 1.5, 2.0, 2.75, and 3.63 in (12.7, 25.4, 38.1, 50.8, 69.9, and 92.2 mm). Thirty powdered concrete samples were taken in May 1992. The samples were taken in the aprons, right wheel path, and center of wheel path locations in both the impregnated and control areas of the eastbound and westbound sides of the bridge. The mean sample depths were 0.5, 1.0, 1.5, 2.0, 2.5, and 3.0 inches (12.7, 25.4, 38.1, 50.8, 63.5, and 76.2 mm).

The difference between the right wheel path chloride contents for the samples collected in 1989 and 1983 and that of 1983 and 1992, for the impregnated and control sections, are presented in Tables 2.1 and 2.2, respectively. This would be a measure of the effectiveness of the impregnation process to exclude or reduce the intrusion of chloride ions. The difference between the eastbound, right wheel path chloride contents were higher for the control section for all depths except 2.5 in (64 mm) for both periods. The mean chloride content at a depth of 2.5 in (63.5 mm) was less than 1.2 lb/yd^3 (0.71 kg/m^3) of concrete in all cases, although there is some variability in the measurement technique. As has been noted earlier, the first powdered concrete samples were obtained a little over 2 years before the section was monomer impregnated.

Though no pre-impregnation measurements were taken in the shoulder and the center of wheel path areas, a relative comparison can be made between the current average chloride content in the impregnated and control sections. The results of these comparisons are shown in Tables 2.3 and 2.4 for the shoulder and center of wheel path, respectively.

Table 2.1 Difference in Average Chloride Content in Right Wheel Path, Eastbound Lane, 1983-1989

Depth (in)	Chloride Content (lbs/yd^3)		Difference (Con-Imp)	Chloride Reduction (%)
	Control	Impregnated		
0.5	5.1	3.5	1.6	29
1.0	4.6	1.7	2.9	63
1.5	2.2	1.9	0.3	9
2.5	0.7	0.7	0.0	0

Note: 1 lb/yd^3 = 0.593 kg/m^3
1 in = 25.4 mm.

Table 2.2 Difference in Average Chloride Content in Right Wheel Path, Eastbound Lane, 1983-1992

Depth (in)	Chloride Content (lbs/yd^3)		Difference (Con-Imp)	Chloride Reduction (%)
	Control	Impregnated		
0.5	7.6	6.6	1.0	29
1.0	4.6	3.0	1.6	35
1.5	2.0	1.0	1.0	45
2.5	0.3	0.3	0.0	0

Note: 1 lb/yd^3 = 0.593 kg/m^3
1 in = 25.4 mm.

Without pre-impregnation chloride content measurements for these areas, it is impossible to draw firm conclusions as to the effectiveness of the impregnation process; however, the results indicate that the impregnation process reduced the rate of chloride diffusion.

Table 2.3 Average Chloride Content in Shoulder, East and Westbound Lanes, 1992

Depth (in)	Chloride Content (lbs/yd^3)		Difference (Con-Imp)	Percent Difference
	Control	Impregnated		
0.5	8.3	5.1	3.2	38
1.0	8.4	4.6	3.8	46
1.5	5.9	2.5	3.4	56
2.5	1.3	0.5	0.8	64
3.0	0.7	0.3	0.4	43

Note: 1 lb/yd^3 = 0.593 kg/m^3
1 in = 25.4 mm.

Table 2.4 Average Chloride Content in Center of Wheel Path, East and Westbound Lanes, 1992

Depth (in)	Chloride Content (lbs/yd^3)		Difference (Con-Imp)	Percent Difference
	Control	Impregnated		
0.5	16.9	15.2	1.7	10
1.0	10.8	3.7	7.1	33
1.5	6.1	3.0	3.1	50
2.5	0.8	0.8	0.0	0
3.0	0.4	0.3	0.1	20

Note: 1 lb/yd^3 = 0.593 kg/m^3
1 in = 25.4 mm.

In addition to the effectiveness of the impregnation process in reducing chloride intrusion, the percent of reinforcing steel presently in critically contaminated concrete is also of interest. The chloride contamination levels at the depth of the reinforcing steel for the impregnated and control sections in May, 1992 were approximately equal. Assuming 1.2 lb/yd^3 (0.71 kg/m^3) of concrete as the corrosion threshold level, 0.03% of the reinforcing steel in the wheel paths was located in critically contaminated concrete, based on the cover depth distributions as of May 1992.

Corrosion Potentials

Corrosion half-cell potentials were measured with a CSE in March 1983 and 1989 and in

May 1992. Table 2.5 presents the mean, standard deviation, and number of observations for all three surveys. The mean corrosion potentials for the control and impregnated sections were approximately equal in 1983, 1989, and 1992. The mean CSE potential increased slightly in both the impregnated and control sections over the 9-year period. For the control section in 1992, approximately 84% of the area surveyed was in the range of uncertain corrosion activity (-200 to -350 millivolts). Similarly, 85% of the impregnated area is in the

Table 2.5 Half-Cell Potential Readings For The Eastbound Boalsburg Bridge Deck

Statistical Parameter	Potential (-mV)					
	Impregnated Section			Control Section		
	1992	1989	1983	1992	1989	1983
Mean	235	192	173	234	200	176
Standard Deviation	34	19	5	39	26	28
Number observations	331	24	9	388	28	72

uncertain corrosion activity range. There were 11 observations with a greater than 90% probability of active corrosion (more negative than -350 millivolts), 2 in the impregnated section and 9 in the control section.

In May 1992, potential measurements were taken on the westbound side of the bridge. Table 2.6 presents the means, standard deviations, and number of observations for that survey. Again the mean corrosion potentials for both the impregnated and control sections were approximately equal. Both mean potentials are slightly lower than those for the eastbound side. This may be due to the cross-slope of the bridge which causes runoff to flow from the westbound to the eastbound side of the deck. Approximately 57% and 56%, respectively of the impregnated and control section were in the uncertain range of corrosion activity. Six observations indicated a greater than 90% probability of corrosion activity, 1 in the impregnated and 5 in the control sections.

Table 2.6 Half-Cell Potential Readings For The Westbound Boalsburg Bridge Deck, 1992

Statistical Parameter	Potential (-mV)	
	Impregnated Section	Control Section
Mean	206	208
Standard deviation	34	32
Number observations	319	405

Petrographic Analysis

Four inch diameter cores were drilled with a water cooled diamond bit for petrographic analysis, two in the impregnated section and two in the control section. The depth of impregnation was determined to be 3 to 4 in (76.2 to 101.6 mmm) which agrees with previous findings (16).

Petrographic analysis indicated that the concrete composition volume values were in the range of typical construction grade concrete. The coarse aggregate was a crushed limestone. The fine aggregate was a highly siliceous natural sand. Both the fine and coarse aggregates were good quality aggregates. However, the quality of the cement paste was poor, showing considerable evidence of excessive mixing water. In addition to drying shrinkage cracks, there was excessive near-surface porosity and bleeding channels and high porosity and large irregularly-shaped voids adjacent to coarse aggregate particles. Cracking was numerous, though minor, and was equally distributed between the impregnated and the control sections.

Two of the 4 cores contained steel rebar; one in the impregnated and one in the control area. The core from the impregnated area showed no corrosion. The core in the control area showed heavy corrosion deposits from a supporting chair. The core was located immediately adjacent to a sliding plate expansion joint at the east end of the span. This was the area where spalling had occurred.

Corrosion Current

In May 1992 and March 1990, corrosion current density (i_{corr}) measurements were taken in both the control and impregnated areas. In March 1990, the measurements were taken using a 3LP device. The device is based on the linear polarization resistance technique with changes in cathodic polarization currents measured at changes in potentials of 0, 4, 8, and 12 millivolts. The value of the Tafel slope constant, B, is 40.76 millivolts. In May 1992, the Geocisa Gecor device was used in addition to the 3LP. The Gecor device is also based on the linear polarization resistance technique with the addition of a guard ring electrode to confine the area of polarization. The value of the Tafel slope constant, B for this device is 26 millivolts. Table 2.7 presents the means, standard deviation, and number of observations for the 3LP and Gecor i_{corr} measurements taken on the eastbound side of the deck. Table 2.8, presents the results of the May 1992 i_{corr} measurements and the cover depth at the test locations.

Table 2.7 Corrosion Current Measurements For Eastbound Boalsburg Bridge Deck

Statistical Parameter	i_{corr}, (mA/ft^2)					
	Impregnated Section			Control Section		
	1990 3LP	1992 3LP	1992 Gecor	1990 3LP	1992 3LP	1992 Gecor
Mean	1.66	2.38	0.13	4.26	5.28	0.46
Standard deviation	0.41	1.28	0.12	1.06	2.56	0.44
Number observations	10	8	8	10	7	7

Note: 1 mA/ft^2 = 1.08 μA/cm^2

In 1990, the control section was corroding at a rate of about 2.5 times that of the impregnated section as measured by the 3LP. In 1992, the control section was corroding at a rate of about 2.2 times that of the impregnated section as measured by the 3LP and 3.5 times as measured by the Gecor device. Also, note that no correlation between the i_{corr} and the corrosion potentials measurements was obtained.

Concrete Resistivity

Concrete resistivity measurements were taken with the Nippon Steel device in the March 1989 survey, and concrete resistance measurements were obtained using the Gecor device in the May 1992 survey, see Table 2.9. Unfortunately, the concrete resistance measurements taken with the Gecor device cannot be directly converted to concrete resistivity at this time.

It is generally believed that corrosion is less likely to occur if the concrete resistivity is greater than 12 Kohms·cm (17,18). The mean resistivity value for the impregnated concrete as measured by the Nippon Steel device was 17% below this value, it was also 48% greater than the value for the control section. The mean concrete resistance measurement from the Gecor device was 118% greater in the impregnated area. Both comparisons indicated that the impregnation process increased the resistance of the concrete, which should decrease the likelihood of corrosion.

Performance of Bethlehem Bridge Deck

Background

The Bethlehem bridge is a dual-lane bridge which carries Pennsylvania Route 378 over Union Boulevard. In March 1975, a test section at the south end of the bridge, 3.5 ft (1.1 m) by 11.5 ft (3.5 m), was deep monomer-impregnated from the surface using the pressure

Table 2.8 Corrosion Current Measurements for the Boalsburg Bridge Deck, 1992

Location	Cover Depth (in)	Corrosion Potentials (-mV, CSE)	Corrosion Current (μ/cm^2)	
			3LP	Gecor
Impregnated Section				
Eastbound				
1	2.7	134	1.4	0.07
2	2.5	178	4.8	0.42
3	2.6	199	3.3	0.45
4	2.5	157	1.0	0.06
5	2.4	186	2.4	0.11
6	2.4	222	2.3	0.06
7	2.8	128	1.6	0.06
8	2.5	184	2.1	0.11
Westbound				
1	2.6	117	1.3	0.10
2	2.6	194	1.9	0.03
3	2.6	160	1.5	0.03
4	2.4	128	0.3	0.02
5	2.7	242	NA	0.08
6	2.4	284	NA	0.04
Control Section				
Eastbound				
1	2.7	359	10.4	1.46
2	2.7	152	4.8	0.23
3	2.6	167	6.1	0.29
4	2.8	127	2.6	0.27
5	2.6	160	3.8	0.22
6	2.6	197	5.7	0.38
7	3.1	153	3.6	0.37
Westbound				
1	2.6	178	7.2	1.31
2	2.5	159	4.1	0.26
3	2.8	188	7.4	0.77
4	2.7	193	6.2	0.25
5	2.2	142	2.6	0.25
6	2.4	147	2.9	0.27

Note: 1 mA/ft^2 = 1.08 μA/cm^2

method. The bridge was 8 years old at the time of impregnation. The wheel path areas were deeply rutted. The chloride content at the reinforcing steel depth in the impregnated area exceeded the corrosion threshold level but the deck was sound, with no spalled or patched areas. Details of the deep impregnation with methyl methacrylate and in situ polymerization of the field test installation are presented by Mason et al. (19).

A visual examination of the bridge in December, 1983 revealed some obvious differences in performance between the deck in general and the deep-impregnated test area. The visual difference in performance initiated an investigation to identify the cause of the difference in the visual corrosion protection performance. An investigation performed in February 1984 consisted of a delamination survey, corrosion potential measurements, chloride content analysis, and a microscopic analysis of drilled concrete cores. The results of the study

Table 2.9 Concrete Resistivity and Resistance Measurements of The Boalsburg Bridge Deck

Statistical Parameter	Impregnated Section		Control Section	
	1989 Nippon Steel (Kohm • cm)	1992 Gecor (Kohm)	1989 Nippon Steel (Kohm • cm)	1992 Gecor (Kohm)
Mean	9.95	1.57	6.72	0.72
Standard deviation	1.66	0.44	1.91	0.17
Number observations	5	8	5	7

have been reported by Cady and Weyers (20). A second investigation, performed in March 1989, consisted of a visual inspection, delamination survey, corrosion potentials and microscopic analysis of drilled concrete cores.

In March 1990 the structure was replaced. Both the deep-impregnated test section and an adjoining section, 4.6 ft (1.4 m) by 10.3 ft (3.1 m), were removed and subsequently placed in the outdoor exposure area of the S&M Lab. Sections of both slabs were damaged during removal.

Visual Inspection and Delaminations

A visual inspection and delamination survey of an area about 14 ft (4.3 m) by 37 ft (11.3 m), encompassing the impregnated test area, was performed at the south end of the northbound traffic lane in March 1989. Approximately, 20% of the non-impregnated area was delaminated or spalled due to reinforcing steel corrosion, whereas, the impregnated area remained sound with no patched spalls, spalls, or delaminations, although one corner of the impregnated area was patched as part of a repair to an adjacent spall in the untreated area.

The 2 deck sections which were transported to S&M Lab in May 1990, a visually inspected and a delamination survey was conducted upon arrival. The impregnated slab area was 38 ft^2 (3.5 m^2). One of the corners of the slab, 3.6 ft^2 (0.3 m^2), was damaged during removal. An additional 1.9 ft^2 (0.2 m^2) of one corner had been patched during the repair of an adjacent spall in an untreated area of the original bridge deck. No delaminations were located. The damaged corner was repaired with LMC.

The control slab area was 47 ft^2 (4.4 m^2) in area. A delamination survey revealed that 10.4 ft^2 (1.0 m^2), roughly 22%, of the control slab was delaminated. In addition, 3.4 ft^2 (0.3 m^2) of the slab had been previously patched. The concrete in the damaged area was removed to the bar level with a 50 lb (23 kg) jack hammer. The exposed rebar was sandblasted to near white metal. The damaged areas were patched with latex modified concrete, and a 2 in (51 mm) overlay was placed over the entire slab in July 1990.

Cracking between the overlay and the substrate concrete was noticed on the edges of the control slab in April 1991. A subsequent delamination survey found that 71% of the overlay had delaminated from the substrate concrete. These delaminations were the result of poor construction practice.

The delaminated area was outlined with a concrete saw to a depth of 3/4 in (19 mm) and the delaminated concrete removed with an impact hammer fitted with a chipper bit. A second delamination survey on the substrate concrete located an additional 1.3 ft^2 (0.1 m^2) of corrosion-induced delamination. The delaminated concrete was removed to a depth of 3/4 in (19 mm) below the rebar. Corrosion products were cleaned from the exposed rebar and a new LMC overlay was placed.

The most recent visual inspection and delamination survey was conducted in June 1992. Neither the impregnated slab or the control slab showed any sign of deterioration at that time.

Concrete Cover Depth and Chloride Content

Prior to the deck replacement, a pachometer was used to determine the concrete cover depth over the reinforcing steel. Forty measurements were taken, 20 within and 20 outside the impregnated area. The mean cover depth was 1.45 in (37 mm) with a standard deviation of 0.40 in (10 mm).

During chloride sampling, the top 0.25 in (6 mm) sample was discarded and 4 samples were taken at depth increments of 0.50 in (12.7 mm). Powdered concrete samples were taken in the right wheel path at ten locations, five within and five outside the impregnated area. The mean depth of the samples was 0.50, 1.00, 1.50, 2.00 and 2.75 in (12.7, 25.4, 38.1, 50.8, and 69.9 mm). Table 2.10 presents the average chloride content for the wheel path locations as a function of depth for the 1984 and 1989 samplings.

The chloride content of the reinforcing steel depth was above the corrosion threshold value in 1975 (19) and there was an insignificant difference between the chloride contents of the impregnated area and the rest of the deck based on a 95% confidence level (20). Thus, any difference in the chloride contents between the impregnated section and the non-impregnated section should be a measure of the efficacy of impregnation to reduce the rate of chloride diffusion rate into concrete.

As presented in Table 2.10, chloride contents in both the impregnated and control area appeared to have continued to increase during the five year time period. The difference in chloride contents between the measurements indicate that more chloride penetrated the impregnated concrete than the control concrete for the top 1 in (25 mm) of concrete. Research by Dutta (21) indicates that at higher drying temperatures, such as those used during drying, not all voids accessible by water would be filled by the monomer, probably due to the large size of the organic monomer molecules. As a result, the impregnation process may make the top 1 in (25 mm) of concrete more susceptible to chloride intrusion.

However, for the depths of 1.5 to 2.75 in (38 to 70 mm) the impregnated concrete reduced the chloride intrusion by an average 1.5 lb/yd^3 (0.9 kg/m^3) of concrete, see Table 2.10. The average chloride reduction percent, which would be a measure of the monomer impregnation

Table 2.10 Difference in Average Chloride Content in Right Wheel Path for Bethlehem Bridge.

Depth (in)	Chloride Content (lbs/yd^3) Difference Between 1989-84		Difference Between Con-Imp	Chloride Reduction (%)
	Control	Impregnated		
0.5	0.17	2.9	-2.7	--
1.0	-0.17	1.5	-1.7	--
1.5	2.5	0.4	1.1	53
2.0	1.9	0.7	0.8	63
2.75	3.0	1.0	2.0	67

Note: 1 lb/yd^3 = 0.593 kg/m^3
1 in = 25.4 mm.

effectiveness was about 60% for the depths of 1.5 in (38 mm) and greater. It is interesting to note that the chloride content, at the reinforcing steel depth, in the impregnated area remained above the threshold level of 1.2 lb/yd^3 (0.7 kg/m^3) for 14 years without spalling or delaminating. The average chloride contents are presented in Table 2.11.

Corrosion Potentials

Corrosion half cell potentials were measured using a CSE. Table 2.12 presents the means, standard deviations, number of observations, the percent more negative than -350 mV and the percent less negative than -200 mV for the field measurements prior to the 1990 deck replacement. The potentials for the non-impregnated area increased slightly in the percent more negative than -350 mV, thus indicating that the percent with a greater than 90% probability of reinforcing steel corrosion increased by 6%.

Table 2.11 Chloride Contents for Bethlehem Bridge Slabs

Depth (in)	Chloride Content (lbs/yd^3) October 1992			
	Impregnated Location		Control Location	
	I-1	I-2	C-1	C-2
Overlay	NA	NA	0.7	0.7
0.5	10.8	11.1	1.9	0.8
1.0	10.6	10.3	8.4	9.8
1.5	13.3	9.4	9.8	14.0
2.0	13.3	3.7	13.1	14.8
2.5	7.8	3.5	14.3	16.5

Note: 1 lb/yd^3 = 0.593 kg/m^3
1 in = 25.4 mm.

Also the percent with greater than 90% probability that no reinforcing steel corrosion is occuring increased by 3%. However, there was no change in the mean or standard deviation. Thus, for all practical purposes there was insignificant change in corrosion potentials of the non-impregnated areas prior to the deck replacement.

However, in the same period, the corrosion potentials in the impregnated area became more negative by 90 mV, from -260 mV to -350 mV, and the standard deviation increased by 30 mV. Also, the percent more negative than -350 mV, indicating that a greater than 90% probability that corrosion is occurring, increased by 50%. Thus, it appears that the corrosion activity increased in the impregnated section during the 5 year period from 1984 to 1989 prior to replacement.

Once the salvaged impregnated slab and non-impregnated control slab arrived at the S&M Lab, a 6 in (15 cm) control grid was established on both slabs for corrosion potential measurements. CSE corrosion potentials were taken on the slabs in July 1990 prior to the initial repair, in July 1991 prior to the replacement of the control slab's LMC overlay, and in June 1992. The means, standard deviations, and number of observations are reported in Table 2.13. The results for the control slab are divided into repaired and non-repaired areas.

Table 2.12 Half Cell Potentials from 1984 and 1989 Field Measurements For the Bethlehem Bridge Deck

	Time, Year	Mean (-mV)	STD (-mV)	No.	More Negative Than -350 (%)	Less Negative Than -200 (%)
Impregnated Area	1984	260	60	5	0	0
	1989	350	90	18	50	0
Non-Impregnated Area	1984	340	110	34	41	9
	1989	340	110	134	47	12

The results presented in Table 2.13 indicate that upon arrival at Virginia Tech, the mean potential for the impregnated slab and the mean of the repaired and non-repaired sections of the non-impregnated slab were approximately the same. After repair, the mean potential in the repaired areas of the non-impregnated slab decreased 61%. The mean potential of the non-repaired area became less negative after placement of the first overlay, and more negative after the placement of the second overlay. The mean potential of the impregnated slab decreased (was less negative) by 39% in the 2 years after it arrived at Virginia Tech. The increase (less negative) of both the impregnated slab and the non-repaired section of the control slab may be due to drying out of the slabs. The stay-in-place metal forms were removed from both slabs upon arrival at the S&M Lab.

Microscopic Analysis

To evaluate the concrete material, 4 in (102 mm) diameter cores were drilled with a water-cooled diamond drill bit. The cores were approximately 5 in (127 mm) long. Vertical sections were cut, polished and examined using a petrographic microscope. The coarse aggregate was a blast furnace slag and the fine aggregate was a natural sand. The cement paste appeared to be of an excellent quality. The depth of impregnation was approximately 3 in (76 mm), which agreed with previous results (19).

The primary interest in the examination was the reinforcing steel corrosion, since the purpose of deep impregnation is to prevent/arrest the corrosion process. Table 2.14 presents the summary of the corrosion examinations. The microscopic examination of polished and fractured sections revealed details of the corrosion state of the deck. With the exception of the Conn. core, corrosion products were observed around the reinforcing steel. Cores A and D from the non-impregnated area showed evidence of slight corrosion. All four cores from the impregnated area showed evidence of corroding reinforcing steel; however, the corrosion products were impregnated. Thus, the deep impregnation process appears to have arrested active corrosion cells in all four of the cores. Fig. 2.1 presents a microphotograph of impregnated core J showing a vertical crack caused by corrosion of the rebar, while Fig. 2.2 is a microphotograph of a fractured surface of core J showing the impregnated corrosion

products. Thus, the microscopic investigation presents direct evidence that the deep monomer impregnation process arrested the steel corrosion in concrete.

Table 2.13 Half-Cell Potentials For the Bethlehem Impregnated and Control Slabs

	Date	Mean (-mV)	STD (mV)	No. of Observations	More Negative Than -350 mV (%)
Impregnated Area	July, 1990	342	40	126	47
	February, 1991	278	39	138	3
	June, 1992	207	41	138	0
Non-Impregnated, Non-Repaired	July, 1990	313	55	119	37
	July, 1991[1]	381	68	119	66
	June, 1992	285	55	119	14
Non-Impregnated, Repaired	July, 1990[2]	454	70	29	97
	July, 1991	178	71	41	0
	June, 1992	193	65	41	0

[1]Readings taken after the delaminated overlay was removed.
[2]Readings taken prior to repairs.

Table 2.14 Microscopical Examination of Polished Vertical Sectional Cores From the Bethlehem Bridge Deck

Core No.	Impreg. Area	Cracking Observed			Rebar Corr.	Cover Depth (mm)	Rebar Corroded
		Drying Shrink	Micro Shrink	Subsi-dence			
A	No	No	No	No	No	56	Slight
D	No	No	No	No	No	33	Slight
Conn	No	Few	No	No	No	36	No
F	Yes	Two	No	Yes	No	38	Y/Arrested
H	Yes	Few	No	No	No	38	Sl/Arrested
I	Yes	(a)	No	(a)	(a)	30	Y/Arrested
J	Yes	No	Minor	No	Yes	36	Y/Arrested

(a) Two cracks originating from rebar -- cannot discern if shrinkage, subsidence, or rebar corrosion related, but definitely pre-exist the impregnation.

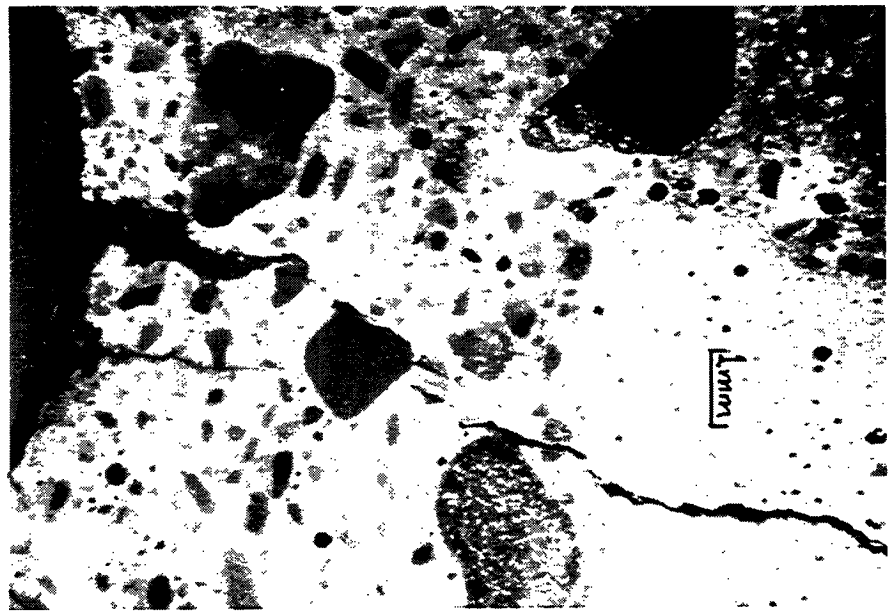

Fig. 2.1 Rebar Corrosion and Associated Vertical Crack, Core J, Bethlehem Bridge

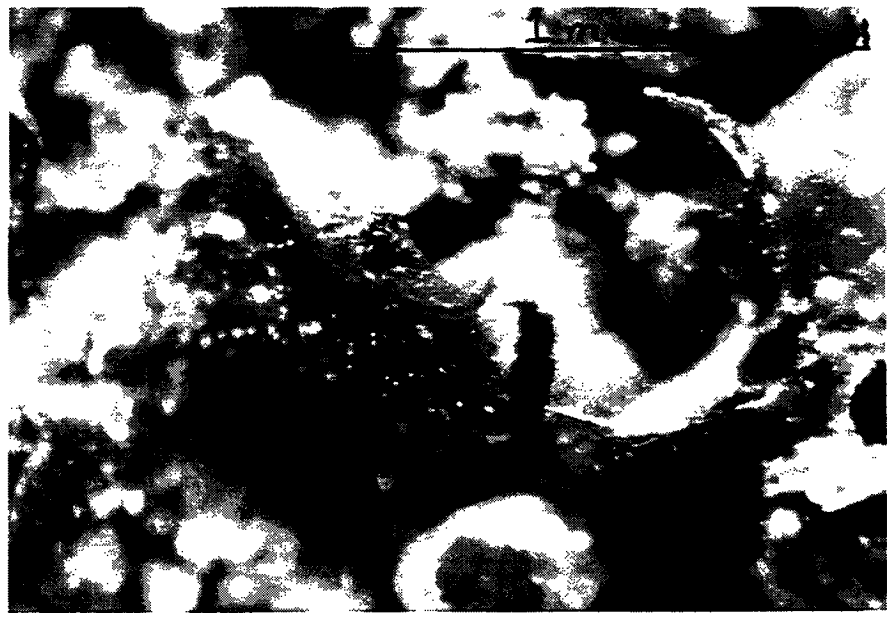

Fig. 2.2 Polymer Impregnated Corrosion Products--Fractured Section, Core J, Bethlehem Bridge

Corrosion Rate

In March 1990, eight i_{corr} measurements were taken in both the control and impregnated areas. The measurements were taken in sound areas for both the impregnated and control areas; no delaminations were detected in the impregnated area. The i_{corr} measurements of the March 1990 using the 3LP device are presented in Table 2.15. No correlations between the corrosion potentials and the corrosion currents were found. Also, the i_{corr} measurements in the impregnated section was found to be significantly less, 15 times lower, than that in the control section.

Table 2.15 Corrosion Current Measurement For Bethlehem Bridge Deck

Location	Impregnated Area		Control Area	
	Corrosion Potential (mV, CSE)	Corrosion Current (μ/cm^2)	Corrosion Potential (mV, CSE)	Corrosion Current (μ/cm^2)
1	475	0.68	354	3.04
2	422	0.38	507	6.86
3	288	0.24	398	4.77
4	280	0.15	280	2.79
5	310	0.15	325	3.27
6	312	0.11	329	3.10
7	342	0.17	403	4.35
8	440	0.33	404	6.08
Mean	358	0.28	375	4.28

Note: 1 mA/ft^2 = 1.08 μA/cm^2

Additional i_{corr} measurements were taken on both the impregnated and the control slabs salvaged from the Bethlehem Bridge deck. The means, standard deviations, and number of observations are presented in Table 2.16.

From Table 2.16, it can be seen that the i_{corr} measured by both the 3LP and Gecor devices was approximately 10 times less in the impregnated section as compared to the control section. Based on the 3LP measurements, it may be estimated that damage may be expected in the impregnated slab in 10-15 years whereas damage would be expected in the control slab in 2-10 years based on the study conducted by Clear (22). It must also be noticed that the mean 3LP i_{corr} for the impregnated slab borders on the threshold of no corrosion activity, given at 0.20 mA/ft^2 (0.22 μA/cm^2) (22).

Table 2.16 3LP Corrosion Current Measurements For Bethlehem Bridge Slabs

	Date	3LP Corrosion Currents			Gecor Corrosion Currents		
		Mean (mA/ft^2)	STD	No. of Observations	Mean (mA/ft^2)	STD	No. of Observations
Impregnated Slab	July, 1990	0.25	0.21	21	N/A	N/A	N/A
	June, 1992	0.27	0.32	24	0.02	0.01	13
Control Slab, Repaired	July, 1990[1]	5.4	3.8	12	N/A	N/A	N/A
	July, 1991	4.2	0.57	12	0.21	0.35	6
	June, 1992	1.8	1.80	12	0.12	0.05	7
Control Slab, Non-Repaired	July, 1990	1.7	0.77	18	N/A	N/A	N/A
	July, 1991[2]	3.9	1.5	18	0.54	0.33	13
	June, 1992	3.4	0.49	18	0.11	0.04	14

[1]Readings taken prior to repairs.
[2]Readings taken prior to removal of delaminated overlay.

Note: 1 mA/ft^2 = 1.08 $\mu A/cm^2$

Estimated Service Life of Monomer Impregnation

Impregnation with monomer and in-situ polymerization is expected to reduce the diffusion of chloride ions to the bar level, increase the resistivity of the concrete, and tend to significantly reduce the corrosion current expected in a similar untreated deck.

The Bethlehem test section has shown no sign of deterioration in the 18 years after impregnation, even though the chloride content was greater than the 1.2 lb/yd^3 (0.70 kg/m^3) at the time of impregnation. The mean 3LP i_{corr} for the impregnated section has remained slightly above 0.20 mA/ft^2 (0.22 $\mu A/cm^2$) during the past three years of testing, which suggests that damage may be expected in 10-15 years. However, it must be noted that for 3LP i_{corr} rates less than 0.20 mA/ft^2 (0.22 $\mu A/cm^2$), no corrosion damage is expected. Therefore, it may be assumed that damage might be expected in 15 years even though the i_{corr} has shown no sign of increase over the past 3 years. Based on the observations of the Bethlehem trial section, it can be estimated that deep monomer impregnation will increase the service life of a bridge deck by at least 30 years, 18 years current service since impregnation and 15 years expected service till damage occurs based on 3LP i_{corr} measurements.

3

Calcium Nitrite Impregnation of Christiansburg Deck

Introduction

The two most common means of rehabilitating concrete bridge components in which steel corrosion has caused distress are the removal and replacement of the concrete and/or the use of cathodic protection. In cases where delaminated and spalled areas are a small percentage of the deck area and the steel has not lost appreciable cross sectional area, cathodic protection is the current method of stopping corrosion without concrete removal. In this project the feasibility of adding a known corrosion inhibitor, calcium nitrite, to repassivate the reinforcing steel in concrete was examined. This rehabilitation method does not require removal of appreciable amounts of sound chloride contaminated concrete, nor does it require long-term maintenance of a cathodic protection system.

Laboratory testing was initiated at W. R. Grace & Co. in the mid 1980s to determine the conditions needed to impregnate hardened concrete with calcium nitrite to below the reinforcement level. Methods examined included vacuum impregnation, pressure impregnation, ordinary soaking and drying the concrete by heating above the boiling point of water with subsequent soaking with an aqueous calcium nitrite solution. Only the last method was successful in impregnating the concrete with calcium nitrite to below the reinforcement level. It was also determined that the cooling of the concrete had to be controlled to prevent thermal shock.

In August 1985, a large scale bridge deck impregnation was performed at the University of Texas at Austin (23). A 20 x 60 ft (6.1 x 18.3 m) bridge deck section was used for the evaluation. Two 10 x 20 ft (8.0 x 6.1 m) sections were dried to above 212°F (100°C) to approximately mid-depth and slowly cooled. Detailed analyses of the heating and cooling profiles as well as the crack distribution before and after heating were performed. There

were no new cracks due to the heating and cooling process and there was no growth in existing cracks. Analysis of the concrete and measurement of liquid consumed in the soaking process both indicated that 18 lbs/yd^3 (10.8 kg/m^3) of nitrite penetrated 2 in (51 mm) into the deck. Thus, the posttreatment process was successful.

In the summer of 1987, a 10 X 20 ft (3.0 x 6.1 m) section of a parking garage was subjected to the calcium nitrite impregnation treatment. This structure was approximately 18 years old and had severe delamination. Chloride levels were over 15 lb/yd^3 (9 kg/m^3) in the top 1.25 in (31.8 mm). The deck was successfully heat treated and slowly cooled without creating cracks. However, nitrite analysis of cores showed that only 3.2 lb/yd^3 (1.92 kg/m^3) of nitrite penetrated to the 1-1.5 in (25-38 mm) depth. It was concluded that the reduced penetration was due to surface contamination and high surface chloride concentrations which blocked the nitrite.

Laboratory experiments showed that removing a contaminated surface layer on other field specimens improved ingress. Thus, it was recommended either to scarify the surface or to cut grooves below the surface to improve the impregnation process.

In this work a 20 x 8 ft (6.1 x 2.4 m) section of a bridge deck breakdown lane in the north span was treated with calcium nitrite during the week of July 23, 1990. The bridge is located on U. S. Route 460 Bypass, East of Christiansburg, VA, spanning Va. Route 732. The bridge consisted of three simple spans, with two travel lanes of 12 ft (3.7 m) each, and a 10 ft (3 m) breakdown lane. The deck was grooved parallel to the expansion joints between the spans, Fig. A-1, Appendix A. Based on previous experience, grooves were precut in the deck to allow the calcium nitrite to ingress without having to penetrate surface impurities (16). Corrosion and chloride content measurements were performed. The section was demonstrating both active and passive corrosion currents which correlated well with the chloride concentrations. There were also a few delaminated areas.

Pretreatment Corrosion Measurements and Chloride Concentrations

Corrosion potentials and i_{corrs} are presented in Fig. 3.1. The results showed that the breakdown lane of the bridge was corroding on the guardrail side of the area that was to be treated.

Chloride analysis results are given in Table 3.1 and correspond to positions in the deck schematic in Appendix A. Location 1-2 is at the guardrail and increasing letter values indicate locations nearer to the traffic line. Chloride content levels were in general much higher near the guardrail (1-2, A4, A26) most likely because traffic caused a buildup of snow and slush containing deicing salts at that location. Chloride content levels at the 2.25 in (57 mm) nominal reinforcement depth were above 1.2 lb/yd^3 (0.9 kg/m^3) at several locations, which is considered a lower limit for chloride induced corrosion.

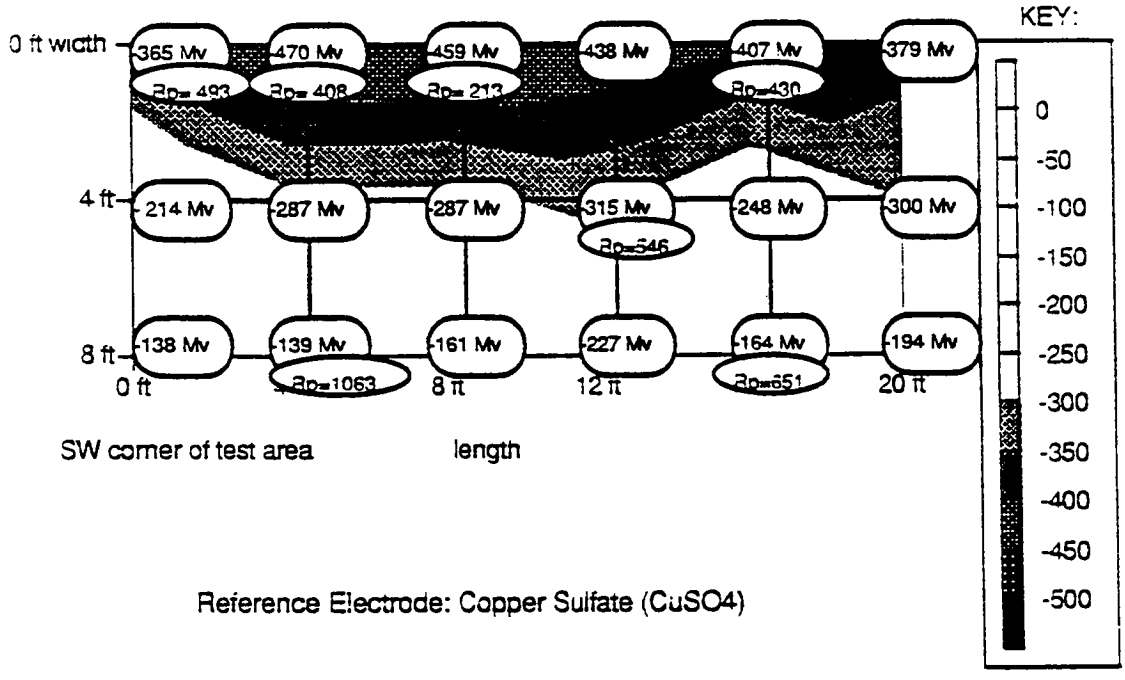

Fig. 3.1 Corrosion Potential Profile and Corrosion Polarization Resistance

Table 3.1 Chloride Content Analysis of Bridge Deck Samples (lb/yd^3)*

	LOCATION					
Depth (in)	1-1	A4	A26	B14	E14	E24
0.5	7.5	18.1	6.7	7.6	6.9	1.9
1.0	4.7	10.6	5.2	3.8	3.7	2.3
1.5	4.0	6.7	3.4	2.0	1.6	1.5
2.0	--	5.9	2.3	2.0	1.1	1.8
2.5	--	4.0	1.6	1.5	0.8	1.1

*Based on concrete unit weight at 140 lb/cf

Note: 1 lb/yd^3 = 0.593 Kg/m^3 1 lbs/yd^3 = 16 Kg/m^3
1 in = 25.4 mm

Corrosion potential and i_{corr} measurements (measured by 3LP) were performed within the 8 x 20 ft (2.4 x 6.1 m) section before drying the deck. It rained the day before so there was no difficulty in obtaining stable corrosion readings. The corrosion potentials (CSE) are shown in Fig. 3.1. Locations of high negative potential occurred near the guardrail which was in good agreement with the chloride data.

Corrosion polarization resistance measurements were measured under potentiostatic control. A portable computer-controlled potentiostat (Thompson Autostat-Software Controlled Potentiostat) was used with a copper wire mesh/sponge counter electrode. The polarization resistance $R_p = \Delta E/\Delta I$ at $I=0$, where E is the potential and I is the current, was determined. R_p is inversely proportional to the corrosion current (25).

Polarization resistance values at several locations are shown in Fig. 3.1. They are not corrected for the area of steel polarized, and as such serve as a relative comparison between corroding and noncorroding sections that can be monitored over time. Since changes over time are of interest rather than absolute values, the need for area correction is not great because the reinforcement pattern is not expected to change. Note that it is likely that at least 11.8 in^2 (76 cm^2) of rebar area is involved (based upon a 6 in (152 mm) long counter electrode and 5/8 in (15.9 mm) rebars). Laboratory studies indicate that R_p values less than 66,000 ohm $\cdot$ cm^2 are indicative of corrosion (25), so if an arbitrary 15.5 in^2 (100 cm^2) area was used, corrosion was occurring at several locations, Fig. 3.1. The low R_p values occurred in regions of high negative corrosion potentials, indicating good agreement between the methods. Note that no correction was made for concrete resistance, but since the concrete was moist and of moderate w/c ratio (above 0.45), the correction is minor in the noncorroding regions, and would mask higher corrosion currents in the corroding regions (26).

The chloride analyses, corrosion potentials, i_{corr}, polarization resistance, and corrosion data are in good agreement. The post-treated area definitely had locations undergoing active corrosion and others that appearred to be in the passive state. As such, the ability of the posttreatment process to arrest or reduce corrosion activity was measurable.

Treatment Process

Equipment

A plan view of the bridge deck and the treated area is presented in Fig. A-1, Appendix A. A series of 0.75 in (19 mm) diameter holes was drilled into the underside of the deck for placement of thermocouples to monitor the heating/cooling of the bridge deck. The approximate location of the holes is shown in Fig. A-2, Appendix A. A pair of holes was drilled at each location. The deepest hole penetrated 4 in (102 mm) into the concrete from the underside of the deck. The distance between the deepest penetration of the hole and the deck surface was 2 in (51 mm). A Type K and Type T TC were inserted into the hole, and

then sealed with a clay plug. The thermocouple leads were then taped to the underside of the deck and brought over the side to temperature measuring instrumentation on the deck surface. The second hole was drilled to a depth of 2 in (51 mm) from the underside into the concrete. A Type T TC was placed in this hole and sealed and taped in the same manner as previously discussed.

A multichannel digital thermometer was used to measure all Type K TCs. A total of 9 Type K TCs were used, with 4 being placed on the surface of the concrete deck. The surface TCs were held in place with clay and blocks to insure solid contact with the surface of the deck. Eight Type T TCs were attached to a portable data logger and serial printer programmed to measure up to 12 temperatures at 15 minute intervals. Due to battery discharge/damage during transit, the data logger did not function properly. A backup hand held two channel digital thermometer was used instead, to take a reading from the eight thermocouples at 15 minute intervals. A ninth Type T TC was used to measure the heated air temperature inside the insulating shell.

To provide fast, effective heating to the deck, a Dayton 600,000 BTU/hr. kerosene heater was utilized. The heater was modified to incorporate a centrifugal blower for an increased output of air. A high temperature controller with adjustable on/off setpoint provided a constant air temperature inside the shell. A Type K TC placed 6 in (152 mm) above the deck surface at the center of the heated deck furnished the temperature signal.

A lightweight modular heating shell was fabricated to trap the heated air above the concrete deck. The shell was built in a layered construction, with reflective aluminum sheeting attached to an inner frame of aluminum angle. Four 1/2 in (13 mm) thick high-temperature fiberglass boards and sheets were glued together with high-temperature silicone caulking, and were then glued to the inside frame. An outside frame of aluminum was then glued to the panels. The outside fiberglass panel had a foil facing for water resistance. A detailed schematic is presented in Appendix A. Panels damaged during shipment and initial handling, were repaired using silicone caulk. The use of aluminum pop rivets to attach additional panels was not completely effective, and thus additional bracing and modifications were made. A connecting duct between the furnace and the shell was assembled and pop riveted onto the shell. Commercial use would require a more rugged and more easily assembled shell. A 3.5 ft^3 (0.1 m^3) gas powered drum mixer was used for grouting operations.

Procedure

The method of impregnating the concrete with calcium nitrite involved driving the free water out of the concrete by heating the deck surface. In order to promote the ingress of calcium nitrite to the bar level, the bridge deck was grooved prior to drying. Grooves 3/4 in (19 mm) wide by 1 1/2 in (38.1 mm) deep were cut into the deck with a walk-behind concrete saw. The grooves were cut 3 in (76 mm) on center on lines of equal contour. A major concern during the heating and subsequent cooling process was the temperature gradient that existed throughout the slab. Instrumentation of the deck was critical for monitoring any

temperature gradients that might have developed, since the deck was being heated from one surface. Temperature monitoring capabilities were provided by a series of Type K and Type T TCs as described in the Equipment section. The thermocouples provided critical information on the depth of dry concrete and temperature gradients for the prevention of thermal cracking, especially during cooling.

Plots of the temperature of the concrete slab at various depth as a function of time are presented in Appendix A, Fig. A-6 through A-9. Furnace shutdown is marked on each plot to delineate between the heating and cooling cycles of the test. Temperatures ranged from over 400°F (204°C) next to the duct from the furnace to 230°F (110°C) at the far end of the shell prior to furnace shutdown. The temperature differences between the various locations within the test area dropped dramatically after 1 hour of cooling. The differential was less than 100°F (38°C) versus over 200°F (76°C) prior to furnace shutdown. After 8 hours of cooling, the temperature differential was only 20°F (11°C). Temperatures at 2 in (51 mm) and 4 in (102 mm) depth of the concrete slab are presented in Fig. A-7 and A-8, Appendix A.

The boiling point was reached at 2 in (51 mm) depth except at the far end of the slab and was reached at the 4 in (102 mm) depth for the center region of the slab. A temperature profile of center region of the slab, with surface, 2 in (51 mm) depth, and 4 in (102 mm) depth is presented in Fig. A-9, Appendix A. During the heating cycle, the concrete at any appreciable depth into the slab was at a relatively constant temperature, with little temperature difference between 2 in (51 mm) and 4 in (102 mm) depth. When the furnace was turned off and the cooling cycle began, within three hours the three temperatures varied by only 15°F (6°C). A large temperature gradient which could cause cracking during the cooling of the deck was avoided by judicious opening of vents and by extending the cooling period until the concrete was slightly above ambient temperatures.

After the deck had been cooled, the heating shell was removed. A wooden 2 in x 4 in (51 mm x 102 mm) dam for trapping any spilled or excess calcium nitrite solution was constructed around the test area and caulked along the concrete-wood interface. The 15% calcium nitrite solution was siphoned from the holding drum with a hose and poured into each of the grooves until the groove was full. The level of calcium nitrite solution was measured in the holding drum prior to application and after the grooves had been filled to estimate the amount applied to the deck. A few small cracks were noticed during the application of calcium nitrite, but it was not known whether these cracks were a result of heating the deck, since a survey of any existing cracks prior to heating had not been done. However, before heating there were several areas of deck delamination due to corrosion in the test section. The deck was then covered with a polyethylene tarp to prevent evaporation of the calcium nitrite solution.

The calcium nitrite solution was ponded for 24 hours. At the end of the 24 hour period, the tarp was removed. An inspection of the underside of the bridge deck slab revealed two small cracks that had leaked some calcium nitrite. The amount of calcium nitrite which leaked

through the cracks was very small, certainly less than 1 quart (0.94 ℓ). The calcium nitrite was then removed from the grooves with a wet-dry shop vacuum.

The 15% calcium nitrite ponded volume was 31.67 gallons (119 ℓ). The recovered product was 10.59 gallons (40 ℓ). Therefore, approximately 20.8 gallons (78.5 ℓ) was absorbed by the deck. This is equivalent to 10.4 gallons (39 ℓ) of 30% calcium nitrite which is the nominal composition of a commercial admixture, DCI Corrosion Inhibitor". Typically, 4 gallons/yd^3 (20 l/m^3) of 30% calcium nitrite is added to protect against 13 lb/yd^3 (7.8 kg/m^3) of ingressed chloride at the reinforcement level (27). The calculated dosages based upon the above absorption are 10.5 gallons/yd^3 (52 ℓ/m^3) if penetration was to the 2 in (5 cm) level and 5.3 gallons/yd^3 (26.2 ℓ/m^3) if penetration was to the 4 in (10 cm) level.

The treated deck was rinsed down with water using burlap as an applicator, in preparation for filling the grooves of the treated area with a calcium nitrite-rich, latex- modified grout. The purpose of the grout was twofold: to prevent diffusion of the calcium nitrite out of the concrete to a region of lower concentration (the higher concentration of calcium nitrite and the lowered permeability of the latex modified grout would counteract the tendency of the calcium nitrite to diffuse out of the treated concrete); and to return the treated deck section to an acceptable riding surface.

The calcium nitrite-latex-modified grout was mixed using a 3.5 ft^3 (0.1 m^3) gas powered drum mixer. Mixture proportions are presented in Table 3.2. Ice and a large quantity of retarder was required to prevent flash set, and more importantly, to preserve initial workability until the grout could be squeezed into the grooves. The retarder used was Daratard-HC", at an addition rate of 10 oz/cwt of cement (38 mL/m^3). This was required even with the use of neutral set calcium nitrite (at normal addition rates), DCI-S Corrosion Inhibitor". The addition rate of latex (DOW Chemical [48% solids]) at 15% s/s (latex solids to cement solids weight ratio) cement was responsible for a smooth, pourable, but homogeneous grout which was ideal for application with a squeegee. Mix #3 had a reduction in latex content (11% s/s) because the supply ran out, and the reduction in latex was reflected in the reduced workability of mix #3.

Wet burlap was applied to the deck after the application of the grout. The burlap was covered with a polyethylene tarp and allowed to wet cure for 24 hours.

Visual Inspection and Delamination Survey

In January 1991, approximately 6 months after treatment, a visual inspection of the treated and control areas of the bridge deck showed the deck to be in excellent condition. Some flaking of the excess latex grout between the grooves in the treated area was observed. No delaminations were located in the treated area at that time. One small delamination, 0.3 ft^2 (0.03 m^2) was detected in the control section.

In July 1991, a visual inspection and delamination survey located delaminations in both the

treated and the control sections of the deck. The total sum of delaminated area was 7.5 ft^2 (0.70 m^2) in the treated section and 7.1 ft^2 (0.66 m^2) in the control section. This represents 4.7% and 3.5% of their respective areas. All delaminated areas were located in the breakdown lane within 3 ft (0.9 m) of the parapet. A cover depth survey showed the mean cover depth to be 2.2 in (56 mm) with a standard deviation of 0.33 in (8.4 mm) based on 80 observations.

Table 3.2 Calcium Nitrite Grout Mixes Used To Fill Grooves in Deck

MIX #	CEMENT (lbs/yd^3)	FINE AGGREGATE (lbs/yd^3)	LATEX (DOW) @ 48% solids (lbs/yd^3)	DCI-S @ 35% solids (lbs/yd^3)	Daratard-HC oz/cwt (lbs/yd^3)	Water (ICE) (lbs/yd^3)
1	816	2465	252 (15% s/s cement)	109 (5% s/s cement)	10 (0.3% s/s cement)	85.2
2	816	2465	252 (15% s/s cement)	109 (5% s/s cement)	10 (0.3% s/s cement)	85.2
3	816	2455	180 (11% s/s cement)	109 (5% s/s cement)	10 (0.3% s/s cement)	121.2

Note: 1 lb/yd^3 = 0.593 Kg/m^3

In July 1992, a visual inspection and delamination survey indicated a growth of the delaminated areas. The total area sum was 8.8 ft^2 (0.82 m^2) for the treated section and 8.6 ft^2 (0.80 m^2) for the control section, representing 5.5% and 4.4% of the the areas sections, respectively. The additional delaminated area resulted from the growth of delaminations identified previously.

Chloride Contamination Levels

In July 1992, powdered samples for chloride analysis were taken at mean depths of 0.5, 1.0, 1.5, 2.0, and 2.5 in (13, 25, 38, 51, and 70 mm). Twenty powdered samples were collected, 10 each in the treated and control sections. The results are reported in Table 3.3.

Both samples from the treated area were greater than 1.2 lbs chloride/yd^3 (0.7 Kg/m^3) of concrete at the bar level. In the control section, sample A4 was significantly greater than the corrosion initiation level at the bar level while E24 was less than the corrosion initiation level. The degree of variance of the 2 samples in the control section probably results from

their location, sample A4 was taken within 2 ft (0.6 m) of the parapet, while sample E24 was taken 10 ft (3.0 m) from the parapet.

In January 1991, three 4 in (102 mm) cores were obtained from the treated section. The chloride and nitrite contents of the cores were analyzed by W. R. Grace as a function of depth. The results are reported in Table 3.4.

Table 3.3 Chloride Contents In The Treated and Control Sections

	Chloride Content (lb/yd^3)			
	Treated Section Locations		Control Section Locations	
Depth (in)	A26	B14	A4	E24
0.5	4.5	5.3	15.2	8.4
1.0	4.2	3.8	18.7	1.8
1.5	2.8	2.9	16.0	0.4
2.0	2.1	1.8	12.3	0.2
2.5	2.0	1.6	8.0	0.3

Note: 1 lb/yd^3 = 0.593 Kg/m^3
1 in = 25.4 mm

Table 3.4 Chloride and Nitrite Analyses

	Cl^- Content (lb/yd^3), NO_2 (gal/yd^3) of 30% Solution*					
Depth (in)	Core A Southwest Corner		Core B Center		Core C Northeast Corner	
	Cl^-	NO_2	Cl^-	NO_2	Cl^-	NO_2
0-0.5	6.1	6.0	2.2	9.4	3.5	7.3
0.5-1.0	6.0	5.5	3.8	8.9	0.7	10.5
1.0-1.5	3.5	6.2	1.6	10.5	0.4	12.6
1.5-2.0	4.3	2.5	2.0	5.3	1.0	8.0
2.0-2.5	3.0	2.1	1.5	6.6	0.9	8.0
2.5-3.0	3.7	1.9	1.5	6.8	0.8	9.3
3.0-3.5	2.6	0.9	1.1	3.9	0.8	9.6

Note: 1 lb/yd^3 = 0.593 Kg/m^3
1 in = 25.4 mm
1 gal/yd^3 = 5.0 ℓ/m^3
There are 2.25 pounds of nitrite in a gallon of 30% calcium nitrite solution.

Research conducted by Berke et al., (27), suggested that for inhibition to occur, the chloride:nitrite ratio must be less than 2. The average nitrite content at the bar level, 2.0-2.5 in (51-64 mm) was 11.6 lbs NO_2/yd^3 (7.0 kg/m^3), and the minimum measured nitrite content 4.7 lbs NO_2/yd^3 (2.8 kg/m^3). Therefore, inhibition should occur at chloride contents up to 23.2 lbs Cl^-/yd^3 (13.9 kg/m^3), based on the average nitrite content at the bar level. All of the pre-treatment chloride contents were below this level.

Corrosion Potentials

Corrosion potentials were measured with a CSE in accordance with ASTM 876-87 (24). Potential surveys were conducted in March 1990 prior to treatment, in January 1991, July 1991, and July 1992. The means, standard deviations, and number of observations for the pre-treatment and post-treatment potential surveys are presented in Table 3.5.

The mean potentials for both the treated and control sections fall into the uncertain range of corrosion activity, -200 to -350 millivolts. The mean potential for the treated section increased slightly and the standard deviation decreased after treatment, indicating that the number of potential measurements more negative than -350 millivolts decreased.

Corrosion Current

Corrosion current density measurements were taken in both the treated and control areas in March 1990 prior to treatment and in January 1991, July 1991, and July 1992. The 3LP device was used to take measurements during all 4 surveys. In addition to the 3LP, the Gecor device was used in the surveys conducted in July of 1991 and 1992. Table 3.6 and 3.7 presents the means, standard deviations, and number of observations for the 3LP and Gecor corrosion i_{corr} measurements, respectively.

Table 3.5 CSE Corrosion Potentials

Measurement Date	Treated			Untreated		
	Mean (-mV)	STD (-mV)	n	Mean (-mV)	STD (-mV)	n
Pre-Treatment						
March, 1990	209	139	24	232	100	4
Post-Treatment						
January, 1991	273	49	24	222	95	4
July, 1991	285	62	24	299	58	4
July, 1992	273	53	44	245	87	29

The 3LP i_{corr} measurements for both the treated and the control section showed little change after treatment. Clear (22) suggested that for corrosion current densities from 1.0 to 10.0

mA/ft^2 (1.1 to 10.8 $\mu A/m^2$), corrosion related damage would be expected in 2-10 years. The mean i_{corr} for both sections is within this range.

The Gecor mean corrosion increased in the treated section, after the initial measurements with the device. However, further surveys will be required to verify this trend and to make an accurate assessment of calcium nitrite as a corrosion inhibitor when applied with the grooving technique.

Conclusions

The ability to dry out a concrete bridge and successfully impregnate it with a known corrosion inhibitor was demonstrated. It appears to be a viable method of bridge rehabilitation that does not require the large-scale removal of sound concrete. The equipment employed is relatively nonsophisticated and can easily be scaled up to treat larger areas. However, cracked and delaminated areas would have to be repaired before the deck is impregnated.

Table 3.6 3LP Corrosion Current Measurements

Measurement Date	i_{corr}, (mA/ft^2) Treated			Untreated		
	Mean	STD	n	Mean	STD	n
Pre-Treatment						
March, 1990	2.48	2.71	8	2.51	3.20	3
Post-Treatment						
January, 1991	2.39	1.46	8	1.61	1.93	3
July, 1991	2.48	2.71	8	2.06	2.42	3
July, 1992	2.01	0.57	8	2.03	1.91	3

Table 3.7 Gecor Corrosion Current Measurements

Measurement Date	i_{corr}, (mA/ft^2) Treated			Untreated		
	Mean	STD	n	Mean	STD	n
Post-Treatment						
July, 1991	0.12	0.05	8	0.09	0.05	3
July, 1992	0.17	0.13	8	0.10	0.10	3

4

Calcium Nitrite Column Repair

Introduction

In July 1990, a 12 ft^2 (1.1 m^2) spalled area on the east pier, southern column of the structure which carries U. S. Route 460 westbound over VA Route 723 was repaired with a calcium nitrite-rich latex-modified concrete. In addition, a series of 1 in (25 mm) diameter holes were drilled in a 24 ft^2 (2.2 m^2) area surrounding the patch. These holes were backfilled with a calcium nitrite rich mortar, so that the inhibitor might migrate into the surrounding concrete to provide additional protection. Post-treatment evaluations were carried out on the treated and adjacent control areas in February 1991 and June 1991.

Equipment

Equipment necessary for the repair of the column with DCI latex concrete and grout was minimal in comparison to that needed for the bridge deck post treatment. A 3.5 ft^3 (0.1 m^3) gas powered drum mixer was utilized for mixing the concrete for the column repair. A plywood form was banded to the column for the concrete patch. A metal chute was used for placing the concrete at the top of the form into the patch. A small Hobart mixer was used to mix the grout. Other equipment required was a scale, batching pails, accurate liquid measuring containers such as measuring cups for admixture dispensing, and concrete/grout finishing tools.

Procedure

A series of 1 in (25 mm) diameter holes had been drilled in a 2 in (5.08 cm) grid pattern outside the spalled area, shown in Fig. 4.1, to the depth of the reinforcement. The area drilled represented an area with corrosion problems. A calcium nitrite rich grout was mixed

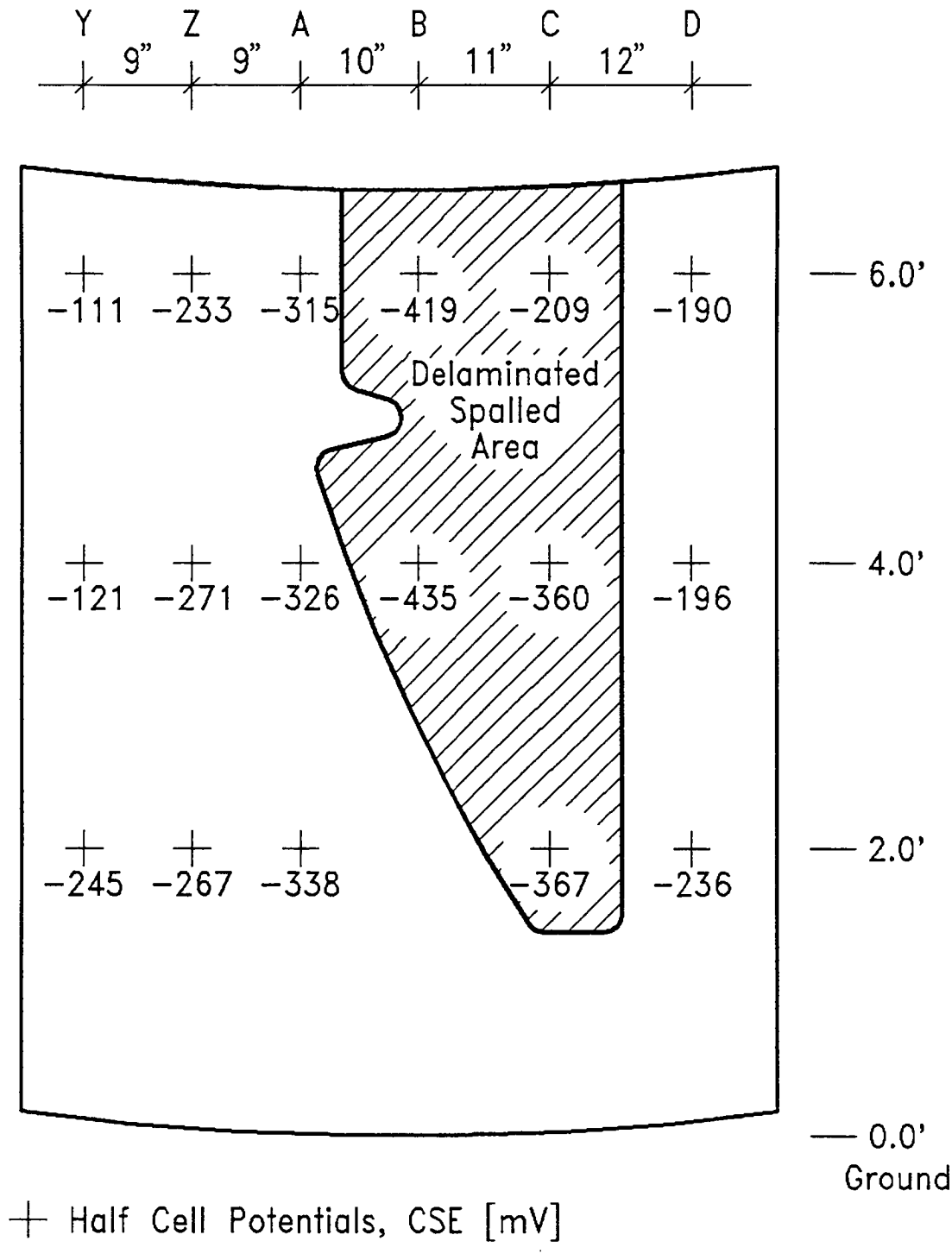

Fig. 4.1 Column Repair Area and Corrosion Potentials

to fill the holes. The mix was based on several trial mixes performed at W. R. Grace & Co. Mixture proportions are presented in Table 4.1. DCI-S Corrosion Inhibitor™, a neutral set corrosion inhibitor at normal dosage levels (2% s/s [calcium nitrite salt solids to cement solids ratio by weight]), was to be used at 7.5 times the normal dosage rate. Latex (DOW Chemical 48% solids) was used at 15% s/s cement. Requirements for the grout were that it had to have some workability but be stiff enough to remain in the drill holes. The first mix, with 15% latex was too fluid during the first 20 minutes after mixing.

For the second grout mix, the latex content was reduced to 10% s/s. The workability of this mix was better initially, but the mix rapidly hardened. Mix #1 exhibited the same behavior after 20 minutes, and not all of the grout could be used due to the accelerated rate of stiffening. The third mix was mixed by hand because the Hobart mixer had developed a mechanical problem. A latex addition rate of 12.5% s/s was used with some success. During this time, the sun had moved into position to shine on the column and exacerbate the stiffening problem. Mix #4 and #5 contained 15% s/s and 17.5% s/s latex, respectively. Latex addition was increased due to the increase in air temperature and the resultant loss of workability of the grout. A skim coat of mortar was placed over the hole pattern to prevent drying out of the grout and for cosmetic purposes.

A concrete mixture was proportioned and batched. The DCI-S Corrosion Inhibitor™ percent solid salt to cement solids (s/s) was 15%. The latex solids to cement solids (s/s) was 10%. Mixture proportions are presented in Table 4.2. Cement content for the mix was 758 pcy (455 kg/m^3), with a design w/c ratio of 0.38. A problem developed with the mixture; the mixture exhibited rapid stiffening and heat evolution and had to be discarded. Even with the addition of Daratard-HC™ (a retarder) at 5 oz/cy (19 mL/m^3), rapid hardening occurred at such a rate that some of the concrete had to be chipped out of the mixer.

A second concrete patch mix was batched with some modifications. DCI-S Corrosion Inhibitor" percent s/s was reduced to 10%, and the initial amount of retarder increased by a factor of 4 to 20 oz/cwt (15-75 mL/m^3). Ice was used for mix water, and the retarder, Daratard-HC was added to the mix water to be present at the start of hydration. During the mixing of the revised mix, additional retarder was added, 12 oz/cwt (45 mL/m^3), and two more points of water were required (final w/c = 0.40) to obtain the desired workability for the repair. The concrete had an estimated slump of approximately 8 in (20 cm), with no noticeable segregation. The concrete was then rapidly placed inside the form by the chute. The outside of the form was vibrated with a hand vibrator to facilitate consolidation of the concrete.

Table 4.1 Grout Mixes For The Column Repair

MIX #	CEMENT (lbs/yd^3)	FINE AGGREGATE (lbs/yd^3)	LATEX (DOW) @ 48% solids (lbs/yd^3)	DCI-S @ 35% solids (lbs/yd^3)
1	825	2475	256 (15% s/s cement)	274.5 (11.6% s/s cement)
2	874	2624	182 (10% s/s cement)	291 (11.6% s/s cement)
3	840	2549	225 (12.5% s/s cement)	283 (11.6% s/s cement)
4	811	2433	277 (16.7% s/s cement)	269 (11.6% s/s cement)
5	798	2393	264.7 (18.3% s/s cement)	265.5 (11.6% s/s cement)

Note: 1 lbs/yd^3 = 0.593 Kg/m^3
1 in = 25.4 mm

Table 4.2 Concrete Mixes Used In Column Repair

MIX #	CEMENT (lbs/yd^3)	COARSE AGG. (lbs/yd^3)	FINE AGG. (lbs/yd^3)	LATEX (DOW) @48% solids (lbs/yd^3)	DCI-S @ 35% solids (lbs/yd^3)	DARATARD-HC (oz/cwt)	WATER (ICE) (lbs/yd^3)
1	758 (w/c=0.38)	1500	1130 (10% s/s cement)	151 (15% s/s cement)	325 (0.16% s/s cement)	5	12
2	751 (w/c=0.40)	1487	1120 (10% s/s cement)	149.7 (10% s/s cement)	214 (1% s/s cement)	32	86.3

(aggregate absorption at 0.5%)
Note: 1 lbs/yd^3 = 0.593 Kg/m^3; 1 in = 25.4 mm; cwt = 100 lbs, 1 oz = 29.6 ml

Visual Inspection and Delamination Survey

In February 1991, a visual inspection of the column, including the patched area, suggested excellent performance. No delaminations were detected at that time.

In June 1992, a visual inspection of the column showed that a 0.2 ft^2 (0.02 m^2) area at the upper edge of the patch was beginning to delaminate. It was not possible to discern whether the delamination was the result of poor construction practice (feathered patch edges) or corrosion activity. A spall approximately 2 ft^2 (0.19 m^2) was observed at the top of the column directly above the patch (above the control area). The delamination survey detected a small delamination 0.4 ft^2 (0.04 m^2) in the plugged section surrounding the patch. It was not possible to obtain accurate cover depths due to the large bar diameters and the small bar spacing.

Chloride Contents

Table 4.3 presents the chloride contents for two positions on the column as a function of depth. As shown, the chloride content exceeded the corrosion threshold level at a cover depth greater than 2.5 in (6.35 cm). Chloride results for 2 positions in column 1 are presented in Table 4.3. The chloride contents were at the borderline for corrosion initiation at the 1.50 in (44 mm) depth. The corrosion potential analysis indicated that corrosion was not occurring since potentials were more noble than -100 mV (CSE), ASTM C876-87, (24).

Table 4.3 Chloride Content of Repaired Column, lbs/yd^3

DEPTH (IN)	COLUMN 1	COLUMN 2
0.5	2.4	3.3
1.0	2.1	1.9
1.5	1.7	1.7
2.0	--	1.4
2.5	--	1.6

Note: 1 in = 25.4 mm 1 lbs/yd^3 = 0.59 Kg/m^3

Corrosion Potentials

Corrosion half-cell potentials were measured with a CSE in May 1990 prior to treatment and in February 1991 and June 1992 after treatment. Table 4.4 presents the means, standard

deviations, and number of observations for all three surveys.

The mean corrosion potential in the patched area showed a 31% decrease after treatment and was accompanied by a substantial decrease in the standard deviation. Both post-treatment mean corrosion potentials are in the uncertain range of corrosion activity, indicating that the calcium nitrite was effective in reducing corrosion activity even though the concrete was only removed to the bar level. The mean potentials in both the plugged and control sections have remained relatively constant since treatment.

Corrosion Currents

Corrosion current density measurements were taken with the 3LP device in February 1991 and June 1992. No pre-treatment i_{corr} measurements were available. Table 4.5 presents the means, standard deviations, and number of observations for the two surveys.

Table 4.4 Southern Column, East Pier CSE Half-Cell Potential Readings

Date	Mean (-mV)	STD (-mV)	Number of Observations
Patched Section			
May, 1990	358	89	5
February. 1991	246	23	6
June, 1992	293	19	6
Plugged Section[1]			
May, 1990	237	74	12
February, 1991	226	55	12
June, 1992	227	103	12
Control Section			
February, 1991	188	100	17
June, 1992	205	112	17

[1] Plugged section refers to the area where holes were drilled and backfilled with calcium nitrite rich mortar.

Table 4.5 3LP Corrosion Current Measurements

Measurement Date	i_{corr}, (mA/ft^2) February, 1991			June, 1992		
	Mean	STD	n	Mean	STD	n
Patched Section	2.92	NA	2	1.59	1.39	3
Plugged Section	2.06	1.54	3	1.90	1.20	5

The mean i_{corr} value for the patched section decreased by 46% over a 16 month period. Corrosion damage would be expected in approximately 10 years based on this value (22). The mean i_{corr} value for the plugged section also decreased slightly, possibly due to the influence of the calcium nitrite plugs.

Conclusions

Due to the localized nature of corrosion attack on substructures, it is difficult and possibly misleading to compare the treated and control sections on the columns. However, the corrosion activity in the patched area appears to have decreased. Further monitoring, particularly corrosion currents, will be necessary to assess the effectiveness of the technique. The measured i_{corr} values may have been higher than the actual corrosion current density due to the difficulty in determining the area of polarization. This would be especially true as the corrosion current density decreased. The small delamination at the upper edge of the patch was alarming, but may have been the result of poor construction practice at the time of repair.

The practicality of using grouts and concretes with high inhibitor contents is somewhat questionable. Overall, the addition of calcium nitrite to concrete patches appears promising and deserves further investigation.

5

Laboratory Investigation of Polymer-Impregnated Concrete

Introduction

Deep impregnation (to depths greater than 3.0 in [76 mm]) of monomer into concrete and subsequent in-situ polymerization will abate corrosion and prevents its initiation. A deep grooving method for impregnating concrete was developed by Weyers and Cady, and its technical and economical feasibility was subsequently demonstrated (14). The polymerized monomer (polymer) fills most of the void spaces of the concrete. The chloride intrusion resistance and the encapsulation of the present chloride stop the flow of corrosion current and prevents the onset or continuation of any corrosive activity.

It has been estimated that about 90% of the voids in concrete are filled by the process of polymer impregnation (28). The factors which control monomer selection are familiarity with its use and its physical, chemical, fire hazard and health hazard properties. The best monomer system to impregnate concrete with is 90% methyl methacrylate (MMA), 10% trimethylolpropene trimethacrylate (TMPTMA), and 0.5% of the above monomer mix of azobisisobutyronitrile (Azo) (28). All of the above proportions are by weight. MMA is the monomer, TMPTMA is a cross linking agent, and Azo is the initiator.

This monomer system is distinguished from other monomer systems by its low viscosity and its rapid auto accelerating polymerization reaction. However, this monomer system is flammable, toxic and has an irritating odor.

The primary objective of this study was to evaluate the effectiveness of monomer impregnation as a possible method for arresting corrosion in chloride contaminated concrete

overlaid bridge deck. To achieve this, reinforced concrete specimens were cast simulating bridge deck conditions and tested under controlled conditions. Specimens were exposed to deicer solution until corrosion was initiated. For comparison, overlaid systems were cast: LMC, and LSDC. For impregnation, the deep grooving technique was applied. Five treatments were evaluated: three control treatments: LMC overlay, LSDC overlay, and polymer impregnation, and two rehabilitation treatments: impregnation of LMC overlaid specimens and impregnation of LSDC overlaid specimens. Control, non-treated, specimens were also cast.

The secondary objective of this study was to determine the optimum drying temperature of the concrete prior to monomer impregnation. This may reduce drying time and energy usage and may substantially reduce impregnation costs. In order to accomplish this task, mortar cubes were cast, polymer impregnated at different temperatures and observed using a Scanning Electron Microscope (SEM) and a Mercury Porsimeter. Comparison cubes were subjected to chloride ponding-drying cycles and the chloride content of powdered samples was measured to determine the effectiveness of polymer-impregnated concrete in reducing the ingress of chloride ions. To validate the hypothesis, several specimens with actively corroding rebars, were impregnated after being dried at a relatively lower temperature.

Experimental Design

Specimen Preparation and Corrosion Initiation

To simulate bridge deck conditions, laboratory reinforced concrete specimens were cast. Eighteen specimens were cast with two triads of rebars in each specimen. Each specimen was 12 in (305 mm) long and 10 3/8 in (264 mm) wide, see Fig. 5.1. Each triad consisted of one top rebar and two rebars equidistant from the top rebar at the bottom, thus forming an isosceles triangle. The bottom rebars were 1 1/4 in (38 mm) from the bottom of the specimens. The rebars were placed along the width of the specimen. They were approximately 11 7/8 in (302 mm) long, such that they extended about 3/4 in (19 mm) beyond the two ends of the specimens. The rebars used were #4 (ASTM specifications A 615) with a 1/2 in (13 mm) nominal diameter. The overall height of the specimens was 4 in (102 mm). The top cover depth was usually 1 in (25 mm).

The forms for the specimens were 3/4 in (19 mm) plywood A-C exterior grade and fastened by 2 in (51 mm) #8 dry wall screws. To accomodate the thermocouple wires, plexiglass spacers (3/4 in x 1/4 in [19 mm x 6 mm]) were used on one side of the forms, two spacers per form. Holes with 5/8 in (16 mm) diameter were drilled in the forms to accommodate the rebars with adequate clearance.

Rebars were cut to size, drilled and tapped at one end to a depth of 5/8 in (16 mm) to accommodate 1/8 in (3 mm) diameter screws. In order to minimize the effects of manufacturing oil and existing rust on the rebars, the rebars were cleaned by soaking them in a hexane solution for about 20 minutes and then wiped clean. The rebars were then dried in

the oven at 240° F (116° C) for 10 minutes. To prevent corrosion from taking place at the exposed ends, the two ends were covered with electroplating tape such that the uncovered length of each rebar was known and hence corrosion currents could be normalized to a square foot (square meter) of surface area of the rebar. To prevent concrete from adhering to the wooden forms, the forms were painted with two coats of form oil.

A type T TC was taped at the bottom center point of each top right hand rebar of each specimen. Type T plugs were attached to the other ends. The rebars along with the TC wire and spacers were assembled in each form in an inverted configuration to minimize consolidation (subsidence) cracking.

Five treatment methods were used and one set of control specimens was not subjected to any treatment. Triplicate specimens were cast for each treatment and for the controls. Therefore, a total of 18 specimens were cast. The two-letter codes assigned to each group were as follows:

- CO: Specimens acted as controls, untreated,
- LM: Specimens overlaid with LMC,
- LS: Specimens overlaid with LSDC,
- PC: Specimens polymer impregnated,
- PM: Specimens overlaid with LMC and polymer impregnated, and
- PS: Specimens overlaid with LSDC and polymer impregnated.

Concrete was then placed; mixture proportions and aggregate properties are presented in Table B.1, Appendix B. The forms were removed after 24 hours of moist curing. Because the specimens were cast inverted, the surfaces were cleaned to remove any possible oil contamination with muriatic acid (diluted hydrochloric acid).

The sides were coated with epoxy to prevent moisture loss and salt ingress from the sides. Plexiglass dikes 1 in (25 mm) high and 5/16 in (8 mm) thick were fixed to the top of each specimen using silicon rubber. Glass covers were used on the specimens to minimize moisture loss during wet cycles. A resistor of 100 Ω was connected between the top rebar and the bottom right rebar of each triad. A jumper cable was fitted between the two bottom rebars of each triad, resulting in a macro-cell cathode-to-anode area of 2.

Prior to the first wet cycle, potential and temperature readings were taken. Temperature readings were measured by a digital type T TC meter. Potential readings were taken with a CSE in accordance with ASTM C-876 (24).

The 3LP was used to monitor the corrosion current density, i_{corr}. The corrosion current of metal is directly proportional to the corrosion rate (Faraday's 1st Law). The 3LP device impresses a current in the reverse direction and polarizes the corrosion current. A description of the test procedure and interpretation of the results are given in the 3LP manual (29), and are repeated here as an aid to the reader. Interpretation of the obtained corrosion current

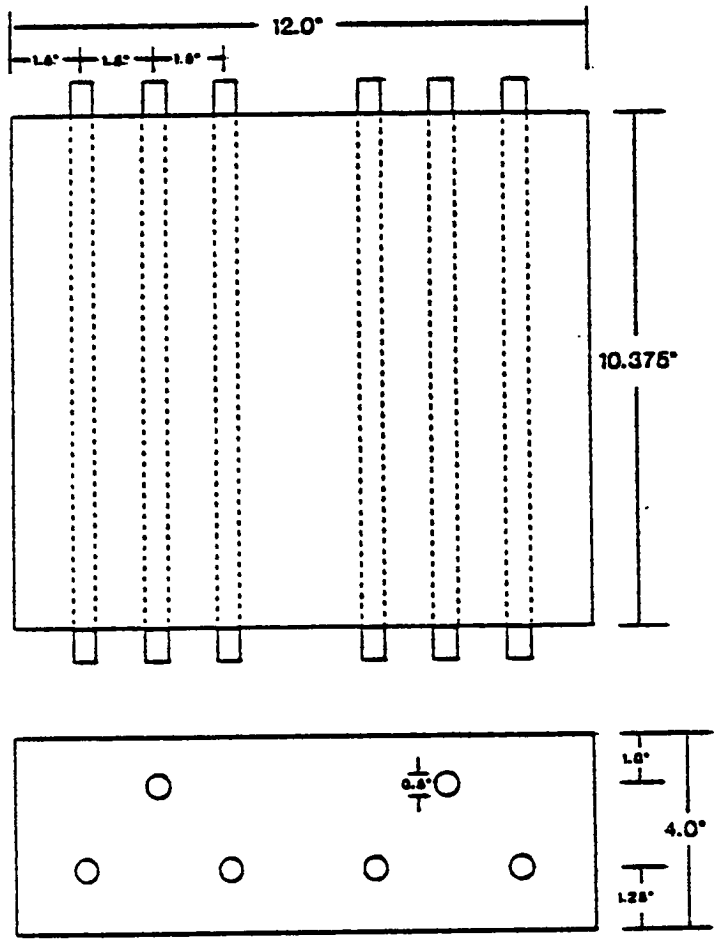

Fig. 5.1 Plan and Elevation of Specimens

density (i_{corr}) values is as follows:

- i_{corr} < 0.2 mA/ft^2 (2.2 μA/m^2) → no corrosion damage is expected.
- i_{corr} between 0.2 and 1.0 mA/ft^2 (2.2 and 10.8 μA/m^2) → corrosion damage is possible in 10 to 15 years.
- i_{corr} between 1.0 and 10 mA/ft^2 (10.8 μA/m^2 and 108 μA/m^2) → corrosion damage is expected in 2 to 10 years.
- i_{corr} > 10 mA/ft^2 (10.8 μA/m^2) → corrosion damage is expected in 2 years or less.

Five days after the concrete was placed, the first wet cycle was started. A 6% (by weight) sodium chloride solution was used as the wet cycle ponding solution. The wet cycle duration was 3 days. At the end of that period, the solution was removed from the specimens using a wet-dry shop vacuum. During the dry cycle the ambient temperature was raised to 120°F (49°C) using several infra-red lamps. The high temperature dried the concrete and made it moisture hungry to increase the penetration of chloride ions during the next wet cycle. The duration of the dry cycle was 4 days.

During the ponding period, chloride contents of selected specimens were determined at different depths using the a specific ion probe test method developed by James Instruments, Inc. (30). The results obtained by specific ion probe method were correlated to that obtained by the standard AASHTO test method, T-260-78 (31).

The literature indicates that several different values of chloride ion concentration have been suggested as a threshold value for the initiation of corrosion. The authors have considered the value of 1.2 lb/yd^3 (0.72 kg/m^3) of chloride ions in concrete as a requirement to initiate the corrosion (32,33).

Treatment activities were started when it was determined that there was active corrosion in most of the top rebars, all the potentials were more negative than -350 mV, the mean corrosion current density was 4.2 mA/ft^2 (4.5 μA/m^2) with most of the values being over 2 mA/ft^2 (2.2 μA/m^2), and the chloride contents at the rebar level of selected test specimens were greater than 1.2 lb/yd^3 (0.72 kg/m^3).

Impregnation Treatment Process

During the treatment processes, the salt water ponding of all 18 specimens was suspended. Twelve forms were made to accommodate the 2-in (51 mm) height overlay. LMC overlays were applied to the LM and PM series, while the LS and PS series were overlaid with LSDC. After the moist curing period (14 days), the sides of the overlays were coated with epoxy. The PC, PM and PS series specimens were grooved in preparation for monomer impregnation.

For all the specimens, the groove width was 0.75 in (19 mm) and 3.0 in (76 mm) on center. The grooving parameters, see Fig. 5.2, were determined in accordance with the procedure

developed by Weyers and Cady (14, 15). The number of grooves in each specimen was three. The depth of impregnation was 0.5 in (13 mm) below the top rebars and the groove depth was 0.5 in (13 mm) above the top rebars. Two depths of impregnation were involved. The specimens of the PC series had the original cover depth of 1 in (25 mm) and the final depth of monomer penetration was 2 in (51 mm). For these specimens, the depth of groove was 0.5 in (13 mm). The overlaid specimens (PM and PS series) had a cover depth of 3 in (76 mm), a groove depth of 2.5 in (64 mm), and the final depth of monomer penetration of 4 in (102 mm). A masonry saw was used to cut along the groove lines which had been marked with a permanent ink marker. Concrete between the lines was then chipped out with a masonary chisel.

The objective of deep monomer impregnation is to encapsulate the steel by impregnating the concrete to about a depth of 1/2 in (13 mm) below the top rebar level. A greater depth is not desired as impregnating the concrete further is redundant and the larger volume of monomer required becomes an unnecessary expense. Encapsulation of the top rebar results in isolating the anode and thus forcing electrical discontinuity between the cathode and anode, consequently decreasing the corrosion current.

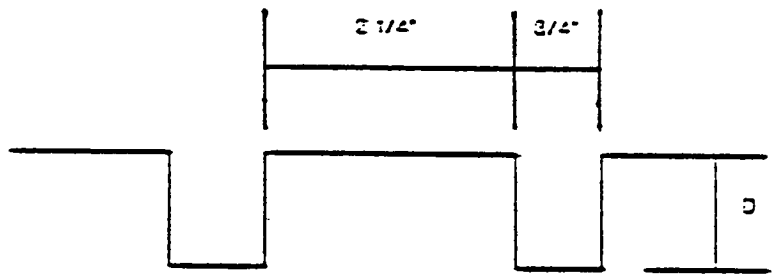

D = 1/2" for PC
D = 2 1/2" for PM and PS

Fig. 5.2 Groove Dimensions

A drying temperature of 230°F (110°C) at 0.5 in (13 mm) below top rebar was used. Monomer impregnation of concrete had been used successfully at this temperature (20). Three propane-fired infrared heaters, placed side by side, were used to dry the specimens. In order to monitor the temperature at a depth of 0.5 in (13 mm) below the top rebar level, high temperature type T TC wires were encased in ceramic tubing and inserted into a hole made in the bottom of the specimens to a depth such that the TC junction was 0.5 in (13 mm) below the top rebar. Nine specimens at a time were set up 9 in (23 cm) below the heaters.

Fiberglass insulation 3.5 in (89 mm) thick was wrapped around the specimens. The fiberglass was supported by a layer of sand and gravel. The specimens were insulated to prevent the entry of heat from the sides. The TC wires were insulated to enable the TC junction to measure the temperature at the proper location. A metal sheet with rectangular holes the same size as the specimen surfaces was placed over the specimens to assure that only the top surfaces of the specimens were exposed to the heaters. Two probes were used to record the shaded ambient temperature and the temperature at the specimen surfaces. Along with the nine specimens, three cylinders 4 in (102 mm) diameter and 8 in (203 mm) long cast from the same concrete mix were also dried. The three cylinders were dried to determine the rate of monomer impregnation through the concrete.

Temperatures were recorded at regular intervals after the heaters were turned on. After 70 minutes of heating, the internal temperatures of two specimens reached 230°F (110°C). Since the internal temperatures of the other seven specimens were substantially lower, the heaters could not be turned off. To remedy the situation, the two adequately dried specimens were covered with a metal sheet to prevent further heating of these specimens. The heaters were turned off at 150 min, when most of the specimens had the internal temperatures at the requisite value.

Because concrete acts as a heat sink, the internal temperatures of all the specimens continued to rise (between 5 and 10°F [5 and 6°C]) until a thermal equilibrium was established. Temperature measurements were taken for about five hours. The specimens were then covered with a layer of fiberglass insulation and left to cool for about 12 hours before impregnation was started. This time was needed to minimize the difference between the surface and internal temperature; the surface temperature had reached 529°F (296°C) when the heaters were turned off.

The ends of the grooves in the nine specimens were sealed with epoxy putty which does not dissolve in methyl methacrylate (MMA). The putty was also used to make 1 in (25 mm) high dikes on the three cylinders. The specimens and the cylinders were covered with plastic sheets. A slit was made in the middle of each plastic cover and covered by duct tape.

A mixture of 90% MMA and 10% TMPTMA was prepared by weight. Then 0.5% Azo, of the MMA and TMPTMA mixture, was added. The monomer was ponded on the top surface of the specimens and cylinders using a 20 ml pipette and placed through the slit in the plastic

cover. The slit was kept covered after the monomer was placed.

The three cylinders had impregnation times of 6, 14, and 23 hours. During that period more monomer was added as needed to assure the availability of monomer for transfer into the concrete. After the designated impregnation time for each cylinder was reached, the residual monomer was drawn off with pipette. The cylinders were then placed in a hot water bath for 4 hours at 185°F (85°C) for polymerization of the monomer. The cylinders were taken out of the bath and cut longitudinally in half using a masonry saw. The cut cylinders were then etched with muriatic acid. The acid etched all portions of the concrete except the impregnated area. Thus, the depth of impregnation of the cylinders could be visually distinguished.

The depth of monomer impregnation in concrete is a function of the square root of time of impregnation (28). Using this relation, the data obtained from the acid etching of the three cylinders indicated that the time corresponding to the required depth was 16 hours. Accordingly, the specimens were impregnated for a period of 16 hours using the same procedure. At the end of that period, the residual monomer was drawn off with a pipette and the specimens were polymerized in a water bath at 185°F (110°C) for 24 hours. The grooves in the PM and PS series were then filled with latex modified mortar (LMM). Application of salt solution was resumed with the same wet and dry cycles used before treatments. Post treatment potential and corrosion current density measurements were taken periodically.

Optimizing Drying Temperature

The objective of this part of the study is to investigate the possibility of using a lower drying temperature and to ascertain an optimum dry temperature of concrete prior to monomer impregnation.

In order to accomplish this task, mortar cubes were cast, monomer impregnated at different temperatures, and observed using a Scanning Electron Microscope (SEM) and a Mercury Porosimeter. The cubes were subjected to chloride solution ponding-drying cycles and the chloride contents of powdered samples were measured to determine the effectiveness of polymer-impregnated concrete in reducing the ingress of chloride ions.

Forty-two 2 in (51 mm), mortar cubes were cast in accordance with ASTM C-109-90; the w/c ratio was 0.47 and the average compressive strength was 4450 psi (30.7 kPa). Fourteen sets of cubes were cast; each set consisted of three cubes: A, B, and C. Set 14 served as the control (CON). The cubes were moist cured for 30 days before air drying. Set 2 cubes were air dried at 75°F (24°C). Cubes in set 3 through 13 were oven dried at higher temperatures ranging from 100°F (38°C) to 600°F (316°C), each set at a specific temperature.

Each cube was fully dried at its designated drying temperature. A cube was considered fully

dry when the decrease in its original weight within a 24-hour period was less than 0.1% of its weight. All cubes were placed in an oven at the same time and the oven was set to the lowest drying temperature, 100°F (38°C). When set 3 cubes were fully dried, they were removed and placed in a desiccator to prevent any moisture absorption before monomer impregnation. The oven was then set at the next higher temperature, 125°F (52°C). This process continued until all cubes were dried.

At low temperatures, the cubes required a relatively longer time to dry, as water requires a longer time to evaporate at temperatures below the boiling temperature of water. It took 7 to 11 days to dry cubes at temperatures below 225°F (100°C). As the temperature increased, the required drying time decreased; the drying time for set 12 cubes was 48 hours, at 500°F (260°C).

The monomer was mixed in the same way as the one applied to the concrete blocks. The monomer impregnation was achieved in this case by submerging the cubes in the monomer for a period of five days. That period was considered sufficient to complete the monomer impregnation of the cubes (14).

After monomer impregnation, set 2 cubes, which were dried to an ambient temperature, showed random surface cracks. One cube had a small piece completely broken off. None of the other cubes which were dried to higher temperatures experienced any cracks. The same behavior was noticed at an earlier time during a feasibility investigation. Repeatability of this cracking phenomenon suggested some expansive physiochemical reaction between the pore water and the monomer.

For polymerization, each cube was individually wrapped in aluminum foil and each set of cubes was placed in water resistant plastic bags and immersed in a hot water bath at 185°F (85°C) for 24 hours. Aluminum foil and plastic bags were used to prevent the intrusion of water during the polymerization process. The cubes were then vacuum saturated and their moisture contents were determined.

Resistivity across opposite sides of each cube was estimated using Nilsson Soil Resistance Meter. The suggested criteria used for interpreting resistivity values are presented below (17,18):

- If resistivity exceeds 12,000 Ω-cm, corrosion is unlikely.
- If resistivity is between 5,000 Ω-cm and 12,000 Ω-cm, corrosion is probable.
- If resistivity is less than 5,000 Ω-cm, corrosion is almost certain.

A separate study on marine structures in California indicated that at resistivity values over 60,000 Ω-cm, no corrosion would occur; but corrosion has been detected below 60,000 Ω-cm (34). Other studies have suggested that corrosion is unlikely above 20,000 Ω-cm and active corrosion may occur at resistivities between 5,000 to 10,000 Ω-cm (35).

A masonry saw was used to cut sections from cube C of each set. Pore size characteristics were determined for one section using a mercury porosimeter. The total mercury intrusion volume was the volume of mercury which could be forced into the specimen per gram of the specimen weight under a maximum pressure of about 50,000 psi (345 MPa).

Chemical compositions were determined for the other section using a scanning electron microscope-energy dispersive X-ray spectroscope system (SEM-EDS). The evaluated sections, in both tests, were approximately 2 x 1 x 1 in (51 x 25 x 25 mm), the maximum size that can be accommodated in the mercury porosimeter. These sections were dried in an oven at 220°F (104°C) until their weight loss in a 24-hour period was less than 0.1% of the original weight before testing.

Although pore size distribution may be studied using other fluids and techniques, the mercury intrusion technique is still the most widely used to examine the pore size distribution of mortar samples. However, some limitations associated with this technique are well recognized. All pores are assumed to be cylindrical and accessible to mercury; although the pressure used is iso-static, breakage in the pore structure may occur; contact angle of surface tension will be different at different drying temperatures; and the volume of specimen relative to the volume of the penetrometer may slightly affect the results.

Cube A of each set was submerged in a 6% (by weight) sodium chloride solution for 3 days followed by 4 days of air drying. The wet and dry alternate cycles were continued for a period of 100 days. After that, resistivity values of the cubes were measured for a surface dry condition. Each cube was then cut in half with a masonry saw. From one half, a powdered mortar sample was extracted from a square 1/4 in (6.4 mm) wide at 1/4 in (6.4 mm) from the edge. Thus, the sampling depth was from 1/4 to 1/2 in (6.4 to 12.7 mm) from the specimen edge. The powdered samples were tested for chloride content using a CL-500 specific ion probe manufactured by James Instruments, Inc. (31).

The other half of each A cube was etched with muriatic acid. The acid was applied to a strip 1 in (25.4 mm) wide across the cube at its center, while the remaining portion of the cut surface was covered with duct tape.

Results of the drying temperature study, which will be discussed in the next section, suggested that a lower drying temperature than the one used for the treated overlay series blocks should be sufficient for effective monomer impregnation of concrete. To validate those results, twelve specimens were cast with the same dimensions and rebar configuration as the previous blocks, except for the cover depth. Six specimens had 2 in (51 mm) cover depth and the other 6 had a 3/4 in (19 mm) cover depth. Four specimens (two of each cover depth) were dried to 150°F (66°C) at 1/2 in (13 mm) below the top rebar level, while the other 4 specimens were dried to 180°F (82°C). The other 4 specimens (two of each cover depth) served as controls and were not impregnated.

Eight specimens were monomer impregnated, using the same procedure described earlier.

However, no grooves were cut in the specimens and the monomer was ponded on the top surface. From the cylinder results, the time of impregnation for the specimens with 2 in (51 mm) cover depth was 50 hours, and for the specimens with 3/4 in (19 mm) cover depth was 16 hours. After polymerization, potential and corrosion current density readings were taken.

Analysis of Results

Polymer Impregnation of Overlaid Specimens

To minimize the effect of temperature on potentials and corrosion current readings, all measurements were taken at 72°F (22°C). The potential values and the corresponding 3LP corrosion current values before and after treatments indicated that post-treatment potential values did not accurately reflect the corrosion activity in the specimens. While the corrosion current values in the treated specimens showed very little active corrosion, the corresponding potential values for most specimens were well above the 90% active corrosion region, more negative than -350 mV. The i_{corr} value is a more direct measure of corrosion activity than corrosion potential.

The results are presented in the categories based on treatments: the first group includes CO, LM, and PM specimens; the second group includes CO, LS, and PS specimens; and the third group includes CO and PC. Throughout this section, the first group will be referred to as the latex group, the second as the low slump group, and the third as the polymer-impregnated group.

The initial pre-treatment potential values ranged from about -225 mV to -260 mV, which is in the 90% no-corrosion region. During the first 50 days, the potential values became less negative indicating less corrosion activity, see Figs. B.1 through B.3 in Appendix B. A possible explanation is due to the formation of a passive layer of gamma iron oxide around the steel which protects the rebar from further corrosion activity.

After 50 days, more negative potential values were measured due to the destruction of the passive layer by the chlorides. At day 214, all specimens had potential values more negative than -350 mV, which is in the 90% active-corrosion region.

Chloride contents were measured in selected specimens on days 71 and 190. At day 190, the chloride content at a depth of 1 to 1 1/2 in (25 to 38 mm), rebar level, for all the tested specimens were well over the generally accepted threshold level for corrosion initiation, 1.2 lb/yd^3 (0.7 kg/m^3).

The third method for monitoring the degree of corrosion was the i_{corr} values obtained by the 3LP device. The mean of six readings were used for evaluation. The mean i_{corr} values at day 214 were over 2 mA/ft^2 (21.5 mA/m^2) for all 6 series of specimens except the LMC overlay specimens.

The specimens were prepared for the different treatments after day 214. It took about 33 days to complete the entire treatment process, the corrosion activity most likely increased during that period. The mean post-treatment potential values are presented in Figs. B.4 through B.6, Appendix B.

The mean values of the corrosion current density (see Figs. 5.3 through 5.5) indicated that the control specimens progressively corroded to extremely high levels with the passage of time, while the corrosion current densities of treated specimens decreased and did not fluctuate significantly over time.

To compare the effectiveness of the different treatment methods, the percent change in each post-treatment i_{corr} value was computed on the basis of the last pre-treatment value as follows:

$$\Delta = \{(B - P)/B\} \times 100 \qquad (5.1)$$

where,

Δ = percent change,
B = last pre-treatment i_{corr} in mA/ft^2, and
P = present i_{corr} in mA/ft^2.

Therefore, a positive "Δ" value indicates that corrosion current has decreased from its pre-treatment level, while a negative "Δ" value signifies a higher corrosion level compared to its pre-treatment value.

At day 181 after the application of the overlays, the control specimens (CO) had a "Δ" value of -223.4% demonstrating the extreme corrosion activity of the untreated specimens as shown in Figs. 5.6 through 5.8. The latex (LM and PM) and polymer impregnated (PC) groups demonstrated values of over +50% at day 181, as presented in Figs. 5.6 and 5.8, respectively. The low slump (LS and PS) group was well below +50% improvement level, as shown in Fig. 5.7. However, they remained in the positive range indicating that the treatments had the desired effect of reducing corrosion levels. The low slump overlay specimens had a value of +22.7% while the low slump overlay with polymer impregnation had a slightly higher value of +36.2%. However, at 41 days after overlays, all treated specimens, except for the polymer-impregnated specimens, had negative "Δ" values. A possible explanation is that a time lag is required before the overlays cause a decrease in the corrosion current densities.

The absolute difference in the "Δ" between the last and first values may be a useful measure of the effectiveness of each treatment procedure. Table 5.1 summarizes this relationship. The maximum value of this measure was 91.03% for the LSDC specimens and the minimum value was 42.30% for the polymer-impregnated specimens with no well defined trend between the 3 groups. This indicates that there was no appreciable difference in the effectiveness of any treatment method. The specimens with only overlays demonstrated higher values than polymer-impregnated overlays. This suggests that impregnation may decrease the effectiveness of the overlays in abating corrosion.

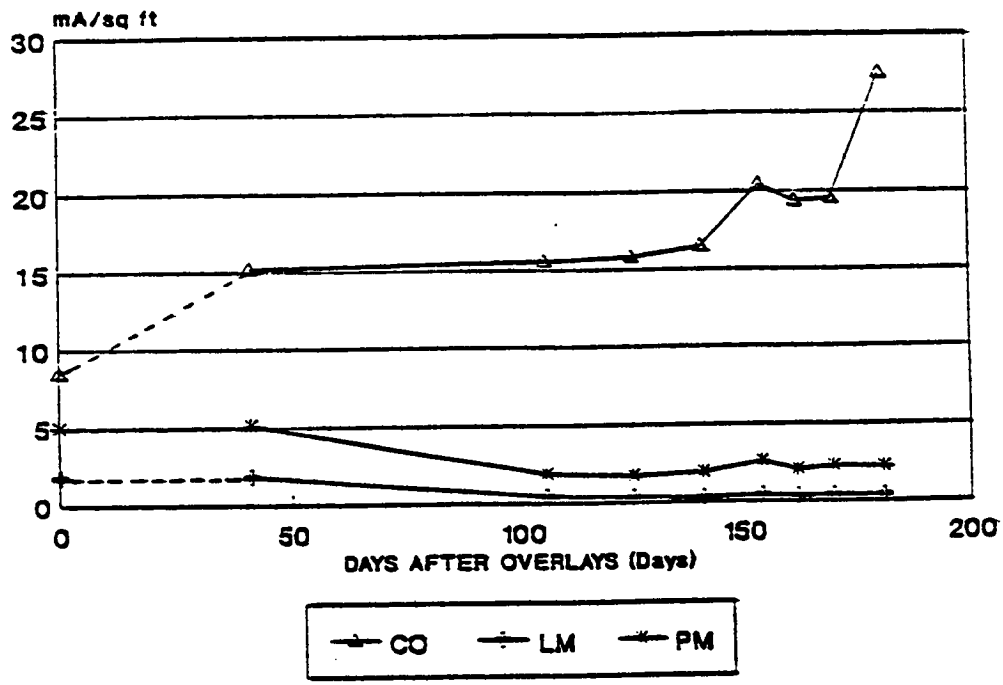

Fig. 5.3 Post-Treatment Mean i_{corr}, Latex Group

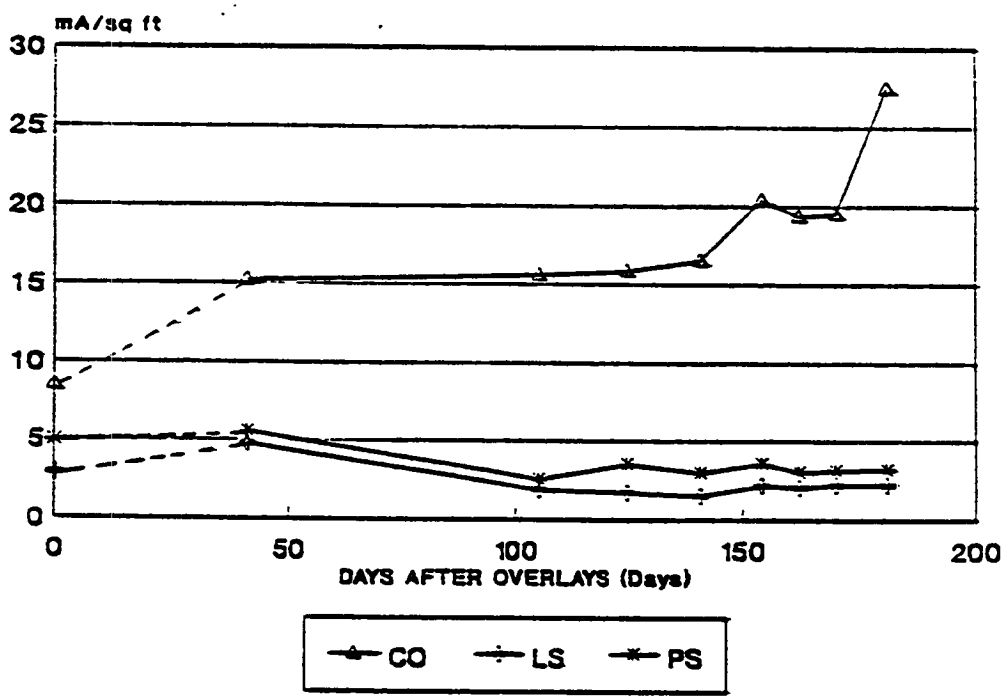

Fig. 5.4 Post-Treatment Mean i_{corr}, Low Slump Group

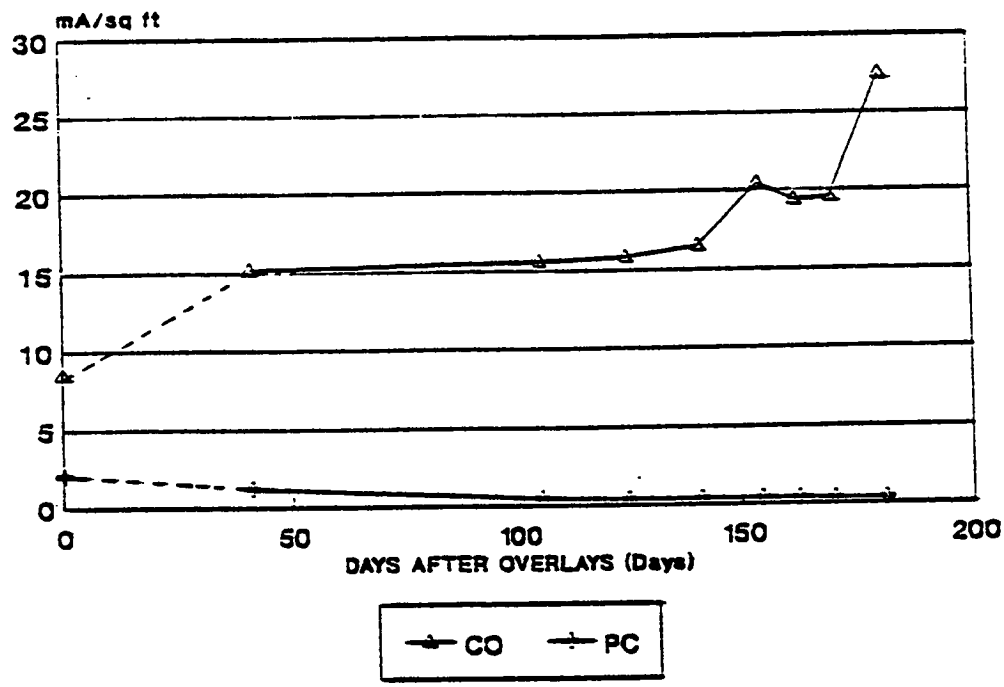

Fig. 5.5 Post-Treatment Mean i_{corr}, Polymer Impregnated Group

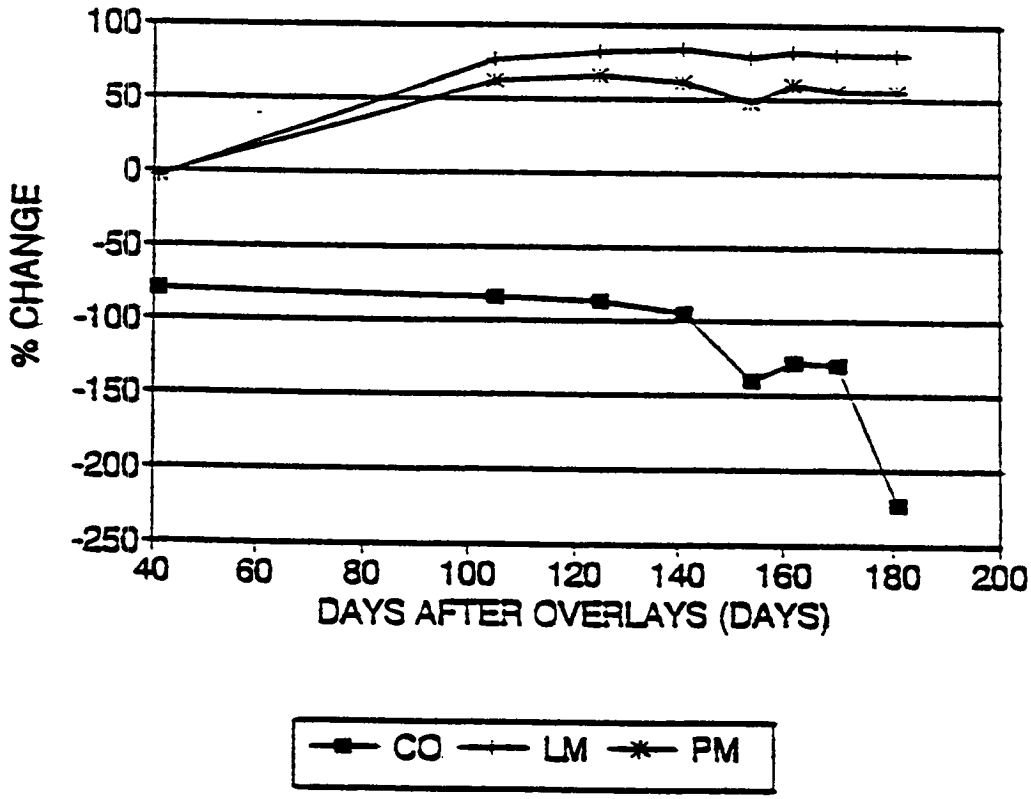

Fig. 5.6 Percent Change in Mean i_{corr}, Latex Group

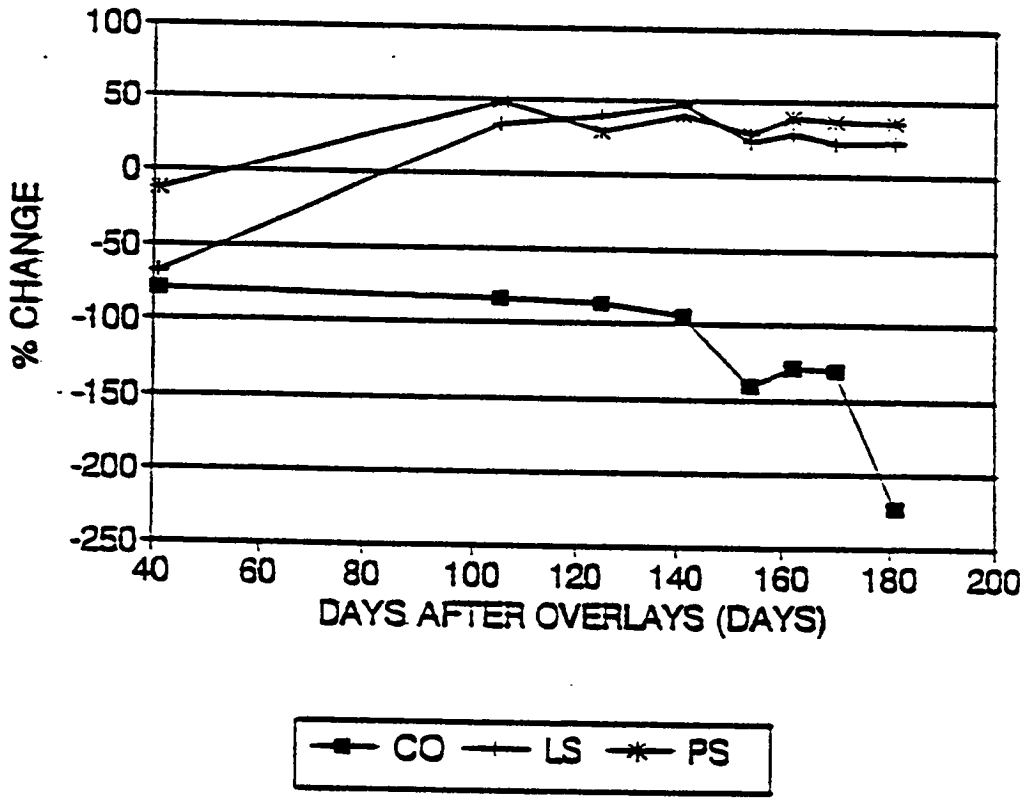

Fig. 5.7 Percent Change in Mean i_{corr}, Low Slump Group

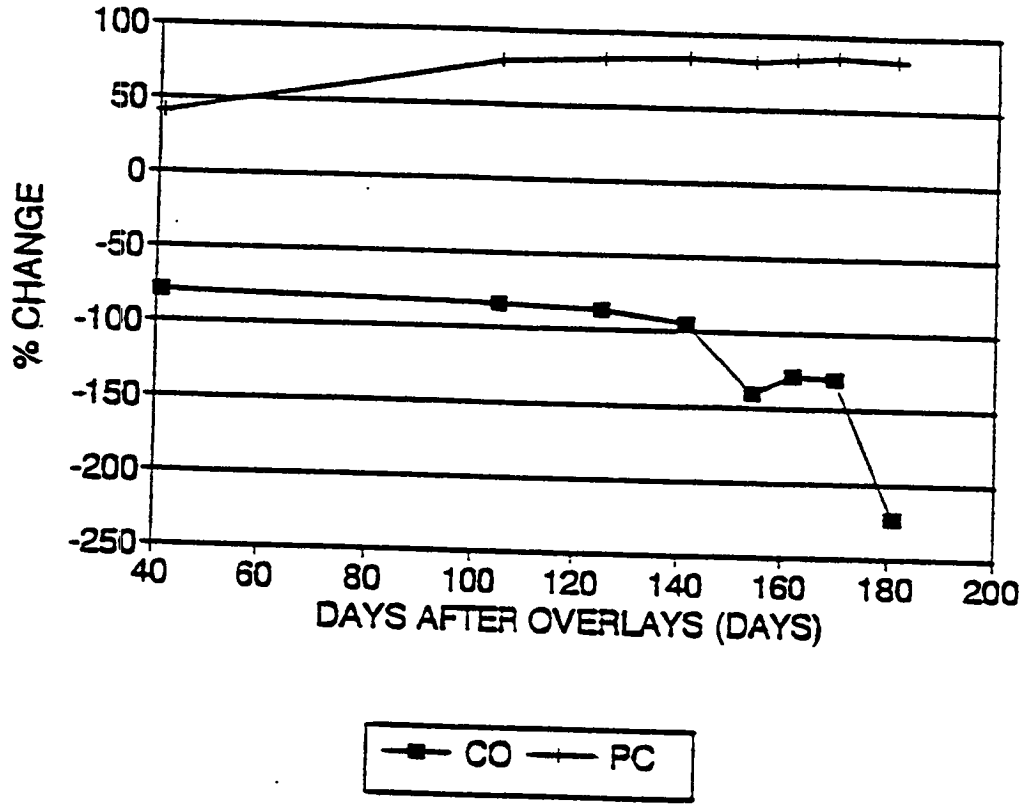

Fig. 5.8 Percent Change in Mean i_{corr}, Polymer Impregnated Group

Table 5.1 Treatment Effectiveness

SPECIMEN	LAST PRE-TREATMENT I_{corr} (mA/sq ft)	% CHANGE AT DAY 41	% CHANGE AT DAY 181	ABSOLUTE DIFFERENCE IN % CHANGE
Latex Group				
LM	1.76	-3.37	+79.85	83.22
PM	4.99	-2.89	+55.84	58.73
Low Slump Group				
LS	2.82	-68.35	+22.68	91.03
PS	4.92	-12.55	+36.19	48.74
Polymer Impregnated Group				
PC	2.07	+41.73	+84.03	42.30

However, it was found that in the series with both overlays and monomer impregnation, the PM series (LMC overlaid-polymer impregnated) and the PS series (LSDC overlaid-polymer impregnated) had the highest pre-treatment corrosion currents of 4.99 mA/ft^2 (5.35 $\mu A/m^2$) and 4.92 mA/ft^2 (5.34 $\mu A/m^2$), respectively. It is conceivable that the higher corrosion current densities had an effect on the "absolute difference in "Δ" values. It is reasonable to expect that any treatment method would be more effective if the initial corrosion current density is low.

By comparing the actual "Δ" values, the low slump group appears to be less effective than the other two groups. However, this measure might not be a very accurate representation of the situation, since it does not indicate the "degree" of the "Δ".

The values of the "Δ" at day 41 (see Table 5.1) indicate that the low slump group had been least effective in abating corrosion at this age. The specimens which had been overlaid with LSDC (LS) had an unusually high negative "Δ" value, -68.35%, compared to the control specimens "Δ" values at the same time, -79.47%. The much lower negative "Δ" value (-12.55%) of the specimens with LSDC overlaid-polymer impregnation (PS) could probably be attributed to the polymer impregnation. However, this value for the PS series was more negative than for the other groups. The higher pre-treatment corrosion current densities could not be considered as a possible cause, since the specimens with LMC overlaid-polymer impregnation (PM) also had similar high pre-treatment corrosion current densities. In the case of the PM series, the "Δ" at day 41 was -2.89% which was comparable to the -3.37% value for the LMC overlaid specimens (LM).

A possible explanation for the apparently lower effectiveness of the low slump group is that the low slump mixture design for the LSDC overlay resulted in an imperfect compaction after the overlay was placed. The LSDC overlay had a rough surface which suggests the presence of more void spaces resulting in increased permeability for more rapid progress of chloride ions after treatment.

Drying Temperature Optimization

The impregnation results of this part of the study are presented in Table 5.2. The amount of water loss increased as drying temperature increased. The volume of impregnated monomer was 20% at 75°F (24°C) and 10.5% at 100°F (30°C). The volume of impregnated monomer was 8.8% at 125°F (52°C) and it increased at higher drying temperatures up to 400°F (204°C) above which it remained constant at 10.3%, see Fig. 5.10.

The cubes at 75°F (24°C) were visibly cracked after the monomer impregnation and the high monomer content was most likely due to direct physical entry of some monomer into the cracked cubes rather than entry by capillary flow. Although cubes dried at 100°F (38°C) were not visibly cracked, the anomaly in the monomer content might be due to direct entry of monomer via micro-cracks invisible to the naked eye. These cracks may be caused by the shrinking of hydrated material while the unhydrated particles act as inclusion in the paste, restraining it from shrinking freely.

The difference in volume between water lost and monomer gained increased with drying temperature. Thus, at higher drying temperatures, water-accessible voids were not being refilled with monomer. A possible explanation is that the monomer molecules, large organic molecules, were filling voids only above a certain limiting size, and void sizes below that limit could not be filled with the large monomer molecules (molecular weight of Azo = 164, MMA = 98, and TMPTMA = 311). Another explanation may be the irrecoverable closure of smaller pores (39).

The moisture content values obtained after vacuum saturation of the cubes are presented in Fig. 5.11. The lowest value of moisture content was at a drying temperature of 200°F (93°C), above which the moisture content increased with increasing drying temperature. At temperatures below boiling point of water, the higher moisture contents are probably due to the result of remaining water after drying. At higher temperatures, the water could refill smaller voids which monomer could not fill. At 200°F (93°C), most available void spaces had been filled with monomer molecules, resulting in a low absorbed moisture content. The moisture contents of the control cubes (Set 14) were much higher (2.67%) than any of the impregnated cubes, as shown in Table 5.2. Thus, some degree of monomer impregnation is possible at low drying temperatures.

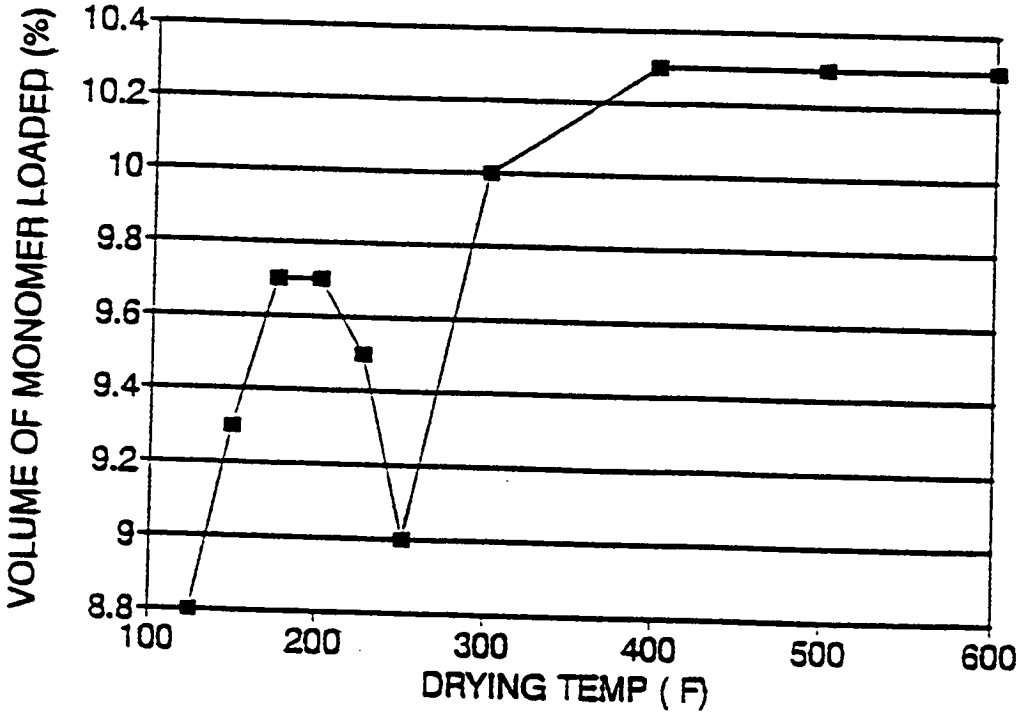

Fig. 5.9 Volume of Monomer Loaded vs Temperature

Table 5.2 Impregnation Results

DRYING TEMP (°F)	VOLUME OF WATER LOST DURING DRYING (%)	VOLUME OF MONOMER GAINED (%)	DIFFERENCE (%)	MOISTURE CONTENT AFTER VACUUM SATURATION (%)	RESISTIVITY BEFORE SALT APPLICATION (1000 ohm-cm)	RESISTIVITY AFTER SALT APPLICATION (1000 ohm-cm)	DIFFERENCE IN RESISTIVITY (1000 ohm-cm)	CHLORIDE CONTENT (lb/cu yd)
75	*	20.0*	*	*	*	*	*	*
100	13.2	10.5	2.7	0.75	406	13.2	392.8	0.61
125	14.0	8.8	5.2	0.70	401	12.5	388.5	0.66
150	15.5	9.3	6.2	0.85	350	13.2	336.8	0.65
175	15.3	9.7	5.6	0.70	654	20.7	633.3	0.65
200	16.0	9.7	6.3	0.37	793+	20.5	772.5	0.61
225	16.5	9.5	7.0	0.58	490	26.0	464.0	0.62
250	16.6	9.0	7.6	0.52	513	16.8	496.2	0.60
300	17.1	10.0	7.1	0.44	849	34.3	814.7	0.60
400	18.3	10.3	8.0	0.59	487	57.8	429.2	0.55
500	19.2	10.3	8.9	0.68	267	35.5	231.5	0.57
600	20.2	10.3	9.9	0.92	200	27.3	172.7	0.54
CONTROL	-	-	-	2.67	4.8	2.8	2.0	14.38

* CUBES FRACTURED DURING POLYMER IMPREGNATION

°F = 9/5 °C + 32

+ MEAN FROM TWO CUBES; THIRD CUBE HAD VERY HIGH VALUES

For the resistivity measurements, resistivity values before salt application showed peak values at drying temperature of 200°F (93°C) and 300°F (149°C) and then decreased at higher temperatures, as shown in Fig. 5.12. The lowest resistivity value was 200,000 Ω-cm. As noted previously, other studies suggested that no corrosion will occur above a resistivity interrange of 12,000 Ω-cm to 60,000 Ω-cm (17; 18; 34). Thus even if the most conservative value is used, the lowest resistivity value obtained was in the no-corrosion region.

Resistivity values followed a trend which supported the corresponding values of moisture content. Around 200°F (93°C), moisture content was the lowest and resistivity was near its peak. Since the ionic solution is a conducting agent, resistivity of concrete increases with decreasing moisture content.

Resistivity values after salt application were much lower than pre-salt application values (see Fig. 5.12). The trend after salt application was similar to that before salt application with respect to drying temperature. Apart from a large downward shift, there was apparently a slight shift to the right (an increase in the drying temperature).

Values of the post-salt application resistivity were low due to the Cl^- ions in the mortar pore water. The value corresponding to 200°F (93°C) was 20,500 Ω-cm, which is greater than the lowest suggested no-corrosion value of 12,000 Ω-cm, but less than the highest suggest value of 60,000 Ω-cm. However, the possibility remained that the surfaces of the cubes were not fully dry. Some micromolecular layers of salt water may have been absorbed on the surface when post-salt application resistivity values were taken, which could have reduced the values.

The results of the mercury porosimeter showed that at lower drying temperatures, the total mercury intrusion volume was high, as fewer voids were filled with polymer. At pre-impregnation drying temperatures of 200°F (93°C) and 225°F (107°C), there was an abrupt decrease in total intrusion volume. Thus, it appears that most of the available voids at these temperatures were filled with polymer (see Table 5.3). At higher temperatures, total intrusion volume increased. More void spaces were present which were too small for monomer molecules to occupy but large enough for mercury to enter. As expected, control cubes had more intrusion volume (0.0606 cc/g) than any of the impregnated cubes except for cubes dried at 175°F (79°C).

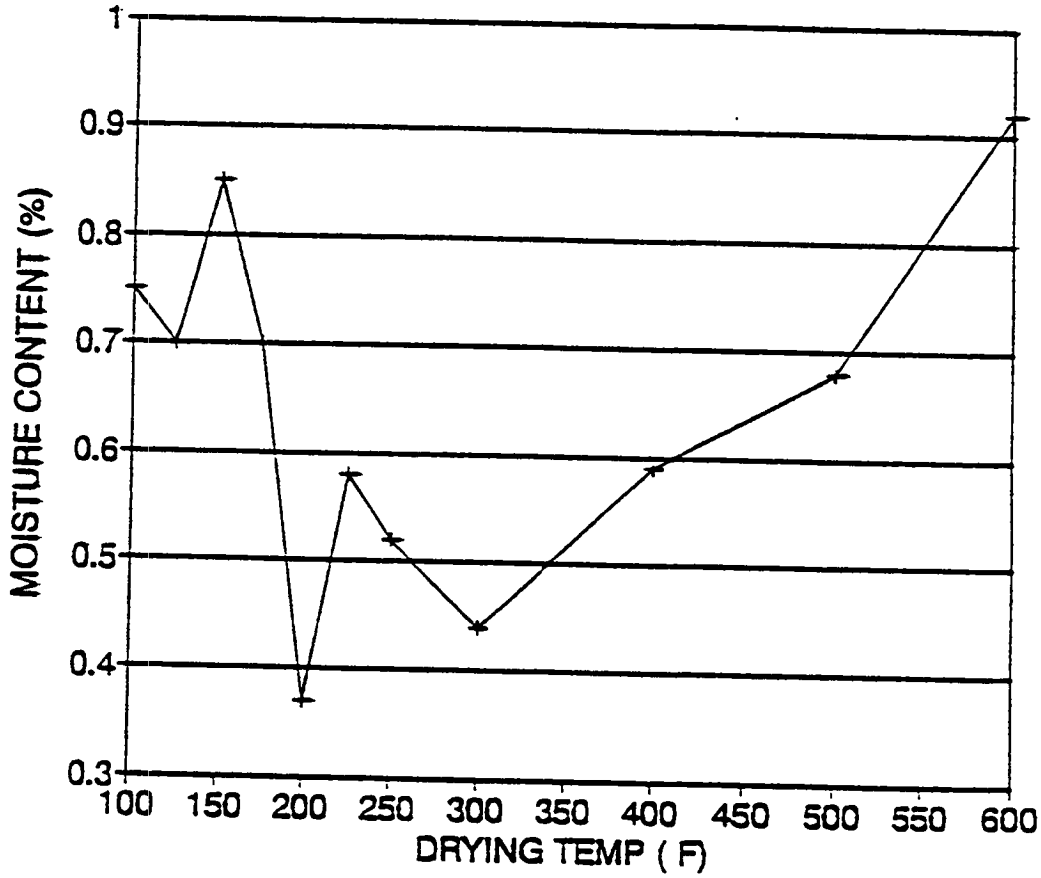

Fig. 5.10 Moisture Content vs Temperature

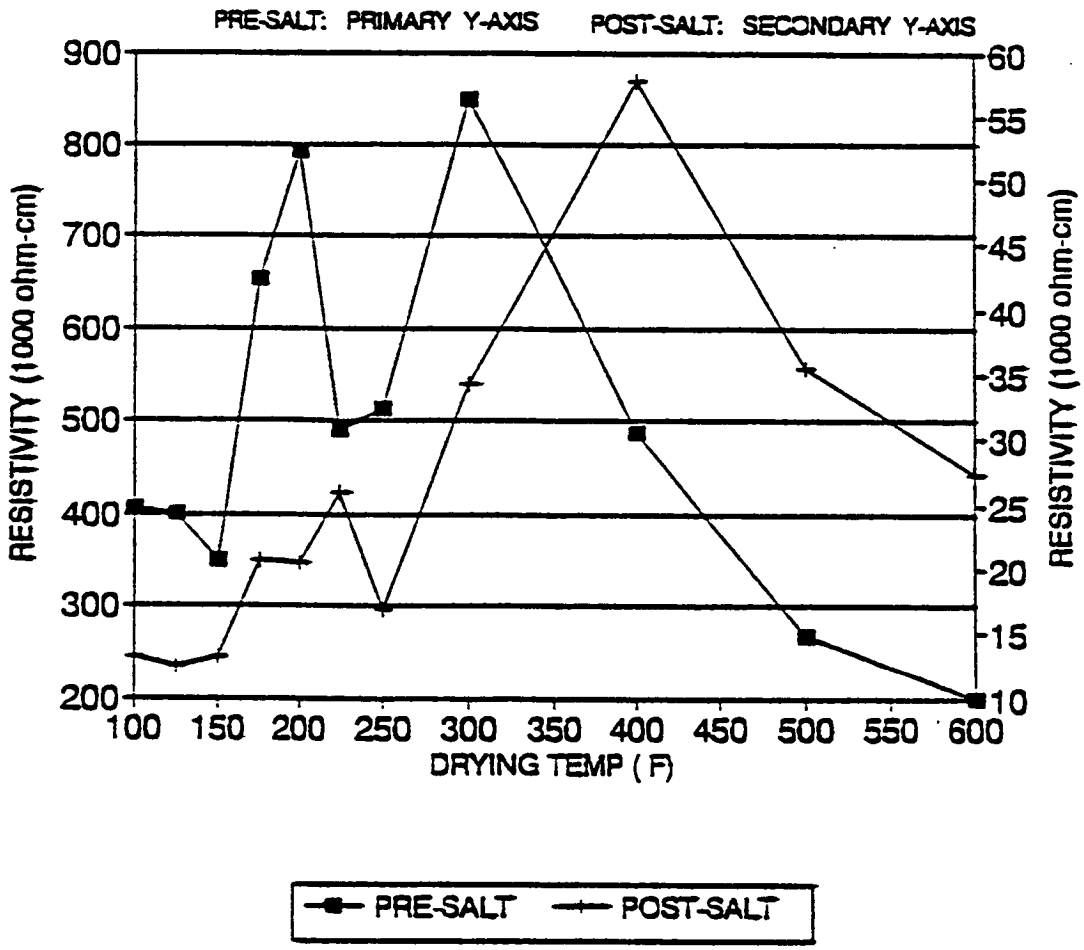

Fig. 5.11 Resistivity vs Temperature

Table 5.3 Porosimeter Test Data

DRYING TEMP (°F)	INTRUSION VOLUME (cc/g)	TOTAL PORE AREA (sq m/g)	AVERAGE PORE DIAM. (micrometers)
100	0.0518	5.2038	0.0398
125	0.0435	5.7887	0.0300
150	0.0520	6.0464	0.0344
175	0.0693	7.1469	0.0388
200	0.0080	1.0022	0.0319
225	0.0042	0.2114	0.0795
250	0.0185	1.0314	0.0716
300	0.0544	5.8839	0.0370
400	0.0426	5.7121	0.0298
500	0.0419	6.1251	0.0273
600	0.0367	5.3034	0.0277
CONTROL	0.0606	7.9242	0.0306

Note: 1 in = 25.4 mm, 1 ft = 0.304 m, 1 lb = 453.6 g

The above conclusion was further supported by total pore area of cubes dried at different temperatures. At lower temperatures, the total pore area was high; at 200°F (93°C) and 225°F (107°C), the total pore area was the least; and at higher drying temperatures, the total pore area increased, see Fig. 5.13. The total pore area of the control cubes was higher than that of any of the impregnated cubes.

The average pore diameter showed a decrease at temperatures over 250°F (121°C). This indicates that, in spite of larger total pore area at higher temperatures, the average pore diameter of available pores is smaller and supports the hypothesis of selective filling of pores by monomer. The high value of average pore diameter at 225°F (107°C) and 250°F (121°C) may be due to the ink-well effect. The ink-well effect usually refers to a void which has a small pore opening and a large cavity so a large amount of mercury is injected into the sample at the size of the small pore opening.

The SEM was used to identify the elements and their relative quantities, as presented in Table 5.4. Since few conclusions could be drawn from the absolute values of the amounts of each element identified, the ratios of carbon to some of the elements were calculated. Carbon does not normally occur in concrete, but it is a major component of polymers. On the other hand, calcium (Ca) and silica (Si) occur only in cements and not in polymers. The values of C/Ca increased abruptly at drying temperatures of 225°F (107°C) and 250°F (121°C), indicating the presence of larger quantities of polymer. The Ca/Si at 225°F (107°C) was very low, possibly because the cementitious particles were masked by polymer in the spots the SEM scanned.

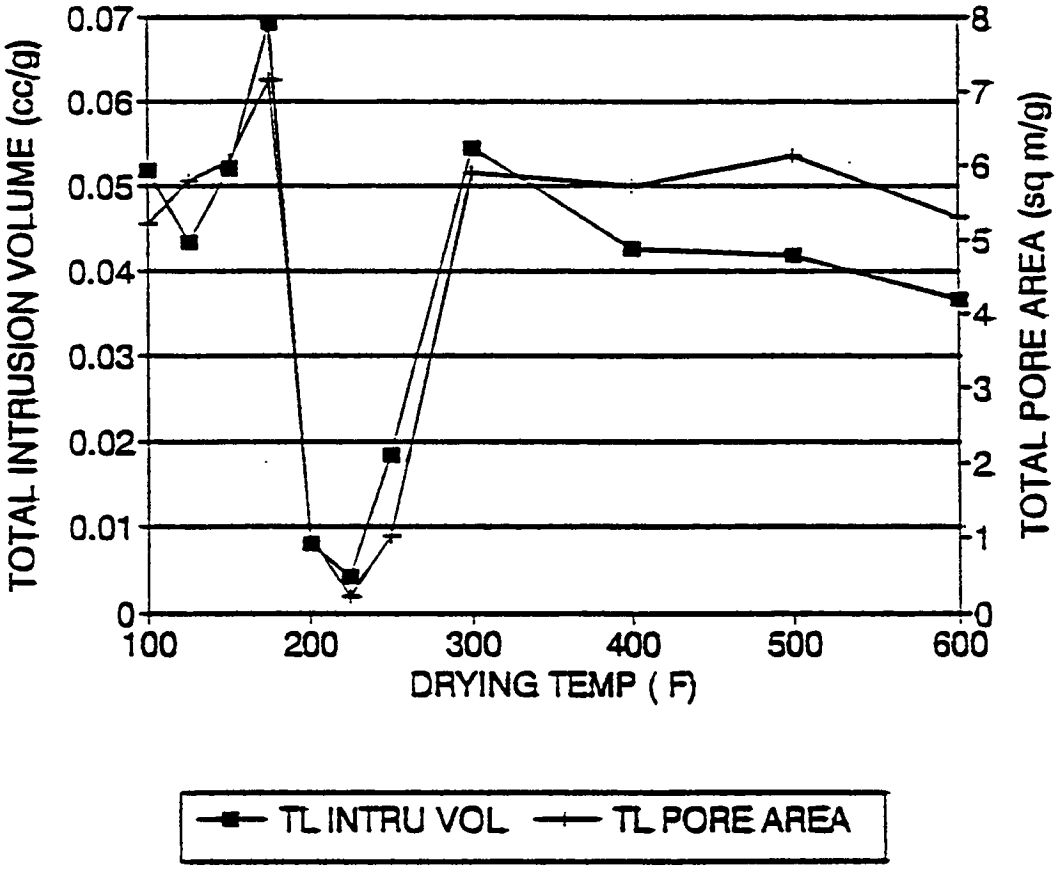

Fig. 5.12 Intrusion Volume Pore Area vs Temperature

Table 5.4 SEM-EDS Test Data

DRYING TEMP (°F)	C/Ca	C/Si
100	0.0413	0.0282
125	0.0256	0.0219
150	0.0118	0.0283
175	0.0136	0.0127
200	0.0199	0.0148
225	0.2584	10.2799
250	0.2327	0.0309
300	0.0344	0.0015
400	0.0257	0.0033
500	0.1393	0.0074
600	0.0456	0.1427
CONTROL	0.0034	0.0066

Note: °F = 9/5 °C + 32

Although the SEM results could be interpreted as supporting previous conclusions, definite inferences should not be drawn from this test for the following reasons:

1. The SEM scans a small area of the sample. As the sample is non-homogeneous, the relative ratios of elements in one spot might be a biased representation of the sample as a whole.

2. The SEM scans only the cut surface; certain elements which might be present in significant quantities below the cut surface would not be represented in the results. Also, obtaining thin layers of mortar cubes to test concrete at different depths was not feasible.

The relationship between chloride content and drying temperature (see Fig. 5.20) indicated that with higher drying temperatures there was a decrease in chloride content as higher volumes of polymer resisted the Cl^- ingress into cubes. This observation is in agreement with resistivity measurements (Fig. 5.13). In general, the increase in chloride content accompanied a decrease in resistivity. The maximum chloride content was 0.66 lb/yd^3 (0.39 kg/m^3) at a drying temperature of 125°F (52°C). For control cubes, the chloride content was much higher, 14.38 lb/yd^3 (8.54 kg/m^3). With the absence of polymer molecules, chloride ions readily diffused into the mortar cubes.

Application of acid had no discernable effect on any of the impregnated cubes. The polymer prevented the dissolving of cement particles. However, in the non-impregnated cubes, the cement portion was attacked by the acid. For a more visual demonstration of this phenomenon, both impregnated and unimpregnated cubes were colored with a permanent marker and then etched with the acid. In the impregnated cubes, the color remained almost the same while in the non-impregnated cubes, the color started to fade after repeated applications of the acid.

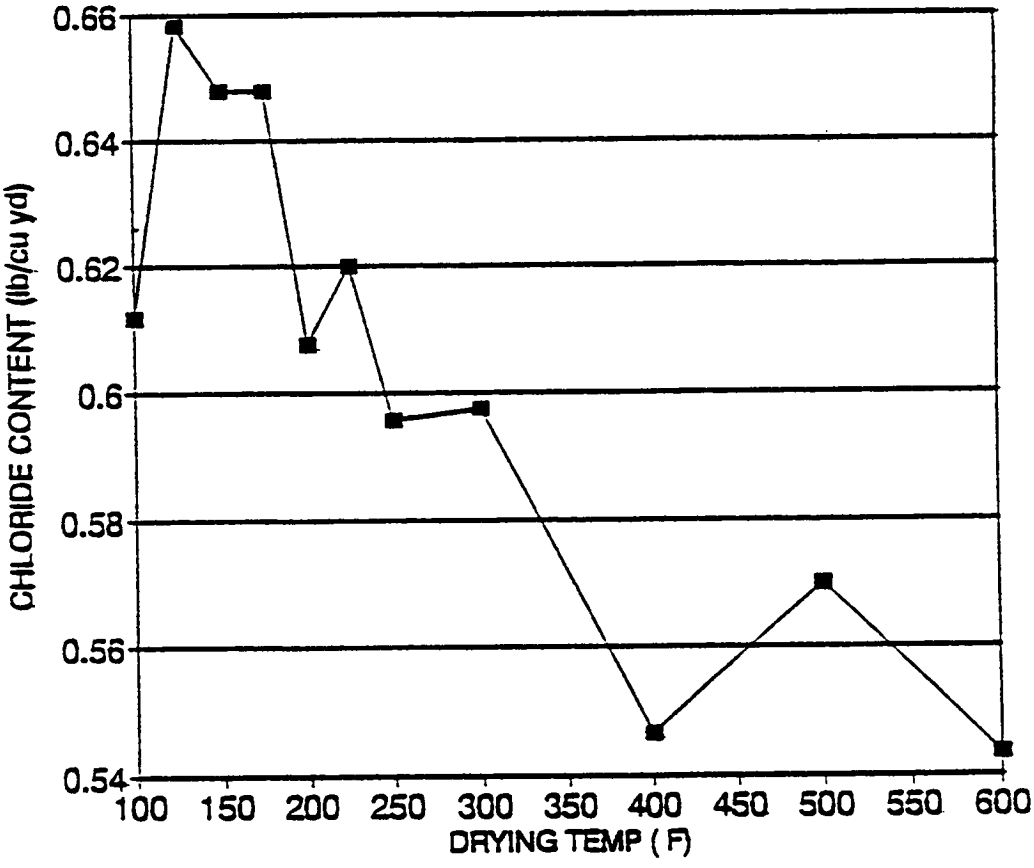

Fig. 5.13 Chloride Content vs Temperature

Corrosion Activity at Different Drying Temperatures

To achieve this objective, three drying temperatures were applied: 150°, 180°, and 230°F (66°, 82°, and 110°C), respectively, at 1/2 in (13 mm) below the rebar level at the time the heaters were turned off.

As indicated earlier, 18 specimens were dried to a temperature of 230°F (110°C) at 1/2 in (13 mm) below the rebar level. All specimens had a 1 in (25 mm) cover depth and 2 in (51 mm) of overlay except the polymer impregnated (PC) series, which attained the requisite temperature before the other specimens, see Fig. 5.15. It took 155 minutes to achieve the needed temperature. The internal temperature for the overlaid specimens increased by 5° to 10°F (3° to 6°C) after the heaters were turned off. The surface temperature reached 529°F (276°C) and then decreased sharply for two hours after the heaters were turned off, after which point the rate of cooling was gradual. After 850 minutes from the time the heaters were turned off, the surface temperature was 50°F (10°C) and the internal temperature was 100°F (38°C).

A one-hour drying was needed for heating to 150°F and 180°F (66°C and 82°C, respectively) at 1/2 in (13 mm) below the rebar level for the 2 in (51 mm) cover depth. The temperature increased by 8° to 18°F (4° to 10°C) after the heaters were turned off in the case of 2 in (51 mm) cover depth. When the cover depth was 3/4 in (19 mm), the temperature increased by 20° to 24°F (11° to 13°C), and the drying time was about 1/2 hour.

At the time of impregnation, the 3/4 in (19 mm) cover depth specimens had very high rates of corrosion (see Fig. 5.16). One of the specimens had a visible crack running on the surface vertically over the left rebar, and another specimen had corrosion products on the top but did not have any visible cracks. There were other specimens with the same cover depth (which were not treated) that had visible signs of active corrosion. It is likely, at that point in time, that most if not all of the specimens with 3/4 in (19 mm) cover depth had some structural damage due to high corrosion currents even though it was not visible in all specimens. After impregnation, the corrosion currents in all specimens decreased. After a period of time, the corrosion currents in the 3/4 in (19 mm) cover depth specimens started to rise. However, the "% change" was still positive at day 89 (see Fig. 5.17). After drying and subsequent impregnation, cracking above the rebar was visually evident in these specimens, most specimens displaying hair-line cracks. The cracks were responsible for allowing large quantities of chloride ions to enter the impregnated specimens resulting in some corrosion despite the presence of polymer in the concrete.

For the 2 in (51 mm) cover depth specimens, the mean corrosion current densities were very low and not in the active corrosion region. The corrosion current at day 89 after impregnation for these specimens were actually higher than their pre-impregnation values. However, the corrosion current was still low and not in the active corrosion region.

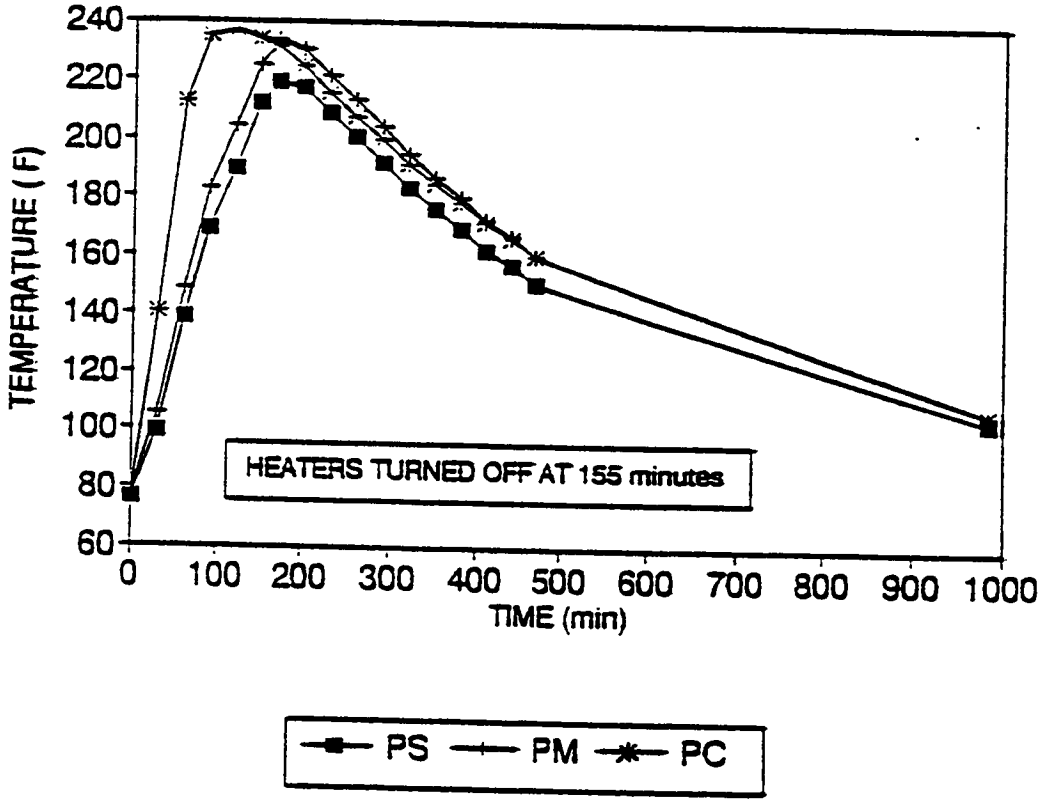

Fig. 5.14 Temperature at 1/2 in (13 mm) Below Top Rebar vs Time

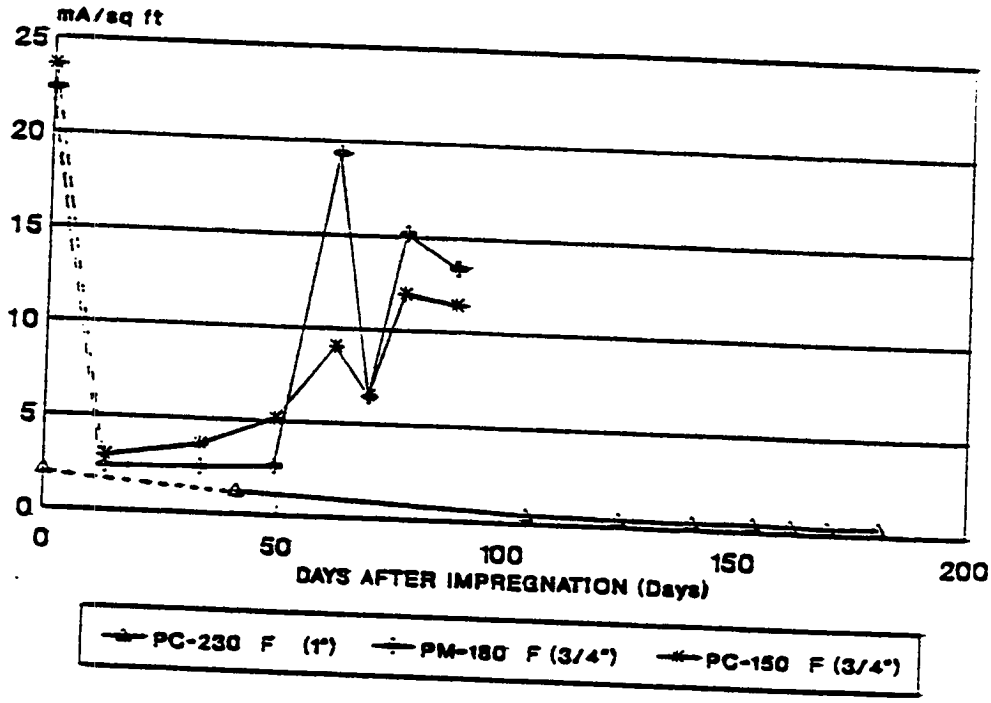

Fig. 5.15 Post-Treatment Mean i_{corr}, (1", 1/4"; 150° F, 180° F, 230° F)

Findings and Conclusions

The following findings were obtained during this part of the study:

1. The CSE was found to be an unreliable instrument after active corrosion cells had been successfully abated by the various treatment methods.

2. Reducing concrete drying temperature from 230°F (110°C) to 180°F (82°C) resulted in a drying time reduction factor of 2.5.

3. Structural damage in concrete impairs the effectiveness of polymer impregnation as a corrosion abatement technique.

4. Polymer molecules, being large organic molecules, fill up voids in concrete selectively, depending on void size.

5. Polymer impregnation of mortar cubes provided good resistance against the ingress of chloride ions.

The following conclusions were reached.

1. This study concluded that there was insignificant difference in the effectiveness of the five treatment methods used in this investigation: LMC overlay, LSDC overlay, polymer impregnation, LMC overlay with polymer impregnation, and LSDC overlay with polymer impregnation. However, the treatments involving LSDC overlay might be less effective than the other four methods investigated.

2. Pre-impregnation drying temperatures can be lowered to 180°F (82°C) at 1/2 in (13 mm) below top rebar level at the time the heaters are turned off. Due to the thermal gradient, the temperature at that depth would continue to rise to about 200°F (93°C).

3. The study on the mortar cubes yielded the conclusion that optimum impregnation is achieved at a drying temperature of about 200°F (93°C).

4. Polymer impregnation of concrete is an effective technique to reduce the chloride intrusion.

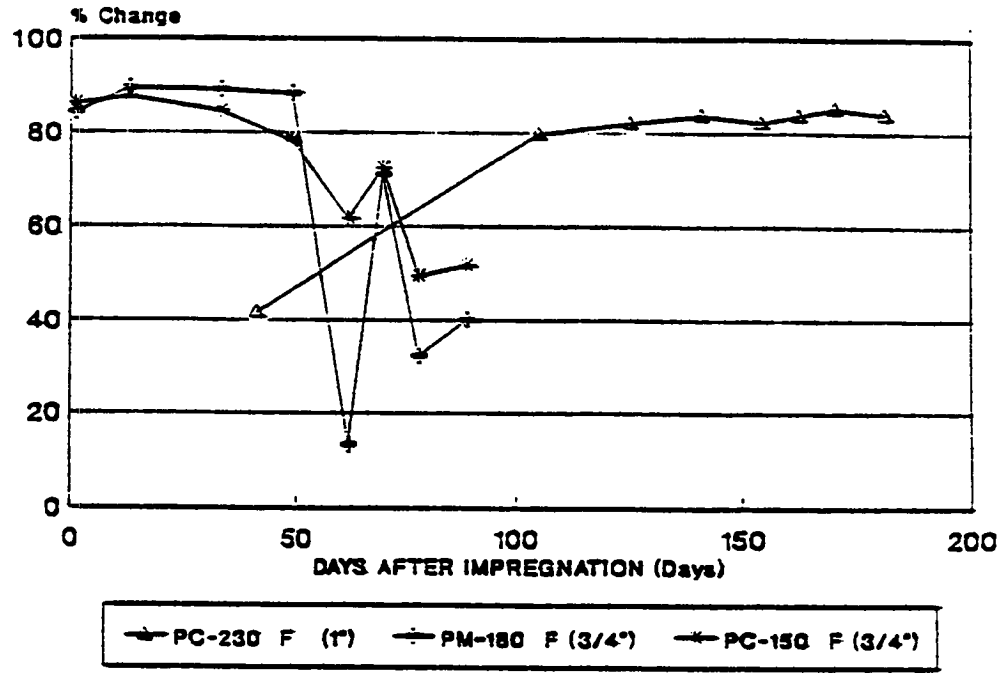

Fig. 5.16 Percent Change in Mean i_{corr} (1", 1/4"; 150° F, 180° F, 230° F)

Part II: Developing New Techniques: Laboratory Investigation of Corrosion Inhibitors

6

Laboratory Investigation of Corrosion Inhibitors

Introduction

As presented in Part I, there are several methods that can be used to rehabilitate reinforced concrete bridge decks which have deteriorated as a result of chloride induced corrosion. A feasibility study on corrosion inhibitors identified four inhibitor combinations (13). In this part of the investigation, procedures were developed to apply corrosion inhibitors on bridge components for which the chloride-contaminated concrete has been removed to at least the top layer of reinforcing steel. Inhibitor effectiveness was evaluated in conditions simulating field construction. The study was performed in three phases: evaluation of corrosion inhibitors, development of field treatment procedures, and estimation of service life.

The first phase employed 1 ft x 1 ft (0.3 m x 0.3 m) laboratory specimens in which corrosion was accelerated by cyclic chloride solution exposure. A treatment matrix was devised to test the effectiveness of the application procedures on varying rates of corrosion. The change in corrosion current was measured using non-destructive techniques.

Treatments proven effective in the first phase were used in the second phase, determining necessary application procedures for field use. Various parameters that would influence constructability were investigated: inhibitor influence on the strength, workability, and durability of modified concrete. This phase culminated in the treatment of sections removed from a deteriorated bridge deck. The third phase attempted to estimate the additional service life resulting from the treatments.

Corrosion inhibitors are used to prevent or delay corrosion of metals exposed to corrosive environments. Corrosion inhibitors are generally classified as anodic, cathodic or mixed inhibitors according to their function. Anodic inhibitors reduce the rate of reaction at the anode. They usually react with the corrosion products to form a protective coating on the metal surface. Cathodic inhibitors act to prevent the reaction at the cathode. Griffin (36)

states, "Reactive products of cathodic inhibitors do not bond to the metal surface as tightly as those of anodic inhibitors and are, therefore, less effective." Cathodic inhibitors act indirectly since they do not prevent metal dissolution. Mixed inhibitors influence both the anodic and the cathodic sites. This is especially advantageous in reinforced concrete due to the prominence of micro-cell corrosion.

Inhibitors are classified as follows (37): adsorbed layer formers, oxidizing inhibitors-passivators, conversion layer formers, and scavengers. Adsorbed layer formers are organic inhibitors which strongly adsorb to the metal surface and interfere with the anodic or cathodic reactions in the area of adsorption. The effectiveness of these inhibitors is measured as a percent reduction as shown in Equation 6-1 (36).

$$\%inhibition = 100\left(\frac{R \cdot R*}{R}\right) \qquad (6\text{-}1)$$

where,

R = corrosion current without inhibitor, and
R* = corrosion current with inhibitor

The percent inhibition is a function of the surface coverage of the adsorbed layer.

Nitrogen is usually the active atom in an adsorbed layer inhibitor acting in a non-acid electrolyte on steel. Typical compounds of nitrogen used as inhibitors are organic nitrates and amines. The bond strength of the adsorbed layers is due to the nitrogen atom's high density of electrons and ability to form co-ordinate bonds (38).

Vapor phase inhibitors (VPI or Volatile Corrosion Inhibitor VCI) are similar to adsorbed layer inhibitors. Miksic (39) stated that: "Volatile Corrosion Inhibitors are secondary electrolyte layer inhibitors that possess appreciable saturated vapor pressures under atmospheric conditions, thus allowing significant vapor phase transport of the inhibitive substance." Aliphatic and cyclic amines and nitrites with a high vapor pressure typically make up these inhibitors (38).

Oxidizing inhibitors or passivators are another form of barrier inhibitor which act by shifting the electrochemical potential of the corroding metal such that an insoluble oxide or hydroxide forms on the metal surface (37). Sodium nitrite and chromates are examples of this inhibitor. Another form of passivators are metal soaps which are a form of the basic pigments (metal oxides) and oxidation products of oil, such as cinnamic and pelargonic acid, which form passivating films on the metal surface (38).

Conversion layer inhibitors form insoluble compounds on metal surfaces without oxidation. In neutral or basic solution, the presence of calcium and magnesium ions inhibits corrosion by the formation of an insoluble calcareous scale on the metal surface (37).

Finally, scavengers act as neutralizing inhibitors by removing concentrations of corrosive materials such as Cl^- ion.

The effect of corrosion inhibitors is generally concentration dependent, which may cause what is called dangerous inhibitors. Dangerous inhibitors increase the rate of attack in unprotected areas, similar to the haloing effect which is sometimes produced around patches due to the increase in the cathodic area after repair. Most anodic inhibitors are dangerous inhibitors (36).

Selection of Corrosion Inhibitors

In research reported in Task 2 (13), seven corrosion inhibitors and two sealers were evaluated to determine their effectiveness in reducing corrosion currents in reinforced concrete specimens (40). The following five corrosion inhibitors were identified as showing promising results and were recommended for further study:

1. Alox 901 (proprietary oxygenated hydrocarbon produced by the partial oxidation of an aliphatic hydrocarbon): An organic inhibitor which forms a protective film by conversion to a metallic soap.

2. Cortec VCI-1337 [MCI-2020] (a proprietary blend of surfactants and amine salts in a water carrier): A secondary electrolyte layer inhibitor with appreciable vapor pressure under atmospheric pressure or volatile corrosion inhibitor, (VCI) (39). The product is designed to migrate in a vapor phase and adsorb on a metallic surface forming a monomolecular film at both anodic and cathodic sites.

3. Cortec VCI-1609 [MCI-2000] (proprietary alkanolamines): This product is designed to migrate and inhibit in a manner similar to VCI-1337 with the difference that it is a concrete admixture.

4. DCI (calcium nitrite, $Ca(NO_2)_2$): The nitrite ions in this inhibitor are thought to compete with the chloride ions for the ferrous ions at the anode. The nitrite and ferrous ions react as follows:

$$2Fe^{++}+2OH^-+2NO_2 \rightarrow 2NO\uparrow +Fe_2O_3+H_2O \qquad \textbf{(6-2)}$$

This reaction forms a stable passive layer on the reinforcement steel (41).

DCI is designed as a concrete admixture for corrosion inhibition. Unlike its predecessor sodium nitrite, it does not adversely effect the strength gain of the concrete. However, it does act as a strong accelerator, normally requiring the addition of a water reducer and a retarder in the concrete mixture.

5. Sodium tetraborate ($Na_2B_4O_7$): An experimental inhibitor which forms a protective layer on the metal surface through the reaction of borate and oxygen. This reaction appears to be highly dependent on the pH of the pore solution. Tests indicate that the borate ion is more mobile in concrete than the chloride ion, indicating an ability to migrate faster to the rebar in concrete (42).

Experimental Design

Overview

The task of developing repair and rehabilitation techniques using corrosion inhibitors for reinforced concrete structures was accomplished in three phases:

I) Evaluation of Corrosion Inhibitors
II) Development of Field Treatment Specifications
III) Estimation of Service Life

Initial corrosion inhibitor evaluations were carried out on 1 ft x 1 ft (0.3 m x 0.3 m) reinforced concrete specimens. Thirty-six specimens with varied ranges of corrosion activity were treated. Specimens were cast having one or two triads of reinforcing steel (rebar). After initial curing, the specimens were alternately ponded with a 6% (by weight) salt water solution and allowed to air dry to induce corrosion.

Half-cell measurements were initially used to monitor corrosion activity in the specimens. Once a drop in the corrosion potential indicated the initiation of corrosion activity, an unguarded linear polarization device, the 3LP, was used to monitor the corrosion current density. Chloride measurements were taken at the bar level prior to treatment.

Overlay bond strength tests were performed initially on 16 well cured 1 ft x 1 ft (0.3 m x 0.3 m) specimens prior to the treatment of 5 ft x 5 ft (1.5 m x 1.5 m) slabs.

Bridge deck slabs were treated in Phase II. The slabs were salvaged from a bridge deck removal project on I-80 in Pennsylvania. Three combinations of inhibitors and modified overlays were applied. Both the 3LP and a linear polarization device with a guard ring electrode (Geocisa Gecor Device) were used to monitor the corrosion current of treated specimens.

Freeze-thaw durability tests were performed on the modified overlay concrete used in Phase II, using ASTM C-666-84 Standard, "Resistance of Concrete to Rapid Freezing and Thawing, procedure A."

Specimen Preparation

Twenty-four specimens with one and two triads of reinforcement steel were cast. Forms were constructed for 12 specimens of each configuration. The dimensions for the one and two triad configurations are presented in Figs. 6.1 and 6.2, respectively.

The forms were made of 3/4 in (19 mm) BC grade exterior plywood fastened with drywall screws. The reinforcement steel was supported by plywood spacers placed at the two ends of the form, and 5/8 in (16 mm) diameter holes were drilled in the spacers to accommodate the ASTM grade 60 #4 bar with a nominal 0.5 in (13 mm) diameter. The three 12 in (305 mm) bars were cleaned with hexane and oven dried to remove any manufacturing latencies. The ends of each bar were covered with electroplating tape to provide a known length of exposed corrodible steel.

Prior to placing the concrete, the forms were twice coated with form oil and the rebar placed in the holding spacers. A type T TC was attached to the center of the top rebar with electroplating tape. To minimize the initiation of subsidence cracking, specimens were cast in an inverted position. A vibratory table was used to consolidate the fresh concrete.

The first set of one triad with 2 in (51 mm) cover specimens was cast with ready-mix concrete in accordance with Virginia A4AE Bridge Deck Air Entrained concrete specifications. A set of two triads, with 2 in (51 mm) cover specimens was cast 20 days later. The ready-mix concrete for both sets, had the same specifications and was produced by the same supplier. The mixture proportions are presented in Appendix C, Table C-1.

The one triad with 1 in (25 mm) cover depth specimens were cast 83 days later. The concrete cover was reduced to decrease the necessary time for the chlorides to diffuse to the top reinforcing steel and initiate corrosion. The concrete for this group of specimens was batched in a 2 ft^3 (0.057 m^3) pan mixer in the laboratory. Four batches were required to produce the 12 specimens. The mixture proportions are presented in Table C-1 and the aggregate properties are presented in Table C-2, Appendix C.

Once the concrete was placed and consolidated, the specimens were covered with moist burlap and polyethylene sheets and allowed to cure for 3 days prior to form removal.

One end of each rebar was tapped to accommodate a No. 10-24 x 3/8 in (9.5 mm) machine screw. The top and bottom layers of steel in each triad were connected with a 100Ω resistor and the two bars in the bottom layer were connected with 18 gauge wire as shown in Figs. 6.1 and 6.2. A male subminiature connector was attached to the type T TC leads.

The sides of the specimens were coated with epoxy to reduce diffusion of oxygen and water-vapor to simulate the boundary conditions on an actual bridge deck.

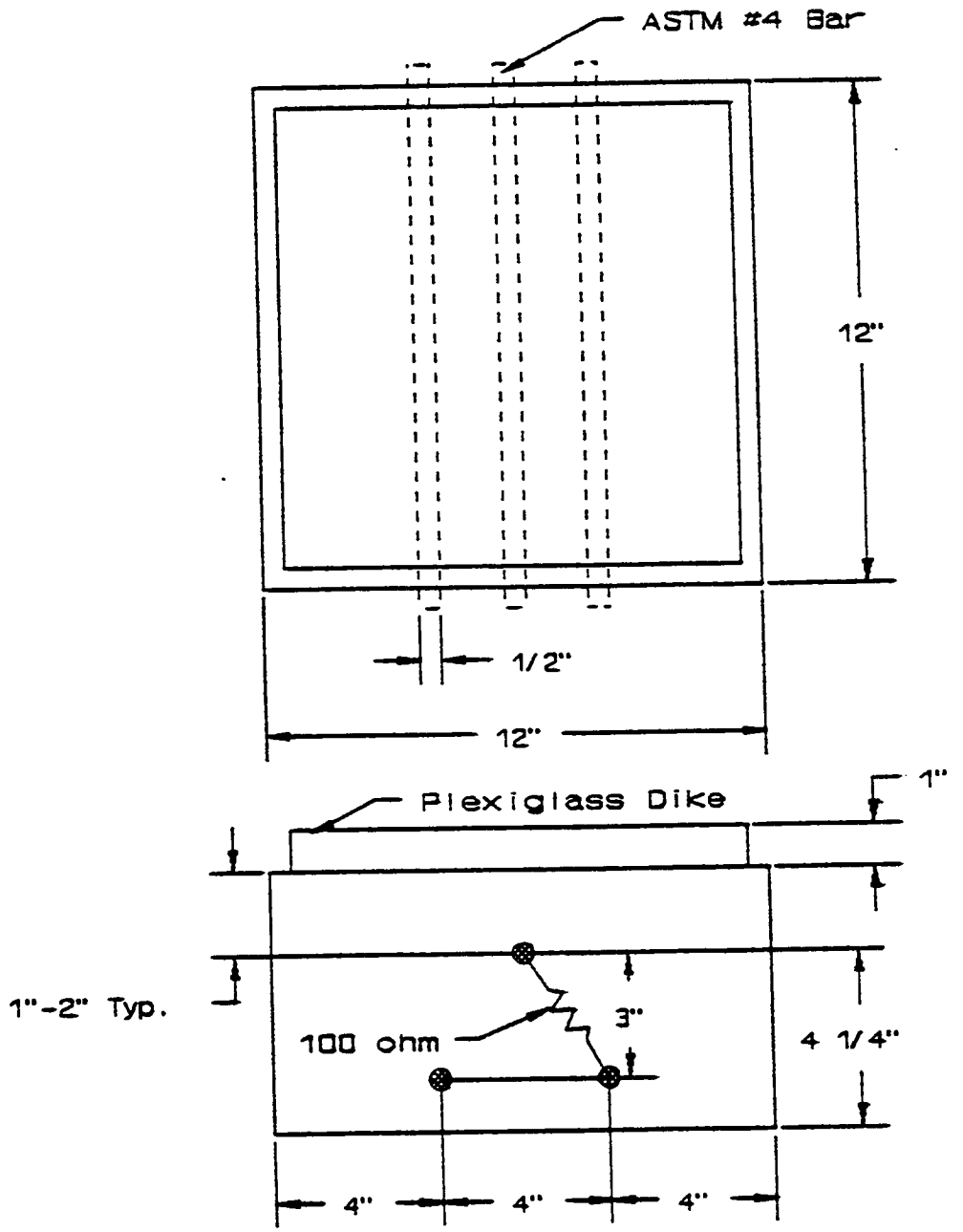

Fig. 6.1 One-Triad Specimen Configuration

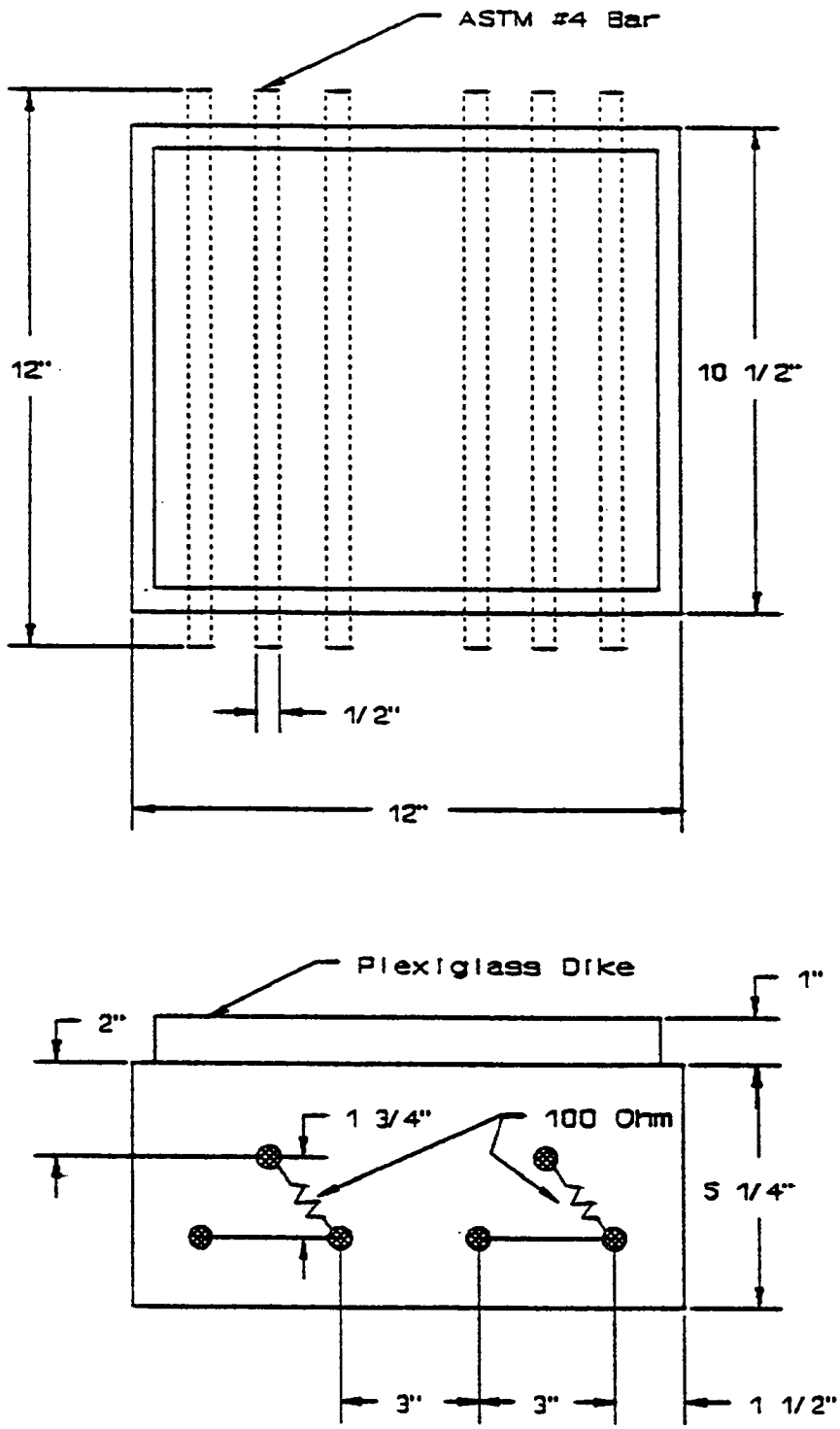

Fig. 6.2 Two Triad Specimen Configuration

Corrosion Initiation

The specimens were ponded with 400 ml of a 6% (by weight) NaCl solution on a weekly basis. The salt water was ponded on the specimens for three days, after which, it was removed with a wet/dry vacuum. The specimens were then allowed to air dry for four days before the cycle was repeated. Plexiglass dikes, 10 in x 10 in x 2 in (254 mm x 254 mm x 51 mm), were attached to the top surface of each specimen using silicone caulk to contain the salt water solution. The specimens were stored in an insulated conditioning room to minimize temperature fluctuations.

One day after the removal of the salt water, half-cell potentials measurements were taken on each specimen. Three measurements were taken along the surface above each bar using a CSE reference half-cell and hand held voltmeter in accordance with ASTM C-876-87 (24). A specimen was considered to be actively corroding when the mean potential value was more negative than -350 mV.

After the probable initiation of corrosion, the specimen's corrosion current density was measured using a 3LP device. The corrosion current density (i_{corr}) was calculated using the Stern-Geary equation. The Tafel slope constant was estimated at B = 40.76 mV (22). According to Farraday's Law, the corrosion current (I_{corr}) is directly proportional to the corrosion rate. Thus, i_{corr} (corrosion current density) measurements provide a relative indication of the corrosion activity in the specimens. Clear (22) correlated the i_{corr} measurement with the time to expected damage of the concrete as presented in Table 6.1.

After the first year of salt water ponding cycles, 3LP estimates were routinely taken on all of the specimens, even those with potentials more noble (less negative) than -350 mV CSE.

Chloride measurements as a function of depth were also taken from the specimens to provide an additional indication of corrosion activity. Powdered concrete samples were collected in ½ in (13 mm) increments starting at a depth of ¼ in (6.5 mm). The samples were collected using a rotary impact hammer equipped with a 1⅛ in (29 mm) masonry bit. The samples were obtained with a vacuum-assisted collection device through a hole in the tip of the bit (31).

Table 6.1 i_{corr} Correlated to Time to Expected Damage

i_{corr} (mA/Ft^2)	Time to Expected Damage
$i_{corr} < 0.20$	Not Expected
$0.20 < i_{corr} < 1.0$	Possible in 10-15 years
$1.0 < i_{corr} < 10$	2-10 years
$I_{corr} > 10$	< 2 years

The Cl^- ion concentration of the sample was measured using the specific ion electrode method (31). The method uses an acid-based solution to digest three grams of the collected powdered concrete sample. The chloride threshold necessary for the initiation of corrosion was considered 1.2 lb/yd^3 (0.7 kg/m^3).

The corrosion inhibitors were divided into four cells of surface ponding agents and concrete admixtures. The application concentrations were based on the research reported earlier (13). An untreated latex-modified overlay was included as a control in each cell combination. The treatments were applied to specimens with chloride-contaminated concrete cover removed to the rebar level. Table 6.2 presents the inhibitor combinations and application concentrations.

Three application methods were used to apply the inhibiting agents: one-day ponding, two-day ponding, and one-day ponding of specimens dried to 180°F (82°C) at ½ in (13 mm) below the top reinforcement.

Three overlay systems were applied to specimens for which the chloride-contaminated concrete cover was not removed. These systems were 1 in (25 mm) LMC overlay, 2½ in (64 mm) hot-mix asphalt overlay with a waterproof preformed membrane, and a thin polymer concrete overlay.

In order to investigate the effectiveness of the treatments on varying corrosion currents, the corroding specimens were divided into three categories based on time to expected damage as correlated to i_{corr} (see Table 6.3). The matrix shown in Table 6.3 was designed to incorporate the effect of different treatment procedures and materials on the range of corrosion current densities.

The specimens were treated in three separate groups. The first group included the blocks with one- and two-day ponding of specimens with low corrosion current densities, 1-day ponding of dried specimens with high initial corrosion current densities, and the overlay controls.

After monitoring the i_{corr} estimates of the one- and two-day ponding groups for two months, it was determined that two-day ponding did not have a significantly different effect on corrosion current densities than did one-day ponding, see Fig. 6.8 and 6.10. Therefore, further treatments with two-day ponding and control overlays were eliminated.

The second treatment group included one-day ponding and one-day ponding with drying of specimens with medium initial corrosion current densities. The third treatment group consisted of one day ponding of dried specimens with low initial i_{corr} estimates.

Prior to the application of the corrosion inhibitors, the chloride contaminated cover concrete was removed to the top layer of reinforcing steel. The top surface of the specimen was sawed perpendicular to the rebar at ½ in (13 mm) intervals using a water-cooled masonry saw with a 1/16 in (1.6 mm) thick diamond blade. The cut depth was set to avoid contact with the rebar. The sawed cover concrete was removed with a hammer and a masonry chisel.

Table 6.2 Treatment Combinations

Surface Ponding Agents	Overlay Admixtures
0.1M Alox 901 in Denatured Ethyl Alcohol, AX	Dow Latex 196 lbs/yd^3
Cortec VCI-1337, (MCI 2020)	Cortec VCI-1609 (MCI 2000) 1 pint/yd^3
0.1M DCI (Calcium Nitrite) in Water, DCI	DCI 6 gallons/yd^3
0.1M Sodium Tetraborate in Water, SB	0.1M Sodium Tetraborate in Mix Water
None	Dow Latex 196 lbs/yd^3

Note: 1 lb = 0.45 Kg; 1 pt = 0.47 ℓ; 1 gal = 3.78 ℓ; 1 yd^3 = 0.76 m^3

After the cover concrete was removed, a ¼ in (6.4 mm) diameter hole was drilled in the bottom of each specimen to be dried, to a depth equal to ½ in (13 mm) below the top rebar. A type T TC with glass braid insulation was installed in the hole and the hole was sealed with duct seal.

The specimens were then placed on a sand bed under a steel frame which supported the heaters. Fiberglass insulation was placed around the sides of the specimens to simulate single surface heating which would occur on a bridge component such as a bridge deck.

Propane infrared heaters were suspended at a height of 16 in (0.34 m) above the top surfaces of the specimens. Once the heaters were lit, the specimen temperature was recorded at 2-minute intervals. A surface probe was used to monitor the approximate specimen surface temperatures. The heaters were shut off when the mean temperature of the specimens at ½ in (13 mm) below rebar level reached 180°F. The temperatures were then monitored for an additional 30 minutes. Drying temperatures as a function of time for each group of specimens are presented in Figs. C.1 - C.3, Appendix C. Specimens were then covered with fiberglass insulation and allowed to cool slowly to help prevent thermal cracking.

The corrosion inhibitors, designated as surface ponding agents, were applied to the surface of the specimens for the time period specified in the treatment matrix (Table 6.3), prior to their overlay. The ponding agent was contained by 2 in (51 mm) height sealed forms prepared to be used for placing the overlay. The corrosion inhibitor was poured into the forms to a depth of ¼ in (6.4 mm). The insides of the forms were coated with an epoxy to provide a nearly non-absorbent surface.

At the end of the ponding period, the excess inhibitor was removed with a wet/dry shopvac. Dry cement was dusted onto the surface of the specimens treated with Alox 901 to help absorb residual petroleum products. These specimens were then placed outdoors in direct sunlight for one hour after which time the surface was blasted clean of loose particles with compressed air.

The batch proportions used for the modified overlay mixtures are presented in Appendix C,

Table C-3 through C-6. The initial mixes were modified with progressive treatment groups to provide improved strength, workability, and freeze-thaw durability. The overlay concrete was batched in a 2 ft^3 (0.057 m^3) pan mixer.

A thick grout was applied to the surface of each specimen immediately prior to placing the concrete. The grout was obtained by sieving out the coarse aggregate from a portion of the concrete mixture. The specimens were placed on a vibratory table to consolidate the overlay concrete. The slump, air content, and unit weight of the plastic overlay concrete was measured. The overlaid specimens were covered with moist burlap and polyethylene sheeting for three days. After curing, the sides of the specimens were recoated with epoxy and the ponding dikes reinstalled. Until 28 days after placement, the specimens were ponded with water.

Six 4 in x 8 in (102 mm x 152 mm) cylinders were cast from each concrete batch. The cylinders were cured at 70° ± 2°F and 100% relative humidity. The compressive strength of pairs of cylinders was measured at 1, 7, and 28 days in accordance with ASTM C-39-86, "Compressive Strength of Cylindrical Concrete Specimens." Fresh and hardened concrete mixture characteristics are summarized in Appendix C, Table C-3 through C-6.

Three control overlays were used for comparison purposes: 1 in (25 mm) LMC overlay, thin polymer concrete overlay, and 2½ in (64 mm) hot-mix asphalt (HMA) overlay with waterproof preformed membrane. The 1 in (25 mm) overlay was placed in the same manner as the above treatments.

A non-skid flexible epoxy-urethane co-polymer, MARK-163 Flexogrid, produced by Polycarb was used as the binder for the thin polymer overlay. The application procedure is described in Appendix C, Table C-7A. The aggregate was a Morie #3 basalt. Particle size gradation and physical characteristics of the aggregate are given in Appendix C, Table C-7B. The overlay was applied in accordance with the manufacturer's specifications.

W. R. Grace's Bituthene preformed membrane system was used with hot-mix asphalt overlay. The preformed membrane was applied according to the manufacturer's specifications. The hot-mix asphalt, a Virginia SM5 surface mixture, was heated and compacted in a 2½ in (64 mm) plywood form built around each specimen. The mixture properties of the HMA are presented in Appendix C, Table C-8.

Table 6.3 Specimen Treatment Matrix

Exposure Type	Time to Expected Concrete Damage in Years, Based on i_{corr}		
	10 - 15 years	2 - 10 years	< 2 years
Ponding 1 Day	Alox 901/LMC Cortec 1307/1609 DCI/DCI Sodium Borate *LMC Control	Alox 901/LMC Cortec 1307/1609 DCI/DCI Sodium Borate *LMC Control	NA
Ponding 2 Day	Alox 901/LMC Cortec 1307/1609 DCI/DCI Sodium Borate *LMC Control	NA	NA
Dried 180°F at ½" Below Bar, Ponding 1 Day	Alox 901/LMC Cortec 1307/1609 DCI/DCI Sodium Borate *LMC Control	Alox 901/LMC Cortec 1307/1609 DCI/DCI Sodium Borate *LMC Control	Alox 901/LMC Cortec 1307/1609 DCI/DCI Sodium Borate *LMC Control
Controls	1" LMC Overlay Membrane w/2½" HMA Thin Polymer Overlay	Untreated	NA

Post-Treatment Corrosion Monitoring

Chloride exposure of specimens to a 6% NaCl solution applied on a three-day ponding and four-day drying cycle was resumed 28 days after the overlay placement. Corrosion current density estimates were taken with the 3LP on a regular basis to monitor the corrosion activity. The readings were taken on the second day of the drying cycle.

Determination of Bond Strength

The bond strength between the modified overlay and base concrete was measured to determine the influence of the corrosion inhibitors. A poor bond strength would indicate that the overlay would probably delaminate and spall under traffic loading and/or freezing and thawing cycles. The bond strength was measured using a method described in ACI 503R (43).

Treatment of Bridge Deck Slabs

The bridge deck slabs were salvaged from a bridge deck replacement project on I-80 in Pennsylvania. The slabs were stored indoors for a month prior to treatment to minimize temperature fluctuation, and covered with moist burlap and polyethylene sheeting to prevent moisture loss.

Prior to treatment, a corrosion survey was conducted on the slabs similar to that which would be conducted on an actual bridge deck. The survey concluded: sounding for delaminations, cover depths, corrosion potentials, i_{corr} estimates with both the 3LP and Gecor devices, and chloride measurements.

The measurements were taken on all the transverse bars across the slab before a second measurement was taken at a different location on a single transverse bar. The 3LP measurements were taken at least one hour after the Gecor measurements. Chloride measurements were taken at two locations on each slab.

Prior to the application of the corrosion inhibitors, the cover concrete was removed to the top layer of reinforcing steel. In order to obtain the same surface texture found on a bridge milled in the field, a commercial milling machine was used by a professional crew. The slabs could not be properly anchored to allow accurate milling, therefore, to avoid damaging the slabs, the remainder of the cover concrete was removed by sawing the slab with a walk-behind concrete saw using a 3/16 in (4.8 mm) thick diamond blade. The sawed concrete was removed with an electric demolition hammer.

The surface ponding technique used for the 1 ft x 1 ft (0.3 m x 0.3 m) specimens would be difficult and expensive under field conditions. Therefore, surface-applied corrosion inhibitors were sprayed on the slabs using a ½ gallon (1.8 L) polyethylene garden sprayer. Three equal spray applications were applied to the slab; the second and third applications were applied ½ hour and 12 hours after the initial spraying, respectively. The spraying rates

for uniformly saturated surface for a single application are shown in Table 6.4.

Table 6.4 Spray Application Rates

Surface Applied Inhibitor	Application Rate (ft^2/gal.)
Alox 901	70
Cortec VCI-1337	225
DCI (Calcium Nitrite)	150

Note: 1 gal = 3.78 ℓ; 1 ft^2 = 0.09 m^2

Sodium tetraborate was not used in the Phase II study because it did not perform as well as the LMC controls where the cover concrete was removed.

After the inhibitors carrying solvent had evaporated, the surface of the slab was blasted clean of loose particles with compressed air. The slabs which were treated with Alox 901 and Cortec VCI-1337 were lightly sandblasted to remove residues left by the inhibitors in order to achieve an acceptable bond strength.

Forms were constructed for the slabs primarily with 5/8 in (16 mm) BC Grade exterior plywood. The slabs were placed in the form with a forklift so that the ends of the transverse bars on 1 side would be accessible after the overlay was placed. This allowed accurate location of the steel after overlay and easy connection to rebars (working electrodes).

Mix designs and batch characteristics are presented in Appendix C, Table C-9 through C-11. The concrete for the slab overlays was mixed in the same manner as the 1 ft x 1 ft (0.3 m x 0.3 m) specimens. However, only three cylinders were cast from each batch, for compressive strength measurement. One cylinder from each batch was tested at seven days, and the remaining pairs were tested at 28 days. Two beams 15 3/4 in x 3 in x 4 in (40 cm x 7.6 cm x 10 cm), were cast from each mix design for rapid freeze-thaw testing.

The plastic overlay concrete was consolidated with a vibratory probe. The surface was screeded with a vibratory screed prior to finishing. After finishing, the slabs were covered with moist burlap and polyethylene sheeting and allowed to cure for three days. The forms were removed after seven days and the sides of the slab were coated with epoxy. The location of the top layer of reinforcement steel was marked on the surface with a permanent marker. The end of a transverse bar was tapped for a lead wire for each slab. While stored in the laboratory, the surfaces were moistened and covered with plastic sheeting.

Concrete Resistance to Rapid Freeze-Thaw Cycles

The concrete beams cast with the slab overlays were tested in accordance with ASTM C-666-84 Procedure A, "Resistance of Concrete to Rapid Freezing and Thawing." The durability

factor for the concrete was determined by measuring the reduction in the fundamental transverse resonant frequency. The resonant frequency was measured using Grindo-Sonic MK4x Instrument.

Results and Discussion

Pre-treatment Corrosion Current Density Measurements

A specimen identification code was developed for the 1 ft x 1 ft (0.3 m x 0.3 m) specimens based on specimen configuration, initial corrosion activity, and applied treatment. For example,

Code: 1H-D1-DCI

1H → A specimen containing 1 triad of reinforcing steel, with a high potential corrosion current density according to Table 6.1.

D1 → Specimen was dried to 180°F (82°C) at a depth of ½ in (13 mm) below the reinforcing steel, and ponded with corrosion inhibitor for 1 day.

DCI → Corrosion inhibitor applied to specimen according to Table 6.2.

The only exceptions to this system were the control overlay specimens presented in Table 6.5 where

2M → Two in (5.08 cm) cover depth medium initial corrosion rate

2L → Two in (5.08 cm) cover depth low initial corrosion rate

Prior to treatment, the specimens were grouped according to their initial corrosion current densities to compare inhibitor effectiveness. The groups were categorized as low, medium, and high according to time to expected damage presented in Table 6.1. In addition, a medium-low category was added for specimens in which the i_{corr} values fell in the low end of the 1-10 mA/ft^2 (10.76 - 107.6 mA/m^2) range, which is the medium category.

The specimen codes will be used to identify treatments throughout this part of the report.

The pre-treatment i_{corr} and E_{corr} values, and Cl^- concentrations at the bar level for the specimens immediately prior to treatment are presented in Table 6.6. The Cl^- content as a function of depth is presented in Appendix C, Table C-14. Since the Cl^- ion concentration represents somewhat of a potential rate for the corrosion reaction, an effort was made to determine if a correlation exists.

Table 6.5 Control Overlay Specimen Identification Codes.

Specimen	Treatment
2M-LMC	1 in LMC Overlay with Cl^- contaminated cover concrete left in place
2L-BC	2½ in Bituminous Concrete Overlay with a preformed membrane; Cl^- contaminated cover concrete left in place
2L-TP	Thin Polymer Overlay, Cl^- contaminated cover concrete left in place
2M-CON	Untreated Control

Table 6.6 **Average pre-treatment corrosion current density, potential, and chloride ion content at the reinforcing steel level for all treated specimens.**

Specimens	i_{corr} (mA/ft^2)	E_{corr} (CSE) (-mV)	Cl^- Ion (lbs/yd^3)
1H-D1-DCI	9.78	476	28.8
1H-D1-SB	12.84	445	26.1
1H-D1-AX	37.48	491	27.3
1H-D1-COR	9.93	489	23.8
1H-D1-LMC	9.72	473	24.7
2ML-1-DCI	1.91	246	2.0
2ML-1-SB	2.34	298	1.6
2ML-1-AX	1.50	303	2.3
2ML-1-COR	1.21	200	1.6
2ML-2-DCI	2.04	294	1.8
2ML-2-SB	0.93	258	1.5
2ML-2-AX	2.53	376	2.0
2ML-2-COR	1.20	213	1.2
2ML-O-LMC	1.31	310	2.3
2M-LMC	2.95	390	2.6
2L-BC	1.63	280	1.4
2L-TP	0.94	261	1.8

Continued.

Table 6.6 **Average pre-treatment corrosion current density, potential, and chloride ion content at the reinforcing steel level for all treated specimens (Continued).**

Specimen	i_{corr} (mA/ft^2)	E_{corr} CSE (-mV)	Cl^- Ion (lbs/yd^3)
1M-1-DCI	4.86	565	12.8
1M-1-SB	4.92	536	14.3
1M-1-AX	4.96	567	16.6
1M-1-COR	5.64	531	13.1
1M-0-LMC	7.32	567	16.8
1M-CON	8.90	534	15.5
1ML-D1-DCI	0.98	404	4.1
1ML-D1-SB	1.24	363	1.9
1ML-D1-AX	1.28	407	1.1
1ML-D1-COR	1.27	430	2.4
1ML-D0-LMC	1.00	388	2.1
1L-D1-DCI	0.30	275	3.6
1L-D1-SB	0.27	172	0.6
1L-D1-AX	0.42	272	1.3
1L-D1-COR	0.36	275	5.8
1L-D0-LMC	0.31	172	1.8
1L-1AX-DCI	0.78	388	1.3
1L-1AX-COR	0.51	325	3.8
1H-1AX-LMC	6.72	564	15.1

Note: $1 mA/ft^2 = 1.08\ \mu A/cm^2$; $1\ lbs/yd^3 = 0.59\ Kg/m^3$

Using the Cl^- content as the predictor variable for i_{corr}, the calculated R^2 was 59.1% (r = 76.9%) including the data representing specimen 1H-D1-AX which had a microcrack in the concrete above the rebar. The influence of 1H-D1-AX was very significant as the standardized residual was 5.64. Another model was developed without specimen 1H-D1-AX. The R^2 value for the model was 90.2% (r = 95.0%), indicating a good correlation between i_{corr} and Cl^- content in lbs/yd^3 as shown in Fig. 6.3. The estimate standard error of the model is 1.099 and number of samples is 35. The regression equation is:

$$i_{corr} = 0.422 + 0.385 \text{ (Cl}^- \text{ Content)} \quad \textbf{(6-3)}$$

This model was developed for specimens with known polarization areas and which were exposed to a relatively constant relative humidity and temperature.

Evaluation of Corrosion Inhibitors

Some of the initial E_{corr} readings fell in the range of -200 to -350 mV of the CSE, all of the specimens' i_{corr} measurements were identified as actively corroding at the time of treatment. The Cl^- ion content was greater than the threshold value, with the exception of specimen 1L-D1-SB, which substantiated the i_{corr} measurements.

All specimen groups were treated in three sets over a five month period. By treating the specimen groups in phases, data from a previous set could be used to determine the best method of application for successive sets. The first set included four groups:

1) Control overlay specimens

2) One-triad, high initial corrosion current density specimens which were dried to 180°F, (82°C), at a depth of ½ in (13 mm) below the bar level, and ponded for one day (1H-1D-***).

3) Two-triad, medium-low initial corrosion current density specimens which were ponded for one day (2ML-1-***).

4) Two-triad, medium-low initial corrosion current specimens which were ponded for two days (2ML-2-***).

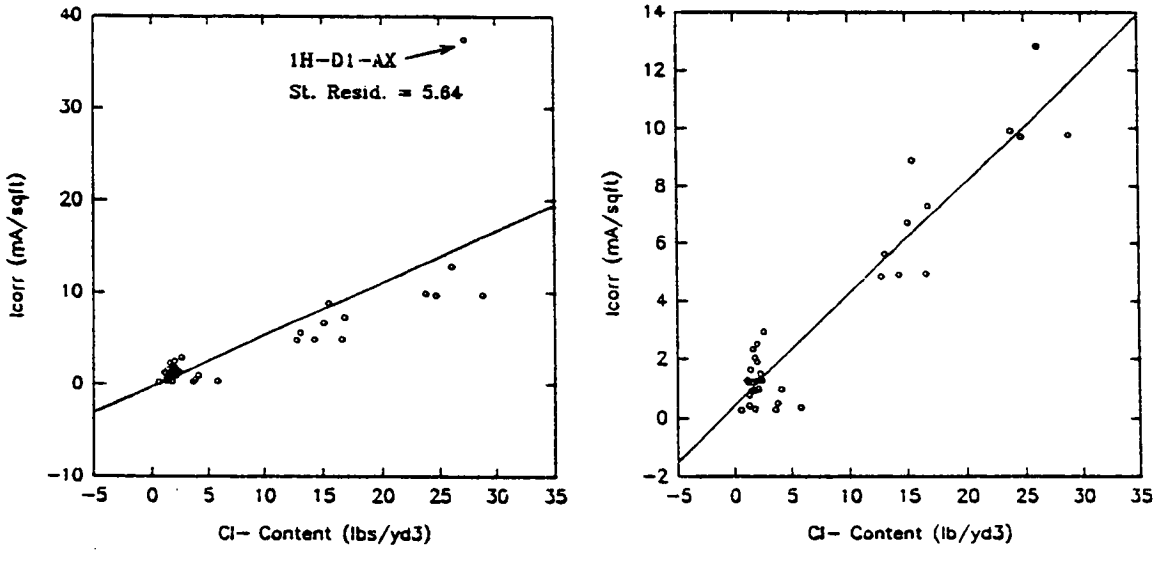

Fig. 6.3 i_{corr} vs. Cl^- Content

The effectiveness of an inhibitor treatment method was based primarily on the i_{corr} measurements obtained from the 3LP. Though the 3LP does not have a guard-ring electrode to confine the area of polarization, the 1 ft x 1 ft (0.3 m x 0.3 m) specimens have a known area of corroding steel which is approximately equal to the 3LP's contact area. E_{corr} measurements were included for comparison. The average values of i_{corr} and E_{corr} for the two top bars were considered in the case of the two-triad specimens.

Control Overlays

The post-treatment i_{corr} and E_{corr} values for the control overlays are presented in Figs. 6.4 and 6.5, respectively. The control overlays represent typical treatment methods used in current practice. One specimen (2L-0-LMC) for which the cover concrete was removed prior to overlay is included as a comparison.

Both of the 1 in (25 mm) LMC overlay (2M-LMC), where the chloride contaminated concrete was left in place, and the 2 in (51 mm) LMC overlay where the chloride contaminated concrete was removed to the bar level, (2L-0-LMC), showed an increase in i_{corr} and E_{corr} immediately after treatment. This is probably due to the increased moisture content in the specimens resulting from the overlays. Measurements taken 63 days after treatment indicate downward trends in the corrosion current densities.

The later decrease in i_{corr} an E_{corr} for 2L-0-LMC was probably caused by a combination of the specimen's drying out, an increase in the pH around the bar resulting from the fresh concrete, and the migration of chlorides into the overlay which decreased their concentration at the bar level. In the case of 2M-LMC, the initial decrease in i_{corr} and E_{corr} was probably due to the specimen's drying out as a result of the decreased permeability of the overlay.

The preformed membrane installed with the hot-mix asphalt overlay (2L-BC) and the thin polymer overlay (2L-TP) specimens were both impervious layers which prevented i_{corr} or E_{corr} measurements from being taken from the top surface. Therefore, the measurements were taken from the bottom of the specimen with the resistor(s) between the upper and lower mats of steel disconnected immediately prior to the measurements. The time period between disconnecting the resistor and taking the measurement was probably too short for the test area to reach a new equilibrium which would have excluded the portion of the i_{corr} related to macro-cell corrosion.

Both 2L-BC and 2L-TP exhibited more than a 50% decrease in corrosion current density after treatment, though neither specimen dropped below 0.2 mA/ft^2 (1.08 mA/m^2), indicate that the corrosion had not ceased. The decrease is probably due to a lack of moisture resulting from the impervious overlays. The fluctuation in the E_{corr} measurements may be due to the high resistance of the concrete resulting from the low moisture content.

High Initial i_{corr}, Dried Specimens

The post-treatment performance of the treated specimens is shown in Figs. 6.6 and 6.7. The LMC control specimen (1H-D0-LMC) displayed a 60% reduction in corrosion current density over a period of 202 days after treatment and remained almost constant at an average i_{corr} of 4.1 mA/ft^2 (43.9 mA/m^2).

The specimens treated with Alox and Cortec showed dramatic decreases in corrosion current density immediately after treatment. Since the corrosion current density of the control specimen did not decrease as rapidly, the decreases in the treated specimens may be assumed to be caused by the reaction of the corrosion inhibitors with the corrosion cells.

The high initial i_{corr} decrease of the Alox-treated specimen (1H-D1-AX) may be somewhat misleading based on the previous discussion of its initial corrosion current density. However, even if the predicted value of i_{corr}, 10.93 mA/ft^2 (117.6 mA/m^2), based on the specimens' Cl^- content is used (equation 6-4), the treatment still showed a significant decrease.

More important, sufficient quantities of the inhibitor seemed to have been absorbed into the specimen, as a result of drying, to have formed a stable metal soap layer on the rebar. This layer reduced metal dissolution so that the average i_{corr} values from 56 to 326 days after treatment was 1.8 mA/ft^2 (19.4 mA/m^2), see Fig. 6.6. This represents an 80% decrease in corrosion current density. However, it is also possible that the inhibitor seeped into a micro-crack surrounding the rebar, allowing greater quantities of the inhibitor to react with the rebar than is normally possible.

Corrosion activity in specimen (1H-D1-COR), which was treated with Cortec, ceased, as indicated by its corrosion current density, (0.20 mA/ft^2 [2.15 mA/m^2]), for the period between 56 and 229 days after treatment. The initial application of Cortec 1337 was apparently sufficient to form a monolayer over the majority of the corrosion sites to stop corrosion. After 229 days, it appears that the gaseous diffusion of the inhibitor from the overlay was not sufficient to maintain a complete monolayer and the i_{corr} values increased slightly.

The specimens treated with DCI and sodium borate (1H-D1-DCI and 1H-D1-SB, respectively) showed increases in corrosion current density immediately after treatment. Though 1H-D1-SB demonstrated a decreasing trend after the initial increase, only 1 value obtained 153 days after treatment, was lower than the initial i_{corr}. However, the data collected by Webster *et al.* (44) in a preliminary study suggested that the effectiveness of sodium borate is pH dependent. The pH of chloride-contaminated corrosion products might not be sufficiently high for the sodium borate to act as an effective inhibitor.

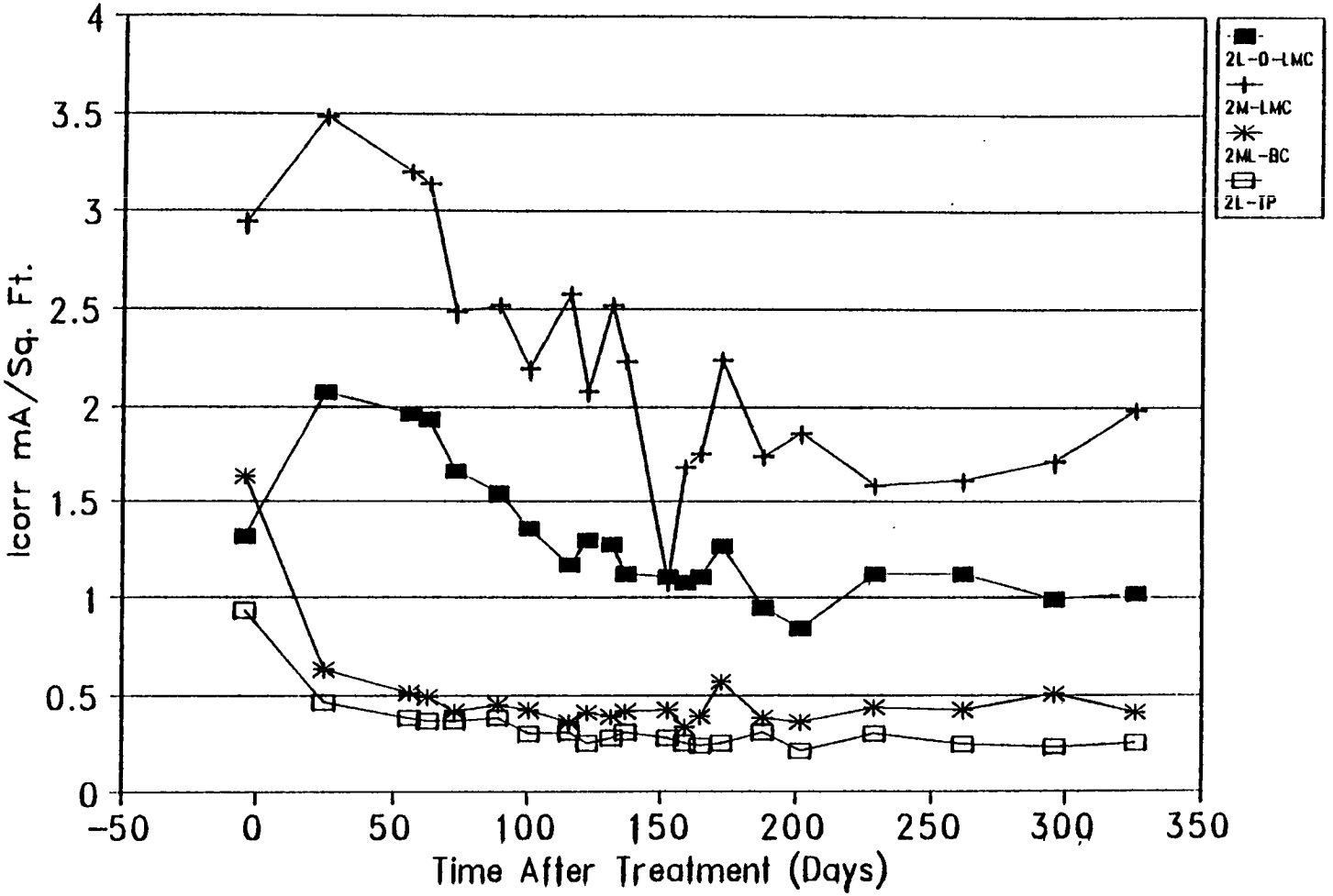

Fig. 6.4 i_{corr} estimates for Control Overlay, with Low initial Corrosion Rates

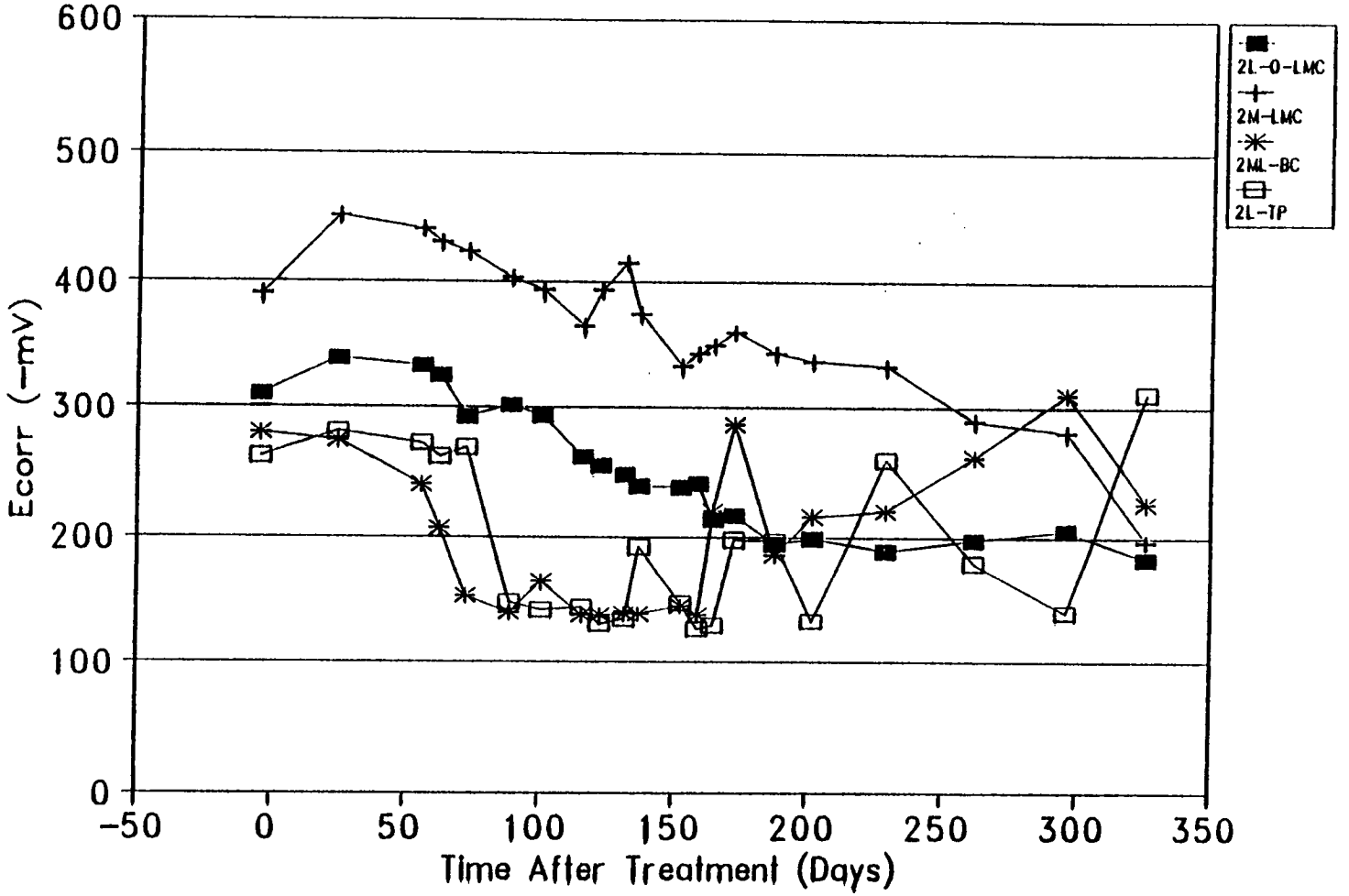

Fig. 6.5 E_{corr} measurements for Control Overlays with Low Initial Corrosion Rate Densities

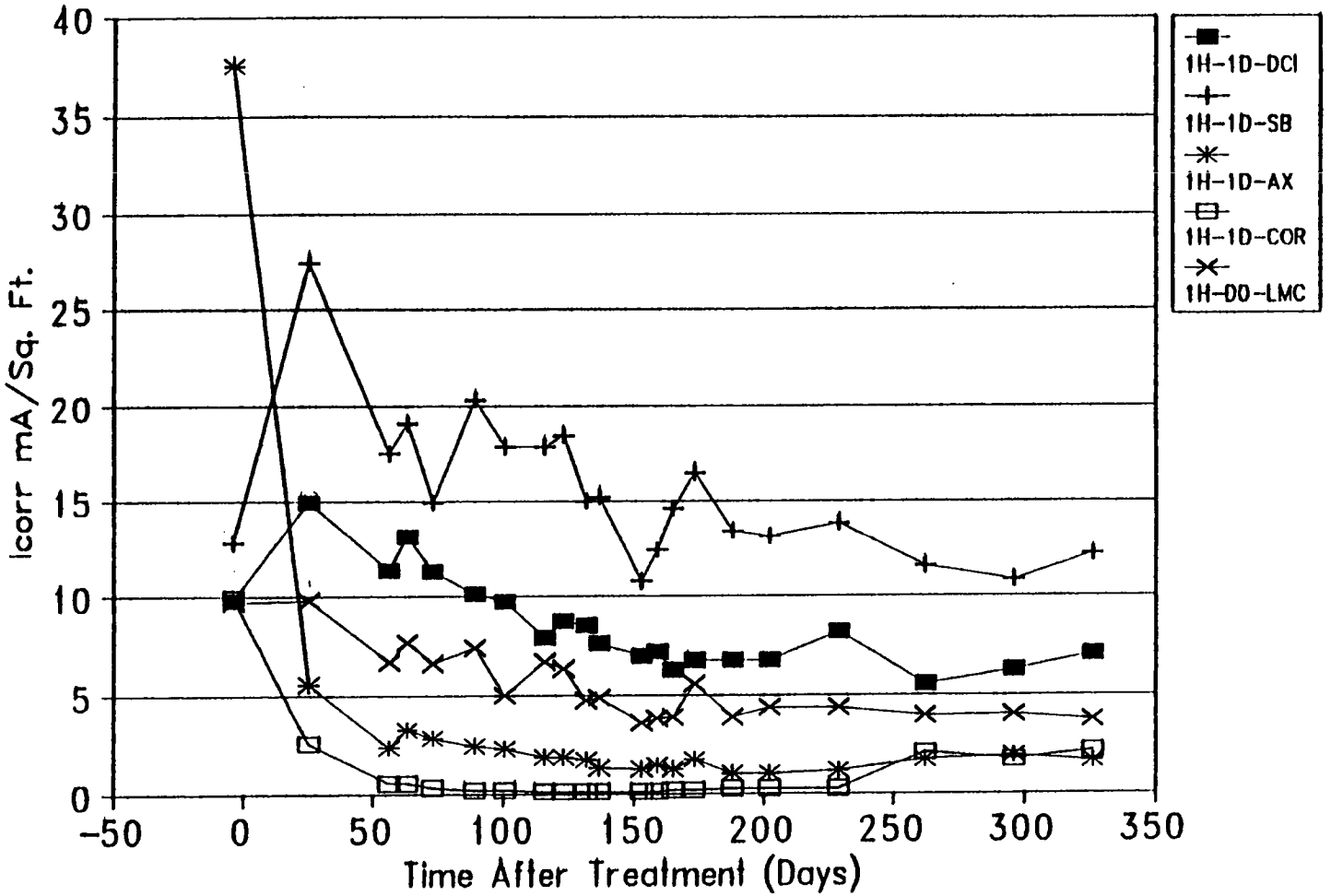

Fig. 6.6 i_{corr} Estimates for Dried Specimens with High Initial Corrosion Rate Densities

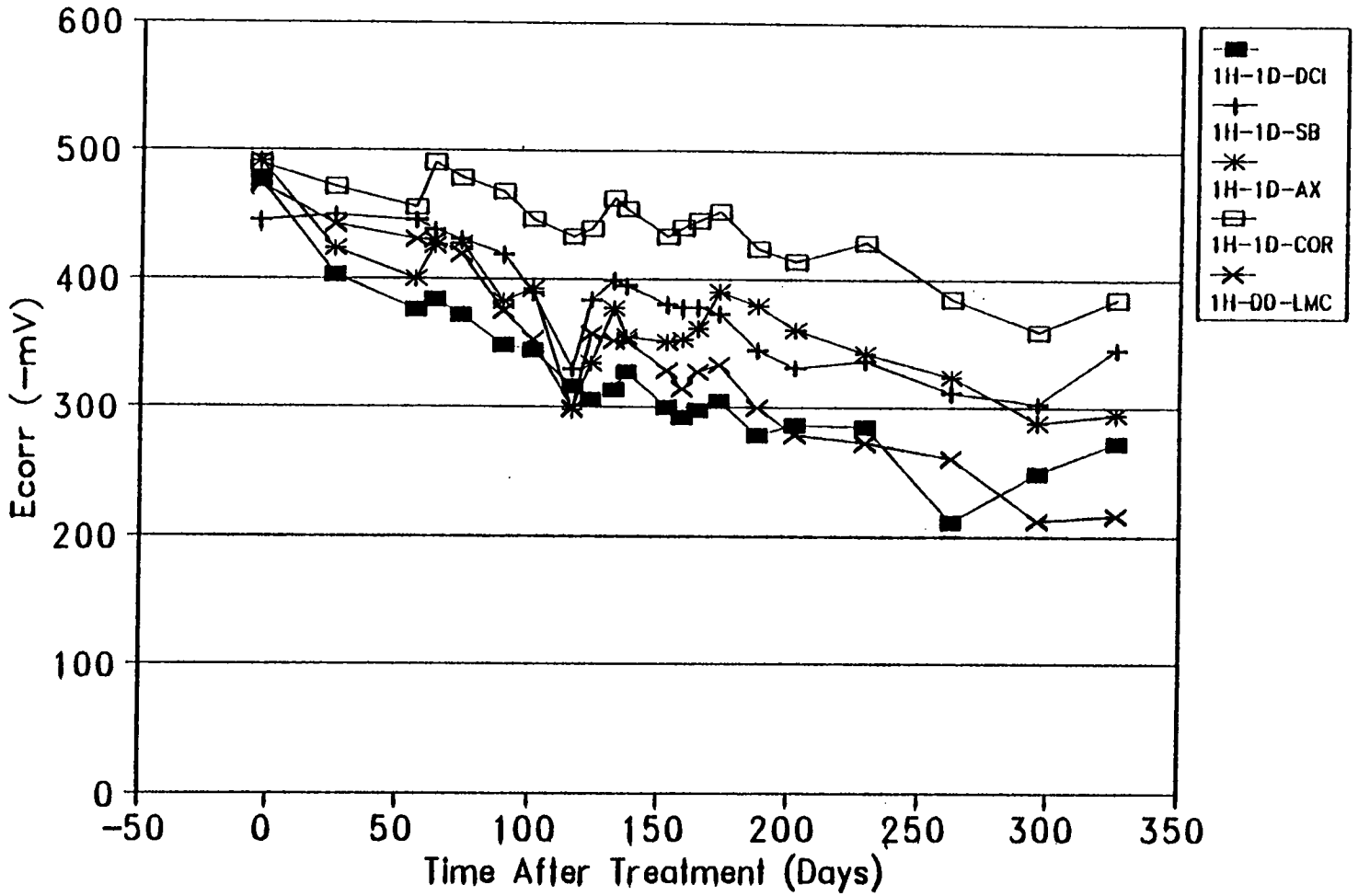

Fig. 6.7 E_{corr} Estimates for Dried Specimens with High Initial Corrosion Rate Densities

The specimen treated with DCI (1H-D1-DCI) showed a relatively consistent decrease in i_{corr} after its initial increase until 159 days after treatment; at that point it appeared to be stabilizing around 6.8 mA/ft^2 (73.2 mA/m^2). The E_{corr} measurements showed a fairly consistent increase until 262 days after treatment, after which they became more negative.

Overall, DCI did not perform as well as the control specimen. The ineffectiveness of DCI may be due to the short ponding period or the low concentration of calcium nitrite used for ponding.

An effort was made to estimate the Cl^-/NO_2 ratio at the bar level for specimens treated with DCI. The Cl^- content was 28.8 lbs/yd^3 (17.3 kg/m^3) immediately prior to treatment. As presented in the previous section, mortar cubes dried to 175°F (79.4°C) had a 9.7% by volume absorption of monomer. From this absorption percentage it was estimated that the nitrite content at the bar level was 1.9 lbs/yd^3 (1.1 kg/m^3), resulting from the application of a 0.1 M calcium nitrite solution as presented in Equation 6.5.

$$Nitrite\ (NO_2^-)\ content = A_v \times U_{wi} \times I_{con} \times \frac{91.9}{132} \qquad (6\text{-}4)$$

where,

A_v = Percent absorption of the concrete by volume expressed as a decimal.

U_{wi} = Unit weight of the inhibitor, 8.5 lbs/gal (1030 kg/m^3).

I_{con} = Inhibitor concentration percent by weight, expressed as a decimal, 0.1 M = 1.32% calcium nitrite.

91.9/132 = Molecular ratio of nitrite to calcium nitrite.

Research conducted by Berke and Rosenberg (41) concluded that for inhibition to occur, the chloride:nitrite ratio must be less than 2. For the DCI-treated specimen, the estimated chloride nitrite ratio was 15.

Medium-Low Initial i_{corr}, 1 day Ponding

The i_{corr} an E_{corr} measurements for the specimens with medium-low initial corrosion current densities were treated with a 1 day ponding application and inhibitor-modified overlay are shown in Figs. 6.8 and 6.9, respectively. Though the initial corrosion current densities were somewhat divergent, the group displays similar trends to the previous group. Although all of the treatments demonstrated a reduction in i_{corr}, the specimen treated with Alox (2ML-1-AX) showed the most significant improvement.

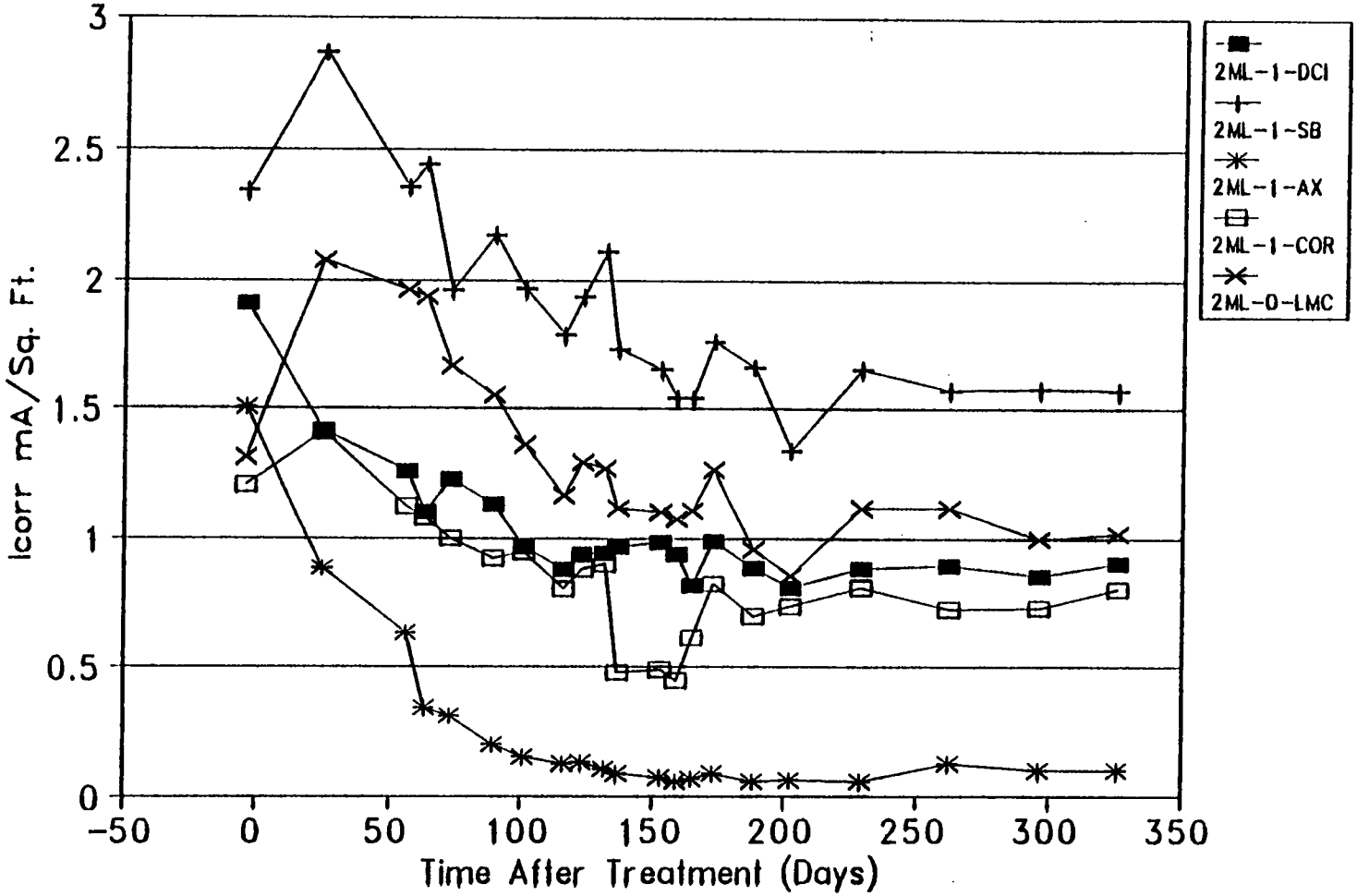

Fig. 6.8 i_{corr} Estimates for 1 day Ponding Specimens with Medium-Low Initial Corrosion Rate Densities

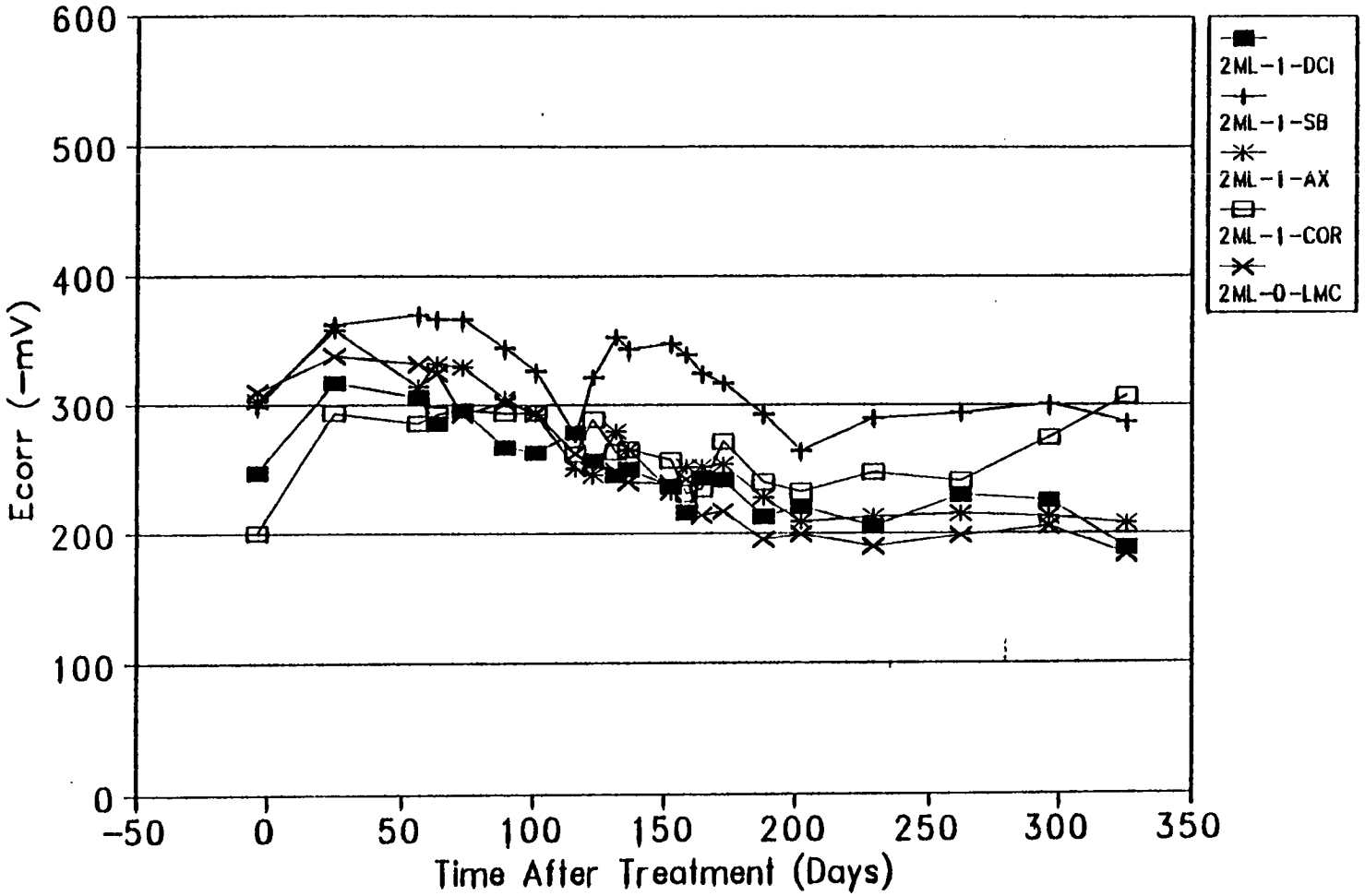

Fig. 6.9 E_{corr} Values for 1 Day Ponding with Medium-Low Initial Corrosion Rate Densities

The mean i_{corr} for the Alox treatment was 0.097 mA/ft^2 (0.10 μA/cm^2) from 89 days after treatment till the end of the study. The corresponding E_{corr} approached 200 mV. These measurements indicate the cessation of corrosion activity in the specimen. The improved performance of Alox in relation to the other inhibitors may be due to its carrier solvent, alcohol. The alcohol may displace some of the capillary water allowing more of the inhibitor to be absorbed. This effect would not have been noticeable in the dried specimens.

The specimens treated with Cortec (2ML-1-COR), DCI (2ML-1-DCI), and the LMC control (2ML-0-LMC) performed almost identically. The specimen treated with DCI had the best numeric improvement, stabilizing at approximately 1 mA/ft^2 (1.08 μA/m^2) below its pretreatment corrosion current. The improved performance of DCI is probably related to the relatively low initial chloride content, 2.0 lbs/yd^3 (1.2 kg/m^3), which required a lower concentration of calcium nitrite to compete with the Cl^- ions for the Fe^{++} ions in order to form a protective layer. Additionally, the initial drop in i_{corr} suggested an inhibitive action since the specimen did not demonstrate the same initial increase as the control.

The chloride:nitrite ratio for DCI treated specimens was estimated in an effort to confirm this theory. Concrete will lose ½% to 3% by weight of evaporable water if it is maintained at a relative humidity of 50% (45). Using a 3% water loss in air drying, and assuming re-saturation of the exposed concrete at the bar level with a 0.1 M calcium nitrite solution, a nitrite concentration of 1.1 lbs/yd^3 (0.66 kg/m^3) can be estimated using Equation 6.6:

$$Nitrite\ (NO_2^-)\ Content = A_w \times W_c \times I_{con} \times \frac{91.9}{132} \qquad (6\text{-}5)$$

where,

A_w = Percent absorption of the concrete by weight expressed as a decimal.

W_c = Unit weight of the concrete, 145 lbs/ft^3 (2349 kg/m^3).

I_{con} = Inhibitor concentration percent by weight, expressed as a decimal, 0.1 M = 1.32% calcium nitrite.

91.9/132 = Molecular ratio of nitrite to calcium nitrite.

The corresponding chloride:nitrite ratio based on this estimation is 1.8 This indicates sufficient nitrite content to control corrosion (41).

The Cortec treatment performed well. However, both the corrosion current density and potential showed an upward trend toward the end of the monitoring period.

The sodium borate treatment also seems somewhat effective in this case. The specimen

stabilized at 1.57 mA/ft^2 (1.69 μA/cm^2), an improvement of 0.77 mA/ft^2 (0.83 μA/cm^2) over its pre-treatment corrosion current density. However, this reduction was not sufficient to move it into the next lowest category for time to expected damage.

Medium-Low Initial i_{corr}, 2-Day Ponding

The progression of post-treatment i_{corr} and E_{corr} group of measurements for the medium-low initial i_{corr} two-day inhibitor ponding group is presented in Figs. 6.10 and 6.11, respectively. A comparison of the overall performance of this group with the previous group, which was ponded for only one-day, indicates no significant reduction in corrosion current density. Since neither set of specimens was dried, the capillaries were probably filled with water, allowing a finite amount of absorption independent of the ponding time. Based on these observations, additional treatments utilizing a two-day ponding period were terminated.

The specimen treated with Alox displayed the greatest decrease in corrosion current density until 159 days after treatment, when it experienced an abrupt increase in i_{corr} and E_{corr}. The increase is probably due to a failure of some portion of the metal soap layer.

It was suspected that since the remainder of the rebar was largely passive, the area where the failure occurred experienced accelerated corrosion as a result of the high anode-to-cathode ratio. However, sufficient quantities of the inhibitor were apparently present to allow a partial healing of the layer. Overall, this may be an example of the reaction caused by a dangerous inhibitor.

The specimen treated with sodium borate also displayed a performance unlike the previous group. In this case, the inhibitor seems to have been completely ineffective. The final i_{corr} value was 73% higher than the pre-treatment value, even though the Cl^- ion content was lower than that in the previous group.

In all 3 treatment groups examined thus far, the control overlay has had the most noble final E_{corr} measurement. This may be due to the fact that the inhibitors block the corrosion process, while in the case of the control the reduction in corrosion current density was most likely due to a decrease in the Cl^- ion concentration.

Medium Initial i_{corr}, 1-Day Ponding

The post-treatment i_{corr} and E_{corr} for the specimens with medium initial i_{corr} values which were exposed to surface applied inhibitors for one-day are presented in Figs. 6.12 and 6.13, respectively. These specimens were included in the second treatment set.

An untreated control specimen (1M-CON) with the chloride-contaminated cover concrete left in place was included in this group of specimens. The decrease in its corrosion current density in the first 50 days after treatment of the other specimens is due to the temporary removal of the specimen from the 6% NaCl ponding cycle which allowed the specimen to

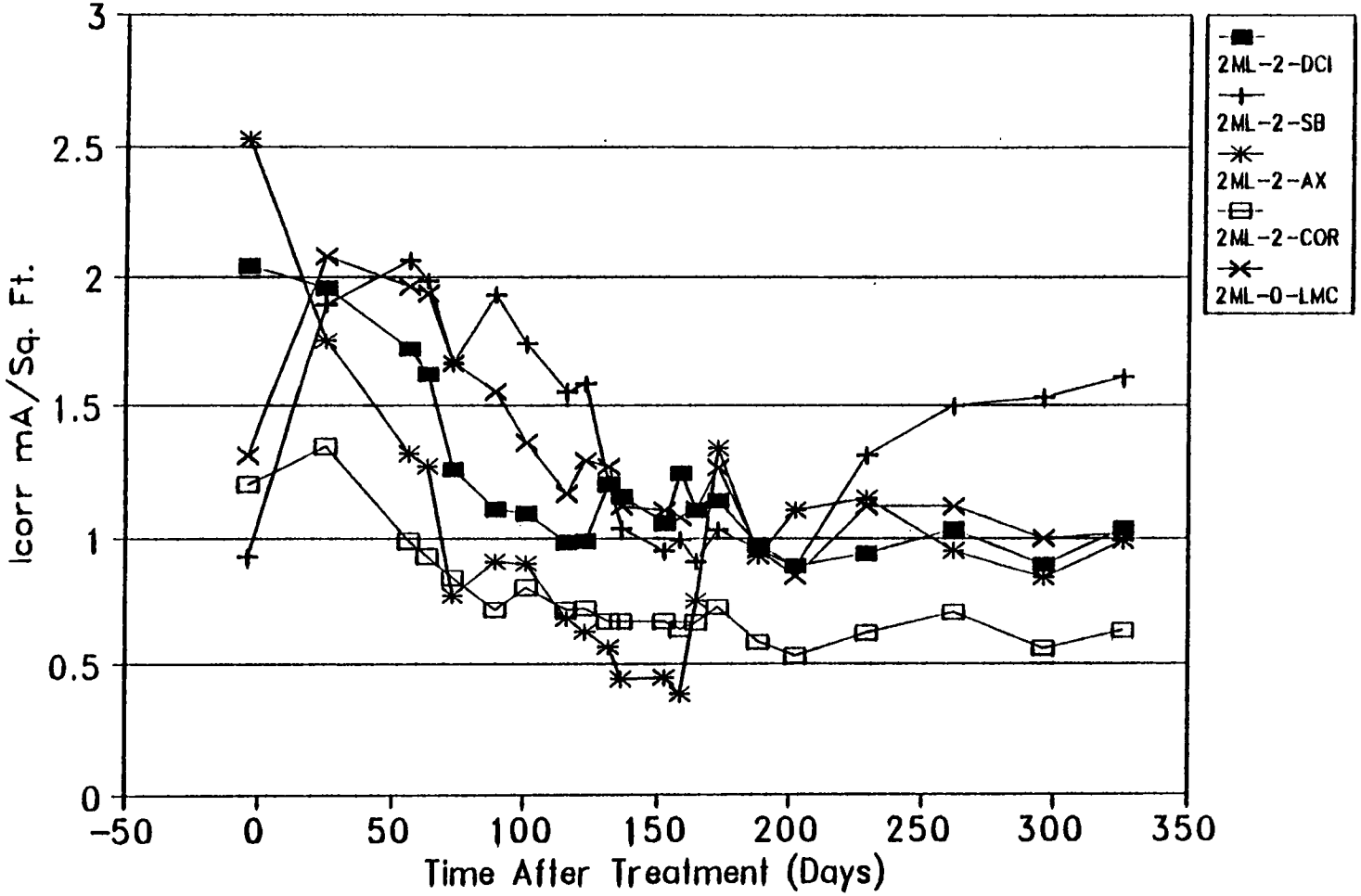

Fig. 6.10 i_{corr} Estimates for Two-Day Ponding Specimens with Medium-Low Initial Corrosion Rate Densities

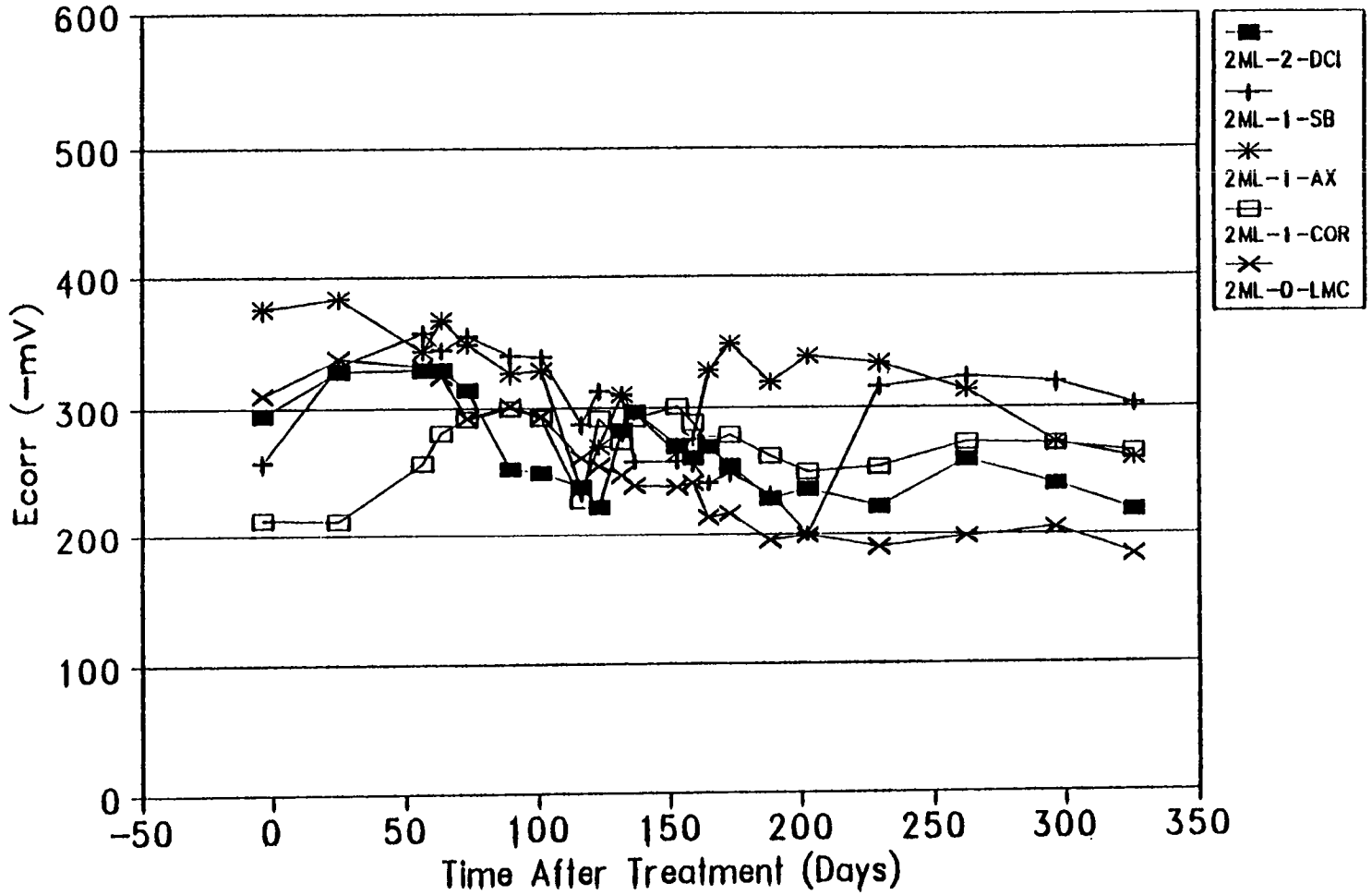

Fig. 6.11 E_{corr} Values for Two-Day Ponding Specimens with Medium-Low Initial Corrosion Rate Densities

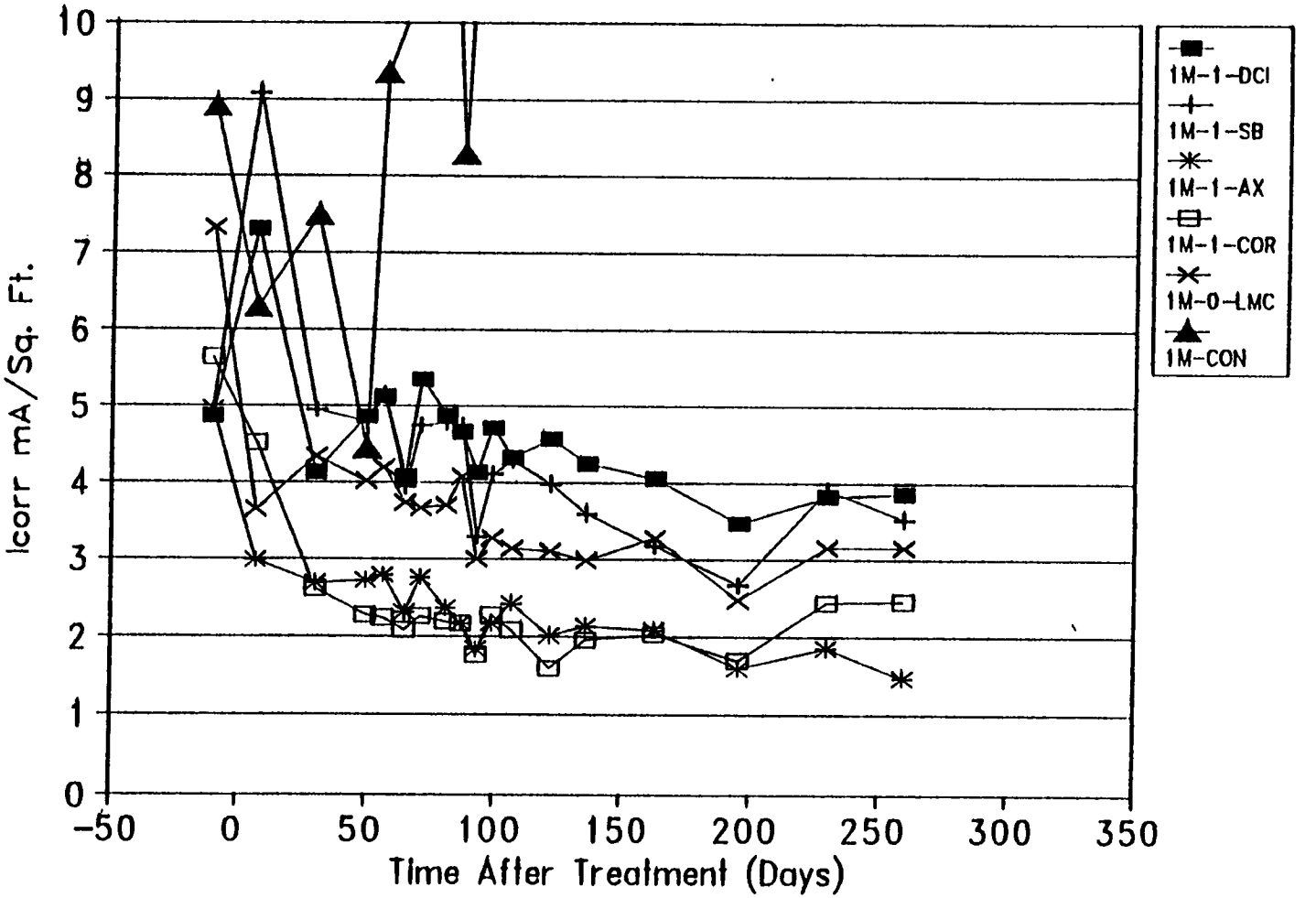

Fig. 6.12 i_{corr} estimates for One-Day Ponding Specimens with Medium Initial Corrosion Rate Densities

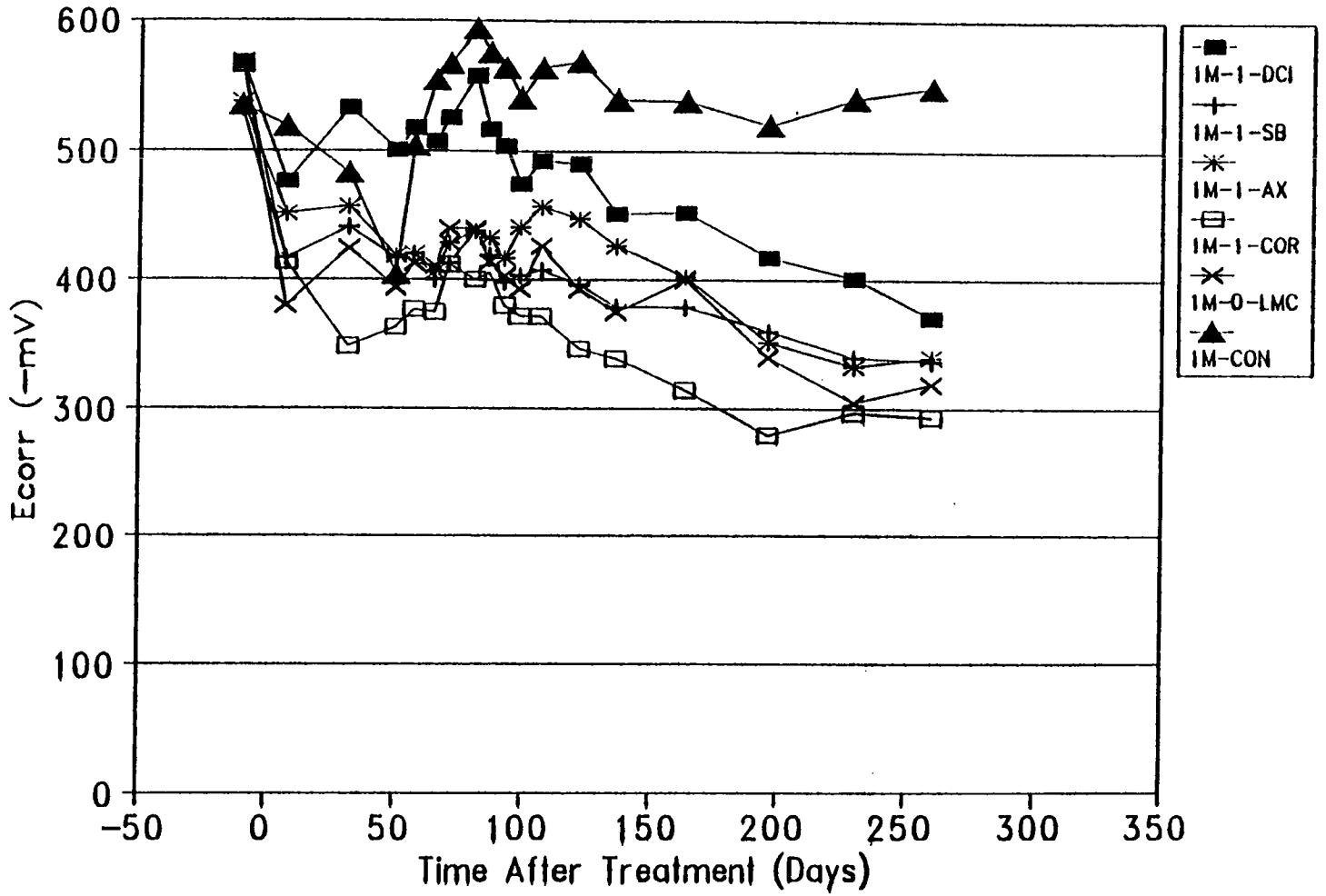

Fig. 6.13 E_{corr} Values for One-Day Ponding Specimens with Medium Initial Corrosion Rate Densities

dry out. The specimen was used to demonstrate corrosion current density measurement devices at an AASHTO convention during that period. A crack was produced in the specimen from the expanding corrosion products 99 days after the treatment of the other specimens. A corrosion current density of 15.0 mA/ft^2 (16.2 μA/cm^2) was measured at that time.

All specimens, for which the chloride-contaminated cover concrete was removed showed improvement after treatment. The specimens treated with Alox and Cortec performed almost identically, tending to fluctuate around a corrosion current of 2.0 mA/ft^2 (2.2 μA/cm^2) from 59 days after treatment till the conclusion of the investigation. This represents approximately a 60% reduction in i_{corr}. The LMC overlay, without any inhibitors, showed a 57% reduction in i_{corr} by the end of the monitoring period. The specimens treated with DCI and sodium borate each improved by about 1 mA/ft^2 (1.08 μA/cm^2) after treatment. However this improvement was less than the controls. The E_{corr} measurements for the DCI treatment did improve, and were more noble than the LMC control.

Medium-Low Initial i_{corr}, Dried Specimens

The post-treatment progression of i_{corr} and E_{corr} values for the group of specimens with medium-low initial corrosion current densities which were dried to 180°F (82°C) at a depth of ½ in (13 mm) below the bar level are shown in Figs. 6.14 and 6.15, respectively. The reduction in i_{corr} estimates shown for all specimens except 1ML-D1-AX prior to 196 days after treatment are inaccurate. The resistors connecting the upper and lower mats or reinforcing steel on those specimens were discontinuous. The resistors were replaced between 163 and 196 days after treatment and all other specimens were checked for a similar problem. The rise in i_{corr} and E_{corr} seen in those specimens 196 days after treatment clearly demonstrates the effect of an increase in anode-to-cathodic ratio. Overall, Alox was the best performing inhibitor in this group.

Low Initial i_{corr}, Dried Specimens

i_{corr} and E_{corr} measurements for the dried specimens with low initial corrosion current densities are presented in Figs. 6.16 and 6.17, respectively. The highest pre-treatment i_{corr} for this group of specimens was 0.42 mA/ft^2 (0.45 μA/cm^2) and the highest E_{corr} was -275 mV. Effectively, these specimens were barely corroding prior to treatment. Considering those observations, it was not surprising that the corrosion current density in the majority of the specimens increased after treatment.

One exception to this trend was the specimen treated with DCI (1l-D1-DCI). In this case, it acted to repress the initiation of corrosion. This explains the reported effectiveness of calcium nitrite as a corrosion inhibitor when included in the concrete during initial construction. Treatments utilizing DCI seem to be effective on areas with low initial corrosion currents and may be effective at higher rates if a sufficient concentration of the inhibitor can be introduced to the corroding area. The concentration used for surface

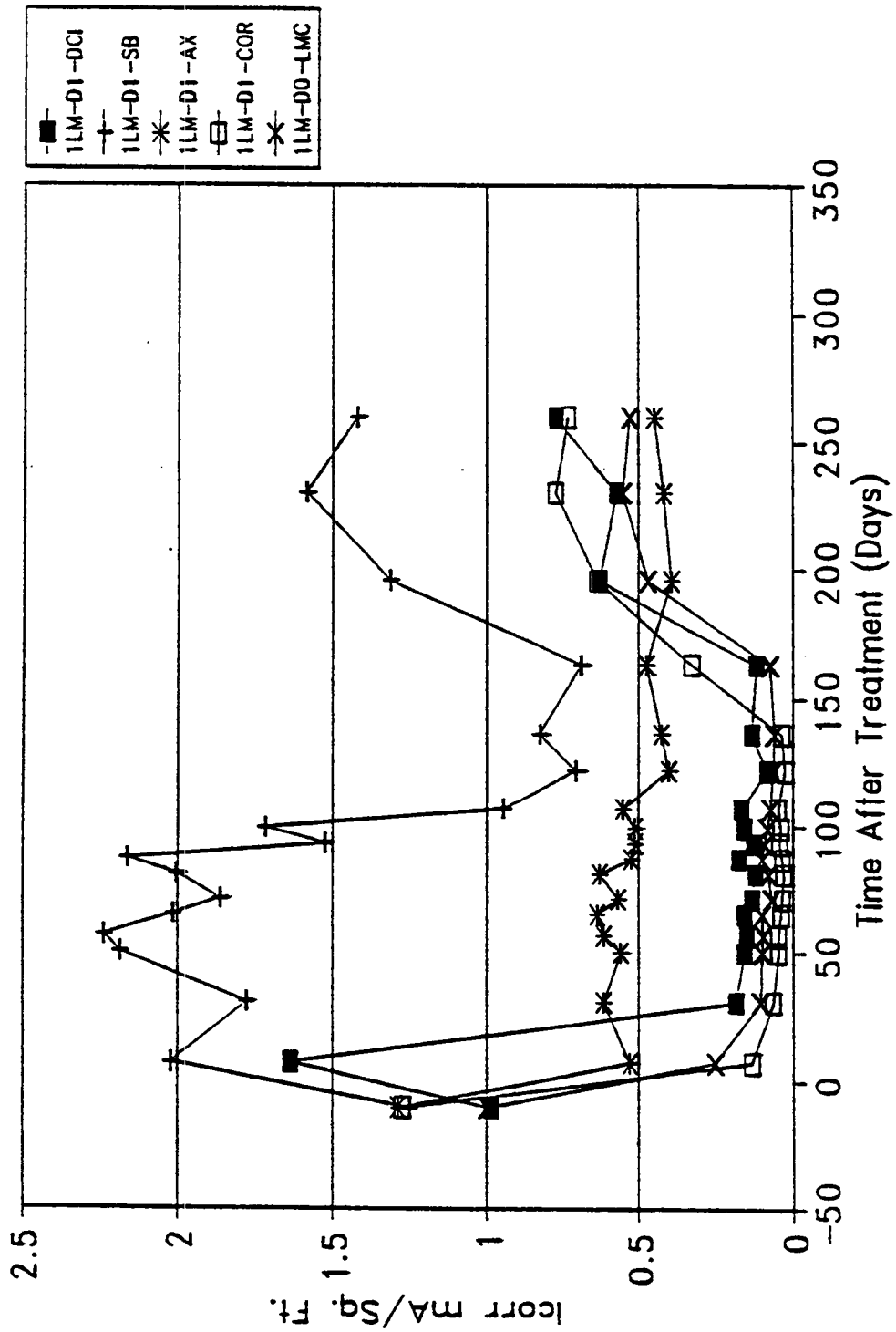

Fig. 6.14 i_{corr} Estimates for Dried Specimens with Medium-Low Initial Corrosion Rate Densities

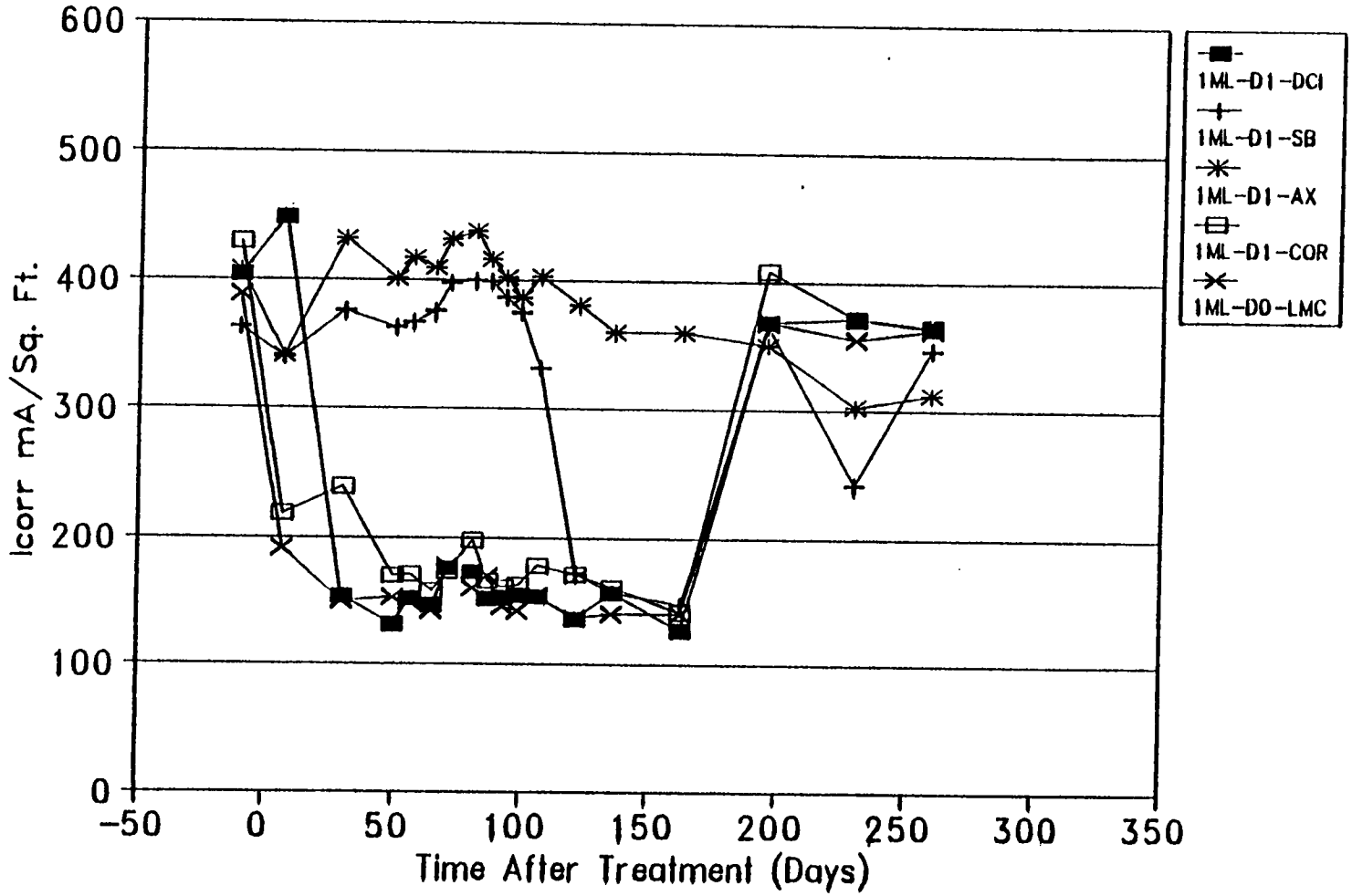

Fig. 6.15 E_{corr} Values for Dried Specimens with Medium-Low Initial Corrosion Rate Densities

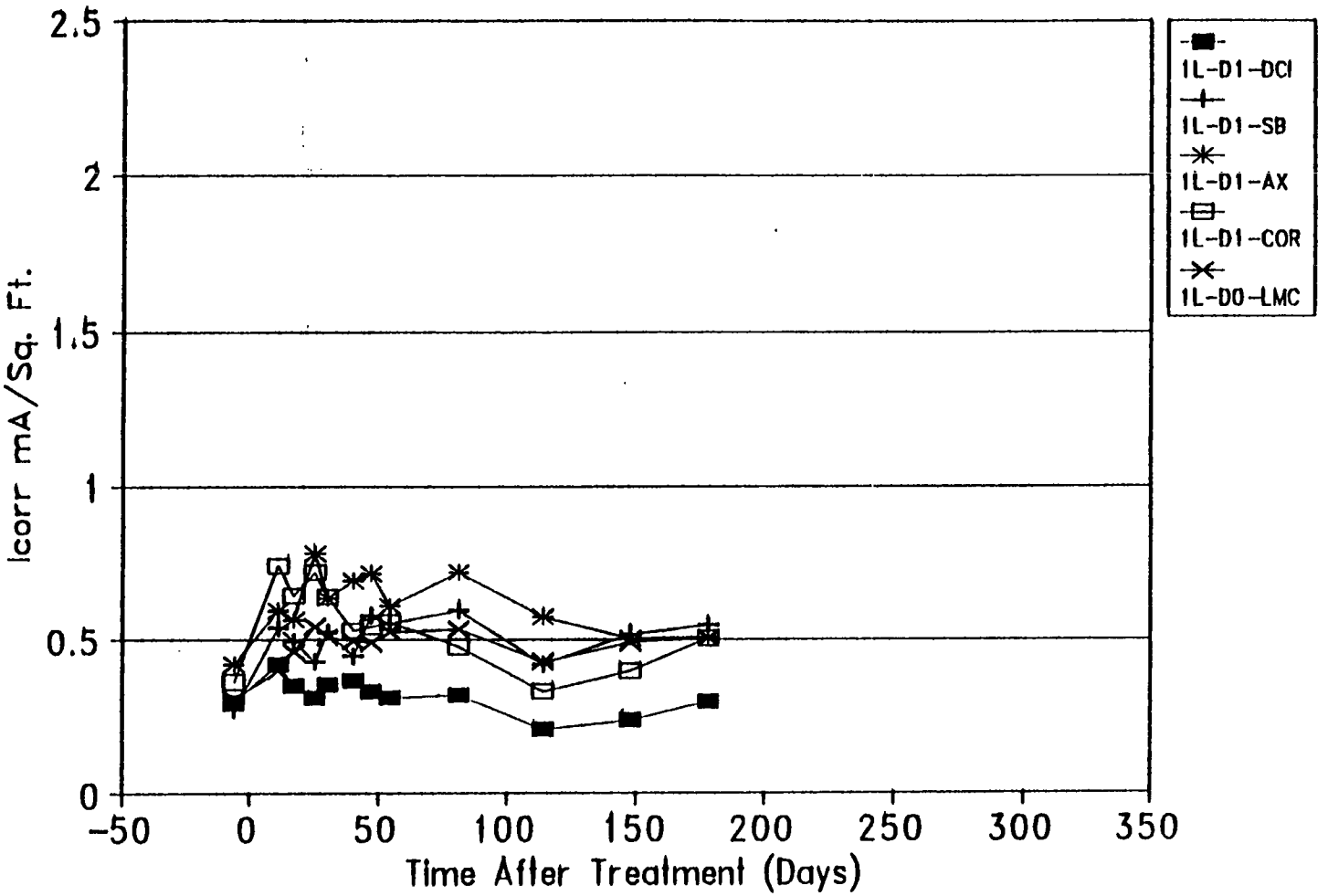

Fig. 6.16 i_{corr} Estimates for Dried Specimens with Low Initial Corrosion Rate Densities

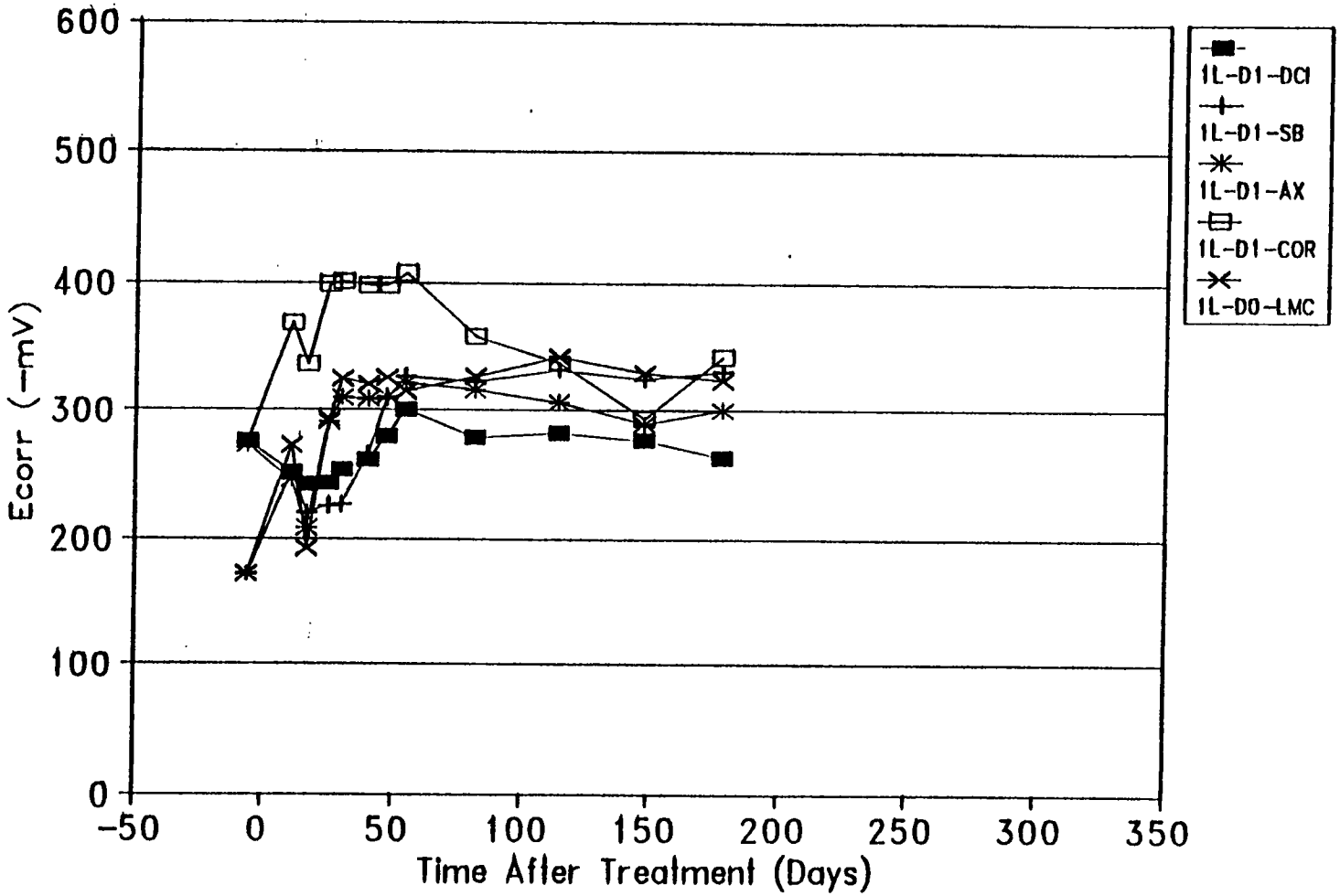

Fig. 6.17 E_{corr} Values for Dried Specimens with Low Initial Corrosion Rate Densities

application on the small scale specimens was 0.1 M as recommended in research performed by Dressman *et al.* (46). As reported earlier in this report, the concentration used in a similar study on U. S. 460 in Virginia was 15% solids by weight which is 11.4 times stronger than 0.1 M.

The chloride content prior to treatment, the estimated nitrite content at the bar level, the chloride:nitrite ration, and the performance relative to the control are presented in Table 6.7 for each specimen treated with DCI. An examination of the specimens with chloride:nitrite ratios less than 2, reveals that all of these specimens performed better than the LMC control. This supports the theory that DCI would be effective if sufficient concentrations of nitrite could be introduced into the treated area. The application of a 15% calcium nitrite solution to a non-dried treatment area should provide sufficient nitrite to control corrosion up to a Cl^- concentration of 24.9 lbs/yd^3 (14.9 kg/m^3) as calculated by Equation 6.6.

Table 6.7 Chloride:Nitrite Ratios for Specimens Treated with DCI.

Specimen Code:	Cl^- Content (lbs/yd^3)	Estimated NO_2^- Content (lbs/yd^3)	Cl^-:NO_2^- Ratio	Performed better than LMC?
1H-D1-DCI	28.8	1.9	15.0	no
2ML-1-DCI	2.0	1.1	1.8	yes
2ML-2-DCI	1.8	1.1	1.6	yes
1M-1-DCI	12.8	1.1	11.6	no
1ML-D1-DCI	4.1	1.9	2.2	no
1L-D1-DCI	3.6	1.9	1.9	yes

Note: 1 lbs/yd^3 = 0.59 Kg/m^3

Alox Ponding and Modified Overlay Combinations

Since Alox is a hydrocarbon, it cannot be included as an admixture in a concrete mix. Therefore, only the initial concentration of Alox absorbed by the specimen during ponding will be available to form a protective layer on the reinforcing steel which makes the long-term effectiveness of the treatment questionable. For this reason, three additional specimens were treated; their post-treatment i_{corr} and E_{corr} measurements are presented in Figs. 6.18 and 6.19.

All three specimens were ponded with Alox; one was overlayed with LMC, one with a Cortec-modified concrete, and one with DCI-modified concrete. Sodium borate was excluded since previous sets showed it to be an ineffective corrosion inhibitor for the application investigated at this point.

Specimen 1H-1AX-LMC displayed an 84% reduction in i_{corr} during the monitoring period. Unfortunately, the initial corrosion current densities on the remaining two specimens were too low to show any meaningful change during the monitoring period.

Summary of Inhibitor Treatment Performance

In this section the most successful inhibitors in abating corrosion chemically were identified as well as the most effective method for their application.

Two inhibitors, Alox and Cortec, demonstrated their ability to reduce corrosion, regardless of the pre-treatment i_{corr} values. Alox seemed to perform better than Cortec if the specimens were not dried prior to ponding, probably because the ethyl alcohol used as a solvent displaced some of the capillary water and allowed more of the inhibitor to be absorbed.

The LMC controls demonstrated the next best overall performance. Removing the chloride-contaminated concrete above the rebar reduced the driving potential for the corrosion reaction. In addition, the fresh concrete helped to reestablish the high pH normally found in uncontaminated concrete.

DCI proved to be an effective treatment when applied to specimens with low initial corrosion currents. Its lack of performance at higher i_{corr} densities may be concentration-dependent.

Although some specimens treated with sodium borate showed improvement, the inhibitor did not perform as well as the LMC controls.

No increased inhibitive effect could be discerned for non-dried specimens with similar i_{corr} values ponded for two days as compared to specimens ponded for only one day. The effectiveness of drying appears to be dependent on the type of inhibitor used and is discussed later in the report.

In order to better evaluate the performance of the inhibitors, an effort was made to separate the portion of reduction in i_{corr} due solely to the inhibitor from the improvement resulting from removing the chloride-contaminated concrete.

Due to the variation in initial corrosion current densities, Equation 6-1 was used to calculate the percent change in i_{corr} for the controls. Equation 6-7 was developed to determine the percent change of a treatment resulting from the application of the inhibitor.

$$\%Change_{inhb} = 100 \; x \; \frac{(\%Change_{treatment} - \%Change_{control})}{\%Change_{control}} \qquad (6\text{-}6)$$

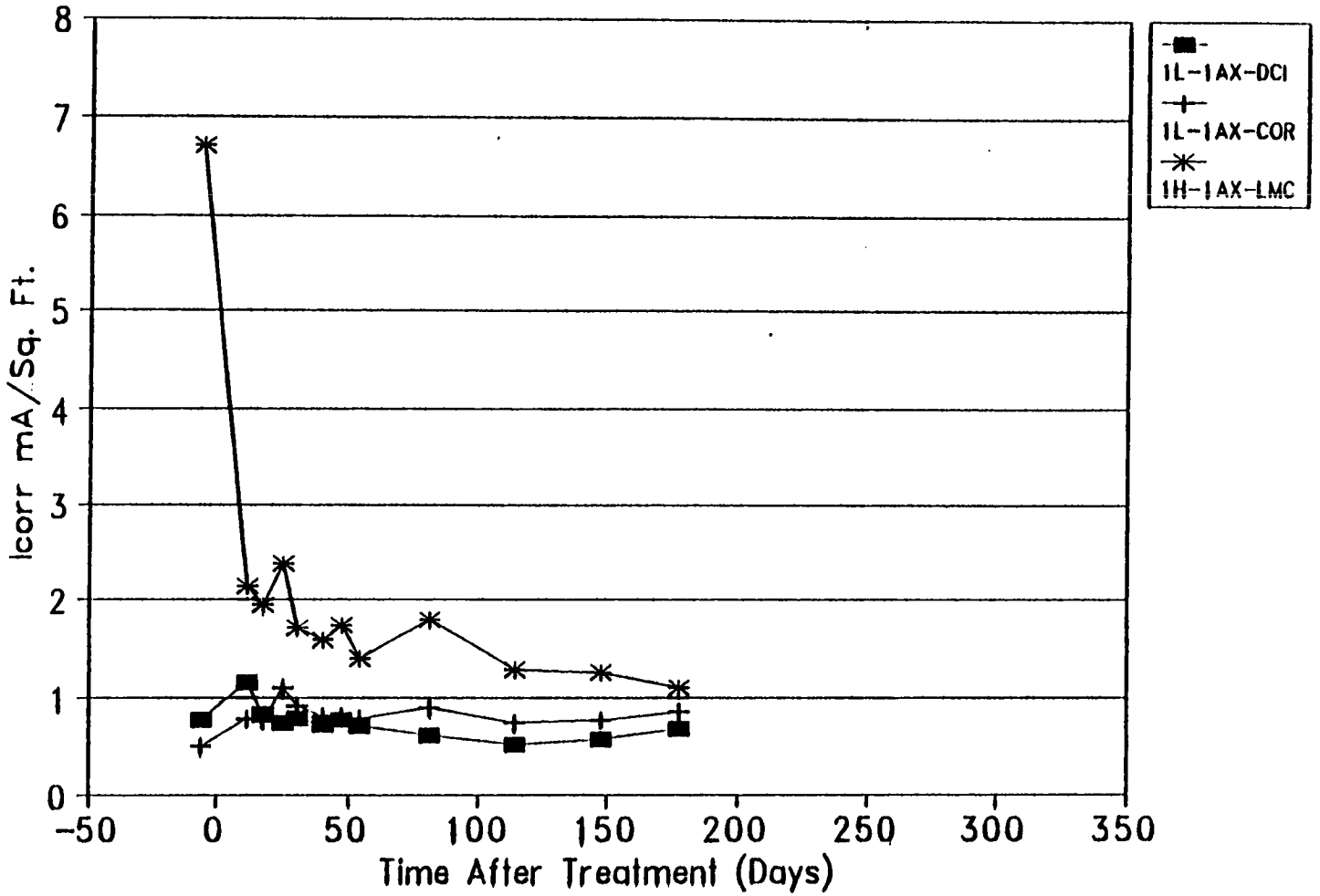

Fig. 6.18 i_{corr} Estimates for Alox Ponding and Modified Overlay Combinations

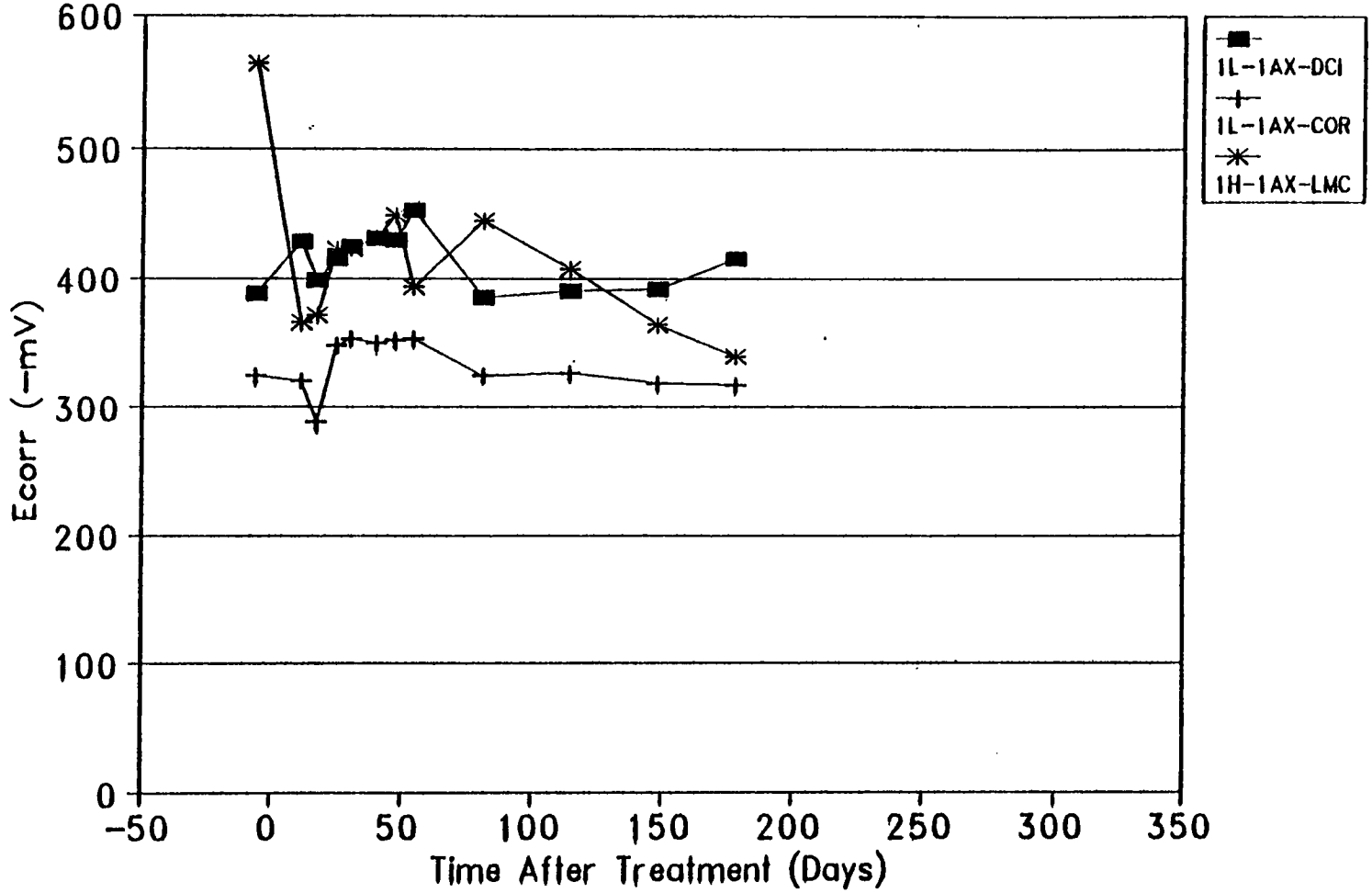

Fig. 6.19 E_{corr} Values for Alox Ponding and Modified Overlay Combinations

The reduction in i_{corr} was found to be highly variable and dependent on the initial corrosion current density as shown in Figs. 6.20 and 6.21. Specimens with medium initial i_{corr} values showed the greatest initial reduction. Specimens with high initial corrosion current densities showed a time dependent reduction. Therefore, corrections based on the percent change of the controls could lead to large errors in the estimation of the inhibitor performance unless their initial i_{corr} values were very close.

The relationship between Cl^- concentration and i_{corr} represents an alternative method to estimate inhibitor effectiveness. Chloride samples were taken from 1H-D0-LMC and 1ML-0-LMC to determine the chloride content at the bar level. A comparison was made between the measured and predicted i_{corr} values based on the Cl^- contents. For specimen 2L-0-LMC, the measured i_{corr} was 1.02 mA/ft^2 (1.10 μA/cm^2) and the predicted value was 0.92 mA/ft^2 (10.7 μA/cm^2). While for 1H-D0-LMC, the measured i_{corr} was 3.73 mA/ft^2 (4.02 μA/cm^2) and the predicted value was 5.58 mA/ft^2 (6.02 μA/cm^2). The Cl^- contents for the specimens are shown in Appendix C, Table C-15. The predicted i_{corr} values are presented in Table 6.8.

Table 6.8 Estimation of the reduction in i_{corr} resulting from the application of corrosion inhibitors.

Specimen	Measured i_{corr} (mA/ft^2)	Predicted i_{corr} (mA/ft^2)	Difference (mA/ft^2)	Percent Reduction[1] (Inhibitor)
1H-D1-DCI	7.06	4.15	-2.91	-29.8%
1H-D1-SB	12.1	4.12	-8.07	-62.9%
1H-D1-AX	1.65	5.74	4.09	37.4%[2]
1H-D1-COR	2.1	5.93	3.83	38.6%

Note: 1 mA/ft^2 = 10.8 μA/cm^2

1 Percent Reduction was calculated by dividing the difference between the predicted and measured i_{corr} rates by the pre-treatment corrosion current density. A negative percent reduction indicates that the reduction of i_{corr} was less than what would be expected from the removal of the chloride-contaminated concrete with no inhibitor applied.

2 The predicted initial i_{corr} of 10.9 mA/ft^2 (11.8 μA/cm^2) was used to arrive at this percentage. If the measured i_{corr} of 37.4 mA/ft^2 (40.5 μA/cm^2) is used, the reduction is 10.9%. The change was made based on earlier observations of the specimens' measured initial i_{corr}.

As shown in Table 6.8, both Alox and Cortec have a sufficient effect on corrosion current density beyond that obtained from removing the chloride contaminated concrete only, and thus should be included in Phase III evaluation.

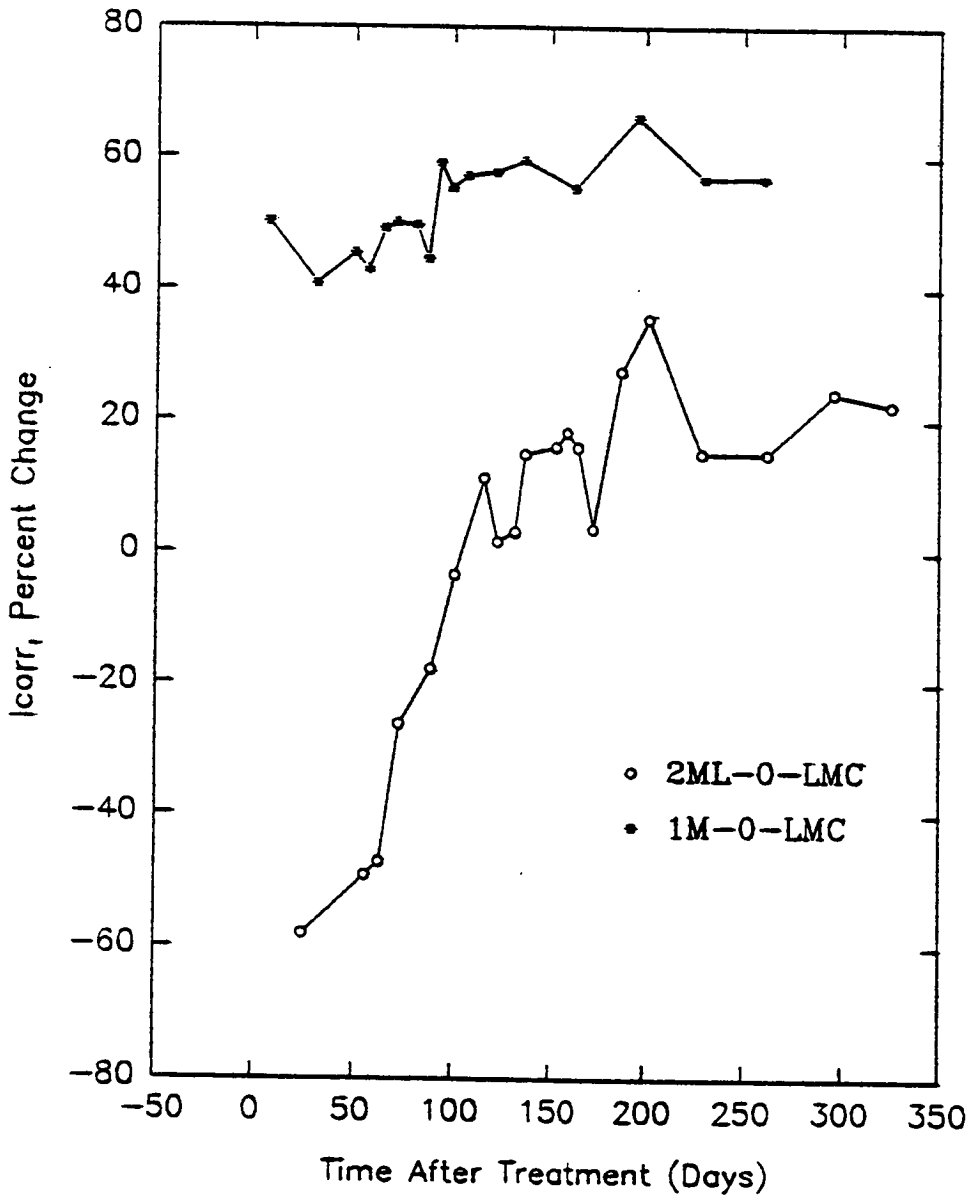

Fig. 6.20 i_{corr}, Percent Change for Non-Dried Specimens

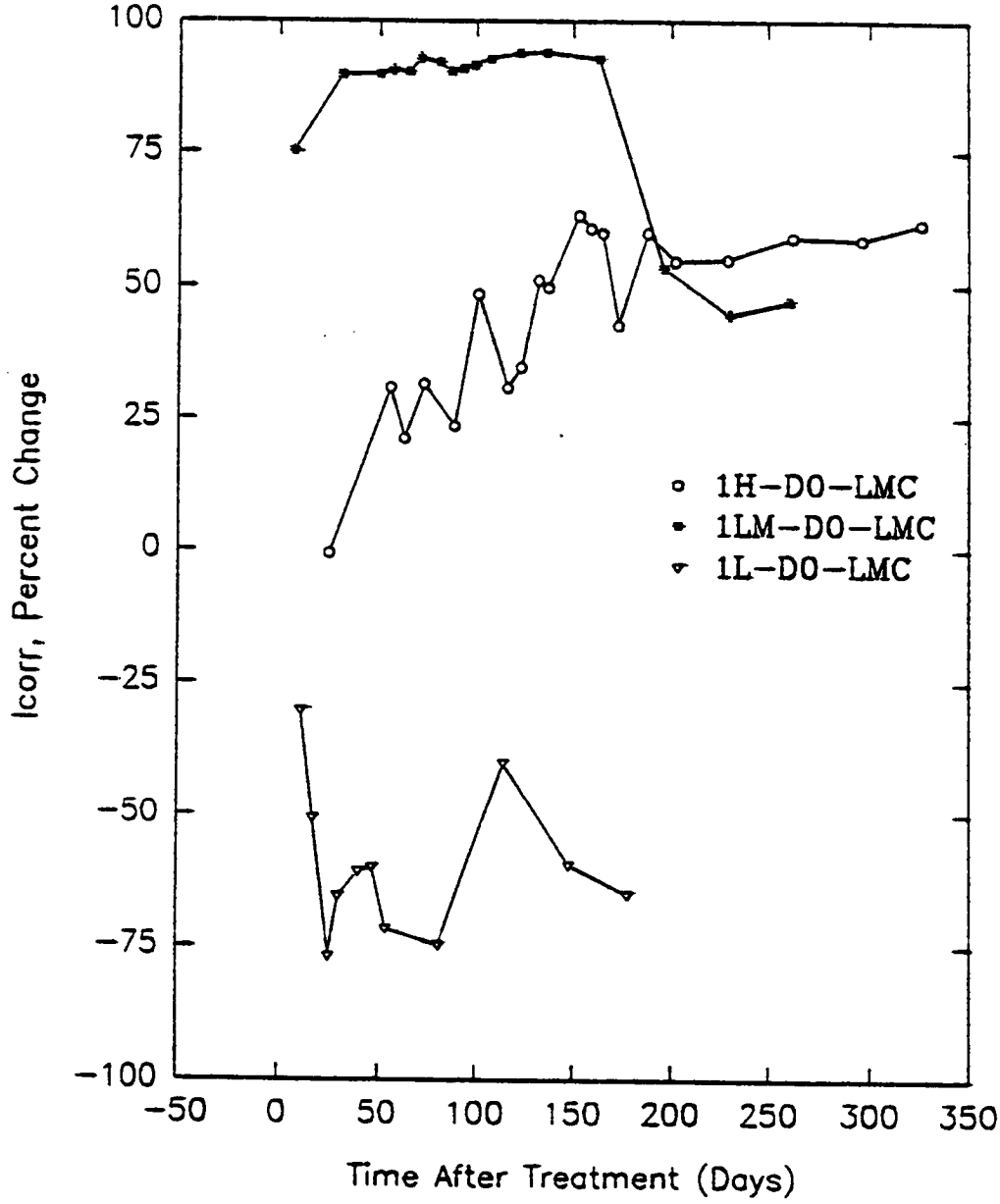

Fig. 6.21 i_{corr}, Percent Change for Dried Controls

Bond Strength Evaluation

The bond strength between the overlays and the substrate concrete was measured 160 days after the treatment of the first set of specimens. The cores were drilled at least 1½ in (38 mm) away from the reinforcing steel in order to minimize any disturbance of the corrosion cell. The bond strength was measured at a minimum of three locations on each specimen in accordance with ACI-503-R (43). The results of these measurements are presented in Table 6.9.

A bond strength of 250 lbs (1112 N) was considered the minimum bond strength needed to prevent the overlay from delaminating under freeze-thaw cycles and traffic loadings. The average bond strengths for two of the Alox and Cortec treated specimens were below this limit. No other treatments showed reduction in bond strength.

The grout appeared to have cured on the specimens treated with Alox, but an oily residue was found between the cured grout and the base concrete. The grout on the specimens treated with Cortec was both porous and powdery. It generally disintegrated under the water pressure from the coring ring.

Three additional specimens were treated in an effort to improve the bond strength, two with Cortex and one with Alox. The Alox specimen and a Cortec specimen were first ponded with the inhibitor. After the excess inhibitor was removed, dry cement was dusted on the surface to absorb any residue. The powdered cement was removed by wire brushing and compressed air. The other Cortec specimen was dried under a heat lamp for 24 hours after the excess inhibitor was removed. The bond strength of these specimens was tested after seven days of curing. An LMC control specimen was cast at the same time to determine the effect of the decreased curing time. The bond strengths for those specimens with inhibitor-modified concrete are shown in Table 6.10. Though the specimen treated with Alox showed some improvement, it was not considered sufficient for field use. The decreased curing time had no significant effect on the LMC control.

A second attempt was made to improve the bond strength by sand-blasting the specimen prior to overlay. Both specimens ponded with Alox and Cortec were tested. In addition, a specimen was overlaid with concrete containing 2 lbs/yd^3 (1.2 kg/m^3) of VCI 1609. This specimen was not ponded. The bond strength for these specimens was measured after seven days of curing.

The results of these tests are shown in Table 6.11. All specimens developed adequate bond strength. Therefore, light sand-blasting was used to improve bond strength for future treatment using Alox or Cortec.

Table 6.9 Overlay Bond Strength for Inhibitor Modified Concrete

Treatment	Specimen	Average Bond Strength (lbs)	STD Bond Strength (lbs)
Alox 901 Ponding	1H-D1-AX	0	0
LMC Overlay	2ML-1-AX	47	42
	2ML-2-AX	257	40
Cortec 1337 Ponding	1H-D1-COR	0	0
Cortec 1609 Overlay	2ML-1-COR	27	46
	2ML-2-COR	323	165
DCI Ponding	1H-D1-DCI	897	162
DCI Overlay	2ML-1-DCI	750	187
	2ML-2-DCI	1037	59
Sodium Borate	1H-D1-SB	797	133
Pond & Overlay	2ML-1-SB	940	295
	2ML-2-SB	937	35
LMC Overlay	1H-D0-LMC	1013	110
Cover Concrete Removed	2ML-0-LMC	850	347
1 in LMC Overlay	2M-LMC	763	171
Thin Polymer Overlay	2L-TP	1240	198

Note: 1 lb = 4.448 N

Table 6.10 Overlay Bond Strength for Inhibitor Modified Concrete

Treatment	Average Bond Strength (lbs)	STD Bond Strength (lbs)
Alox 901 Surface Pond. Surface dusted with dry cement and wire brushed prior to overlay.	67	31
Cortec 1337 Surface Pond. Surface dusted with dry cement and wire brushed prior to overlay.	0	0
Cortec 1337 Surface Pond. Specimen dried under a heat lamp for 24 hours.	0	0
LMC Control	847	151

Note: 1 lb = 4.448 N

Table 6.11 Overlay Bond Strength For Inhibitor Modified Concrete

Treatment	Core #	Bond Strength (lbs)	Failure Plane
Alox 901	1	860	Base Concrete
Surface Pond,	2	640	50/50 Base Concrete/Bond
Sandblasted prior to	3	1240	50/50 Base Concrete/Bond
overlay	AVG	913	
	STD	304	
Cortec 1337	1	650	Grout Failure
Surface Pond,	2	1040	50/50 Base Concrete/Bond
Sandblasted prior to	3	860	50/50 Base Concrete/Bond
overlay	AVG	850	
	STD	195	
Cortec 1609	1	940	Base Concrete Failure
2 lbs/yd^3	2	740	Base Concrete Failure
	3	830	Base Concrete Failure
	AVG	837	
	STD	100	

Note: 1 lb = 4.448 N

Freeze-Thaw Durability of Inhibitor-Modified Concrete

Beams were cast for rapid freeze-thaw testing from the same mixture proportions used for the large scale specimens. In addition, beams were cast from a normal concrete without any inhibitors added, as a comparison. The mixture proportions, and properties of the fresh and hardened concrete are presented in Appendix C, Table C-12. The inhibitor-modified beams were exposed to the number of cycles shown in Table 6.12. The mixture proportions are given in Appendix C, Tables C-9 through C-11. The flexural and longitudinal frequencies are shown in Appendix C, Tables C-17 and C-18.

Table 6.12 Durability Factors for Inhibitor Modified Concrete

Mix Design	Initial Air Content	Number of Cycles of Exposure	Durability Factor[1]
DCI-M4	9.0%	49[2]	13.3
DCI-M4[3]	5.3%	240	91.0
Cortec-M1	7.4%	315	100.0
Cortec-2-M1	6.4%	315	100.0
Cortec-M-4	6.5%	315	100.0
Normal-M1	6.8%	265	100.0
LMC-M2	10.5%	215	100.0

1 The calculated durability factor is the average of 2 beams with the exception of the LMC beam.

2 Since the relative modules dropped below 50% after 49 cycles, the durability factor was calculated at 49 cycles. Further exposure led to the disintegration of the specimen.

3 Retest of DCI.

From this data the only inhibitor which appears to have a detrimental effect on the freeze-thaw durability of the concrete is DCI. However, the following observations should be mentioned.

1) DCI has been used in the field for 26 years with no previous reports of significant freeze-thaw deterioration.

2) The mix had not reached its initial set nine hours after the concrete was placed. This was originally believed to be the result of using very cold mix-water, but later evidence indicates a cement problem.

3) Similar problems were noticed with other mixes made with the same cement and high-range water reducers.

4) This mix exhibited a percent decrease in 28-day strength compared to previous mixes.

The portland cement was replaced by another cement from a different manufacturer. New beams were cast from a DCI mixture prepared with the new cement. The beams had an initial air content of 5.3%. The mixture proportions and properties of the fresh and hardened concrete are presented in Appendix C, Table C-13. After 240 FT cycles, the average durability factor for these beams was 91. The improved durability supports the previous contention that the low durability factor was due to the portland cement.

Evaluation of Bridge Deck Specimens

The treatment of the bridge deck specimens was to provide an opportunity to test the field application methods prior to the field validation work. Since it would be difficult to pond the inhibitor on an entire deck, spray application techniques were developed. The specimens sprayed with Alox and Cortec were lightly sandblasted prior to overlay in order to improve bond strength. DCI was included in the bridge deck slab treatments at the manufacturer's recommended concentration. To validate previous observations regarding the low calcium nitrite concentration.

A delamination survey indicated that the deck sections were sound. Two complete sets of potentials, i_{corr}, and chloride measurements were taken on the slabs prior to treatment. Prior to treatment, slab damage accrual at the time of the slabs' removal from the PA I-80 deck prevented complete survey measurements. Potential measurements were taken on the transverse rebar between the longitudinal bars. i_{corr} measurements were performed with both 3LP and Gecor devices. The correlation between 3LP and Gecor i_{corr} was poor, $r = 7.7\%$. Theoretically, the guard-ring electrode on the Geocisa device should confine the area of polarization and provide a better estimate of the corrosion activity after treatment.

All three slabs were in the medium-low initial i_{corr} category prior to treatment. The mean i_{corr}, as measured by 3LP, was approximately 1 mA/ft^2 (1.08 $\mu A/cm^2$) higher on the slab treated with DCI.

Because of the amount of time required to take i_{corr} readings on the slabs using both 3LP and Gecor devices, measurements were taken simultaneously on different slabs. Therefore, measurements were taken on the same date, and not the same number of days before or after treatment. For this reason only trends can be compared.

A comparison between the pre- and post-treatment potentials are presented in Table 6.13. The treatment demonstrated a reduced potential after treatment. The slabs treated with both Alox and DCI show an increase in i_{corr} as measured by the 3LP after treatment. This may be due in part to the increasing moisture content of the treated slab caused by the overlay concrete, which allowed a greater area of polarization and/or decreased the concrete's resistance at the rebar level and thus increased the corrosion current density. Another possible explanation could have been that the slabs dried out while being stored indoors, and when the overlays were placed, the added moisture reactivated the corrosion cell. However, since the slabs were covered with saturated burlap and polyethylene sheeting for almost a month prior to the second set of pre-treatment readings, the second explanation was not valid. The second set of readings on the Alox slab demonstrated a decreasing trend in 3LP i_{corr}. However, the mean value was still greater than the pre-treatment values.

Table 6.13 Pre- and Post-Treatment Mean Potentials and Mean i_{corr} Values for the Inhibitor Modified Slabs

Treat-ment	Pre-Treatment				Post Treatment			
	Time After Treat. (days)	AVG Poten (-mV)	AVG 3LP i_{corr} mA/ft^2	AVG Geosica i_{corr} mA/ft^2	Time After Treat. (days)	AVG Poten (-mV)	AVG 3LP i_{corr} (mA/ft^2)	AVG Geocisa i_{corr} (mA/ft^2)
Alox 901	77	318	1.28	0.066	34	273	2.94	.053
	50	300	1.16	0.068	52	233	2.29	.068
Cortec	70	260	1.31	0.123	40	138	1.10	.033
	44	191	1.34	0.156	58	125	1.20	.048
DCI	46	342	2.34	0.099	36	228	4.08	.293
	20	320	2.25	0.152	65	244	4.46	.306

Note: 1 mA/ft^2 = 1.08 μA/cm^2

The slab treated with Alox demonstrated a 21% decrease in i_{corr} (Gecor); this decrease may be a more accurate indication of the trend in corrosion activity than the increase in 3LP measurements. Cortec was shown to be very effective, with a 77% decrease in i_{corr} from the mean pre-treatment readings (Gecor). This reduction corresponds to the trend indicated by both the CSE potential and the 3LP i_{corr} measurements, which showed a 17% decrease in i_{corr} after treatment.

The deck section treated with DCI showed a 96% increase in i_{corr} (Gecor) between its highest pre-treatment average, and the mean of its post-treatment average. This indicates an increase in corrosion activity after treatment even though the slab was sprayed with the manufacturer's recommended concentration of DCI. Though this research indicates DCI may not be successful at corrosion abatement, long term data is needed to draw a firm conclusion.

Additional monitoring to assess the effectiveness of the corrosion treatments for the slabs is required.

Three cores were drilled into each of the treated slabs after 28 of days curing. The average bond strengths measured for those cores are as follows: Alox 901, 217 lbs (960 N); Cortec 1337/1609, 400 lbs (1780 N); and DCI, 680 lbs (3020 N). The average bond strength for the slab treated with Alox 901 was below the acceptable limit of 250 lbs (1112 N). Previous data had shown that a good bond could be obtained with sand blasting.

Prediction of Service Life

An estimate of the increase in treatment service life was calculated based on the reduction in corrosion current density of the blocks. The estimate cannot predict the actual time of inhibition provided by the inhibitors, nor does it include the possibility of premature failure due to debonding. However, it helps maintenance engineers in assessing the treatment cost effectiveness.

The following assumptions were made to develop the prediction model:

1. The service life of a typical LMC overlay is 20 years (10).

2. At the time of a typical LMC deck overlay placement, 40% of the bridge deck is delaminated or spalled. The chloride-contaminated concrete would be removed in these areas. Therefore, the average reduction of the non-dried LMC control specimens was used to represent the area of a bridge deck where the chloride-contaminated concrete was removed. The average i_{corr} reduction for the controls is weighted by a factor of 0.4 since it represents only 40% of the components area in a typical rehabilitation process.

3. The reduction in corrosion current seen in specimen 2M-LMC was used to model the other 60% of a typical LMC deck overlay where the chloride-contaminated cover concrete is left in place. The reduction in i_{corr} was weighted by a factor of 0.6.

4. The corrosion current densities on the deck at the time of rehabilitation are assumed to be equally represented by the specimens with low, medium-low, medium, and high initial corrosion current densities such that the average reduction seen in the blocks could be used, with one exception. The results from the low initial i_{corr} dried specimens were not included.

The model is presented in Equation 6-8.
where,

T_p = Predicted service life (years)

$$T_p = 20x\left[\frac{\%R_{INHB}}{(0.60\ (LMC_L) + 0.40(LMC_R))}\right] \quad (6\text{-}8)$$

$\%R_{INHB}$ = Average percent reduction in i_{corr} of the inhibitor-treated specimens.

LMC_L = The percent reduction in i_{corr} of the LMC control specimen with the chloride-contaminated concrete left in place.

LMC_R = The average percent reduction in i_{corr} of the LMC control specimens with the cover concrete removed.

The percent reductions were calculated according to Equation 6-1, based on the last corrosion current densities taken in the monitoring period. The results of the calculation are shown in Table 6.14.

Table 6.14 Service Life Predictions

Treatment	Predicted Service Life
Alox 901, 1 Day Ponding[1]	46 years
Cortec 1337/1609, 1 Day Ponding	26 years
Alox 901, Dried and 1 Day Ponding	42 years
Cortec 1337/1609, Dried and 1 Day Ponding	34 years

[1] The predicted initial i_{corr} of 10.93 was used to calculate the percent reduction, not the measured value of 37.48.

From this estimation, Alox provides a 100% increase in service life. It should also be noted that drying provides no increase in estimated service life for the Alox treatments. However, concrete would need to be dried prior to the application of Cortec in order to gain a significant benefit.

DCI treatment service life estimates could not be calculated using Equation 6-8, since only 1 of the blocks in the non-dried one day pond group and one specimen in the dried group had chloride nitrite:ratios less than two, as discussed earlier.

Conclusions and Recommendations

The following conclusions can be made, based on the results of the preceding research:

1. The removal of chloride-contaminated concrete above reinforcing steel and its

subsequent replacement with fresh concrete is an effective means of reducing corrosion.

2. The removal of the cover concrete facilitates the direct application of corrosion inhibitors.

3. Alox 901 is a very effective surface-applied corrosion inhibitor and potentially capable of doubling the service life of an overlay.

4. Cortec 1307 and Cortec 1609 are effective inhibitors when applied as ponding agents and concrete admixtures, respectively.

5. Alox 901 and Cortec 1337 have a detrimental effect on bond strength. This problem can be mitigated with sand-blasting.

6. DCI (calcium nitrite) is somewhat effective at reducing low corrosion currents when applied at the .1M concentration.

7. Cortec 1609 has no adverse effects on the freeze-thaw durability of concrete.

8. A correlation can be derived between the chloride content at the bar level and the corrosion current density of the reinforcing steel for laboratory conditions where moisture content and temperature are relatively constant.

9. Ponding corrosion inhibitors for two days has no significantly different effect than does pondings for one day.

Based on the limited time and scope of this study, the following recommendations can be made for further research:

1. Long-term monitoring to determine the period of inhibition needs to be investigated, in order to more accurately predict the service life of inhibitor treatments.

2. The chloride threshold for the initiation of corrosion after treatment should be determined in order to understand the effectiveness of inhibitors.

3. Further research should be conducted towards the improvement of overlay bond strength.

4. A better corrosion current measurement device which utilizes a guard-ring electrode should be developed.

7

Laboratory Evaluation of Asphalt Portland Cement Concrete Composite

Introduction

Presently, many bridge deck overlay materials are used in bridge deck repair. However, many of these overlay materials in addition to their high costs, are rigid and lack flexibility.

A material new to the United States, Asphalt Portland Cement Concrete Composite (APCCC), which is a combination of hot-mix asphalt (HMA) and modified portland cement grout, showed some promise when used in the field (47). APCCC has been extensively used in Europe as an overlay in airports where heavy loads and oil spillage occur. Recently, the Army Corps of Engineers applied this technique as airport pavement overlay (47). It is reported that this material provides greater resistance to wear and abrasive forces and also to oil spillage. However, the durability performance of the material relative to United States environments has not been evaluated.

In this research, an effort has been made to evaluate this material, which is a combination of HMA and portland cement concrete (APCCC) to utilize the unique properties of both materials. Thus, this material possesses both flexible and rigid characteristics. It is neither as rigid as portland cement concrete nor as flexible as HMA. A proposed use of the material is the rehabilitation of bridge decks with HMA preformed membrane protection systems. Because of its expected higher resistance to chloride ions, it may not be necessary to remove the existing membrane. The present HMA overlay would be milled off and replaced with APCCC and possibly result in significant cost savings.

Background

Asphalt Portland Cement Concrete Composite (APCCC), or the Salviacim process as it is known in Europe, was developed in France by the Jean Lefebvre Group as a cost-effective alternative to portland cement concrete and hot-mix asphalt to withstand fuel spillage and

abrasive forces. APCCC can be best described as semi-flexible or semi-rigid material which possesses the fuel, abrasion, and wear resistance characteristics of portland cement concrete and the flexible characteristics of hot-mix asphalt. It is an open graded HMA with an air void content of 25 to 30% that is later filled with resin modified cement grout. The materials and mixture proportion requirements are modified to produce a suitable air void content in the hot-mix asphalt and the grout mixture design is modified to ensure full penetration through the hot-mix asphalt.

HMA is designed to act as a support layer and is used to determine the thickness of the APCCC. The placement of HMA in the field does not require any special skilled labor; however total quality control is required throughout. The open graded HMA is placed with conventional asphalt paving equipment. It is not compacted but only smoothed with a 3-ton roller. The asphalt content generally ranges between 3.5 and 4.5%.

The grout consists of cement, fly ash, sand, water and resin additive. Resin additive, Prosalvia (PL7), is a cross polymer resin of styrene-butadiene. It acts as a water-reducing agent. The grout is designed to ensure full penetration through voids. Water to cement ratio is between 0.65 and 0.70. The grout can be mixed in a conventional concrete batch plant or in a small portable mixer. The grout is placed after the hot-mix asphalt is cooled. It should be poured immediately after mixing in order to avoid segregation of material. A 3-ton vibratory roller is usually used to assure the penetration of the grout through the voids.

In the 1970's, the U.S. Army Corps of Engineers at Waterways Experiment Station (WES) evaluated this material. The results were not favorable, due to lack of technical guidance. They achieved an air void content of only 15 to 20% and had thick grout which resulted in insufficient penetration; as a result, tests failed. In 1987, they re-evaluated this material because it was yielding very good results in European countries. The evaluation included site observations in France, Great Britain and Australia. The research at WES was aimed at evaluating the effectiveness of the material for abrasion and oil spillage resistance (47). Some pilot projects have been completed since 1987.

To evaluate APCCC as a potential pavement material, the U.S. Army Corps of Engineers at WES constructed test strips of 150 x 150 ft (48 x 48 m) and evaluated them for abrasive resistance. Track vehicle maneuvers were conducted and an Accelerated Loading Facility (ALF) was used to evaluated the APCCC under heavy rubber tired traffic.

For rubber abrasive resistance evaluation, loading included M1 and M60 tanks with gross weights of 113,000 lb (51,000 kg) and 100,000 lb (45,000 kg), respectively; 600 180° pivot steer turns and 5000 straight passes were applied with tracked vehicles to test the strip. After 420 turns at the same location, the vehicle produced sufficient rough abrasion and high-stress that ravelling occurred. After 600 pivot steer turns, the turning traffic was stopped because the abrasion action produced a ravelled area 1-in deep covering 35 ft^2 (3.3 m^2). The 5000 straight passes produced only surface wearing.

Five different oils and fuels, namely, jet aviation fuel, gasoline, diesel, synthetic oil, and hydraulic oil were used to evaluate the fuel resistance of APCCC. Spillage area was 8 x 10 ft (2.4 x 3.0 m) and materials were spilled from a height of 30 in (76 cm) at a rate of one quart per 20-30 minutes. The fuels and oils were allowed to remain for 30 days after 30 cycles of spillage before evaluation.

Visual observations showed no significant damage, but field cores showed penetration of fuels and oils into APCCC causing various levels of deterioration. Diesel fuel penetrated 1 in (25 mm) and caused the most damage; other fuels and oils penetrated less than 1/2 in (13 mm). This test is more severe than observed in the field as real field spills are cleared regularly and are not allowed to soak for several months.

FHWA's Accelerated Loading Facility (ALF) was used to traffic an APCCC test strip of 48 ft (14.6 m). ALF-simulated truck traffic used a load of 19,000 lbs (8,600 kg) to a dual wheel assembly with tire pressures 140 psi (965 kPa) and applied 80,000 passes. No appreciable damage except slight wearing of excess grout was observed in the wheel path, which indicated that vehicular traffic had no significant effect on APCCC and suggested that APCCC should have good field performance.

APCCC pilot projects have been constructed since the late 1980s, including 10,000 yd^2 (8,000 m^2) as a taxiway at John Wayne Airport in late 1990. APCCC performed well when tested after a year. At Miami International Airport, APCCC also performed well except for some hairline shrinkage cracks due to improper application of the grout. A 2600 yd^2 (2174 m^2) pilot project was constructed at the Tampa International Airport. Some excess grout was noticed along the outside areas and some hairline shrinkage cracks in the center. Otherwise, the overall appearance was excellent.

The performance of APCCC in Europe has been evaluated over a longer period of time. At Merignac Airport in Bordeaux, France, APCCC was rated good-to-excellent after 12 years of service. Although random cracks were observed, APCCC withstood fuel spillage and loading without showing any rutting. APCCC was used also as an overlay on portland cement concrete pavement in the same airport and was able to control reflection cracks. In general, APCCC performed better than an adjacent HMA section.

Other sites in France and England have been evaluated in the past decade. The sites included helicopter fields, airports, and tank facilities. No appreciable damage was found after almost 10 years of service.

Scope and Objective

To reduce the chloride intrusion into bridge decks, new materials other than portland cement concrete have been considered in the past two decades as bridge deck overlays. With the availability of various alternative materials, the selection has become a complicated procedure. It is necessary to assess not only the initial cost, but also future maintenance

costs. Existing bridge deck overlays, except HMA, possess high strength but are rigid and costly.

The excellent performance of APCCC in Europe for the last 30 years and the successful completion of pilot projects and airport pavements by USACE at WES and their reasonably good performance promoted more thorough evaluation of this material under laboratory conditions so that it may be considered as a bridge deck overlay material.

The research reported here has evaluated the mechanical properties of APCCC and its durability characteristics. The research involved development of mix designs for HMA and for the resin modified cement grout. The specimens cast from this design were then evaluated for mechanical and durability characteristics. As this material had a cement component, the tests were conducted after various curing periods. The research involved two phases: Phase I involved the design of the two components of APCCC, namely HMA at the required air void content and resin modified cement slurry grout which can penetrate the HMA. Phase II involved the evaluation of APCCC for mechanical characteristics: stability and flow, compressive strength, indirect tensile strength and resilient modulus; and durability characteristics: stripping, freezing-thawing, and chloride intrusion.

Research Approach

In order to evaluate the performance of this material, a valid HMA was designed. An optimum mix was chosen with an air void content in the range of 25 to 30%. The resin modified cement grout was also investigated to obtain the required viscosity which would allow the grout to penetrate through the HMA.

A preliminary study was conducted using the Marshall method to develop a HMA specimen which had the required air void content. Different compactive efforts and different asphalt contents were used. A mix design was chosen based on optimum unit weight, optimum air void content, and optimum voids in mineral aggregate. Resin modified grout was designed such that it would penetrate through the HMA specimen under low vibration.

In order to evaluate the performance of APCCC, tests were conducted for different moist and air curing periods and after different weathering conditions. All tests were performed at laboratory temperature. Specimens were tested for three curing conditions namely no moist curing, one day moist curing, and three day moist curing. Stability testing was conducted at 1, 3, 7, 21, and 28 days for all three curing conditions. Compressive strength, indirect tensile, and resilient modulus tests were performed at 1, 3, 7 and 28 days for all moist curing conditions. Effects of weathering on APCCC were tested at 3, 7 and 28 days by subjecting specimens to rapid freezing and thawing and water sensitivity tests at the end of the curing period. The weathering effects were evaluated by means of determining indirect tensile strength and resilient modulus before and after conditioning. The ratio of strength values obtained before and after conditioning should be no less than 0.75. Chloride intrusion specimens were subjected to 7, 11, and 15 wet/dry ponding cycles of 3% NaCl solution. A

wet/dry ponding cycle is seven days, four days of air drying followed by three days ponding with the NaCl solution.

Experimental Program

Materials

The materials used in the HMA were Virginia Department of Transportation (VDOT) #68 and #10 dolomitic limestone aggregate supplied by Acco Stone Company located in Blacksburg, VA; the asphalt cement was AC-20. Hydrated lime was used as an anti-stripping agent in HMA specimens of resin modified concrete and VDOT SM-5 HMA was used as the control. The materials used for the grout were Type I portland cement, fly ash, water, standard sand, and resin additive. The fly ash was provided by Marshall Concrete Company of Christiansburg, VA. Resin additive, Prosalvia 7 (PL7), was manufactured by Jean Lefebvre Construction Company in France. Daravair air-entraining agent was used in the control portland cement concrete specimens. The properties of the aggregate used in the HMA are presented in Table 7.1.

Table 7.1 Aggregate Properties

	FINE AGGREGATE	COARSE AGGREGATE
Bulk Specific Gravity	2.79	2.65
Apparent Specific Gravity	2.82	2.68
Absorption	0.7%	0.4%
Average Bulk Specific Gravity of Aggregate Blend		2.67
Average Apparent Specific Gravity of Aggregate Blend		2.71

Mix Design

HMA Design

The primary objective of the HMA design is to provide a mixture with maximum possible density in the desired range of air void content. Various methods may be used such as the Marshall method, Hubbard-Field method, Hveem method, Smith or Asphalt Institute Tri-Axial method, Gyratory testing method, and Laboratoire Central des Ponts et Chaussees (LCPC) rubber tire method. These methods are empirically based and have been standardized to reach worldwide acceptance. Any of these methods may be used to design a

mixture for a given aggregate and aggregate gradation meeting criteria based on past experience. These methods have been developed to measure stability and to establish a correlation between laboratory specimens and field mixture. Methods used to establish this correlation vary from direct compression with or without hand rodding, to hand tamping, impact hammer, kneading action, gyrating shear, vibration and simulated rolling.

In this research, the Marshall method was used to design the HMA. It is the standard in the State of Virginia, where this research was conducted, and it is the most widely used method in the United States, and abroad. The objective of the Marshall method, used in this study, was to design an optimum compactive effort, and optimum asphalt content for the given aggregate in order to achieve desired air void content. The HMA design, in this study, involves aggregate gradation, optimum compactive effort, and optimum asphalt content.

Aggregate gradation was chosen as standardized by the additive manufacturer, Jean Lefebvre Construction Company, and is presented in Table 7.2. In order to determine the optimum number of blows required to produce the required air void content for a given asphalt content and aggregate gradation, different compactive efforts were used. Asphalt content of 3.9% by weight of aggregate was chosen to determine the optimum compactive effort. As the void content required was in the range of 25-30%, the required compactive effort would be very small. Thus, five different compactive efforts were used, 10, 15 and 20 blows on each side and 15 and 20 blows on only one side of the specimen. Marshall specimens were prepared in accordance with ASTM D-1559 and were evaluated for bulk specific gravity and air void content. The compactive effort that gave the optimum percent of air void content was chosen as optimum compactive effort (number of blows). The analysis is presented in Table 7.3 In this research, 10 blows on each side provided the optimum percent of air void content and was used throughout the research. Although 15 blows on 1 side resulted in a lower bulk specific gravity, the researcher elected to use 10 blows on each side because the Marshall method compacts specimens on both sides.

Optimum asphalt content is the one which produces maximum stability and maximum density in the desired range of air void content. It depends on the type and shape of aggregate, compactive effort and desired final voids. In order to design the optimum asphalt content, different amounts of asphalt were used and Marshall specimens were cast and evaluated for density, percent air voids and voids in mineral aggregate (VMA). In practice, 2½% increments are normally used below and above the expected optimum asphalt content. In this research, 0.2% increments were used below and above the expected optimum asphalt content. Expected optimum asphalt content can be calculated using empirical formulas based on the surface area concept, such as California Highway Department formula, Nebraska formula, and French formula.

Table 7.2 Aggregate Gradation

SIEVE	% PASSING			
	#68 Aggregate	#10 Aggregate	Aggregate* Blend	Specified Limits
1"	100.0	100.0	100.0	100
3/4"	100.0	100.0	100.0	100
1/2"	59.3	100.0	67.0	65 - 75
3/8"	31.0	100.0	44.0	50 - 65
#4	6.0	90.0	22.0	23 - 33
#8	2.0	55.0	12.0	9 - 17
#16	0.0	44.7	8.5	7 - 13
#30	0.0	26.3	5.0	5 - 10
#50	0.0	16.0	3.0	4 - 8
#100	0.0	13.0	2.5	2 - 6
#200	0.0	10.0	0.95*	1 - 3

* Additional 0.95% (by weight of aggregate) hydrated lime was used

Note: 1 in = 25.4 mm

The *California Highway Department formula is*

$$P = 0.015a + 0.013b + 0.17c \quad (7\text{-}1)$$

where,

P = percent of bitumen in the mix by weight,
a = percent of aggregate retained on #10 sieve,
b = percent of aggregate passing #10 sieves and retained on #200 sieve, and
c = percent of aggregate passing #200 sieve.

The numerical factors used with a, b, c are related to surface area of aggregates. This method is limited to locally available materials as it employed only two sieve sizes.

The *Nebraska formula is*

$$P = AG(0.2a) + 0.06b + 0.10c + Sd \quad (7\text{-}2)$$

where,

P = percent of bitumen residue by weight of mixture at the time of laying,

A = absorption factor for aggregate retained on #50 sieve,
G = specific gravity correction factor of aggregate retained on #50 sieve,
a = percent of aggregate retained on #50 sieve,
b = percent of aggregate passing #50 sieve and retained on #100 sieve,
c = percent of aggregate passing #100 sieve and retained on #200 sieve,
d = percent of aggregate passing #200 sieve.

This method is preferred over the California Department Highway formula because it makes use of more aggregate sizes. However, these methods do not include shape, surface texture and adsorption of aggregate. Other state highway departments have their own formulas to evaluate optimum asphalt content based on their experiences.

In this research, the French formula was used to evaluate the estimated optimum asphalt content as described below (47):

$$(\alpha)(k)(\sum)^{1/5} \qquad (7\text{-}3)$$

$$\alpha = \frac{2.65}{\gamma_G} \qquad (7\text{-}4)$$

where,

γ_G = apparent specific gravity of aggregate,
k = richness modulus having a value of 3 to 3.5 depending upon the maximum aggregate size and gradation,
Σ = conventional specific surface area
$= 0.25G + 2.3S + 12s + 135f$,
G = percent of material retained on 1/4-in,
S = percent passing 1/4-in and retained on #50 sieve,
s = percent passing #50 and retained on #200 sieve, and
f = percent passing #200 sieve.

The estimated optimum asphalt as calculated using the French formula was found to be 4.1% of the aggregate weight using a K value of 3.25. Marshall specimens were prepared using 10 blows on each side with asphalt contents of 3.7%, 3.9%, 4.1% and 4.3% by weight of aggregate to determine the actual optimum asphalt content. The optimum asphalt content was chosen as the one which produced optimum unit weight, optimum air void content, and optimum voids in mineral aggregate (VMA).

Table 7.3 Optimum Compactive Effort

No. of Blows	Sample No.	Average Bulk Sp. Gr.	STD Bulk Sp. Gr.
15	1	1.781	0.051
1 Side	2		
20	1	2.013	0.166
1 Side	2		
10	1	1.875	0.003
Each Side	2		
15	1	1.897	0.017
Each Side	2		

F = Specific gravity of parafilm = 0.9

Theoretical maximum specific gravity was calculated for each mixture of different asphalt content in accordance with ASTM D 2041-78, and the results are presented in Table 7.4. Bulk density of HMA specimens was determined using parafilm wrapping rather than using uncoated or melted paraffin coating as suggested by ASTM standards D 2726-88 and 1188-83 because of the extreme openness of the mixture and coarse surface texture. If the specimen was left uncoated, water will enter the voids and reduce the effective volume of specimens and give erroneously lower values of air voids. Even when melted paraffin coating is used it is difficult to apply the coating without filling surface voids. Also, the coating cannot be removed easily, and the specimens cannot be used for further testing. The parafilm (sheet) wrapping could be removed and thereby specimens could be used for further testing. The specific gravity of parafilm material is the same as melted wax, and the formula used in ASTM 1188-83 is applicable in calculating air void contents. The results are presented in Table 7.5.

Unit weight, air void content and voids in mineral aggregate was determined and plotted as a function of asphalt content. Optimum asphalt contents from three plots were selected, and the average of the three values was chosen as the average optimum asphalt content for the mixture. The average optimum asphalt content was 4.05%.

Resin Modified Cement Grout

The primary objective of the cement grout design is to assure its penetration through the voids in HMA under vibration. The primary design parameter for the grout design is its flow rate. The grout flow rate is determined by the time needed for 0.26 gal (1 ℓ) of grout to flow through a Marsh Flow Cone and is expressed in seconds. The dimensions of the

cone are presented in Fig. 7.1.

The flow rate of the grout should be slightly greater than that of water, with maximum possible strength in order to have full penetration. If the flow rate is too high, i.e, if the grout is too thick, it will not penetrate fully through the voids. If the flow rate is too low, i.e., the grout is too thin, the grout does not have sufficient strength. The flow rate of the water is six seconds, so a flow rate between seven and nine seconds is considered optimum.

The composition of the grout was adjusted to provide optimum flow rate. The mixture proportions of the grout and resulting flow rate are presented in Table 7.6.

Table 7.4 Theoretical Max. Specific Gravity For HMA (APCCC)

Asphalt Content %	Theo. Max. Specific Gravity	Average Theo. Max. Sp. Gr.
3.7	2.517 2.538	2.527
3.9	2.537 2.545	2.541
4.1	2.531 2.536	2.534
4.3	2.527 2.537	2.532

Table 7.5 Bulk Specific Gravity and Air Void Content of HMA (APCCC)

Asphalt Content %	Wt. in Air "A" (gm)	Wt. of Specimen w/Parafilm in Air "D" (gm)	Sub. Wt. "E" (gm)	Parafilm Factor "K" = (D-A)/F*	Volume "V" = (D-E-K) (cc)	Bulk Sp. Gr. "B"= A/V	Theo. Max. Sp. Gr. "M"	Air Void Content (1-B/M) (x100)	Air Void Content Average (%)
3.7	932.9	948.6	430.7	17.4	484.8	1.864	2.531	26.3	26.6
	888.0	903.7	396.2	17.4	474.4	1.812		28.4	
	981.9	994.8	463.5	14.3	504.1	1.899		25.0	
3.9	914.6	931.1	413.1	18.3	483.2	1.830	2.537	27.8	26.6
	920.2	938.7	423.8	20.6	475.8	1.861		26.6	
	867.7	880.0	397.0	13.7	457.0	1.849		27.1	
	946.8	960.5	447.8	15.2	483.8	1.903		25.0	
4.1	949.0	966.3	437.7	19.2	492.1	1.863	2.528	26.3	26.5
	937.5	955.8	421.0	20.3	496.2	1.822		27.9	
	872.1	886.3	414.6	15.8	441.7	1.913		24.3	
	891.7	905.3	405.5	15.1	471.7	1.840		27.2	
4.3	981.4	999.0	458.7	19.6	503.1	1.885	2.532	25.6	26.1
	912.9	926.9	419.1	15.6	478.2	1.855		26.8	
	912.6	926.6	425.1	15.6	471.9	1.878		25.8	
	903.7	917.5	418.2	15.3	470.2	1.867		26.3	

*Specific Gravity of Parafilm = 0.9, 1 lb = 453.6 gm

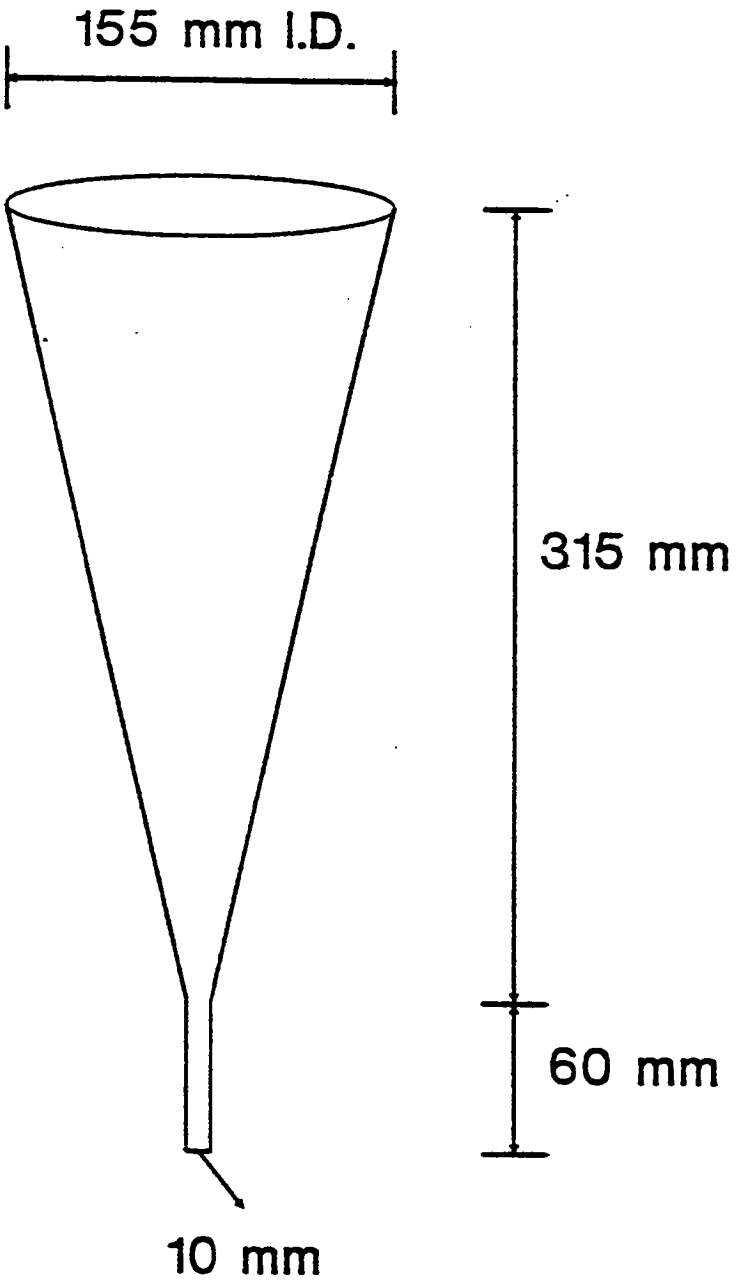

Fig. 7.1 Schematic Diagram of Marsh Flow Cone

Table 7.6 Mix Design of Slurry Grout

MATERIAL	% BY WEIGHT
Cement (Type I Portland Cement)	38.5
Fly Ash	19.2
Sand (Standard)	12.7
Water (W/C ratio 0.7)	26.8
Resin Additive (Prosalvia PL7)	2.8

	AVERAGE	STD	NUMBER OF TESTS
Marsh Flow, sec.	8.1	0.2	17
Specific Gravity	1.74	0.10	17

APCCC Specimen Preparation

After the HMA and grout proportions were determined, the next step was specimen preparation. HMA specimens were prepared using the average optimum asphalt content of 4.05% of the aggregate weight at compactive effort of 10 Marshall blows on each side. The specimens were then wrapped with duct tape to contain the liquid grout. Care was taken to make sure that the grout did not leak through the openings in the duct tape, especially when the specimens were exposed to mechanical vibration. The grout was then prepared; it was stirred with a mechanical stirrer to achieve a homogenous mixture. The grout was poured into the specimen which was placed on a vibrator table. The specimens were vibrated until no bubbles were seen. The duct tape was removed after 12 hours, when the grout had cured. Moist cured specimens were wrapped with wet burlap. After moist curing, specimens were kept in the laboratory and exposed to laboratory air curing until tested.

The average percent of the voids in HMA (APCCC) filled with grout was 91.4%, thus the average remaining air voids in APCCC specimens is 2.2%. Detailed results are presented in Table 7.7.

Table 7.7 Air Void Content Analysis of APCCC Specimens

Specimen No.	Bulk Sp. Gr.	% of Air Voids	Wt. of Grout* Filled In Specimen	% of Voids Filled With Grout
1	1.904	25.2	194.9	89.5
2	1.812	28.8	193.3	85.3
3	1.880	26.1	188.4	89.8
4	1.933	24.0	169.1	84.5
5	1.974	22.4	156.4	88.6
6	1.967	22.7	196.5	95.8
7	1.938	23.8	170.9	87.0
8	1.909	24.9	182.9	86.9
9	1.811	28.8	212.2	88.1
10	1.866	26.6	208.8	93.1
11	1.853	27.2	190.1	88.9
12	1.861	26.8	212.8	95.4
13	1.975	22.4	167.3	87.9
14	1.948	23.4	179.4	85.9
15	1.945	23.5	170.9	84.2
16	1.900	25.3	189.5	89.3
17	1.932	24.0	175.1	84.0
18	1.900	25.3	191.7	90.2
19	1.923	24.4	189.5	90.0
20	1.953	23.2	170.1	85.5
21	1.886	25.9	184.1	86.7
22	1.867	26.6	195.2	85.3
23	1.915	24.7	180.2	90.2
24	1.905	25.1	182.8	85.0
25	1.900	25.3	179.8	84.5
27	1.844	27.5	210.7	88.8
28	1.853	27.2	206.3	88.5
29	1.883	26.0	194.3	84.8
30	1.915	24.7	219.7	100.0
31	1.902	25.2	181.2	84.4
32	1.890	25.7	179.1	84.0
33	1.880	26.1	180.7	83.2
34	1.897	25.4	195.7	88.8
35	1.881	26.1	197.9	89.6

*Specific Gravity of Grout = 1.742

Table 7.7 Air Void Content Analysis of APCCC Specimens Cont'd.

Specimen No.	Bulk Sp. Gr.	% of Air Voids	Wt. of Grout* Filled In Specimen	% of Voids Filled With Grout
36	1.897	25.4	187.0	86.9
37	1.917	24.6	176.4	83.6
38	1.923	24.4	184.8	82.6
39	1.859	26.9	214.7	94.2
40	1.826	28.2	236.9	98.9
41	1.821	28.4	234.2	97.7
42	1.884	25.9	188.4	84.4
43	1.893	25.6	198.3	92.3
44	1.893	25.6	180.3	83.5
45	1.924	24.4	178.1	83.5
46	1.915	24.7	194.2	91.6
47	1.903	25.2	197.7	93.2
48	1.908	25.0	205.7	100.0
49	1.891	25.7	185.2	86.7
50	1.892	25.6	195.4	90.0
51	1.938	23.8	178.3	85.0
52	1.880	26.1	183.4	85.2
53	1.925	24.3	175.6	84.4
54	1.932	24.1	172.3	85.1
55	1.890	25.7	188.8	83.7
56	1.926	24.3	175.9	85.3
57	1.846	27.4	205.7	86.2
58	1.831	28.0	212.7	85.4
59	1.896	25.5	186.4	85.2
60	1.853	27.2	198.1	88.3
61	1.920	24.5	176.9	85.6
62	1.911	24.9	183.7	86.0
63	1.895	25.5	238.5	100.0
64	1.938	23.8	243.2	100.0
65	1.952	23.3	203.2	100.0
66	1.936	23.9	212.8	98.6
67	1.949	23.4	219.5	100.0
68	1.917	24.6	228.3	100.0
69	1.932	24.1	218.8	100.0
70	1.904	25.2	205.0	87.8

*Specific Gravity of Grout = 1.742

Table 7.7 Air Void Content Analysis of APCCC Specimens Cont'd.

Specimen No.	Bulk Sp. Gr.	% of Air Voids	Wt. of Grout* Filled In Specimen	% of Voids Filled With Grout
71	1.909	25.0	211.5	95.9
72	1.917	24.6	209.2	100.0
73	1.912	24.8	211.1	96.3
74	1.848	27.3	217.5	88.9
75	1.855	27.1	243.5	97.3
76	1.891	25.7	204.5	93.4
77	1.872	26.4	231.9	95.3
78	1.935	23.9	237.2	100.0
79	1.920	24.5	235.2	100.0
80	1.922	24.4	195.8	94.1
81	1.910	24.9	207.7	100.0
82	1.896	25.5	219.6	99.1
83	1.848	27.3	246.1	98.5
84	1.909	24.9	211.7	99.8
85	1.898	25.4	208.7	97.1
86	1.847	27.4	232.2	100.0
87	1.871	26.5	222.7	100.0
88	1.866	26.7	212.3	95.8
89	1.916	24.7	216.2	100.0
90	1.908	25.0	196.2	90.6
91	1.927	24.2	198.5	96.8
92	1.903	25.2	233.2	100.0
93	1.894	25.5	218.3	95.4
94	1.917	24.6	212.1	96.2
95	1.927	24.2	210.6	100.0
96	1.914	24.8	205.9	97.1
97	1.891	25.7	197.4	91.0
98	1.920	24.5	194.9	94.6

*Specific Gravity of Grout = 1.742

Control Specimens

To evaluate the performance of the APCCC, the mechanical and durability properties were compared with those of HMA, but chloride intrusion resistance was compared to that of portland cement concrete.

HMA control specimens were Virginia surface mixture SM-5. The aggregate gradation and the control HMA properties are presented in Table 7.8. Portland cement concrete control specimens used for the chloride intrusion comparison were prepared as typical bridge deck mixes used in the state of Pennsylvania. The composition of materials and the properties of the portland cement concrete are presented in Table 7.9.

Table 7.8 Aggregate Gradation and HMA Properties of Virginia Surface Mix (SM-5)

SIEVE SIZE	PERCENT PASSING
2/4"	100.0
1/2"	100.0
3/8"	97.4
#4	71.8
#8	45.5
#16	31.2
#30	23.0
#50	15.9
#100	10.7
#200	7.2
Hydraulic Lime	1% of aggregate weight
Voids in Total Mix, VTM	5.4%
Voids in Mineral Aggregate, VMA	17.9%
Voids Filled in Aggregate, VFA	69.5%
Asphalt Content	5.4%
Unit Weight	147 lb/ft^3
Stability	1950 lb
Flow	14.7 1/100-in
Indirect Tensile Strength	109 psi
Tensile Strength Ratio (TSR)	
Water Sensitivity	0.87
Freeze-Thaw	0.70
Resilient Modulus	2956 ksi
Resilient Modulus Ratio (M_rR)	
Water Sensitivity	0.83
Freeze-Thaw	0.68

Note: 1 lb = 4.448 N, 1 in = 25.4 mm, 1 psi = 6.89 kPa; 1 ksi = 6.89 MPa

Table 7.9 Mix Design and Properties of Portland Cement Concrete

Type I Portland Cement	635.0 lb/yd^3
Fine Aggregate	1193.0 lb/yd^3
Coarse Aggregate	1777.0 lb/yd^3
Water	33.0 gal/yd^3
Air Entraining Agent, Daravair	7.0 oz
Slump	3.5 in
Unit Weight	137 lb/ft^3
Air Voids	6.8%
Compressive Strength	
1 day	2500 psi
7 day	3900 psi
28 day	5570 psi

Note: 1 lbs/yd^3 = 0.59 Kg/m^3; 1 gal/yd^3 = 4.95 ℓ/m^3; 1 oz = 29.6 mℓ; 1 in = 2.54 cm; 1 psi = 6.89 kPa.

Mechanical Tests

Marshall Stability

Marshall stability, designated as ASTM D 1559-82, is one of the most widely used quality control tests of HMA. The objective of this test is to predict the rutting potential of a standard specimen prepared in the laboratory. Marshall stability is defined as the maximum load carried by a compacted specimen tested at 140°F (60°C) at a loading rate of 2 in/min (51 mm/sec). Flow index, or flow value, is the total deformation in 1/100 inches (or in mm) of the specimen at maximum load.

The testing procedure involved applying compressive load to the standard cylindrical specimen, 4 in (101.6 mm) diameter and 2 1/2 in (63.5 mm) height, through semi-circular heads. Specimens were placed in a water bath at a temperature of 140 $\pm$ 1.8°F (60 $\pm$ 1°C) for 30 to 40 minutes before testing. Testing was completed within 30 seconds after removal from the water bath as per specification.

Fifty-one specimens of resin modified concrete were prepared for this test. The specimens were grouped into three moist curing conditions, namely no moist curing, one-day moist curing, and three-day moist curing. Specimens were tested at 1, 3, 7, 21, and 28 days (air cured after termination of moist curing). For comparison, HMA specimens of Virginia surface mix SM-5 were used.

Compressive Strength

Specimens for compressive strength were prepared differently, because they require a

minimum height to diameter ratio of one. The specimens for testing compressive strength were prepared in a 4-in (101.6 mm) mold and the HMA was placed in three layers and hand compacted using a Marshall hammer and applying 10 blows on each layer. This provided the specimens with an air void content in the range of 25 to 30%. The specimens were then filled with resin modified cement slurry grout in accordance with the procedure presented earlier.

Thirty-three specimens were prepared. Specimens were grouped into the three-curing periods, no moist curing, one-day moist curing, and three-day moist curing. Specimens were tested at 1, 3, 7, and 28 days (air cured after termination of moist curing). Specimens were capped with sulfur capping compound before testing, to provide a smooth, flat load surface.

Indirect Tensile Strength

Tensile strength is one of the most widely used tests to determine the characteristics of HMA materials. Thirty-three APCCC specimens were prepared. Specimens were air cured after moist curing (no curing, one-day moist curing and three-day moist curing) until tested at 3, 7, and 28 days. The test was performed in accordance with ASTM D 4123-87. The rate of loading used was 2.0 in/min (51 mm/min). Tensile strength was calculated as follows:

$$\text{Tensile } \textit{Strength} = \frac{2P}{\pi d \ell} \qquad (7\text{-}5)$$

where,

P = maximum load applied to specimen, lb (N);
ℓ = length of the specimen, in (m); and
d = diameter of the specimen, in (m).

Resilient Modulus

Diametral modulus measures the stiffness and temperature susceptibility of asphalt paving mixtures. Several moduli such as Young's, shear, complex, dynamic, double punch, resilient and Shell nomograph are commonly used for structural evaluation of asphalt mixtures. Resilient modulus is more appropriate for use in multilayer elastic programs than are other moduli, because it represents the elastic stiffness of material after repeated loadings (48).

The modulus or elastic stiffness depends on time and temperature. Resilient modulus is defined as the ratio of the applied stress to the recoverable (resilient) strain after repeated loading. The diametral resilient modulus was determined using a MTS and Mark II Resilient Modulus testing apparatus.

The resilient modulus of specimens under dry conditions (without conditioning) were determined at the Virginia Transportation Research Council in Charlottesville, VA. A 0.1 second load pulse is applied every three seconds across the vertical diameter of a cylindrical specimen and the resultant deformation along the horizontal diameter is measured. Thus, Poisson's ratio is needed to determine the resilient modulus. For SM-5 HMA specimens, a Poisson's ratio of 0.35 was used. But, for resin modified concrete specimens the Poisson's ratio cannot be found in the available literature; hence it is necessary to determine the Poisson's ratio to calculate the resilient modulus.

In order to determine Poisson's ratio, it is necessary to determine the vertical and horizontal deformations. An MTS machine was used to determine vertical and horizontal deformations. The Poisson's ratio calculated for these specimens was used to evaluate the resilient modulus for unconditioned specimens tested using the Mark II Resilient Modulus device.

The resilient modulus is calculated as given in the equation below:

$$\text{Modulus}(M_r) = \frac{L*(\nu+0.273)}{(t*\Delta H)}*10^6 \qquad (7.6)$$

where,

M_r = Resilient modulus, psi (Pa)
L = Load, lb (N)
ν = Poisson's ratio
t = Thickness of specimen, in (m)
ΔH = Horizontal strain, micro inches (microns)

Durability Tests

Water Sensitivity (Stripping)

Moisture susceptibility or deterioration of asphalt mixture due to the detrimental effects of water (stripping) causes loss of bond strength (adhesion) at the aggregate-asphalt interface and/or loss of cohesion of asphalt due to the presence of moisture, and external and internal forces. Therefore, moisture in HMA can cause severe damage to its long-term performance. This damage manifests itself as stripping and softening which cause structural strength and mixture stiffness loss. Flushing may occur when some of the stripped asphalt cement rises to the surface. This may develop deformations in the form of shoving and rutting and may also reduce the resilient modulus.

Stripping has been recognized as a critical problem since the early 1970's, reducing the serviceability and durability of HMA, with costly consequences. Thus the evaluation of materials for stripping resistance has gained importance. An aggregate-asphalt system not

prone to water susceptibility has to retain strength when subjected to moisture conditioning. There are 3 different categories in which the evaluation is conducted:

(a) stripping evaluation using loose compacted mixture;
(b) stripping evaluation using compacted specimens;
(c) stripping evaluation by determining weight loss of specimen when subjected to abrasive forces after conditioning.

Laboratory compacted or field extracted specimens are conditioned to simulate inservice conditions and compared with those unconditioned specimens using strength and stiffness tests such as indirect tensile strength, stability, compressive strength and resilient modulus.

Various methods exist today to predict the stripping phenomenon quantitatively; however, none of them provide accurate prediction. The following are most commonly used in the United States: Immersion Compression Test (AASHTO T-165, ASTM D 1075); Lottman Test (49); Tunnicliff/Root Test (50); Marshall Immersion Test (ASTM D 1664); Freeze-thaw Pedestal Test (51); and Boil Test (ASTM D 3625).

In this study, the modified Lottman method (53), was used to evaluate the stripping resistance of the resin modified concrete. This method is more severe than the Tunnicliff/Root method or original Lottman method as the specimens are subjected to freezing cycles also. Resistance to stripping was determined by evaluating the tensile strength and resilient modulus before and after specimen conditioning.

Tensile Strength Ratio (TSR) and Resilient Modulus Ratio (M_rR) were determined as below:

Tensile Strength Ratio (TSR) = Ratio of tensile strength obtained after conditioning to the tensile strength obtained before conditioning.

Resilient Modulus Ratio (M_rR) = Ratio of modulus retained after conditioning to modulus obtained before conditioning.

The suggested minimum value for TSR and M_rR which indicates that the material may not be susceptible to water damage is 0.75 (53).

Thirty-six specimens were prepared for moisture damage evaluation of the APCCC over time for the three different moist curing periods. Two specimens of each moist curing period, no moist curing, one-day moist curing, and three-day moist curing, were air cured for the remaining time of 3, 7, and 28 days before being water conditioned.

Water conditioned specimens are vacuum saturated. Specimens are immediately wrapped in plastic sheet and were kept in a plastic bag containing 10 ml of water. The specimens were then placed in a freezer for 15 hours at 0 $\pm$ 4°F (-32 $\pm$ 2°C). After removal from the freezer the specimens were unwrapped and kept in a water bath for 24 hours at 140 $\pm$ 1.8°F

(60 ± 1°C). The specimens were then removed from the water bath and kept at testing temperature for three hours (room temperature) before testing. Resilient modulus and indirect tensile strength were then performed on the water conditioned specimens. Indirect Tensile Strength for conditioned specimens was tested in accordance with ASTM D 4123-87.

For the resilient modulus testing, cyclic loads between 0.1 to 0.4 of tensile strength were used. The load was transmitted through the curved strips of 1/2 in (13 mm) wide and 2 1/2 in (63.5 mm) long. The load was applied in the square wave form of 0.1 second of load application and releasing the load for 0.9 seconds, thus the frequency was 1 Hz.

The data were acquired by LTN (Lab Tech Notebook) data acquisition system, using four channels. One channel was used to measure the load, one for vertical deformation and the other two to measure the horizontal deformations through LVDTs mounted on either side of the specimen. The data were acquired at a rate of 100 points per second to accurately represent the deformation curve.

Freezing and Thawing

Freezing and thawing is the foremost test used to evaluate the performance of concrete under environmental conditions. Repeated freezing and thawing cycles produce disruptive forces caused by the volume expansion of water during freezing will cause damage to inadequately protected materials (54). Water in the capillary pores of cement paste expands upon freezing, and if the volume is greater than the available space, then the excess water flows under the pressure of expansion. If flow pressure exceeds the tensile strength of paste, cracking occurs, allowing more water to enter during the thawing cycle, and causing more damage during freezing.

The apparatus, the temperature of the freeze thaw cycles, and the duration of each cycle used in this study were in accordance with *ASTM C-666-84, Standard Test Method for Resistance of Concrete to Rapid Freezing and Thawing*; however the specimen shape and size were different. The temperature changed from 40°F to 0°F (4°C to -32°C) during freezing and 0°F to 40°F (-32°C to 4°C) during thawing. The time for one freezing and thawing cycle is ranged between about four hours, thus achieving an average of six cycles per day.

APCCC specimens prepared using the Marshall procedure 4 in (101.6 mm) diameter and 2 1/2 in (63.5 mm) thick, were used to evaluate the effect of freezing and thawing cycles on this material. As the depth-to-diameter ratio is less than one, the dynamic modulus of the specimens could not be determined by the transverse frequency method.

As a result, the effects of freezing and thawing were determined by calculating the indirect tensile strength and resilient modulus before and after conditioning. Because no procedure exists to evaluate the freeze-thaw effects on HMA specimens, resin modified concrete specimens were evaluated after being subjected to 25 rapid freeze-thaw cycles.

Thirty-six specimens were prepared for evaluating the resistance of APCCC to rapid freezing and thawing conditioning for the different curing periods.

Chloride Intrusion

Chlorides arrive at the reinforcing steel in concrete in three different ways: they may be present in the original mix at the time of concrete placement, for example in mixing water, in aggregates, or in accelerators; they may enter through cracks; and they may ingress through pore structure, i.e., by diffusion.

In this research, the Specific Ion Probe method was used to determine chloride contents of specimens based on the results of SHRP C-101 (55). Nine APCCC specimens exposed to three moist curing periods, no moist curing, one-day moist curing and three-day moist curing, air cured to 28 days. After curing, three specimens from each group were subjected to 7, 11 and 15 wet/dry ponding cycles using 3% sodium chloride solution. Each cycle consisted of four days of air curing and three days of salt solution ponding.

After completion of dry/wet cycles, the specimens were cut into quarters and each quarter was then cut into three parts and at least 3 grams of powdered grout was collected at two depths from the top surface; 0.75 in (19 mm), between 0.25 in (6 mm) and 1.25 in (32 mm), and 1.75 in (44 mm), between 1.25 in (32 mm) and 2.25 in (57 mm). The collected grout at different depths from various specimens was stored in labeled plastic containers until chloride contents were measured.

Extreme care was taken during drilling to avoid collecting any asphalt or crushed aggregates. Asphalt cement contains chemicals which may influence the specific ion probe readings. Powdered samples were collected from the control portland cement concrete specimens at corresponding depths to correlate the results of the two materials.

The specific gravity of the grout was 1.742 and unit weight was 2935 lb/yd^3 (17.1 kN/m^3). Thus, to convert the percentage of chloride ions into lb/yd^3 a factor of 29.3 was used. However, the sample was extracted only from the grout and this constituted only 25.3% of the whole material by volume (volume of grout and air voids). In order to convert the chloride into weight per volume of the APCCC the above obtained factor was reduced by 74.7% to measure the amount of chloride in weight per volume of APCCC.

The multiplier for the portland cement concrete was 39.5 to determine the amount of chloride content in lb/yd^3 of portland cement concrete.

Results and Discussion

Marshall Stability

The stability results for all three moist curing levels of APCCC specimens are presented in Table 7.10 and Fig. 7.2. The results indicate that stability of APCCC increases with time for all moist curing levels. For example, at three-day testing, the stability of APCCC was 2111 lb (9389 N) for no moist curing, 2218 lb (9866 N) for one-day moist curing, and 2239 lb (9961 N) for three-day moist curing, whereas the corresponding values at 28 day testing were 3017 lb (13421 N), 4028 lb (17918 N), and 4264 lb (18968 N), respectively.

The stability, in general, increased with the moist curing period. For example, at seven-day testing, the stability was 2259 lb (10047 N) for no moist curing, 2289 lb (10180 N) for one-day moist curing, and 2396 lb (10658 N) for three-day moist curing. For all moist curing conditions, the stability values were higher than for the control mixture SM-5 HMA, which had an average stability of 1956 lb (8700 N). The results also showed that the stability of APCCC for one-day moist curing was 17% greater than that of SM-5 HMA at three-day testing, and 205% greater at 28 days.

Compressive Strength

The results of compressive strength measurements for APCCC specimens at all three moist curing periods are presented in Table 7.11 and Fig. 7.3. The compressive strength of the APCCC was found to increase with curing and time as does that of portland cement concrete. The compressive strengths at three day testing were 300 psi (2070 kPa) for no moist curing, 316 psi (2180 kPa) for one-day moist curing, and 332 psi (2290 kPa) for three-day moist curing, whereas the corresponding values at 28 day testing were 799 psi (5510 kPa), 894 psi (6160 kPa), and 1013 psi (6990 kPa), respectively.

Compressive strength of APCCC at 28 day testing was found to be three times that of HMA. Compressive strength gained between one-day and three-day moist curing was insignificant at three and seven day testing. However, a greater difference was noticed between one day and three day moist curing at 28 day testing.

Indirect Tensile Strength

The results of the indirect tensile strength test for APCCC for all three moist curing periods are presented in Table 7.12 and Fig. 7.4. An increase of about 40% in tensile strength was observed between three day and 28 day testing.

Tensile strengths of APCCC at three day testing were 110 psi (756 kPa) for no moist curing, 117 psi (806 kPa) for one day moist curing, and 123 psi (894 kPa) for three day moist curing, whereas the tensile strengths for corresponding moist curing levels at 28 day testing are 143 psi (985 kPa), 169 psi (1166 kPa), and 174 psi (1197 kPa), respectively.

Table 7.10 Stability and Flow Results

TIME (DAYS)	MOIST CURING	AVERAGE STABILITY (LBS)	STANDARD DEVIATION (LBS)	AVERAGE FLOW (0.01 IN)	STANDARD DEVIATION (0.01 IN)
1	NO	1801	336	27.8	10.4
	1 DAY	1983	171	28.5	7.9
3	NO	2111	273	24.0	3.3
	1 DAY	2218	18	16.5	0.5
	3 DAYS	2239	173	14.5	1.1
7	NO	2259	206	10.3	1.9
	1 DAY	2289	1	20.5	3.5
	3 DAYS	2396	2	14.5	0.5
21	NO	2536	242	21.0	0.0
28	NO	3017	143	13.6	5.1
	1 DAY	4028	278	18.5	1.5
	3 DAYS	4264	68	30.0	2.0

Note: 1 lb = 4.448 N, 1 in = 25.4 mm

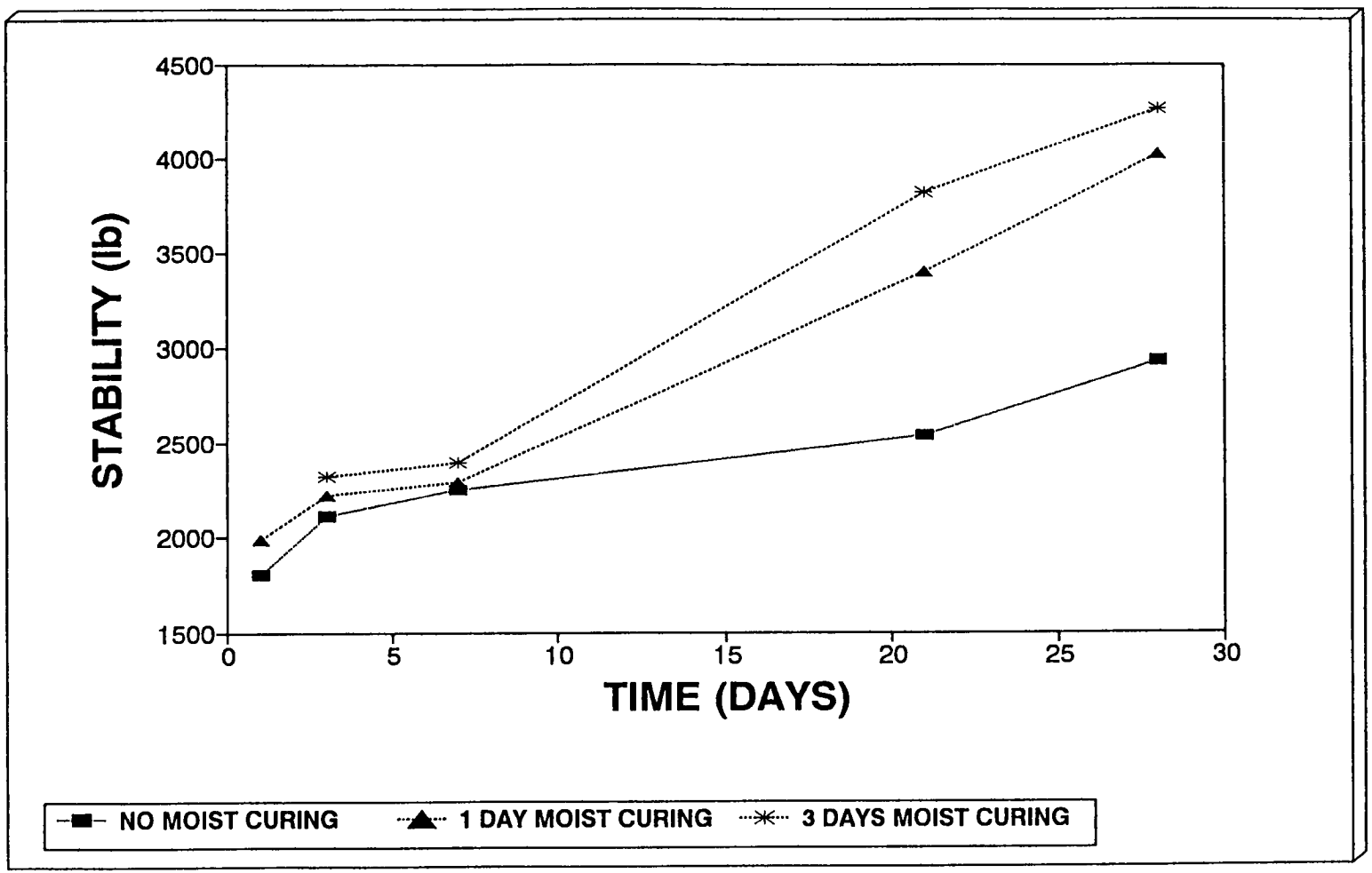

Fig. 7.2 Marshall Stability At Various Curing Periods

Table 7.11 Compressive Strength Results

CURING TIME (DAYS)	MOIST CURING	AVERAGE COMPRESSIVE STRENGTH (PSI)	STANDARD DEVIATION (PSI)
1	NO	270	25
	1 DAY	316	25
3	NO	301	17
	1 DAY	316	13
	3 DAYS	332	11
7	NO	464	33
	1 DAY	509	35
	3 DAYS	513	13
28	NO	799	13
	1 DAY	894	154
	3 DAYS	1013	27

Note: 1 psi = 6.89 kPa

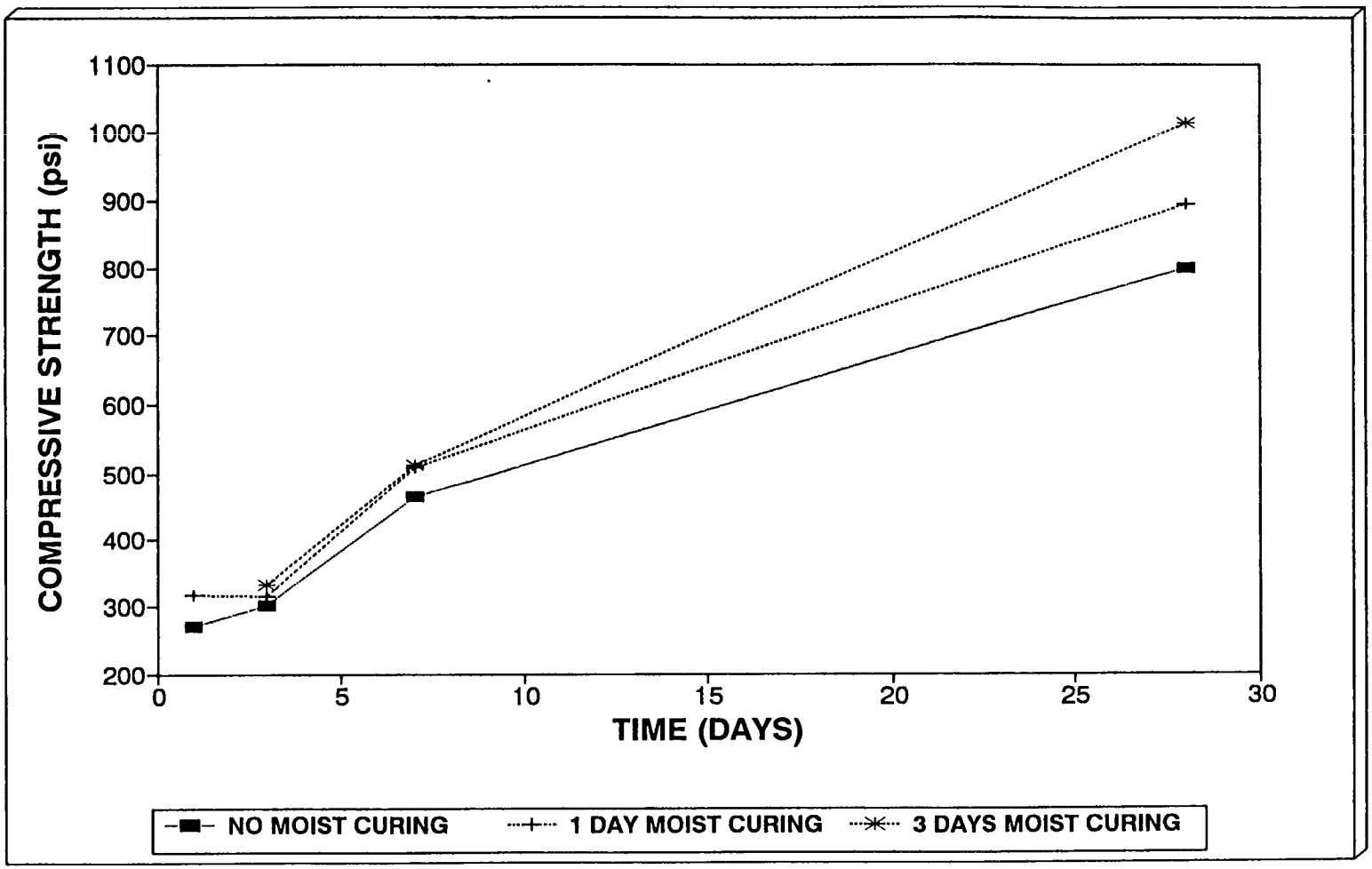

Fig. 7.3 Compressive Strength of APCCC

Table 7.12 Indirect Tensile Strength Results

CURING TIME (DAYS)	MOIST CURING	AVERAGE TENSILE STRENGTH (PSI)	STANDARD DEVIATION (PSI)
1	NO	108	10
	1 DAY	105	3
3	NO	110	11
	1 DAY	117	5
	3 DAYS	123	5
7	NO	142	8
	1 DAY	147	9
	3 DAYS	152	4
28	NO	143	8
	1 DAY	169	13
	3 DAYS	174	3

Note: 1 psi = 6.89 kPa

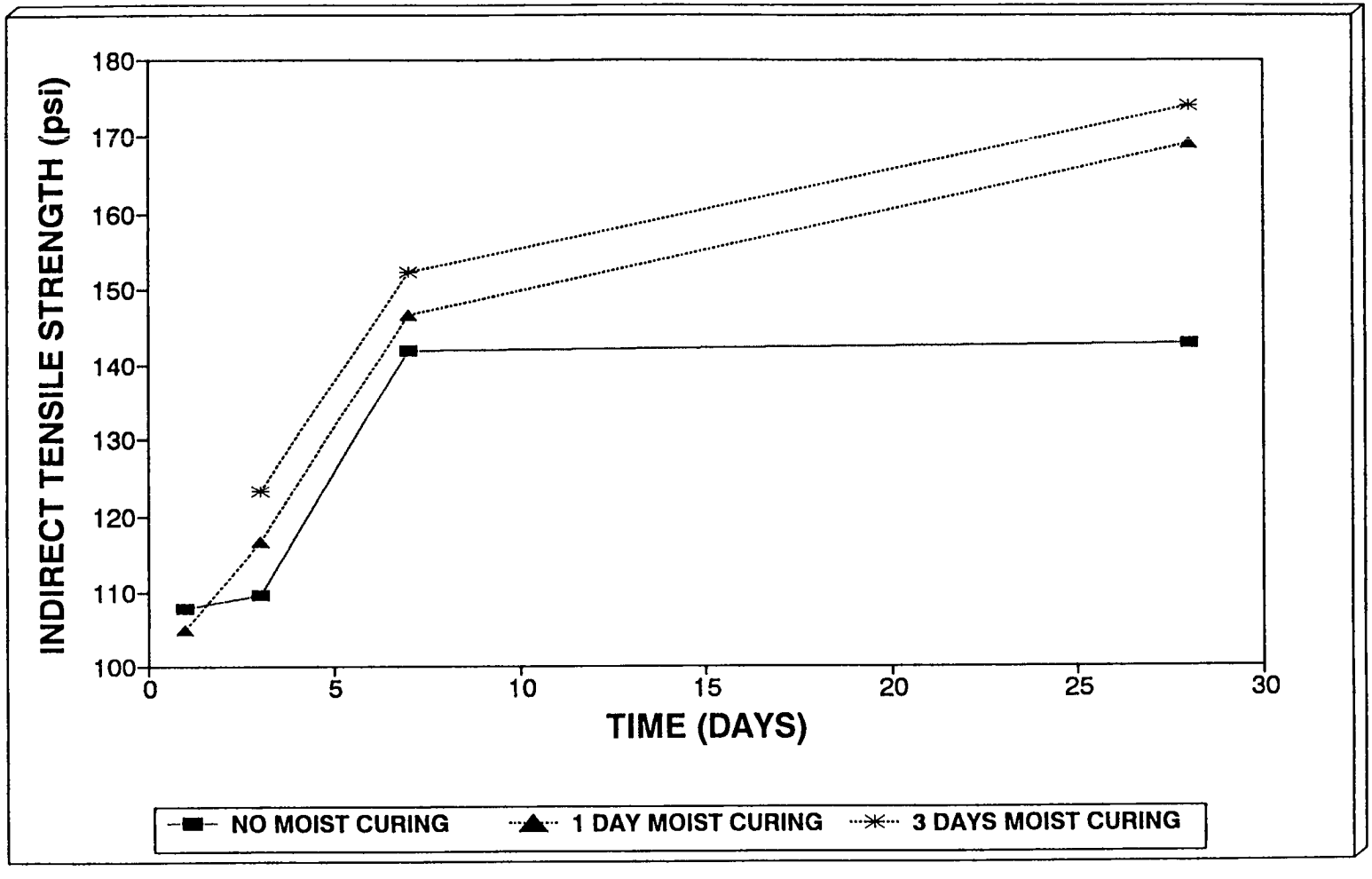

Fig. 7.4 Indirect Tensile Strength of APCCC

An increase of 30% for no moist curing, 55% for one day moist curing, and 59% for three day moist curing is observed at 28 day testing compared to tensile strength of SM-5 HMA. Indirect tensile strength of SM-5 HMA was found to be 109 psi (715 kPa). Insignificant difference in tensile strength was found between one day and three day moist curing.

Resilient Modulus

The results of resilient modulus tests at 1, 3, 7, and 28 days testing for all three moist curing levels of APCCC are presented in Table 7.13 and Fig. 7.5. The resilient modulus at room temperature for APCCC was found to be higher than that of SM-5 HMA at all investigated curing periods and increased with time. The resilient modulus increased by 73% for no moist curing, 71% for one-day moist curing, and 73% for three-day moist curing, when tested at and 28 days. The resilient modulus was found to increase with moist curing; at seven-day testing, the resilient modulus was 489 ksi (3370 MPa) for no moist curing, 507 ksi (3490 MPa) for one day moist curing, and 522 ksi (3600 MPa) for three-day moist curing.

The average resilient modulus for SM-5 HMA was found to be 296 ksi (2040 MPa). APCCC, tested at 28 days, showed an increase of 212% in resilient modulus over SM-5 HMA for no moist curing, 225% for one-day moist curing, and 242% for three-day moist curing when tested at room temperature.

Water Sensitivity

The tensile strengths of the water-conditioned specimens using modified Lottman method are presented in Table 7.14 and Fig. 7.6. Comparison between tensile strengths of unconditioned and water-conditioned APCCC specimens are presented in Figs. 7.6 through 7.9.

The results showed that all tensile strength ratio (TSR) values for APCCC exceeded 0.75 at all times for all moist curing levels except for one-day moist curing and three-day moist curing at 28 day testing. TSR for SM-5 HMA was 0.87. The tensile strengths of conditioned specimens of APCCC for all moist curing levels were found to exceed the unconditioned specimens of SM-5 HMA at all periods.

Tensile strength ratios (TSR) were, in general, found to decrease with moist curing and also decrease with time, which is contradictory. Visual observations indicated that the surfaces of conditioned specimens were not similar to those of unconditioned specimens; because of water conditioning, the surface grout peeled off, making the surface irregular. As a result, the loading strips were not in a good contact along the loaded strip, resulting in concentrated loads and thereby lower tensile strength values. The specimens, did not have any cracks.

Resilient moduli of the water conditioned APCCC specimens are presented in Table 7.14. The comparison of the resilient modulus of APCCC with that of SM-5 HMA are presented in Fig. 7.10. Comparisons between resilient moduli of unconditioned and water conditioned specimens, for all moist curing levels are presented in Figs. 7.11 through 7.13.

Table 7.13 Resilient Modulus Results

CURING TIME (DAYS)	MOIST CURING	AVERAGE RESILIENT MODULUS Mr (KSI)	STANDARD DEVIATION (KSI)
1	NO	333	59
	1 DAY	364	12
3	NO	364	4
	1 DAY	390	3
	3 DAYS	414	33
7	NO	489	30
	1 DAY	507	23
	3 DAYS	522	73
28	NO	629	93
	1 DAY	666	36
	3 DAYS	717	12

Note: 1 ksi = 6.89 MPa

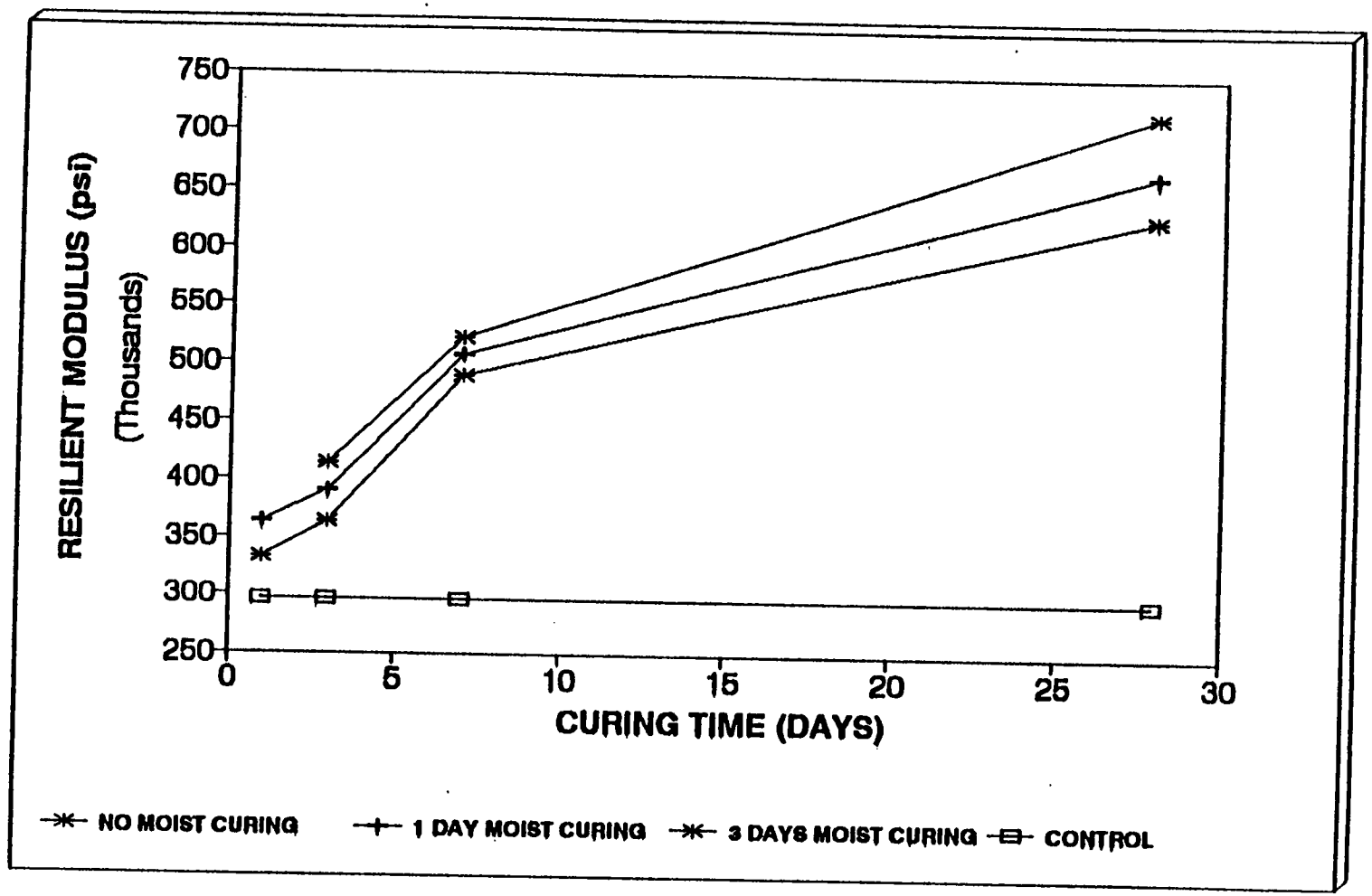

Fig. 7.5 Resilient Modulus of APCCC and HMA

Table 7.14 Tensile Strength and Resilient Modulus Results for Conditioned Specimens

CURING TIME (DAYS)	MOIST CURING	AVERAGE TENSILE STRENGTH (PSI)	STANDARD DEVIATION (PSI)	AVERAGE TENSILE MODULUS (KSI)	STANDARD DEVIATION (KSI)	AVG. RES MODULUS (KSI)	STANDARD DEVIATION (KSI)
3	NO	117	4	107	4	330	4
	1 DAY	113	9	97	8	347	4
	3 DAYS	113	3	92	3	367	4
7	NO	121	5	85	4	430	9
	1 DAY	121	6	83	4	468	125
	3 DAYS	125	10	82	7	481	25
28	NO	122	4	85	2	520	15
	1 DAY	126	7	72	0	563	44
	3 DAYS	126	5	72	3	587	46

Note: 1 psi - 6.89 kPa; 1 ksi = 6.89 MPa

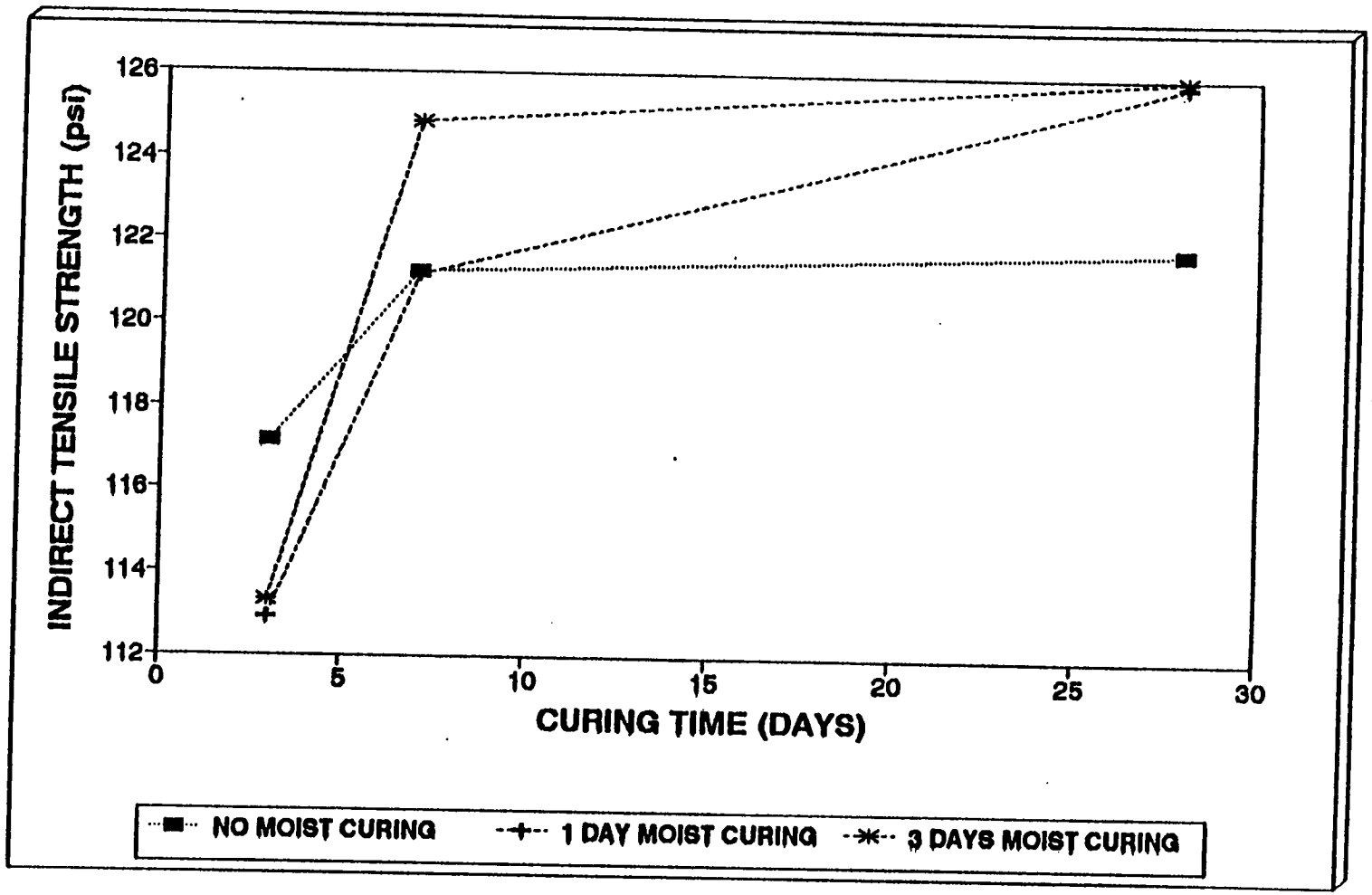

Fig. 7.6 Tensile Strength of Water Conditioned APCCC

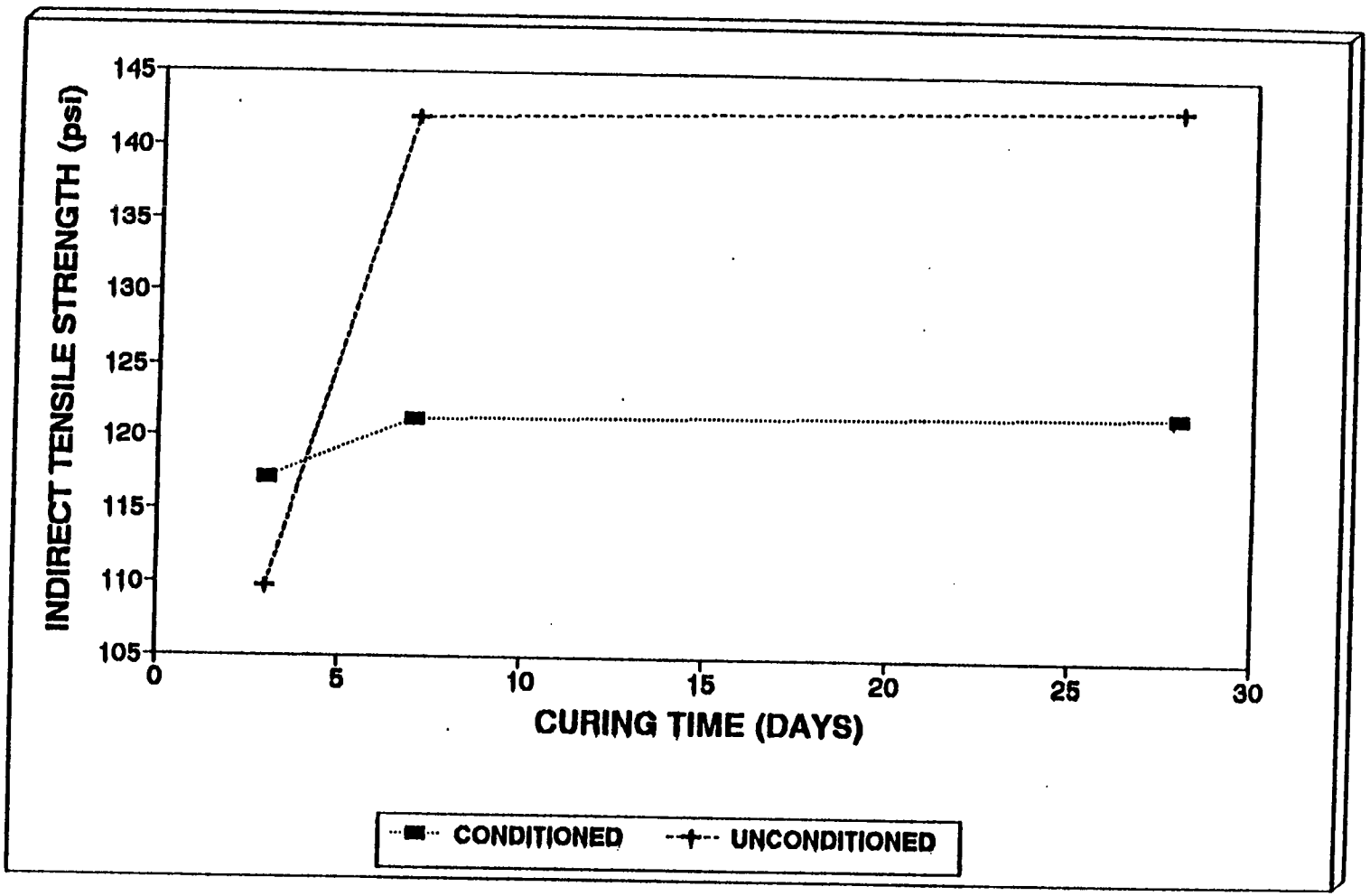

Fig. 7.7 Water Conditioning Effects on the Tensile Strength of Non-Cured APCCC

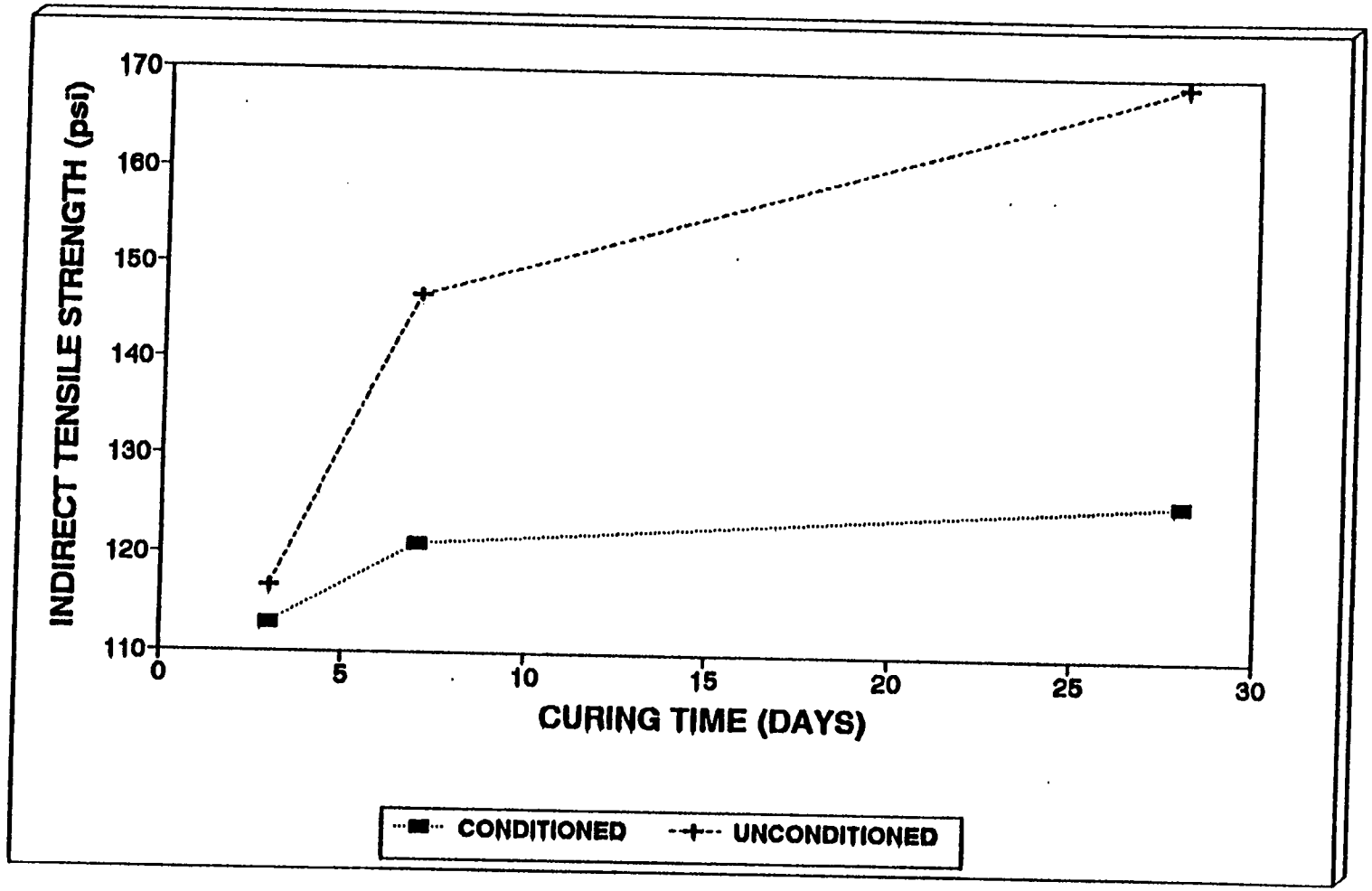

Fig. 7.8 Water Conditioning Effects on the Tensile Strength of 1-Day Moist-Cured APCCC

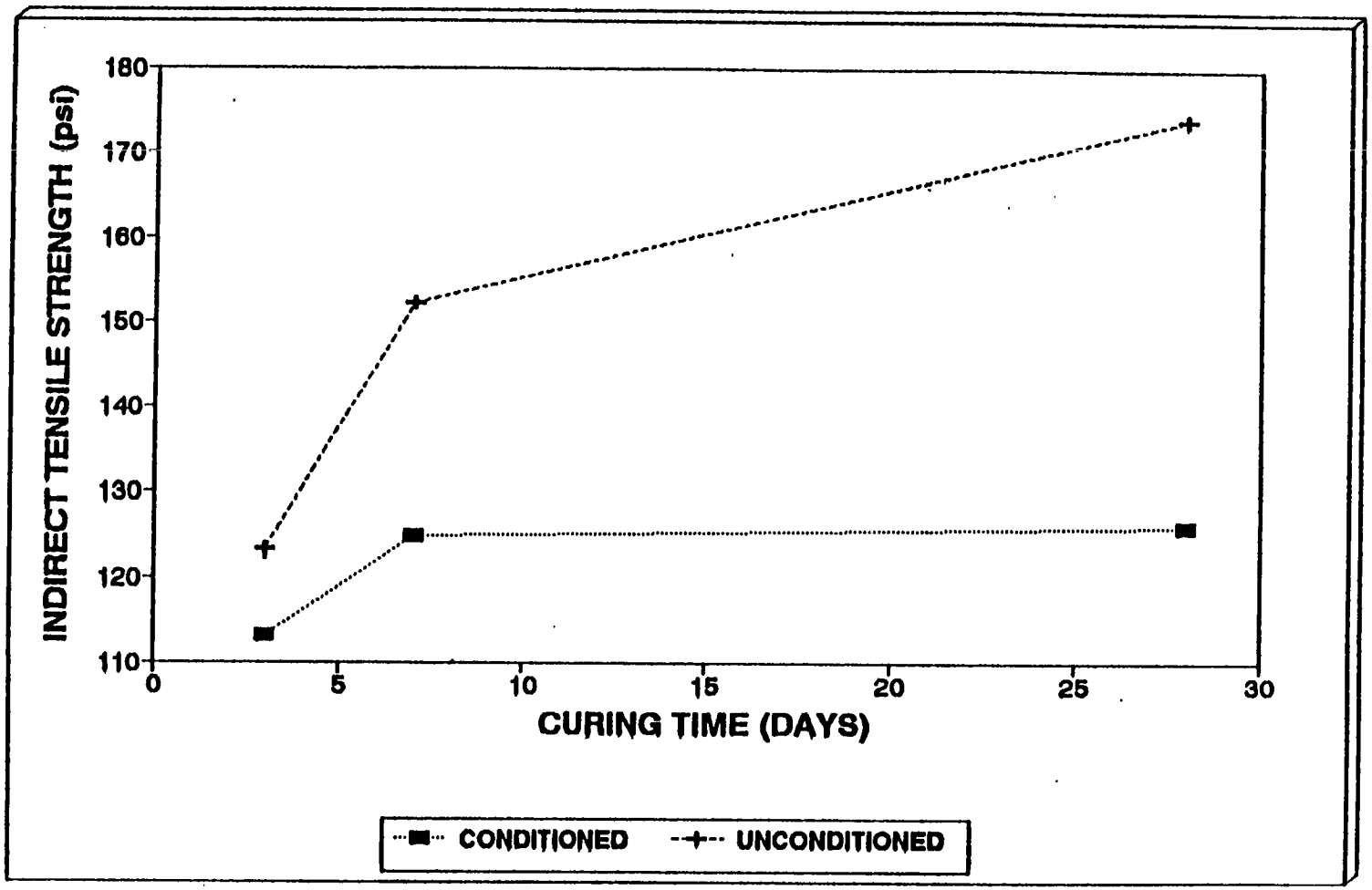

Fig. 7.9 Water Conditioning Effects on the Tensile Strength of 3-Days Moist-Cured APCCC (Tensile Strength)

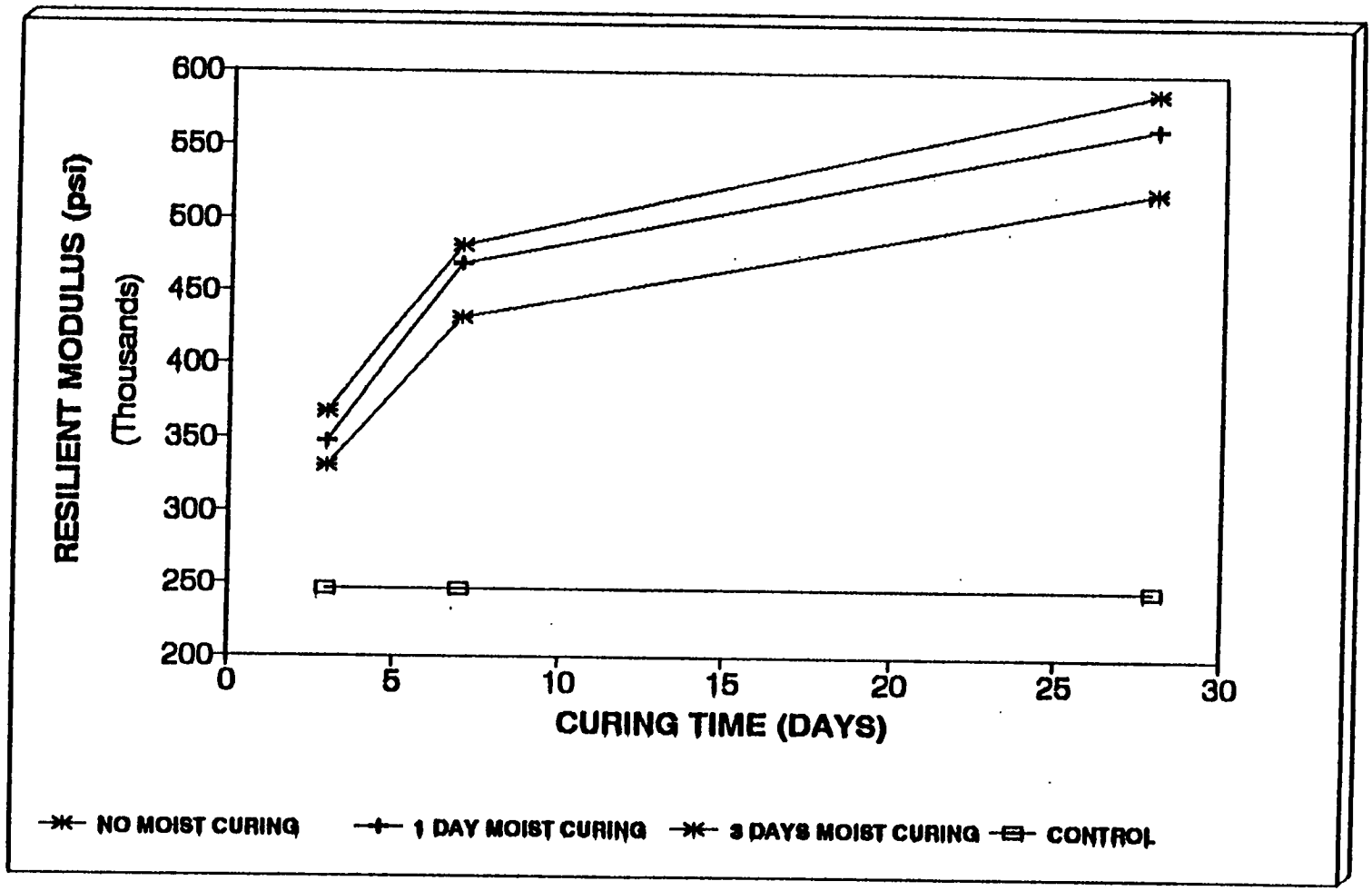

Fig. 7.10 Resilient Moduli of Water Conditioned APCCC

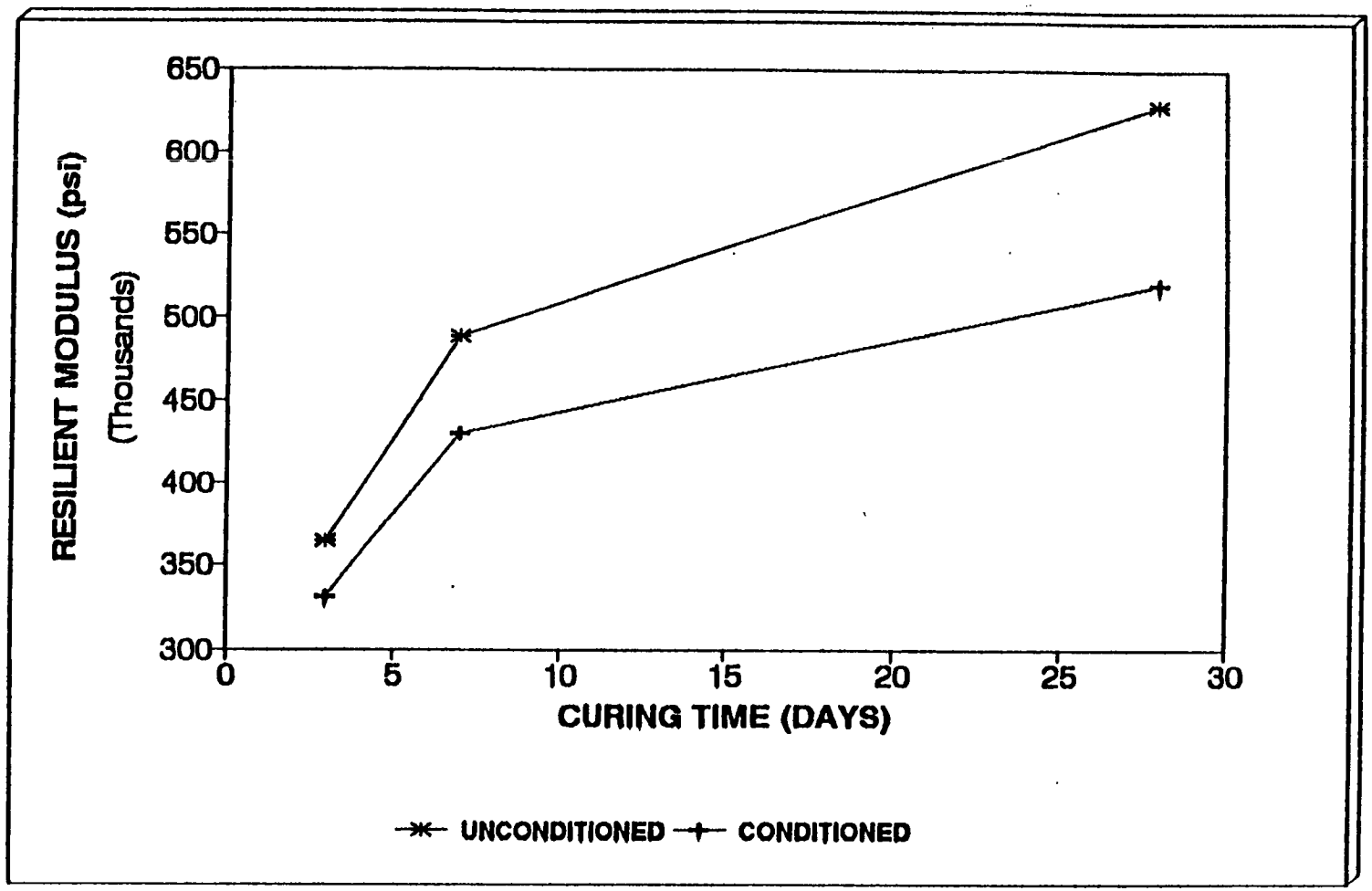

Fig. 7.11 Water Conditioning Effects on the Resilient Modulus of Non-Moist-Cured APCCC

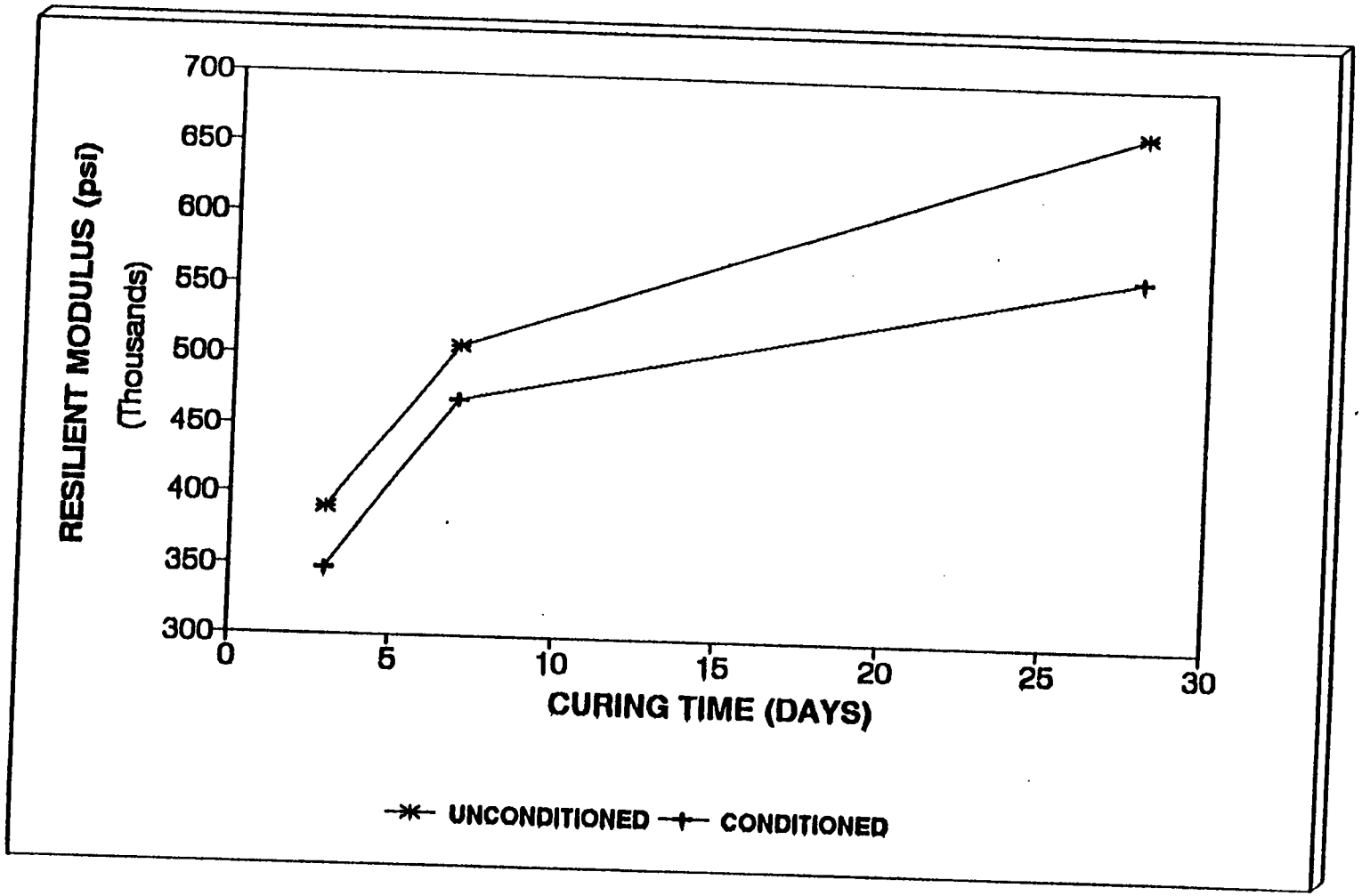

Fig. 7.12 Water Conditioning Effects on The Resilient Modulus of 1-Day Moist-Cured APCCC

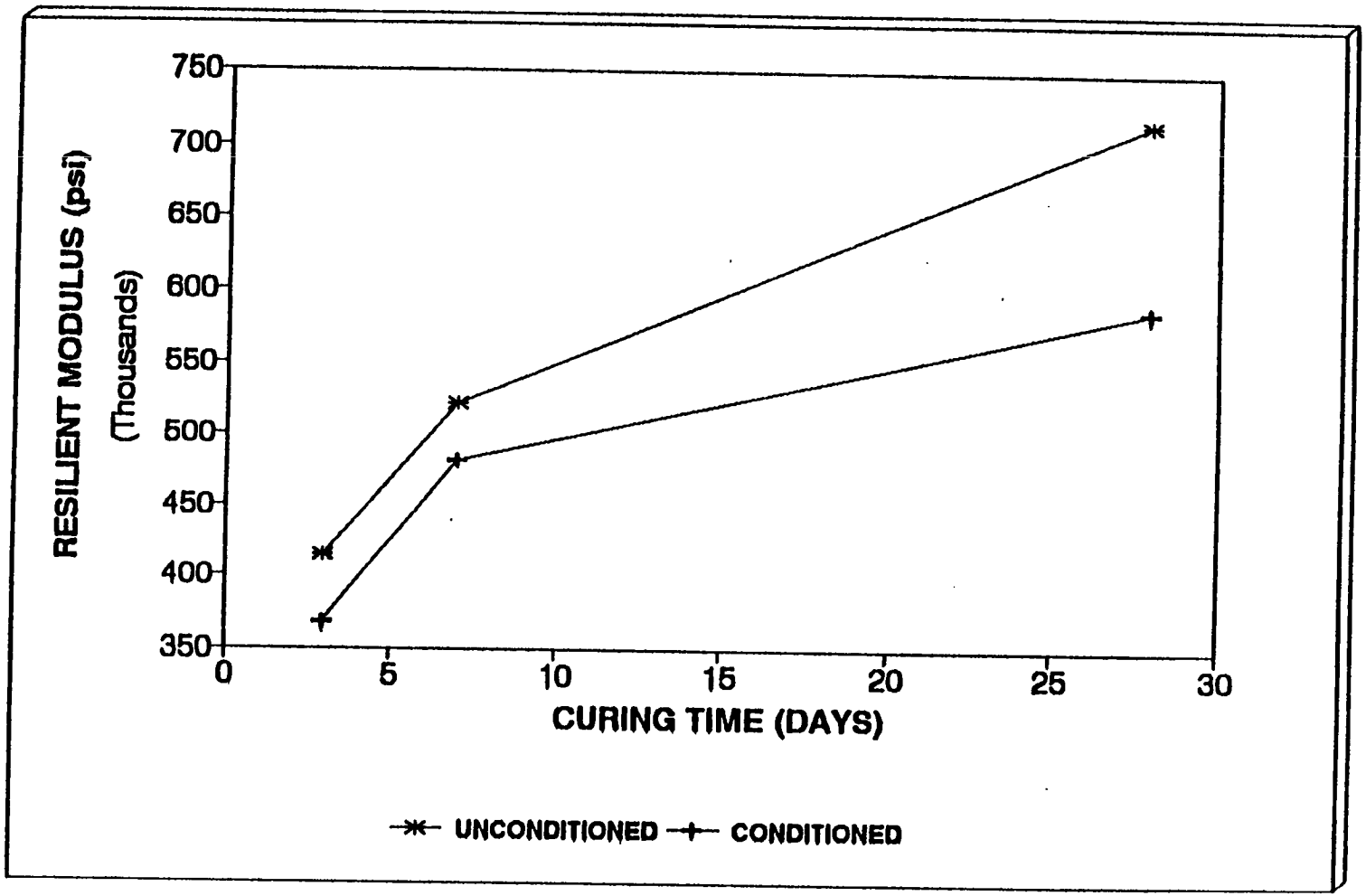

Fig. 7.13 Water Conditioning Effects on the Resilient Modulus of 3-Days Moist-Cured APCCC

Resilient modulus ratio (M_rR) of the SM-5 HMA was found to be 0.83. Resilient modulus ratios (M_rR) of the APCCC for all moist curing levels were found to exceed 0.82, at all times. One day moist curing was, in general, found to have the highest M_rR values compared to no moist curing and three-day moist curing.

The resilient modulus of the water-conditioned APCCC specimens was found to exceed even the resilient modulus of the unconditioned SM-5 HMA. Resilient moduli of the water conditioned APCCC specimens at 28 day testing were found to be 620 ksi (3580 MPa) for no for no moist curing, 563 ksi (3880 MPa) for one-day moist curing, and 5870 ksi (4050 MPa) for three-day moist curing compared to resilient modulus of 296 ksi (2040 MPa) of the unconditioned SM-5 HMA.

Freeze-Thaw

So far, the effects of freeze-thaw have not been well investigated for HMA. However, the freeze-thaw effects of portland cement concrete have been studied extensively using ASTM C-666 and C-672.

Tensile strengths of the APCCC specimens tested after being subjected to 25 rapid freeze-thaw cycles are presented in Table 7.15 and Fig. 7.14 . Tensile strength ratios of the APCCC specimens ranged between 0.66 and 0.89, whereas tensile strength ratio of SM-5 HMA was found to be 0.70.

Tensile strength of conditioned specimens was found to increase with moist curing and time; however, the tensile strength ratios were found to decrease with time, possibly because the surface grout had slightly peeled off, causing an irregular surface area. However, no visual cracks were observed after specimens were subjected to freeze-thaw conditioning, tending to support the observation that specimens were not highly prone to freeze-thaw deterioration after 25 cycles of freeze-thaw. Specimens of no moist curing yielded highest TSR values at three and 28 day testing. Whereas one-day moist curing yielded highest TSR at seven-day testing, followed by three-day moist curing and no moist curing, see Figs. 7.15 through 7.17.

Resilient moduli of the APCCC specimens tested at 3, 7, and 28 days for all three moist curing periods are presented in Table 7.15 and Fig. 7.18. Comparisons between unconditioned and conditioned specimens at all moist curing levels are presented in Figs. 7.19 through 7.21.

The resilient modulus ratio of SM-5 HMA was found to be 0.68. Resilient modulus ratio (M_rR) of the APCCC specimens ranged from 0.51 to 0.78. No moist cured specimens yielded the highest M_rR values at seven and 28 day testing, followed by the one-day moist curing and three-day moist curing. However, differences between the M_rR values of no-moist-curing and one-day-moist-curing specimens were insignificant.

At three-day testing, one-day moist curing had the highest MrR value followed by 3 day moist curing and no moist curing.

Table 7.15 Tensile Strength and Resilient Modulus Results of Freeze-Thaw Conditioned Specimens

CURING TIME (DAYS)	MOIST CURING	AVERAGE TENSILE STRENGTH (PSI)	STANDARD DEVIATION (PSI)	AVG. RES. MODULUS Mr (KSI)	STANDARD DEVIATION (KSI)
3	NO	98	14	248	2
	1 DAY	98	5	304	45
	3 DAYS	101	10	296	6
7	NO	99	7	265	8
	1 DAY	110	1	265	14
	3 DAYS	111	5	278	8
28	NO	110	2	327	4
	1 DAY	111	2	340	15
	3 DAYS	117	6	389	16

Note: 1 psi = 6.89 kPa; 1 ksi = 6.89 MPa

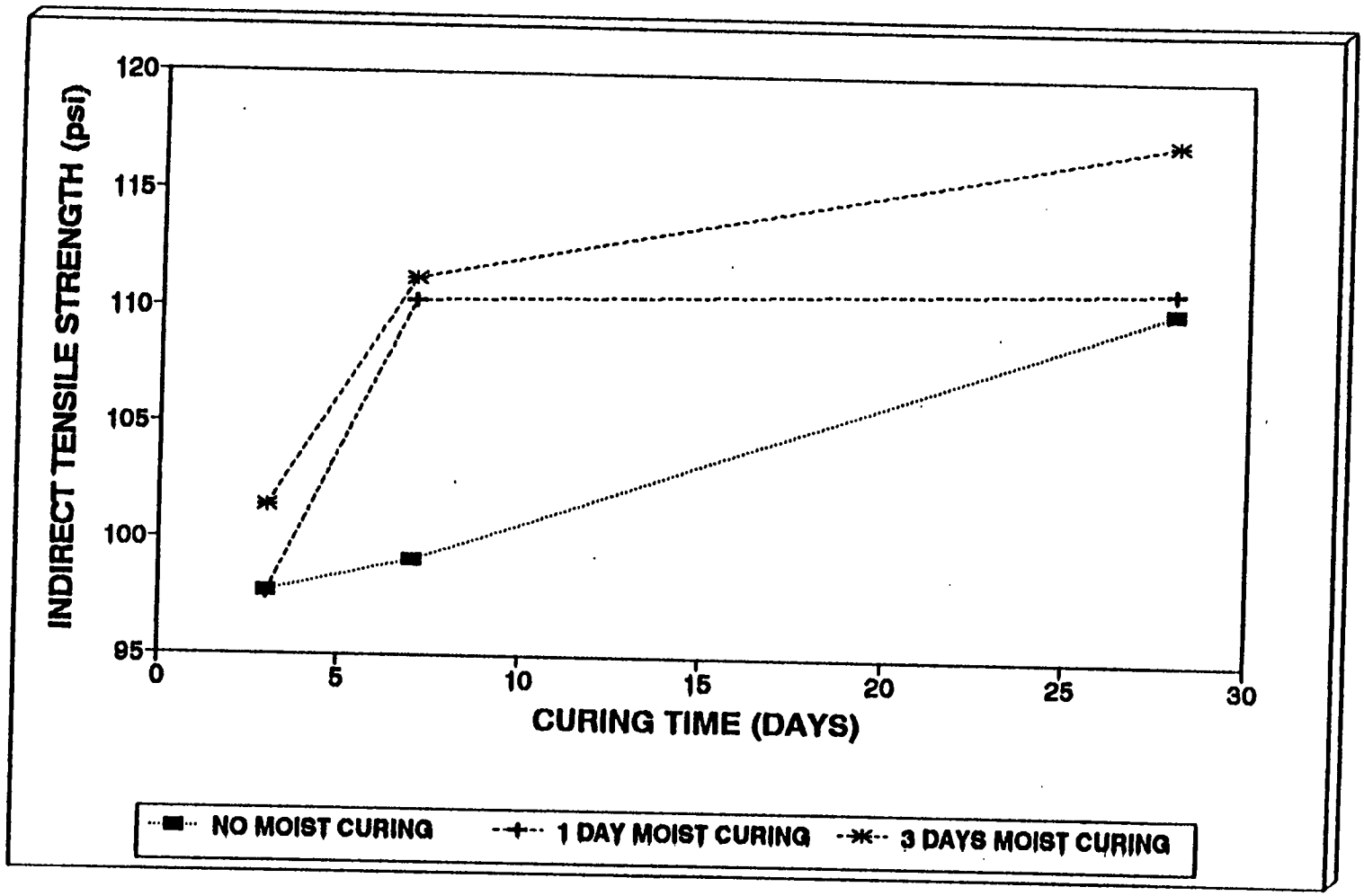

Fig. 7.14 Tensile Strength Results of Freeze-Thaw Conditioned Specimens

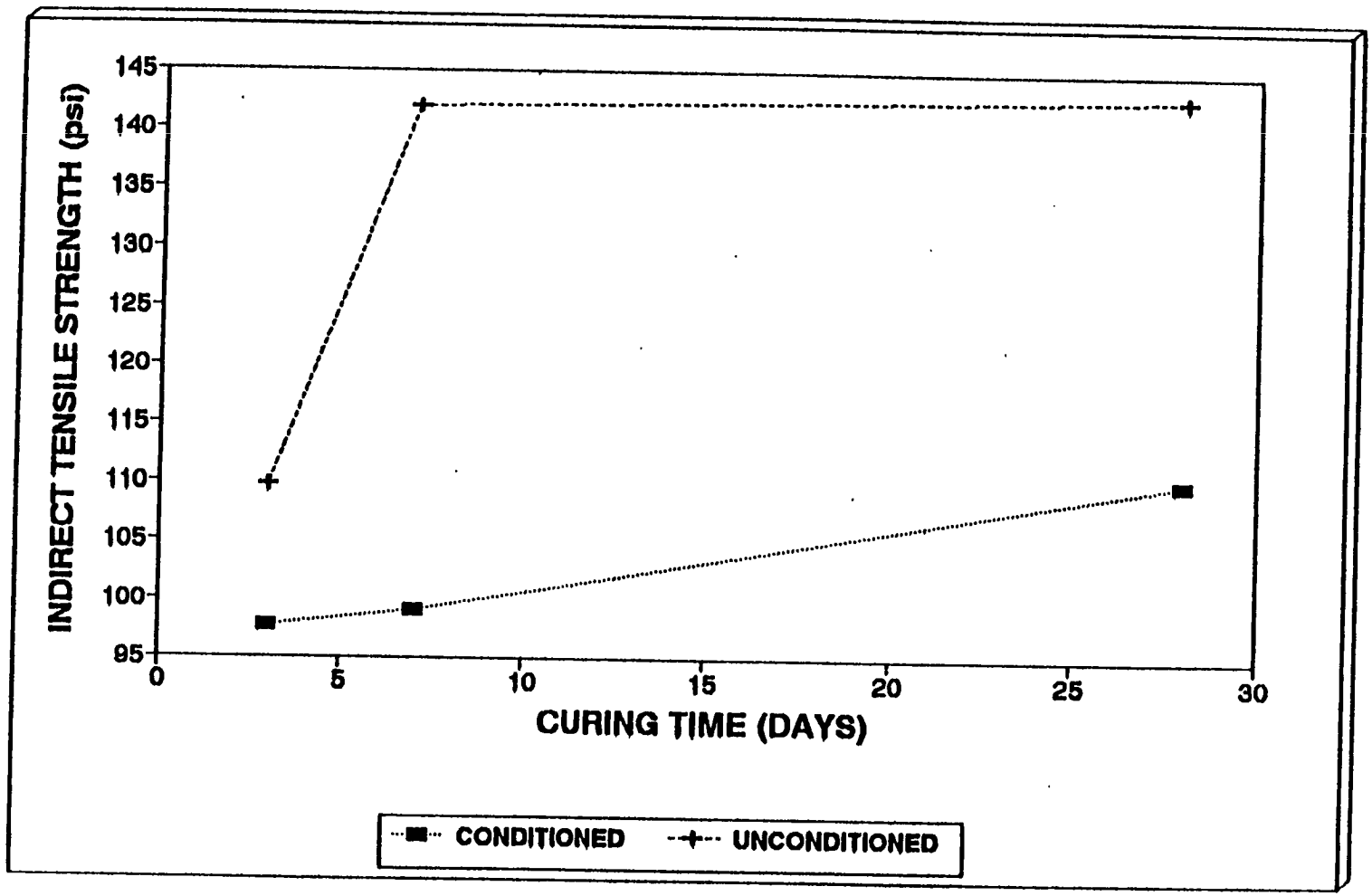

Fig. 7.15 Freeze - Thaw Effects On No Moist Curing Specimens (Tensile Strength)

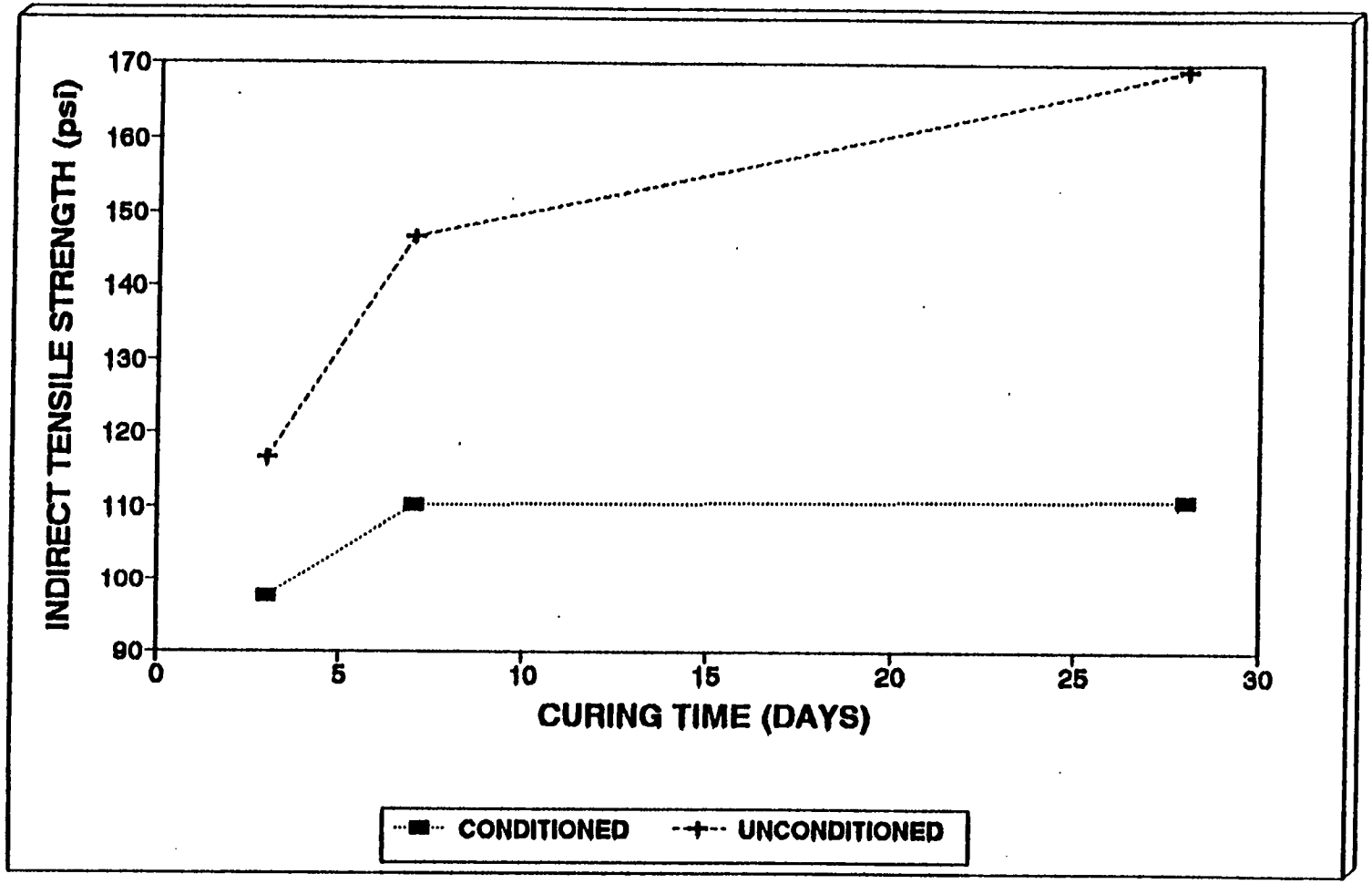

Fig. 7.16 Freeze - Thaw Effects On 1-Day Moist Curing Specimens (Tensile Strength)

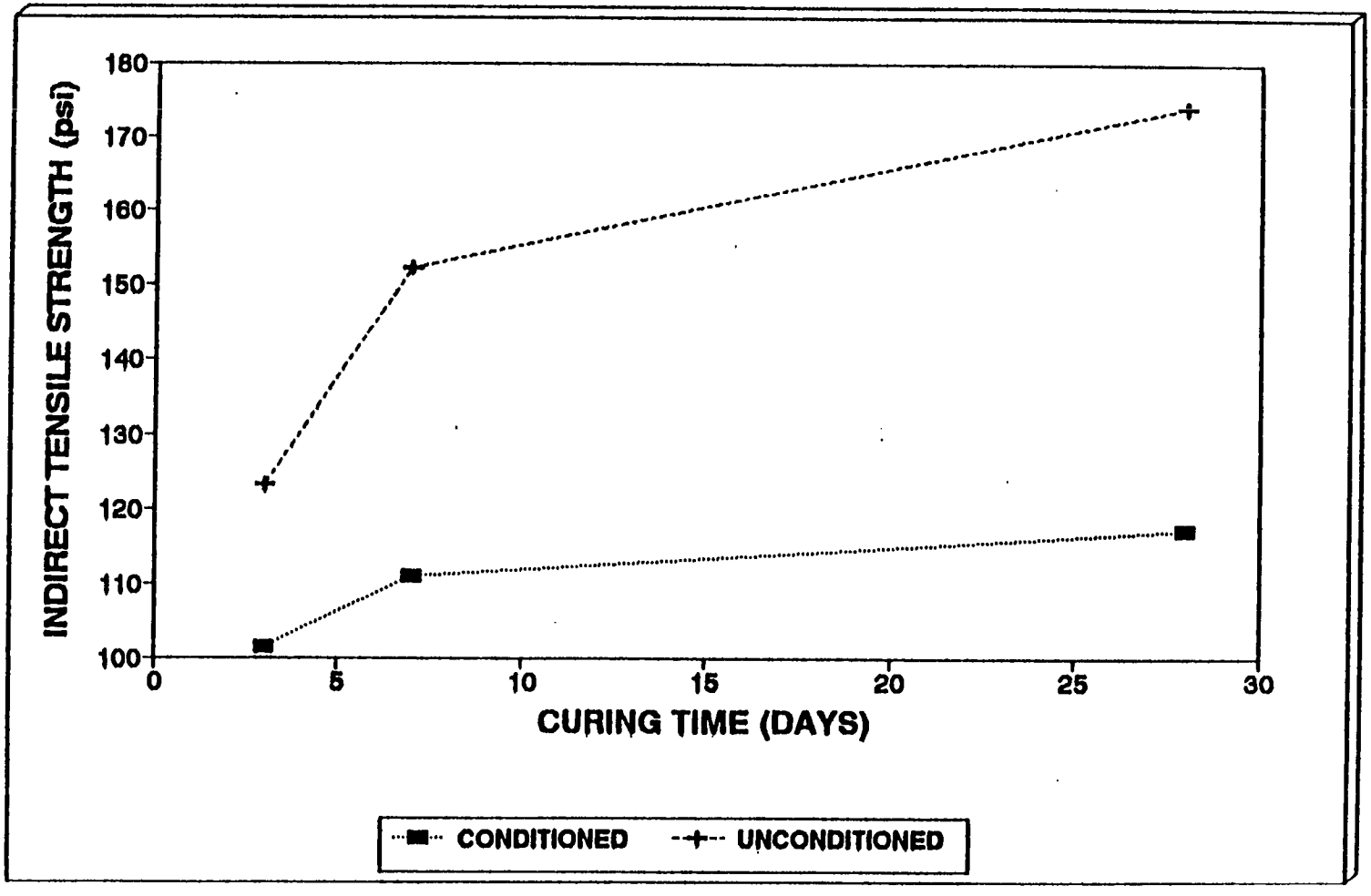

Fig. 7.17 Freeze - Thaw Effects On 3-Day Moist Curing Specimens (Tensile Strength)

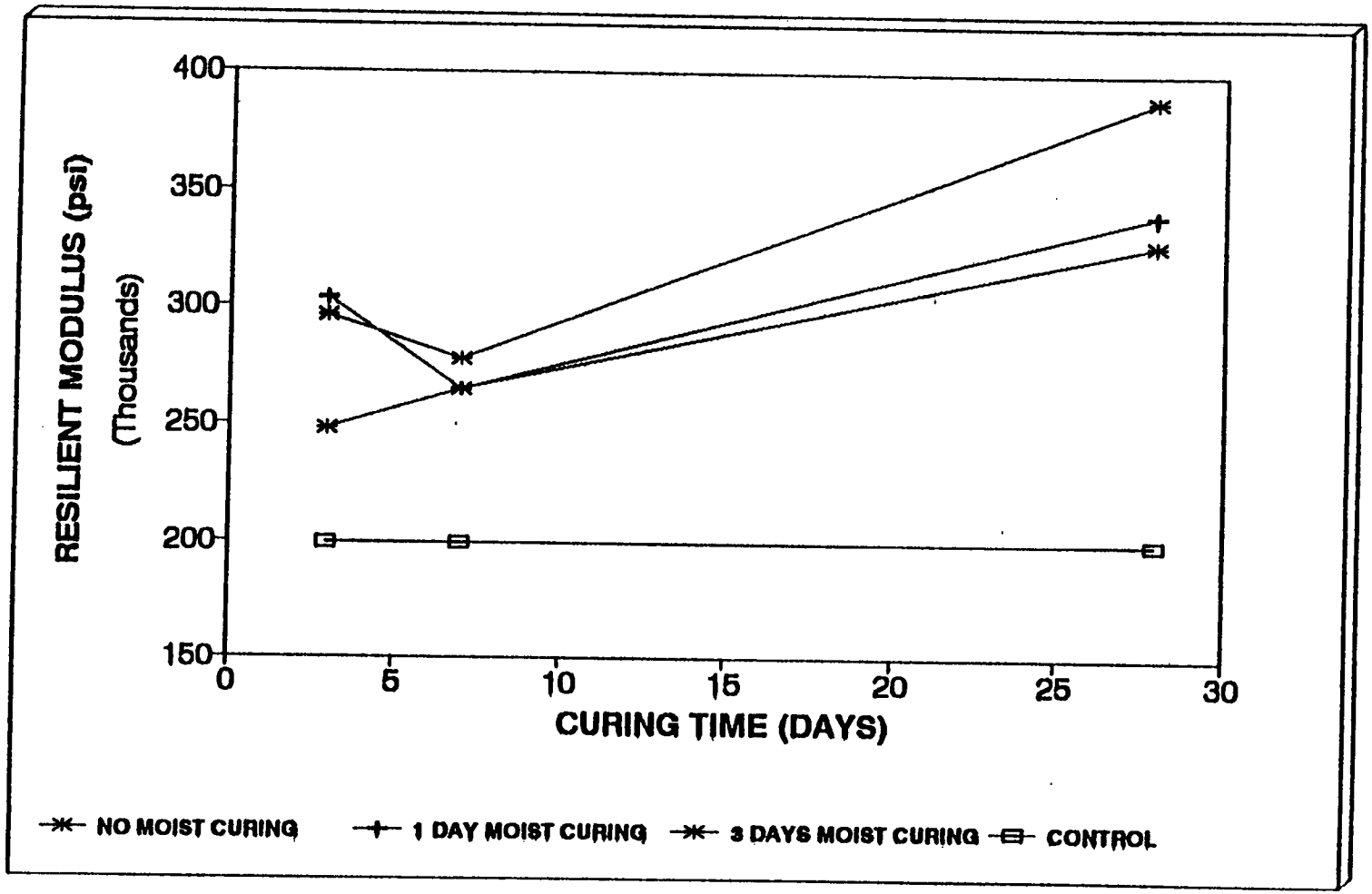

Fig. 7.18 Resilient Moduli Results of Freeze - Thaw Conditioned Specimens

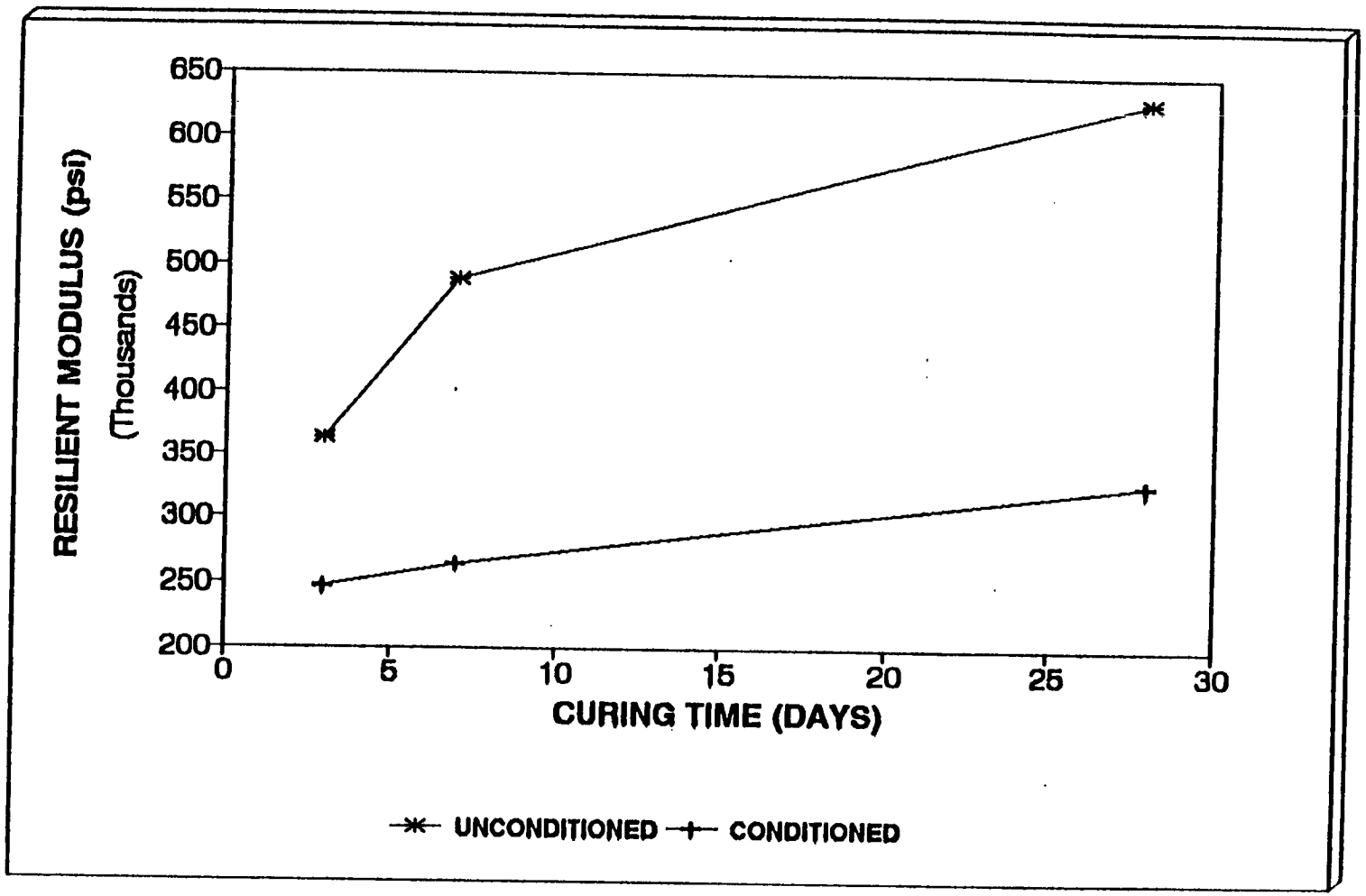

Fig. 7.19 Freeze - Thaw Effects on No-Moist Curing Specimen (Resilient Modulus)

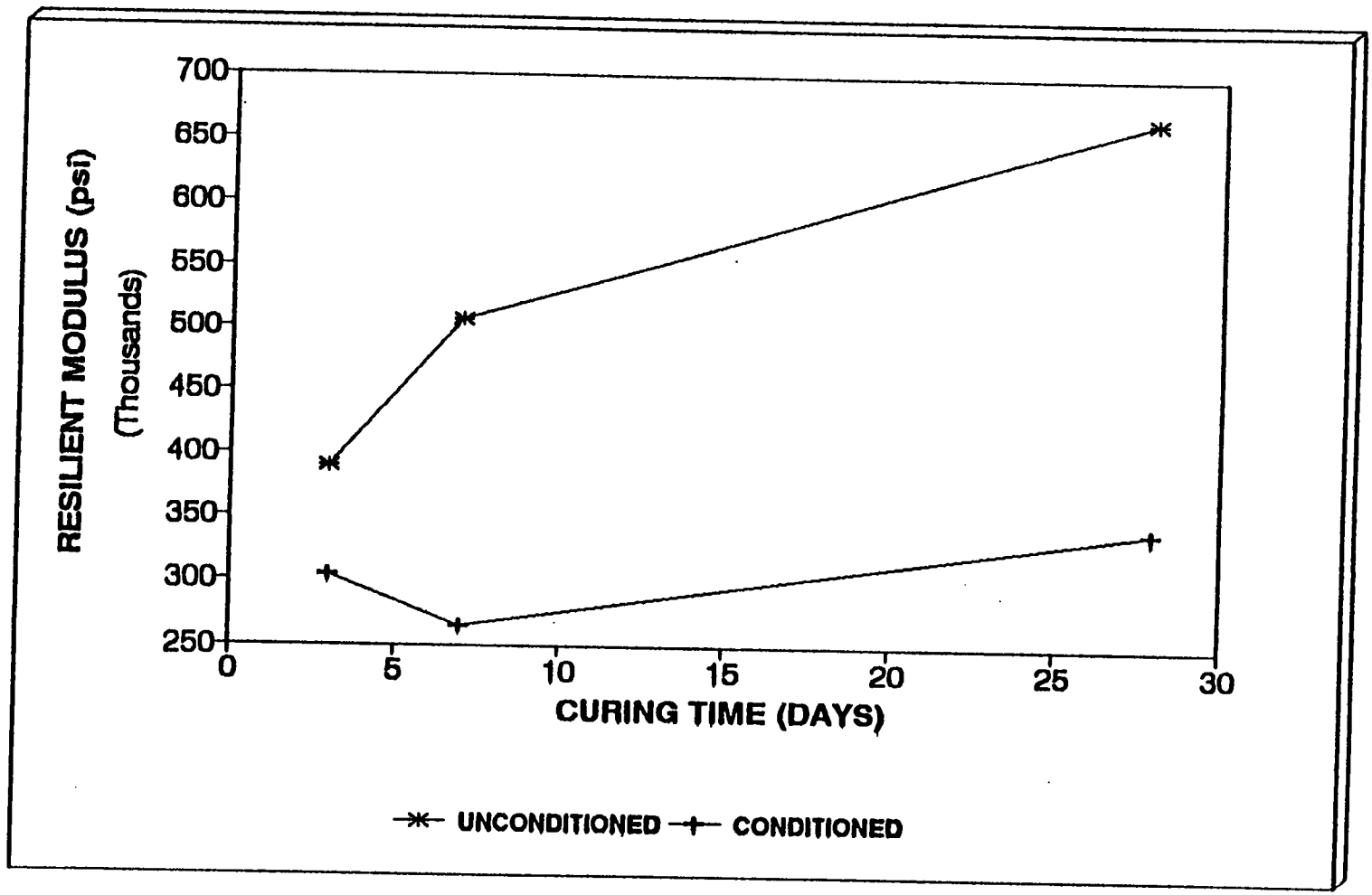

Fig. 7.20 Freeze - Thaw Effects On 1-Day Moist Curing Specimens (Resilient Modulus)

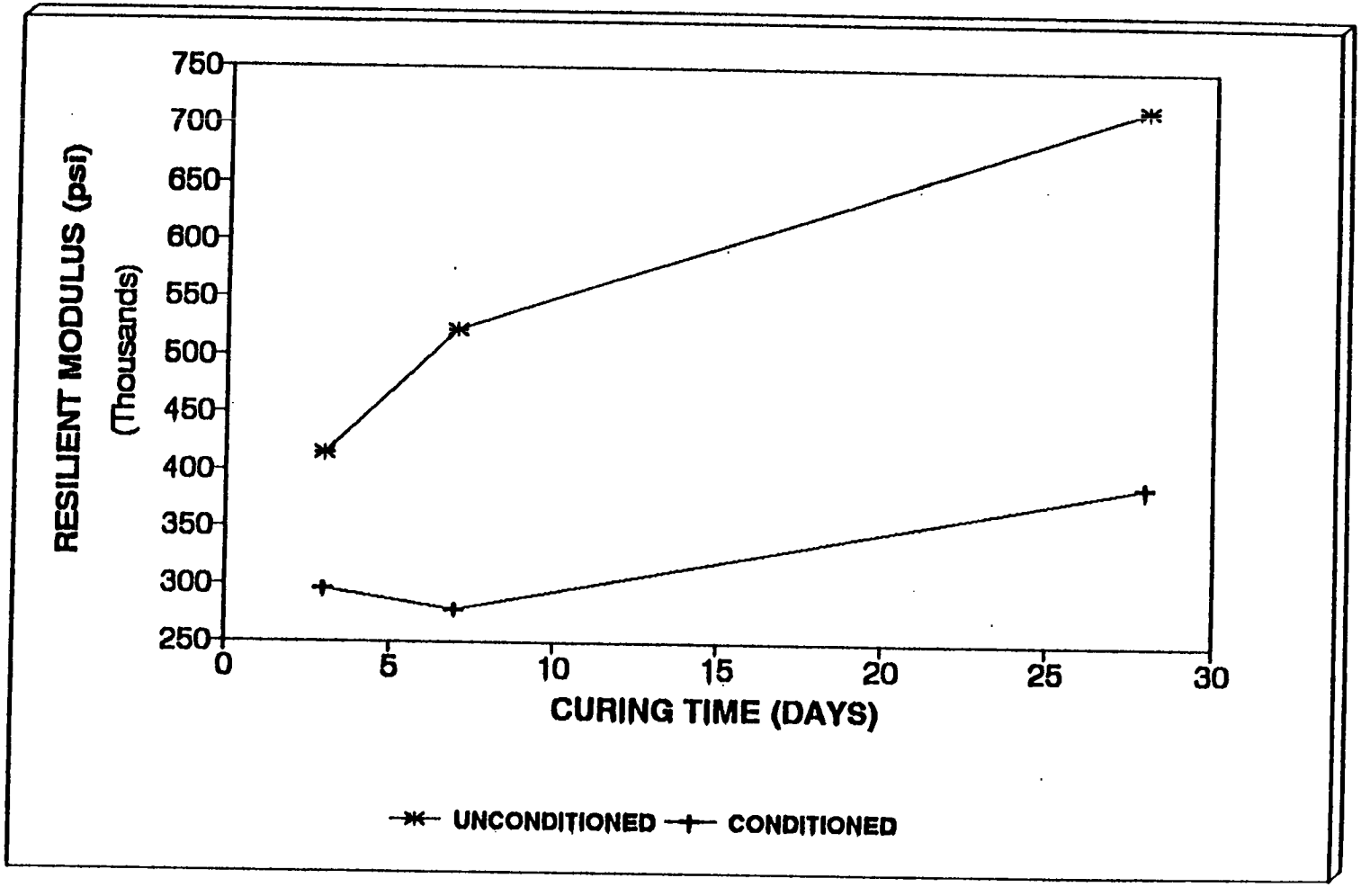

Fig. 7.21 Freeze - Thaw Effects on 3-Day Moist Curing Specimens (Resilient Modulus)

Chloride Content

The chloride content of APCCC and portland cement concrete specimens, after dry/wet cycle pondings are presented in Table 7.16 and Figs. 7.22 and 7.23. The background chloride content of the resin grout for all moist curing levels was 0.06 lb/yd^3 (0.03 kg/m^3), for the portland cement mortar it was 0.2 lb/yd^3 (0.12 kg/m^3).

The results show that chloride content increased with time of exposure to salt solution. After seven dry/wet cycles, the chloride content of the APCCC at 0.75 in (19 mm) and 1.75 in (44 mm) were 0.67 lb/yd^3 (0.40 kg/m^3) and 0.47 lb/yd^3 (0.28 kg/m^3) for no moist curing, 0.63 lb/yd^3 (0.38 kg/m^3) and 0.17 lb/yd^3 (0.10 kg/m^3) for one-day moist curing, and 0.7 lb/yd^3 (0.42 kg/m^3) and0.3 lb/yd^3 (0.18 kg/m^3) for three-day moist curing, whereas after 15 dry/wet cycles of pondings the chloride contents at corresponding depths were 2.6 lb/yd^3 (1.6 kg/m^3) and 2.1 lb/yd^3 (1.3 kg/m^3) for no moist curing, 1.8 lb/yd^3 (1.1 kg/m^3) and 0.5 lb/yd^3 (0.3 kg/m^3) for one-day moist curing, and 1.8 lb/yd^3 (1.1 kg/m^3) and 0.4 lb/yd^3 (0.2 kg/m^3) for three-day moist curing, respectively.

The chloride intrusion decreased with moist curing as presented in Table 5-16. For example, after 11 pondings, at 0.75 in (19 mm) and 1.75 in (44 mm) from the top surface, the chloride contents were 1.1 lb/yd^3 (0.66 kg/m^3) and 0.57 lb/yd^3 (0.34 kg/m^3) for no moist curing, 1.0 lb/yd^3 (0.6 kg/m^3) and 0.43 lb/yd^3 (0.26 kg/m^3) and 0.13 lb/yd^3 (0.08 kg/m^3) for three-day moist curing, respectively. The values for portland cement concrete at corresponding depths were found to be 2.2 lb/yd^3 (1.3 kg/m^3) and 0.8 lb/yd^3 (0.48 kg/m^3), respectively.

The discrepancy in the values of the chloride content of APCCC may be explained by the possibility of the presence of small amounts of asphalt cement in the drilled powder of the resin grout, despite the extreme care taken during the sampling. A possible indication of that is the high standard deviation especially for the samples obtained at 1.75 in (44 mm) from the specimens exposed to 15 cycles of ponding. However, the results showed that the chloride content, in general, in APCCC was lower than that in portland cement concrete.

In the field, moist cured for one-day, APCCC may resist chloride intrusion two to three times longer than would portland cement concrete.

SUMMARY AND CONCLUSIONS

An investigation was undertaken of the effectiveness of APCCC as a potential bridge deck overlay. The study included stability, compressive strength, indirect tensile strength, resilient modulus, water sensitivity (stripping) and freezing and thawing effects. To investigate the potential of APCCC as a corrosion abatement technique, an attempt was made to evaluate the resistance of APCCC to chloride intrusion.

Each investigated property was evaluated over a period of 28 days to determine the effect of time; however, the chloride intrusion test was conducted over a period of 15 weeks of

exposure to salt solution. The specimens were also investigated for three different moist curing conditions, namely no moist curing, and one- and three-day moist curing, in order to evaluate the optimum amount of curing required in the field.

The investigation concluded that APCCC possesses higher strengths, and higher resistance to stripping and freeze-thaw effects when compared to SM-5 HMA. The resistance of APCCC to chlorides intrusion was found to be two to three times greater than that of portland cement concrete.

The investigation concluded that the one-day moist curing would be optimum, although the strengths and resistances for three-day moist curing were found to be higher in certain cases. Based on the results of this research, the study recommends the use of APCCC as bridge deck overlay, especially with preformed membrane, because of its high strength and durability.

Table 7.16 Chloride Content At Various Depths

ASPHALT PORTLAND CEMENT CONCRETE COMPOSITE*					
PONDING (NO. OF CYCLES)	MOIST CURING (DAYS)	CHLORIDE CONTENT (LB/CU.YD)			
		AVERAGE @ 0.75 IN	STD @ 0.75 IN	AVERAGE @ 1.75 IN	STD @ 1.75 IN
7	NO	0.67	0.32	0.47	0.25
	1 DAY	0.63	0.40	0.17	0.06
	3 DAYS	0.70	0.70	0.30	0.10
11	NO	1.10	0.98	0.57	0.23
	1 DAY	1.03	0.80	0.43	0.40
	3 DAYS	0.43	0.29	0.13	0.06
15	NO	2.60	0.82	2.07	0.81
	1 DAY	1.77	0.93	0.50	0.14
	3 DAYS	1.83	0.75	0.40	0.28

PORTLAND CEMENT CONCRETE**		
PONDINGS	CHLORIDE CONTENT (LB/YD^3)	
	0.75 IN	1.75 IN
7	0.8	0.5
11	2.2	0.8
15	4.0	1.5

*Background chloride content for APCCC is 0.06 lb/yd^3 (0.036 kg/m^3)
**Background chloride content for PCC is 0.2 lb/yd^3 (0.12 kg/m^3)

Note: 1 in = 25.4 mm, 1 lbs/yd^3 = 0.59 Kg/m^3

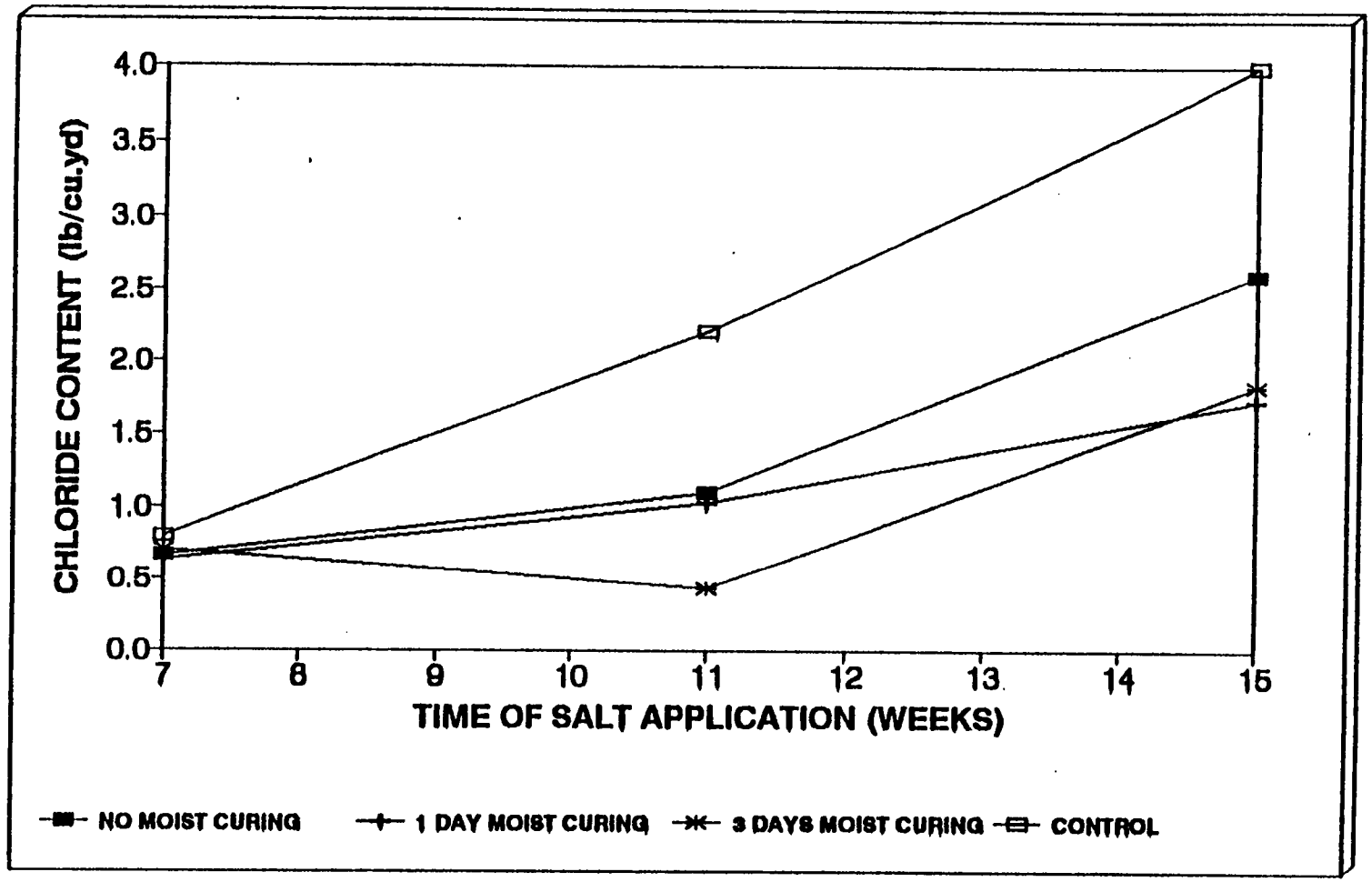

Fig. 7.22 Chloride Content at 0.75 in (19 mm) From Surface

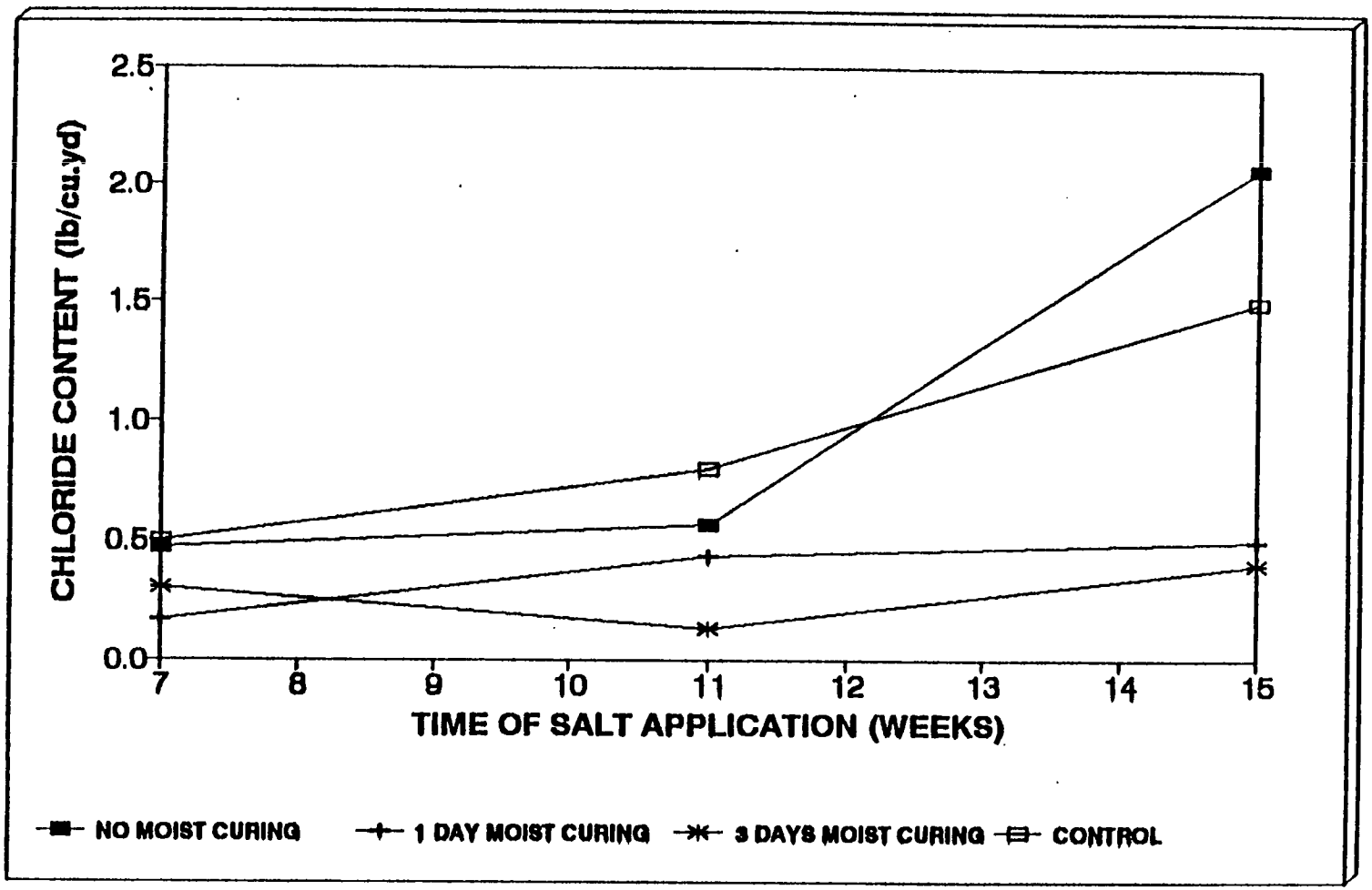

Fig. 7.23 Chloride Content at 1.75 in (42 mm) From Surface

Appendix A

Virginia 460 Bridge Data and Analysis

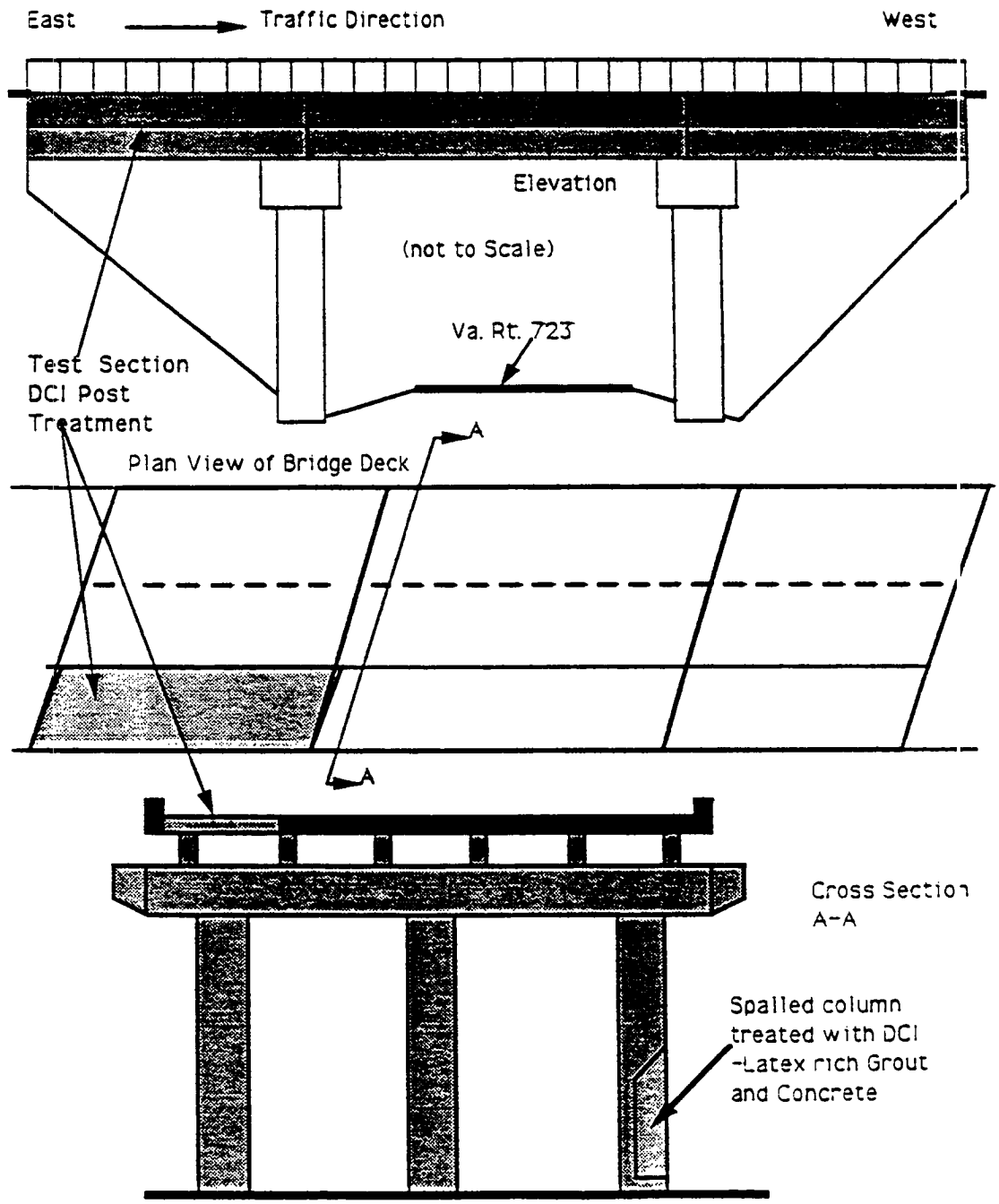

Fig. A.1 Sketch of Post Treatment Test Site
US Rt. 460 Bypass West Between Christiansburg and Blacksburg, VA

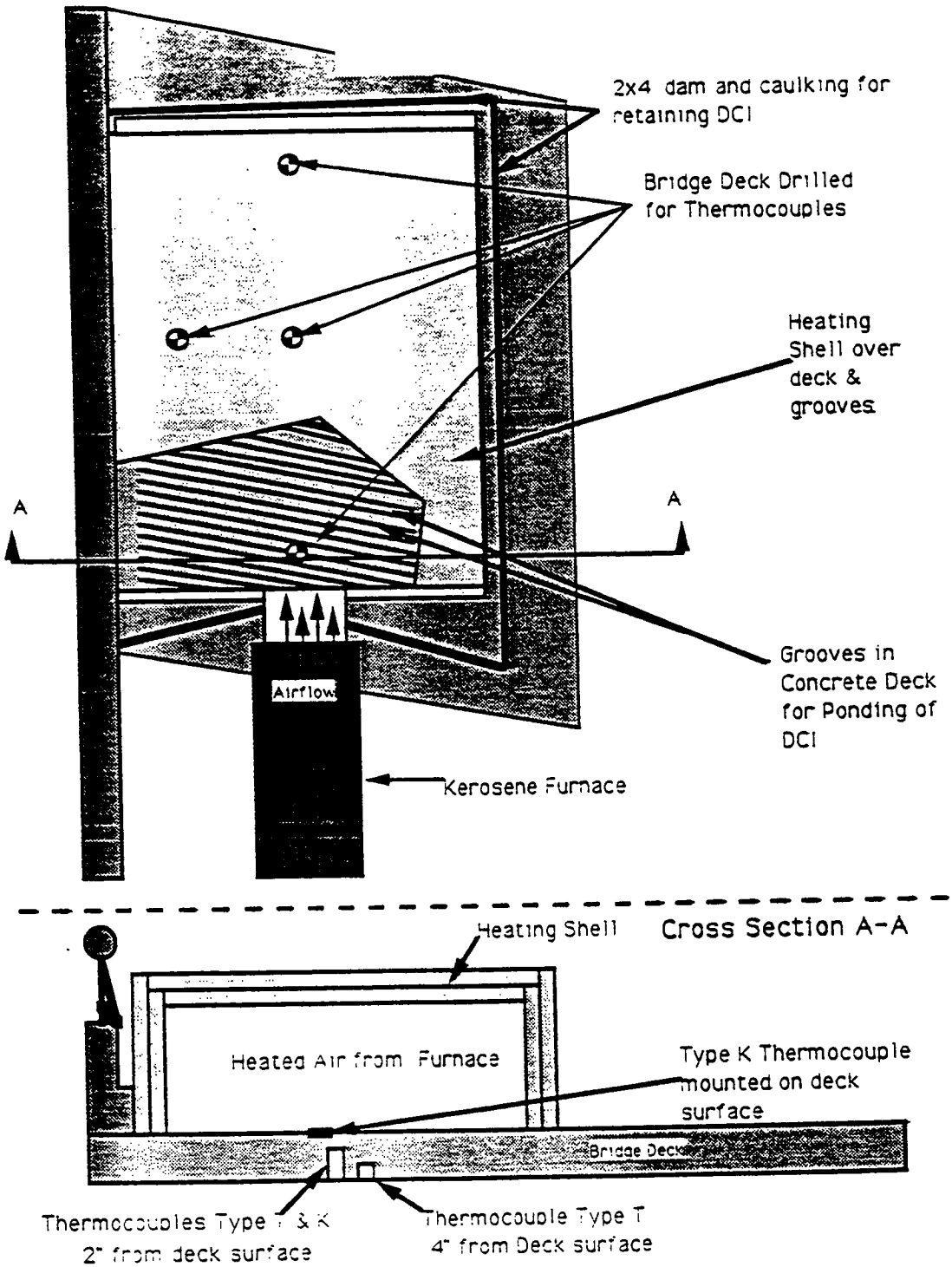

Fig. A.2 Plan View of DCI Post Treatment Test and Thermocouple Placement

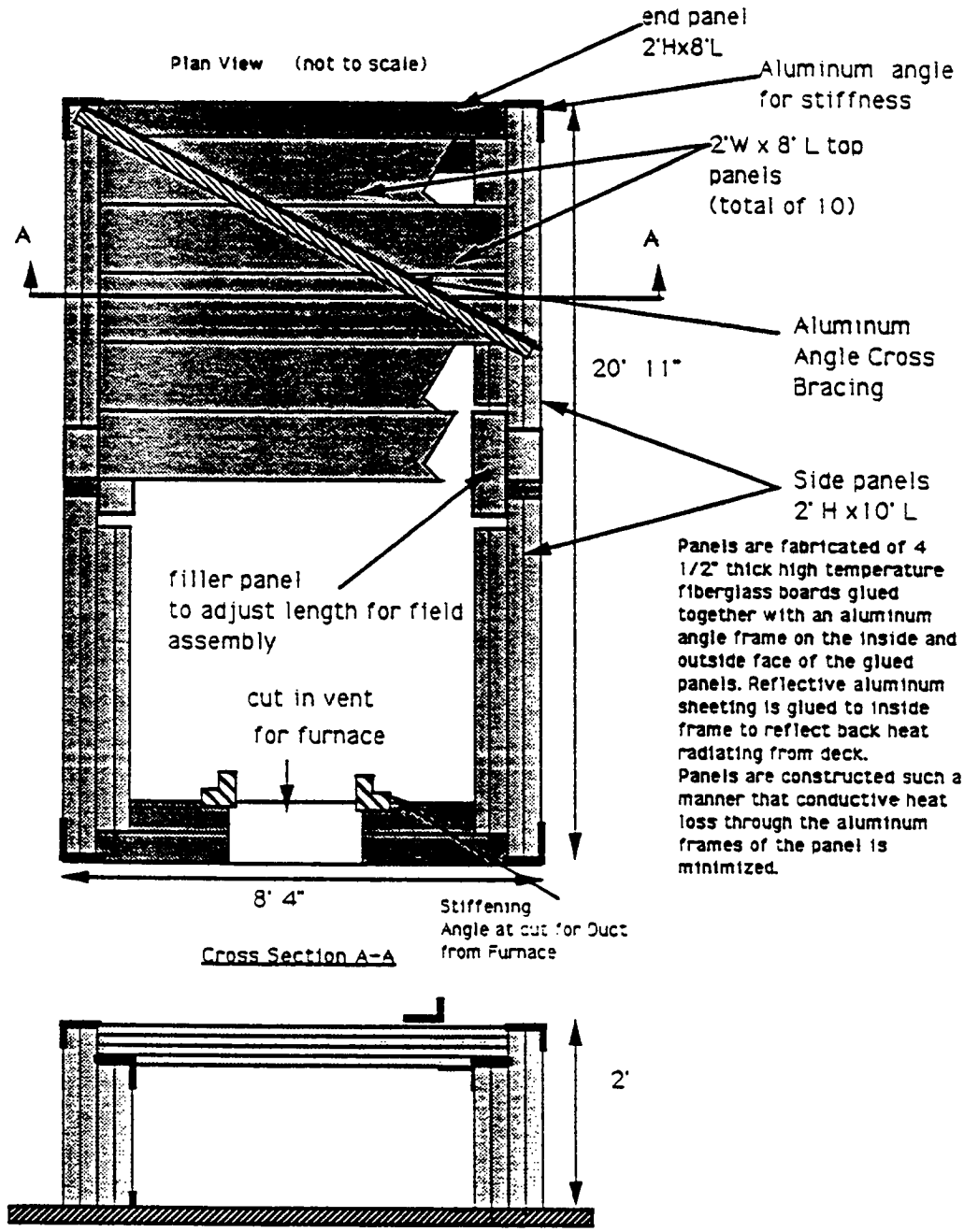

Fig. A.3 Heating Shell Schematic

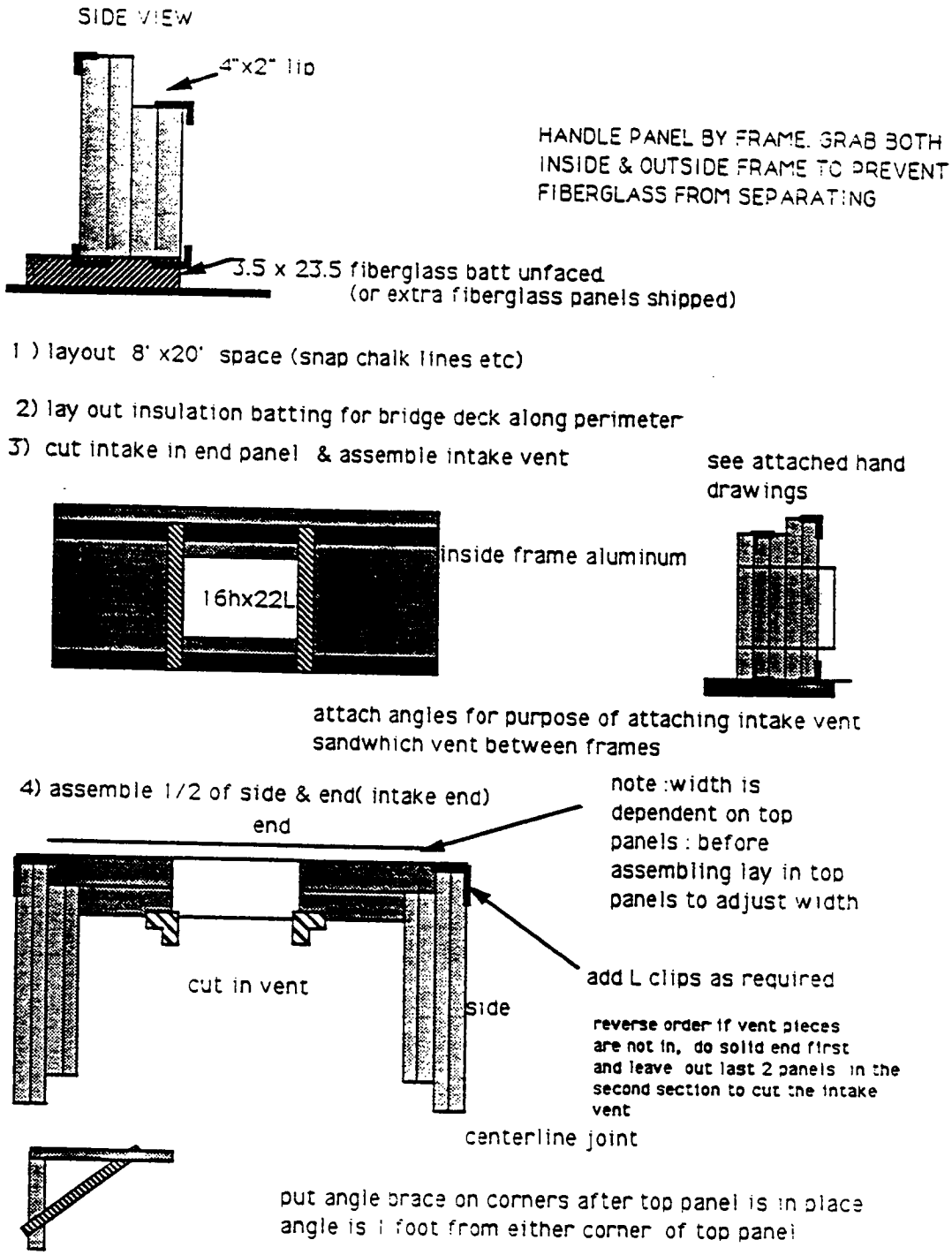

Fig. A.4 Heating Shell Assembly Details

5) lay in 3 top panels loose (total of 4 , one was rivetted in in step #4) and measure expansion factor for center joint)
6) place sides in place for adjusting center joint
see drawing adjust center joint it must be
20' + slop from imperfect fit of top panels 3-4"?
more or less

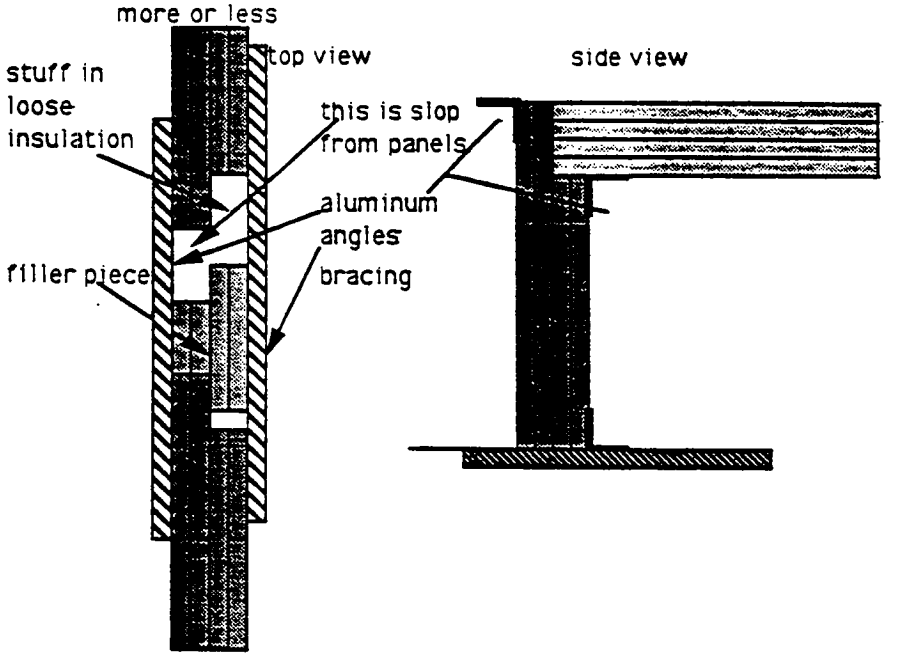

calculate slop based on placing 3 loose panels as tight as possible with the fixed panel . it should be 8' then t there is no slop otherwise . measure along the side walls and calculate slop ((8+slop - 8')/4)x11)

7) install end panel see #4 for details

8) check/install thermocouples now (on top deck)

9) place top panels in, stating from vent intake end, apply angle as required to make frame rigid & tight

10) finish fabricating sheet metal intake vent

Fig. A.5 Heating Shell Assembly Details

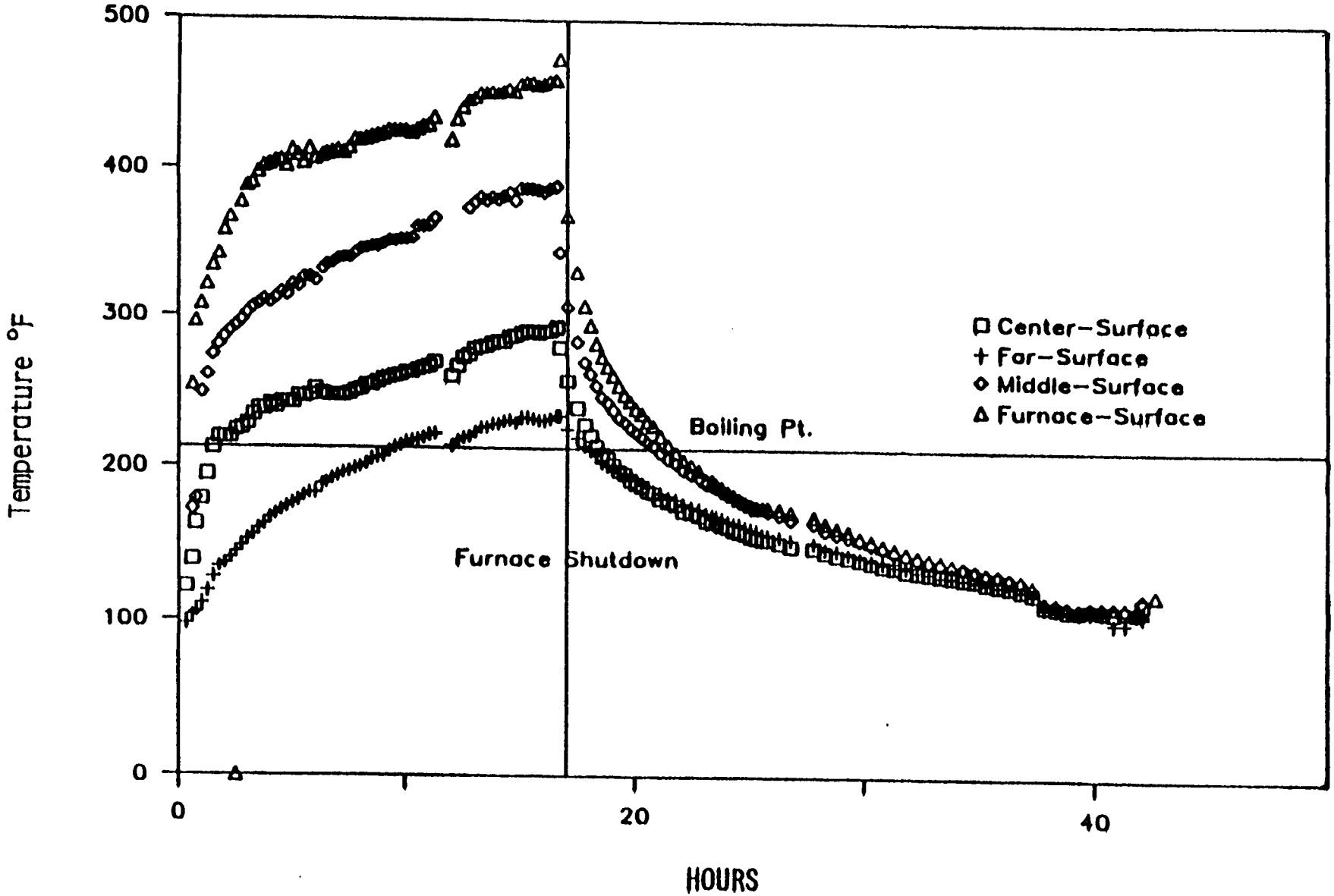

Fig. A.6 Concrete Temperature @ Surface

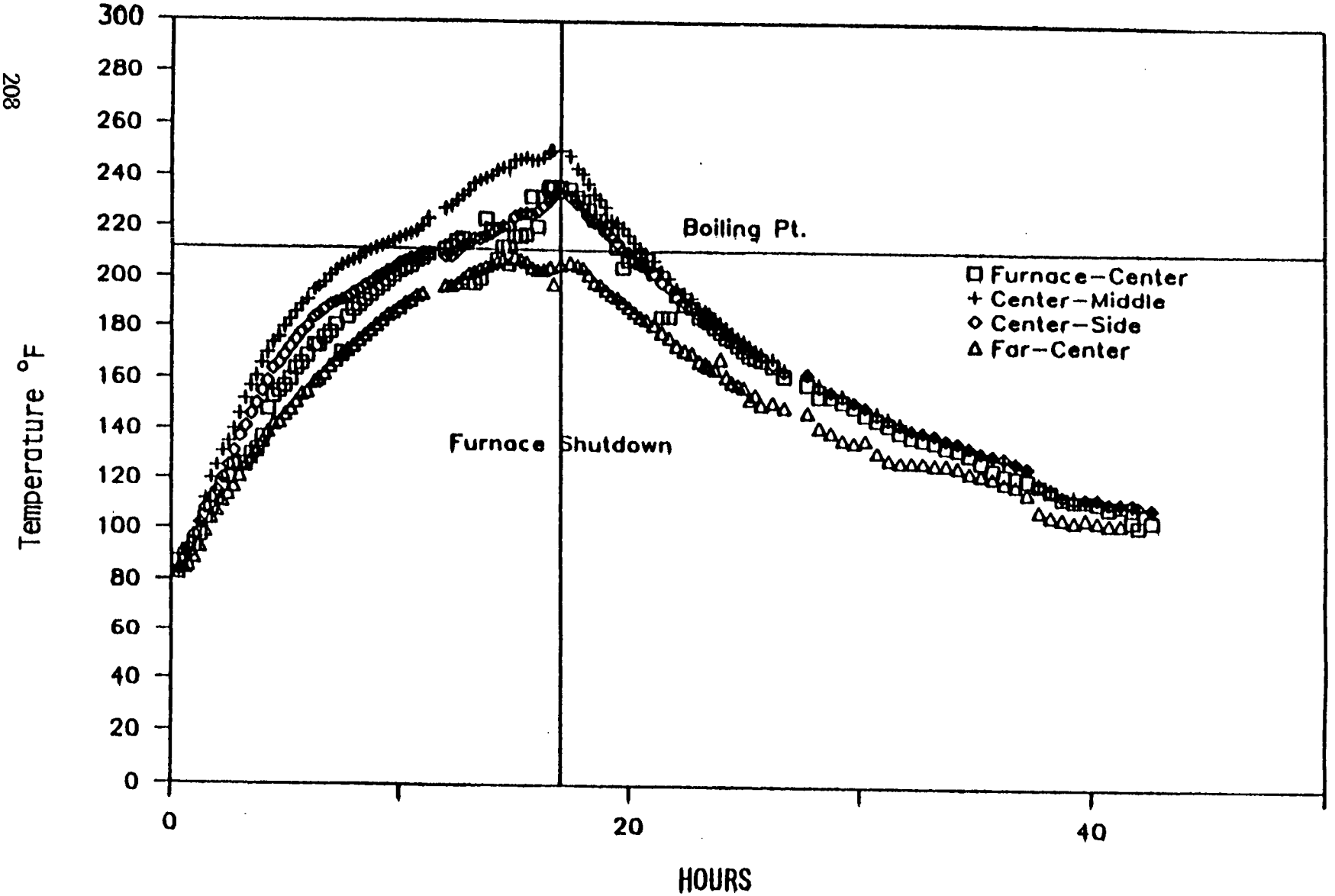

Fig. A.7 Concrete Temperature @ 2" Depth

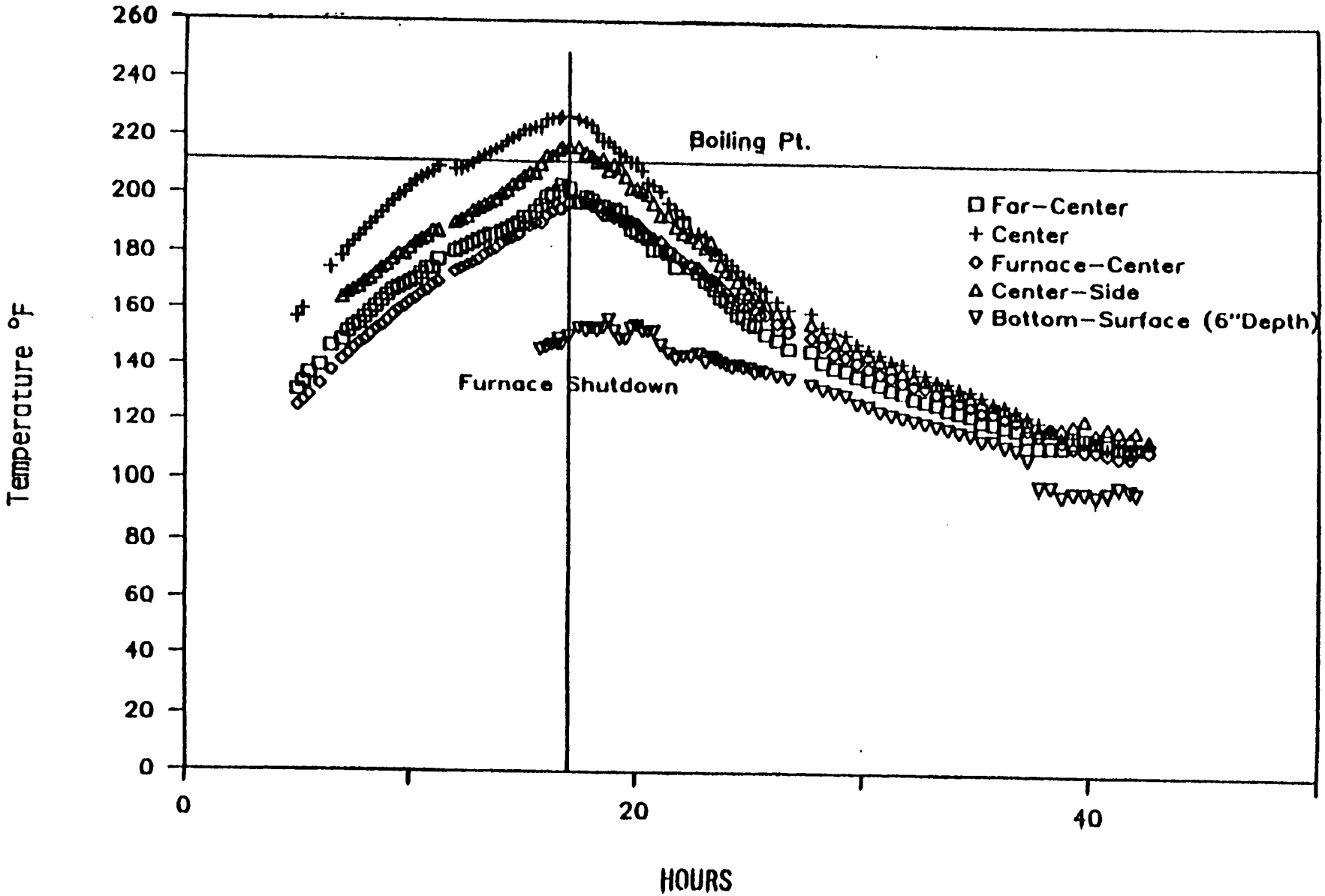

Fig. A.8 Concrete Temperature @ 4" Depth in Slab

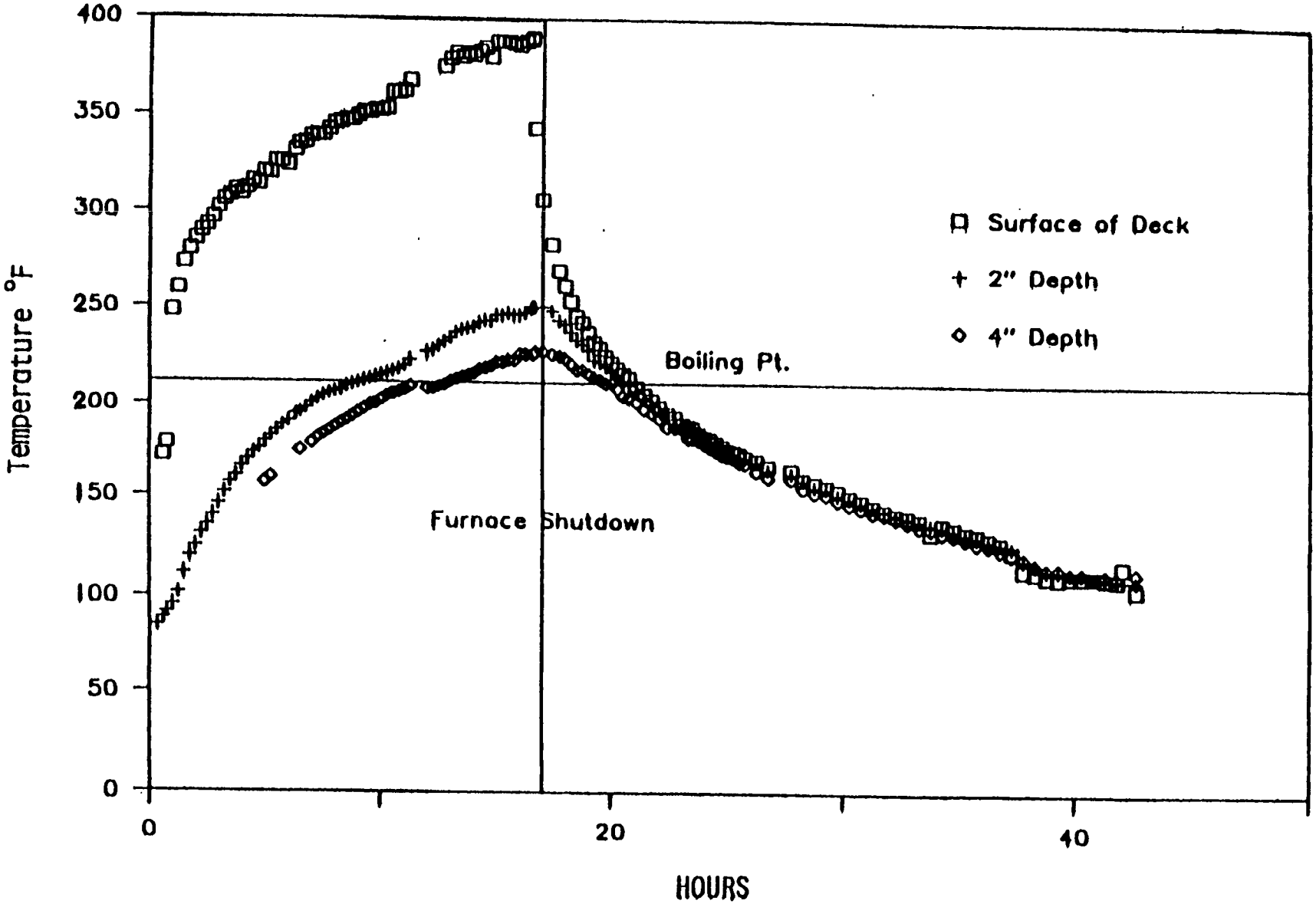

Fig. A.9 Concrete Temperature Profile Center-Middle

Appendix B

Polymer Impregnated Concrete Materials Properties and Select Corrosion Results

Table B.1 Mixture Proportions and Aggregate Properties

MIX DESIGN					
Material/ Property	Concrete	LSDC Overlay	LMC Overlay	LM Mortar	Mortar Cubes
Cement (lb)	677.12	842.71	484.96	778.30	925.53
Water (lb)	269.32	298.65	88.62	632.74	435.00
Coarse Agg (lb)	1151.94	1357.81	965.25	--	--
Fine Agg (lb)	1739.49	1361.83	1080.70	--	--
Sand (lb)	--	--	--	2257.10	2554.47
Latex (lbs emulsion)	--	--	1295.46	245.92	--
Avg. Slump (in)	2.5	0.25	5.5	--	--
Avg. Air (%)	7.3	6.5	4	--	--
Avg. Temp (°F)	57.5	--	--	--	--
Comp. Str. @ 7 day (psi)					
Comp. Str. @ 14 days (psi)	3700	6000	6050	--	--
Comp. Str. @ 28 days (psi)	5450	6550	6700	--	4450

AGGREGATE PROPERTIES			
PROPERTY	COARSE AGG.	FINE AGG.	COARSE AGG. IN OVERLAY
Unit weight (lb/ft^3)	96.5		95.2
Voids in Dry Rodded Agg. (lb)	44.18		43.1
Bulk Spec. Gravity (Dry)	2.77	2.61	2.68
Bulk Spec. Gravity (SSD)	2.78	2.66	2.71
Apparent Spec. Gravity	2.81	2.66	2.77
Absorption	0.57	0.36	1.26
Fineness Modulus		3.39	

NOTE: 1 lb = 0.454 Kg
1 lb = 0.593 Kg/m^3

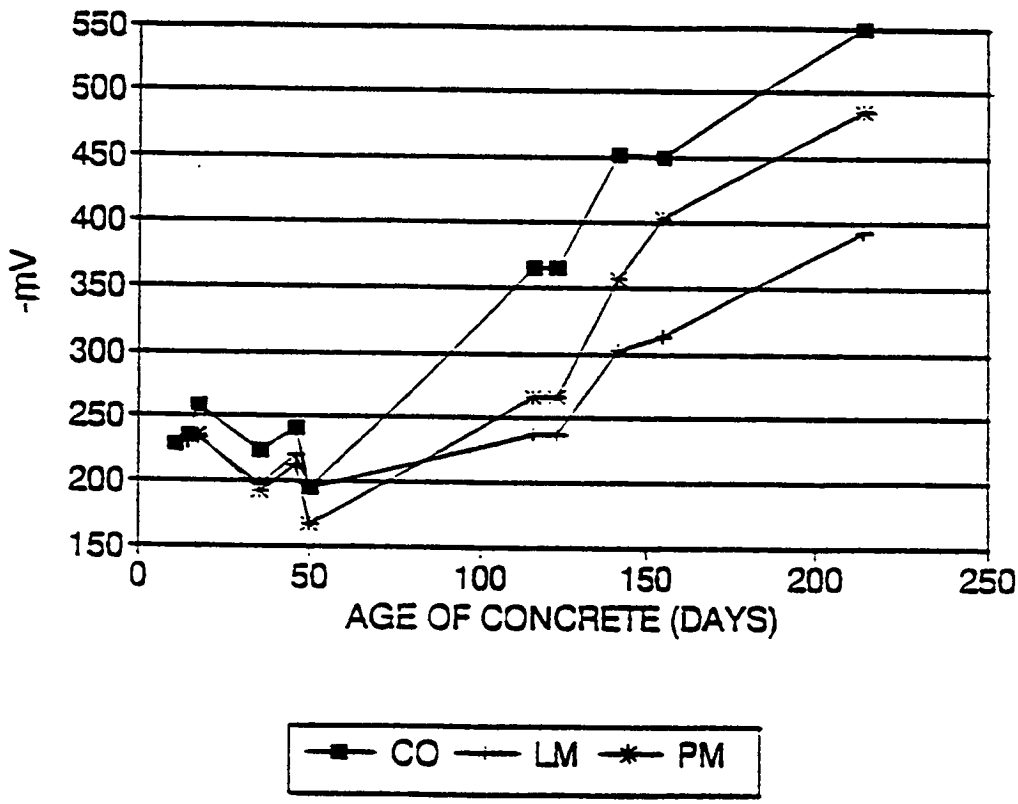

Fig. B.1 Pre-Treatment Mean Potential, Latex Group

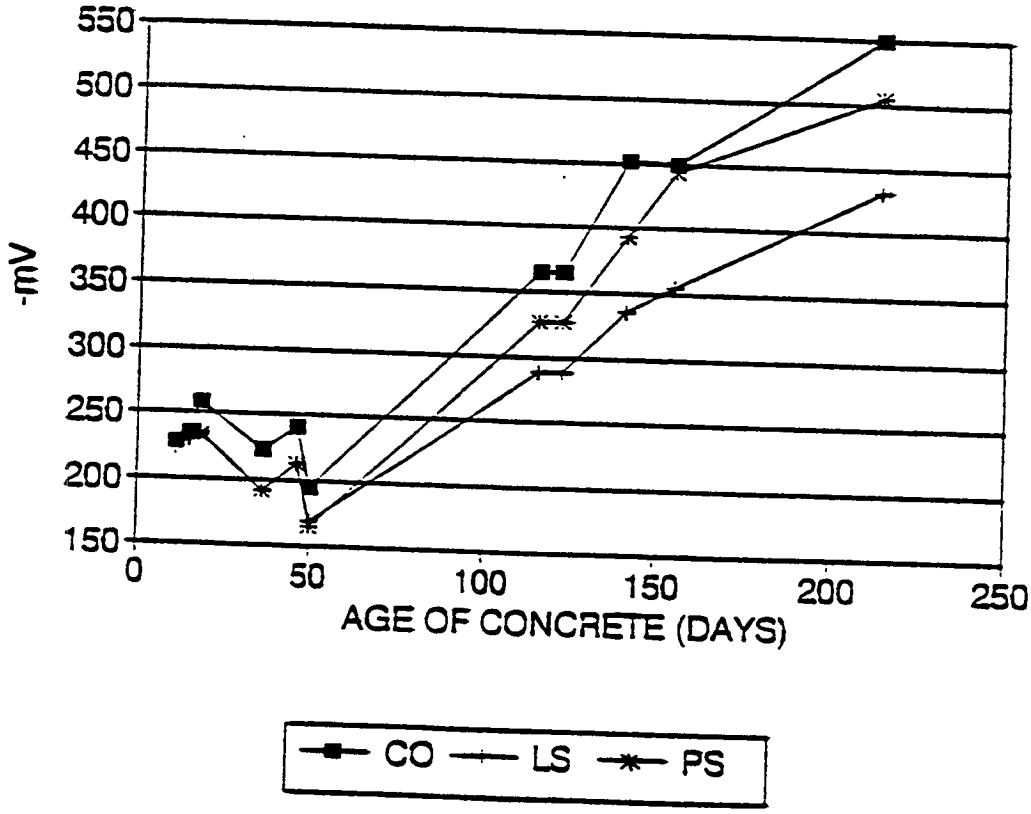

Fig. B.2 Pre-Treatment Mean Potential, Low Slump Group

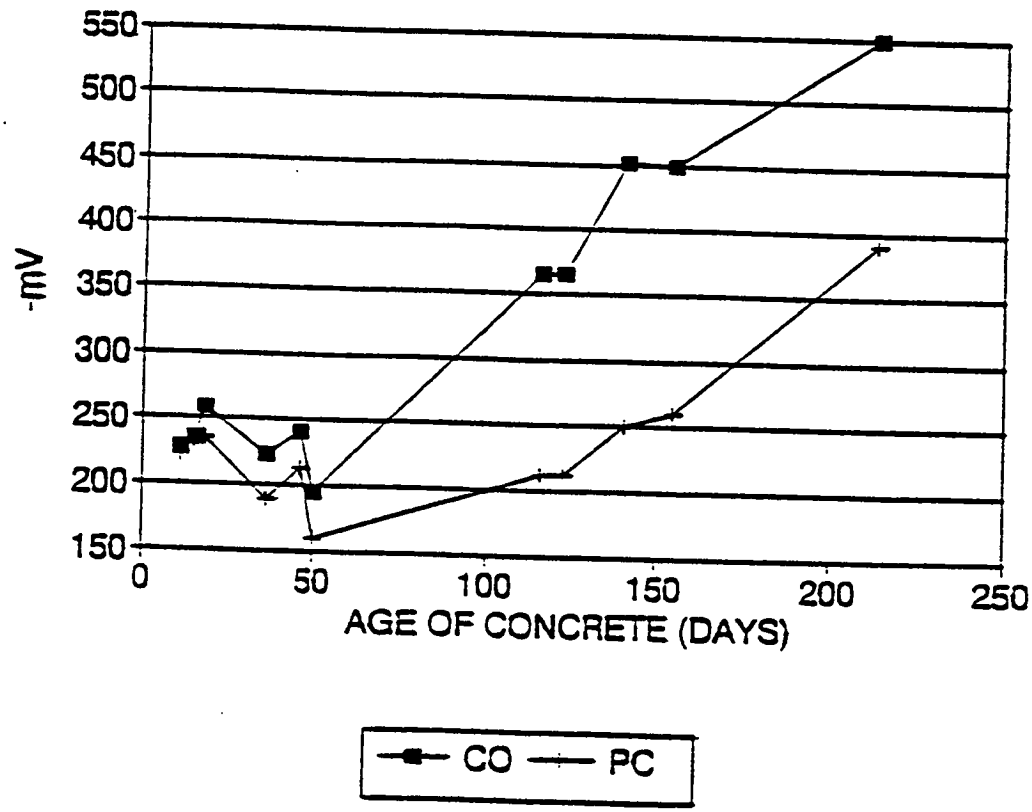

Fig. B.3 Pre-Treatment Mean Potential, Polymer Impregnated Group

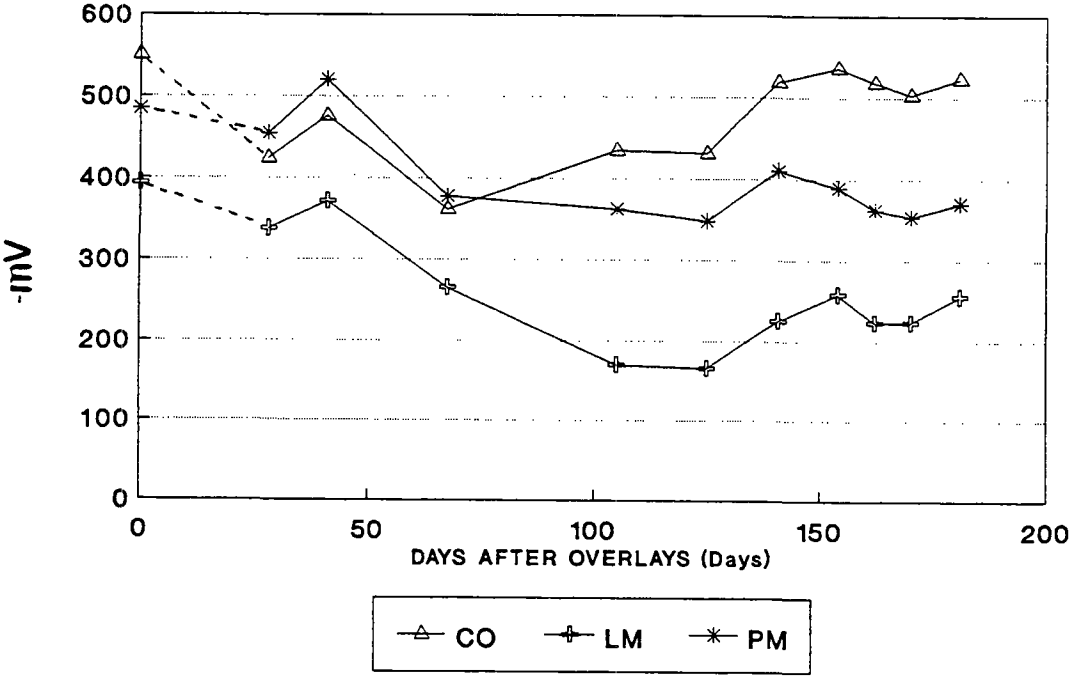

Fig. B.4 Post-Treatment Mean Potential, Latex Group

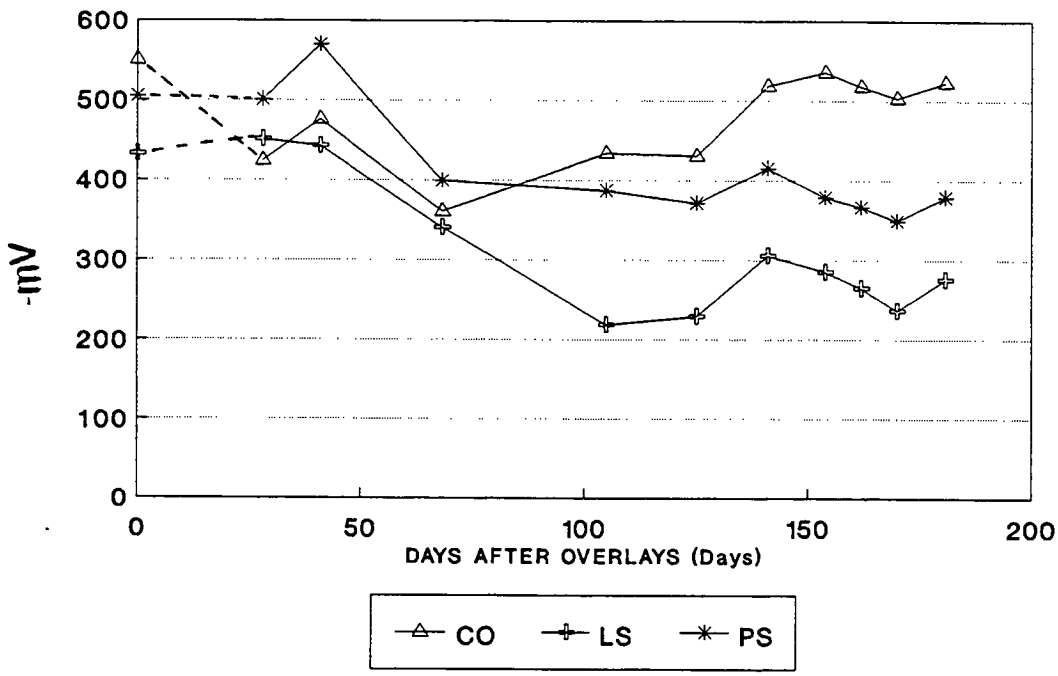

Fig. B.5 Post-Treatment Mean Potential, Low Slump Group

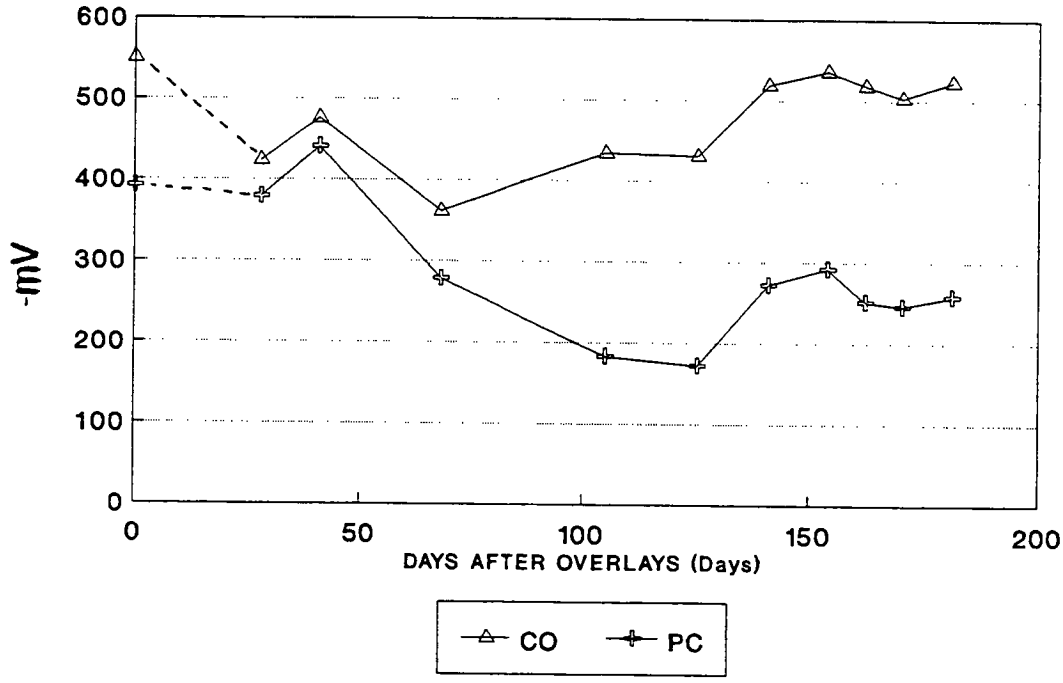

Fig. B.6 Post-Treatment Mean Potential, Polymer Impregnated Group

Appendix C

Corrosion Inhibitors Material Properties and Performance Characteristics

Table C-1. Virginia A4AE Bridge Deck Air Entrained Concrete, Batch Quantities, lb/yd^3.

Item	SSD Basis
Cement	635
Water	212
Coarse Aggregate	1200
Fine Aggregate	1878
Air Entrainment Agent (AEA)	8.0 oz
Super Plasticizer	19.2 oz
Air Content	5.5 %
Slump	2 ½ "

Concrete Batch Quanities and Mix Characteristics for 1" Cover Depth Specimens, lb/yd^3.

Item	SSD Basis
Cement	635
Water	204
Coarse Aggregate	1882
Fine Aggregate	1208
AEA	8.0 oz
Superplasticizer	19.2 oz

Table C-2. Gradation and Properties of Coarse and Fine Aggregates.

Sieve No.	Fine Agg.	Coarse Agg.
1/2"	100	100
3/8"	99.1	97.5
# 4	96.1	14.0
# 8	83.2	0.8
# 16	68.6	0.7
# 30	47.6	0.6
# 50	11.8	0.5
# 100	1.7	0.4
# 200	0.2	0.2
Pan	0.0	0.0

Property	Fine Agg.	Coarse Agg.
Bulk Specfic Gravity, Dry Basis	2.58	2.58
Bulk Specific Gravity, SSD Basis	2.58	2.60
Absorption, (%)	0.16	0.69
Fineness Modulus	2.92	_
Dry Rodded Unit Weight (lbs)	_	91.3

Table C-3. **Cortec 1609 Modified Mix Designs, SSD Basis Batch Quantities (lb/yd^3), and Properties of Fresh and Hardened Concrete for 1 ft x 1 ft Specimen Overlays.**

Batch Number	1	2	3
Type I Cement	637	631	632
Water	292	305	304
Fine Aggregate	1118	1107	1108
Coarse Aggregate	1929	1912	1913
Cortec 1609	1	1	1
AEA (ml)	188	224	184
W/C Ratio	0.46	0.48	0.48
Slump (inches)	2.50	0.75	1.25
Entrained Air (%)	5.7	3.8	6.6
Unit Weight (lb/yd^3)	137	146	142
1 Day Strength (psi)	1990	2350	2110
7 Day Strength (psi)	3960	4580	4120
28 Day Strength (psi)	4740	5450	4640

Table C-4. DCI Modified Mix Designs, SSD Basis Batch Quantities (lb/yd^3), and Properties of Fresh and Hardened Concrete for 1 ft x 1 ft Specimen Overlays.

Batch Number	1	2	3
Type I Cement	653	647	647
Water	251	264	264
Fine Aggregate	1146	1135	1135
Coarse Aggregate	1978	1960	1960
DCI (gallons)	6	6	6
Daratard 17 (oz)	39.2	33.6	25.9
Daracen 100 (oz)	78.3	96.1	77.6
AEA (ml)	194	229	229
W/C Ratio	0.46	0.49	0.49
Slump (inches)	1.50	0.50	1.50
Entrained Air (%)	5.5	4.2	6.1
Unit Weight (lb/yd^3)	138	144	143
1 Day Strength (psi)	3380	2090	2980
7 Day Strength (psi)	6070	6170	5200
28 Day Strength (psi)	6650	7560	6470

Table C-5. Latex Modified Mix Designs, SSD Basis Batch Quantities (lb/yd^3), and Properties of Fresh and Hardened Concrete for 1 ft x 1 ft Specimen Overlays.

Batch Number	1	2	3
Type I Cement	691	687	696
Water	110	130	108
Fine Aggregate	1578	1567	1589
Coarse Aggregate	1361	1344	1364
Latex	206	205	208
W/C Ratio	0.33	0.35	0.31
Slump (inches)	6.0	8.5	5.0
Entrained Air (%)	7.9	11.0	11.0
Unit Weight (lb/yd^3)	133	131	130
1 Day Strength (psi)	2670	2610	2880
7 Day Strength (psi)	4080	3800	4300
28 Day Strength (psi)	4700	4750	4970

Table C-6. Sodium Borate Modified Mix Designs, SSD Basis Batch Quantities (lb/yd^3), and Properties of Fresh and Hardened Concrete for 1ft x 1 ft Specimen Overlays.

Batch Number	1	2	3
Type I Cement	622	637	637
Water	325	292	292
Fine Aggregate	1094	1118	1118
Coarse Aggregate	1897	1929	1929
Sodium Borate (in Mix Water)	11.6	11.6	11.8
AEA (ml)	160	164	223
W/C Ratio	0.52	0.46	0.46
Slump (inches)	1.50	4.25	2.00
Entrained Air (%)	3.0	4.9	6.8
Unit Weight (lb/yd^3)	140	145	140
1 Day Strength (psi)	1340	1340	0
7 Day Strength (psi)	3540	3280	3900
28 Day Strength (psi)	4460	4280	NA

Table C-7A. Application Procedure for Thin Polymer Overlay.

1. Sandblast area to be overlayed.
2. Immediately apply epoxy-urethane co-polymer (Poly-Carb Mark-163 FLEXOGRID) at the rate of 2 pounds per square yard.
3. Broadcast fine aggregate (see Table A-9B for gradation) until there is an excess.
4. Wait 1-2 hours, then air blast surface to remove excess aggregate.
5. Apply a second coat of the epoxy-urethane co-polymer at the rate of 4 pounds per square yard.
6. Repeat steps 3 and 4.

Table C-7B. Gradation of Fine Aggregate, Morie #3 Basalt.

U.S. Standard Sieve	% Retained	% Passing
# 6	0.1	99.9
# 12	94.3	5.6
# 20	5.6	0.0
# 30	0.0	0.0

Table C-8. Hot-Mix Asphalt Mix Design. Virginia Type SM-5

Gradation	
Sieve Size	Percent Passing
1/2 in.	100.0
3/8 in.	97.4
No. 4	71.8
No. 8	45.5
No. 16	31.2
No. 30	23.0
No. 50	15.9
No. 100	10.7
No. 200	8.2
Marshall Results Using 50 Blows Compaction	

VTM = 5.4 percent

VMA = 17.9 percent

VFA = 69.5 percent

Stability = 1950 lb

Flow = 1950 lb

Flow = 14.7

Density = 147.1 pcf

Asphalt content = 5.4 percent

Table C-9. Cortec 1609 Modified Mix Designs, SSD Basis Batch Quantities (lb/yd^3), and Properties of Fresh and Hardened Concrete for Large Scale Specimen Overlays.

Batch Number	1	2	3	4
Type I Cement	714	714	714	713
Water	308	307	320	309
Fine Aggregate	1588	1589	1586	1587
Coarse Aggregate	1361	1361	1352	1360
Cortec 1609	1	1	1	1
AEA (ml)	217	217	217	217
W/C Ratio	0.43	0.43	0.43	0.43
Slump (inches)	2.50	2.25	2.25	5.50
Entrained Air (%)	6.9	6.5	5.5	6.5
Unit Weight (lb/yd^3)	141	143	144	138
7 Day Strength (psi)	4260	4580	4620	3660
28 Day Strength (psi)	5750	5630	5930	4730

Table C-10. DCI Modified Mix Designs, SSD Basis Batch Quantities (lb/yd^3) and Properties of Fresh and Hardened Concrete for Large Scale Specimen Overlays.

Batch Number	1	2	3	4
Type I Cement	678	673	678	681
Water	265	276	265	259
Fine Aggregate	1138	1128	1138	1142
Coarse Aggregate	1955	1939	1955	1963
DCI (gallons)	6	6	6	6
Daratard 17 (oz)	27.1	26.9	27.1	27.2
Daracen 100 (oz)	54.3	53.8	54.3	54.4
AEA (ml)	231	229	231	210
W/C Ratio	0.47	0.49	0.47	0.46
Slump (inches)	1.5	6.0	8.0	3.25
Entrained Air (%)	6.4	13.5	16.0	9.0
Unit Weight (lb/yd^3)	NA	NA	NA	135.0
7 Day Strength (psi)	4970	NA	1950	3980
28 Day Strength (psi)	6130	3410	2470	4700

Table C-11. Latex Modified Mix Designs, SSD Basis Batch Quantities (lb/yd^3) and Properties of Fresh and Hardened Concrete for Large Scale Specimen Overlays.

Batch Number	1	2[1]
Type I Cement	690	693
Water	124	117
Fine Aggregate	1573	1580
Coarse Aggregate	1350	1356
Latex	205	206
W/C Ratio	0.34	0.33
Slump (inches)	9.5	9.0
Entrained Air (%)	10.0	10.5
Unit Weight (lb/yd^3)	134	134
7 Day Strength (psi)	3700	3820
28 Day Strength (psi)	4020	4000

[1] Freeze-Thaw Specimen LMC M-2 Cast From This Mix.

Table C-12. Normal Concrete Mix Designs, SSD Basis Batch Quantities (lb/yd^3) and Properties of Fresh and Hardened Concrete for Freeze-Thaw Testing.

Batch Number	1[1]
Type I Cement	729
Water	315
Fine Aggregate	1625
Coarse Aggregate (max size ½ in [1.27 cm])	1399
AEA (ml)	233
Daracem 100 (oz)	29.0
W/C Ratio	0.43
Slump (inches)	3.50
Entrained Air (%)	6.8
Unit Weight (lb/yd^3)	142
7 Day Strength (psi)	4500
28 Day Strength (psi)	5490

[1] Freeze-Thaw Specimen Normal M-1 Cast From This Mix.

Table C-13. DCI Modified Mix Designs, SSD Basis Batch Quantities (lb/yd^3) and Properties of Fresh and Hardened Concrete for Freeze-Thaw Testing.

Batch Number	1[1]
Type I Cement	658
Water	214
Fine Aggregate	1103
Coarse Aggregate	1896
AEA (oz)	4.9
Daracem 100 (oz)	79.0
Daratard 17	13.2
DCI (gallons)	6
W/C Ratio	0.40
Slump (inches)	1.0
Entrained Air (%)	5.3
Unit Weight (lb/yd^3)	144.5
1 Day Strength (psi)	3180
7 Day Strength (psi)	6740
28 Day Strength (psi)	7660

[1] Freeze-Thaw Specimen DCI Remix Cast From This Mix.

Note: For following Chloride Content Tables, the following sample depth designations apply:

A = 1/4 to 3/4"
B = 3/4 to 1 1/4"
C = 1 1/4 to 1 3/4"
D = 1 3/4 to 2 1/4"
E = 2 1/4 to 2 3/4"

These codes will trail the specimen identification code.

Table C-14 Pretreatment Chloride Contents

Corrosion Inhibitor Evaluation		SHRP C-103 CHLORIDE CONTENTS		PROBE: A DATE: 6/23/91	
Specimens	Measured mV	Measured % Cl	Predicted % Cl	Predicted lbs/cy	Standard %Cl
1H-D1-DCI-A	NA				
1H-D1-DCI-B	21.2	0.0807	0.7192	28.8	
1H-D1-SB-A	19.9	0.0857	0.7689	30.8	
1H-D1-SB-B	23.1	0.0739	0.6517	26.1	
1H-D1-AX-A	20.8	0.0822	0.7342	29.4	
1H-D1-AX-B	22.2	0.0770	0.6830	27.3	
1H-D1-COR-A	20.5	0.0833	0.7456	29.8	
1H-D1-COR-B	24.8	0.0683	0.5961	23.8	
1H-D1-LMC-A	20.3	0.0841	0.7533	30.1	
1H-D1-LMC-B	24.1	0.0706	0.6185	24.7	
2L-1-DCI-A	NA				
2L-1-DCI-B	33.5	0.0457	0.3704	14.8	
2L-1-DCI-C	41.8	0.0311	0.2245	9.0	
2L-1-DCI-D	59.4	0.0138	0.0493	2.0	0.0329
2L-1-SB-A	NA				
2L-1-SB-B	25.8	0.0652	0.5654	22.6	
2L-1-SB-C	40.7	0.0327	0.2408	9.6	0.2204
2L-1-SB-D	60.9	0.0129	0.0399	1.6	
2L-1-AX-A	24.8	0.0931	0.8429	33.7	
2L-1-AX-B	30.4	0.0527	0.4408	17.6	
2L-1-AX-C	43.3	0.0290	0.2035	8.1	0.1751
2L-1-AX-D	58.0	0.0147	0.0587	2.3	
2L-1-COR-A	26.4	0.0732	0.6448	25.8	
2L-1-COR-B	37.0	0.0388	0.3021	12.1	
2L-1-COR-C	56.2	0.0160	0.0717	2.9	
2L-1-COR-D	60.9	0.0129	0.0399	1.6	
2L-1-DCI-A	NA				
2L-1-DCI-B	27.6	0.0600	0.5135	20.5	
2L-1-DCI-C	46.1	0.0255	0.1680	6.7	
2L-1-DCI-D	60.2	0.0133	0.0442	1.8	
2L-1-SB-A	20.7	0.0826	0.7380	29.5	
2L-1-SB-B	32.1	0.0487	0.4010	16.0	
2L-1-SB-B	46.8	0.0247	0.1597	6.4	
2L-1-SB-B	61.2	0.0127	0.0380	1.5	

Table C-14 Pretreatment Chloride Contents - Continued

Corrosion Inhibitor Evaluation		SHRP C-103 CHLORIDE CONTENTS		PROBE: A DATE: 6/23/91	
Specimens	Measured mV	Measured % Cl	Predicted % Cl	Predicted lbs/cy	Standard %Cl
2L-1-AX-A	20.4	0.0837	0.7494	30.0	
2L-1-AX-B	31.4	0.0503	0.4170	16.7	
2L-1-AX-C	44.7	0.0272	0.1851	7.4	
2L-1-AX-D	59.2	0.0139	0.0506	2.0	
2L-1-COR-A	NA				
2L-1-COR-B	27.3	0.0608	0.5219	20.9	
2L-1-COR-C	48.6	0.0227	0.1399	5.6	
2L-1-COR-D	62.7	0.0118	0.0293	1.2	
2L-0-LMC-A	25.6	0.1039	0.9498	38.0	
2L-0-LMC-B	27.3	0.0608	0.5219	20.9	
2L-0-LMC-C	38.7	0.0359	0.2726	10.9	
2L-0-LMC-D	58.0	0.0147	0.0587	2.3	
2M-1LMC-A	21.1	0.0811	0.7229	28.9	
2M-1LMC-B	31.2	0.0508	0.4217	16.9	0.3681
2M-1LMC-C	41.5	0.0315	0.2288	9.2	
2M-1LMC-D	57.0	0.0154	0.0658	2.6	
2L-BC-A	25.0	0.0677	0.5899	23.6	
2L-BC-A	33.4	0.0459	0.3725	14.9	
2L-BC-A	50.7	0.0206	0.1186	4.7	
2L-BC-A	61.8	0.0123	0.0345	1.4	
2L-TP-A	NA				
2L-TP-B	31.4	0.0503	0.4170	16.7	
2L-TP-C	47.9	0.0235	0.1474	5.9	
2L-TP-D	60.2	0.0133	0.0442	1.8	

Table C-14 Pretreatment Chloride Contents - Continued

Corrosion Inhibitor Evaluation		SHRP C-103 CHLORIDE CONTENTS		PROBE: B DATE: 8/9/91	
Specimens	Measured mV	Measured % Cl	Predicted % Cl	Predicted lbs/cy	Standard %Cl
1M-CON-A	27.6	0.0651	0.5642	22.6	
1M-CON-B	34.9	0.0473	0.3866	15.5	
1M-0-LMC-A	27.9	0.0642	0.5558	22.2	
1M-0-LMC-B	33.3	0.0507	0.4208	16.8	
1M-1-DCI-A	31.3	0.0554	0.4672	18.7	
1M-1-DCI-B	38.3	0.0407	0.3211	12.8	
1M-1-SB-A	30.4	0.0576	0.4894	19.6	
1M-1-SB-B	36.4	0.0443	0.3565	14.3	
1M-1-AX-A	27.6	0.0651	0.5642	22.6	
1M-1-AX-B	33.6	0.0501	0.4142	16.6	
1M-1-COR-A	29.5	0.0599	0.5125	20.5	
1M-1-COR-B	37.9	0.0415	0.3283	13.1	
1LM-0-LMC-A	29.0	0.0612	0.5257	21.0	
1LM-0-LMC-B	40.6	0.0368	0.2820	11.3	
1LM-0-LMC-C	51.0	0.0234	0.1464	5.9	
1LM-0-LMC-D	62.6	0.0141	0.0521	2.1	
1LM-1-DCI-A	27.6	0.0651	0.5642	22.6	
1LM-1-DCI-B	34.3	0.0485	0.3991	16.0	
1LM-1-DCI-C	43.9	0.0319	0.2322	9.3	
1LM-1-DCI-D	55.8	0.0189	0.1016	4.1	
1LM-1-SB-A	29.1	0.0610	0.5230	20.9	
1LM-1-SB-B	41.7	0.0351	0.2646	10.6	
1LM-1-SB-C	51.9	0.0225	0.1373	5.5	
1LM-1-SB-D	63.4	0.0136	0.0472	1.9	
1LM-1-AX-A	32.9	0.0516	0.4298	17.2	
1LM-1-AX-B	44.1	0.0316	0.2294	9.2	
1LM-1-AX-C	59.2	0.0163	0.0751	3.0	
1LM-1-AX-D	66.7	0.0117	0.0285	1.1	
1LM-1-COR-A	28.7	0.0620	0.5338	21.4	
1LM-1-COR-B	39.1	0.0393	0.3071	12.3	
1LM-1-COR-C	48.5	0.0261	0.1737	6.9	
1LM-1-COR-D	61.5	0.0148	0.0592	2.4	

Table C-15 Chloride Content, 333 Days After Treatment

Corrosion Inhibitor Evaluation		SHRP C-103 CHLORIDE CONTENTS		PROBE: A DATE: 4/25/92	
Specimens	Measured mV	Measured % Cl	Predicted % Cl	Predicted lbs/cy	Standard %Cl
2L-0-LMC-A	64.7	0.0155	0.1251	5.0	
2L-0-LMC-B	100.8	0.0034	0.0037	0.1	
2L-0-LMC-C	98.3	0.0038	0.0075	0.3	
2L-0-LMC-D	86.1	0.0063	0.0328	1.3	
1H-D0-LMCA	54.8	0.0236	0.2057	8.2	
1H-D0-LMCB	83.5	0.0070	0.0401	1.6	
1H-D0-LMCC	53.5	0.0249	0.2190	8.8	
1H-D0-LMCD	44.4	0.0366	0.3357	13.4	
1H-D1-DCI-D	51.4	0.0272	0.2421	9.7	
1H-D1-SB-D	51.5	0.0271	0.2409	9.6	
1H-D1-AX-D	43.8	0.0375	0.3451	13.8	
1H-D1-COR	43.1	0.0386	0.3564	14.3	
1L-D1-DCI-A	24.9	0.0834	0.8036	32.1	
1L-D1-DCI-B	36.0	0.0522	0.4915	19.7	
1L-D1-DCI-C	58.9	0.0198	0.1682	6.7	
1L-D1-DCI-D	71.0	0.0119	0.0889	3.6	
1L-D1-SB-A	33.0	0.0592	0.5620	22.5	
1L-D1-SB-B	45.5	0.0349	0.3191	12.8	
1L-D1-SB-C	66.8	0.0142	0.1119	4.5	
1L-D1-SB-D	94.2	0.0045	0.0146	0.6	
1L-D1-AX-A	39.1	0.0458	0.4275	17.1	
1L-D1-AX-B	47.9	0.0315	0.2854	11.4	
1L-D1-AX-C	67.4	0.0138	0.1084	4.3	
1L-D1-AX-D	85.9	0.0063	0.0333	1.3	
1L-D1-COR-A	32.5	0.0605	0.5747	23.0	
1L-D1-COR-B	44.6	0.0363	0.3326	13.3	
1L-D1-COR-C	52.2	0.0263	0.2330	9.3	
1L-D1-COR-D	61.9	0.0175	0.1446	5.8	
1L-D0-LMC-A	30.9	0.0647	0.6170	24.7	
1L-D0-LMC-B	46.4	0.0336	0.3061	12.2	
1L-D0-LMC-C	NA				
1L-D0-LMC-D	82.2	0.0074	0.0440	1.8	
1L-AX-DCI-A	35.2	0.0539	0.5095	20.4	
1L-AX-DCI-B	43.0	0.0388	0.3580	14.3	
1L-AX-DCI-C	61.1	0.0181	0.1506	6.0	
1L-AX-DCI-D	86.2	0.0063	0.0325	1.3	

Table C-15 Chloride Content, 333 Days After Treatment - Cont'd

Corrosion Inhibitor Evaluation		SHRP C-103 CHLORIDE CONTENTS		PROBE: A DATE: 4/25/92	
Specimens	Measured mV	Measured % Cl	Predicted % Cl	Predicted lbs/cy	Standard %Cl
1L-AX-COR	32.0	0.0618	0.5876	23.5	
1L-AX-COR	45.2	0.0354	0.3236	12.9	
1L-AX-COR	55.4	0.0230	0.1998	8.0	
1L-AX-COR	69.9	0.0125	0.0945	3.8	
1H-AX-LMC	33.9	0.0570	0.5399	21.6	
1H-AX-LMC	41.8	0.0408	0.3782	15.1	

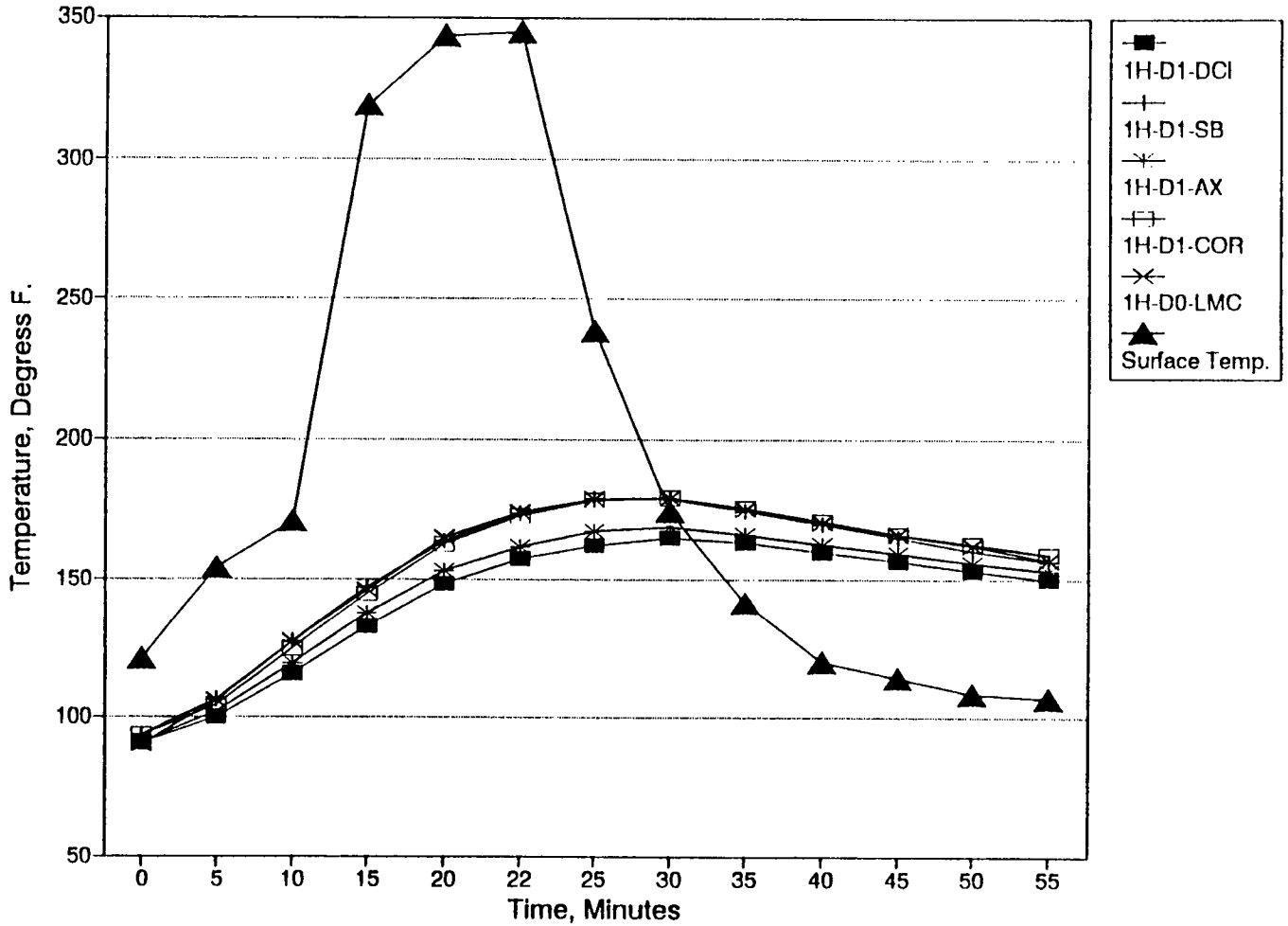

Fig. C-1 Drying Temperatures Effect on High Initial Corrosion Rate Specimens

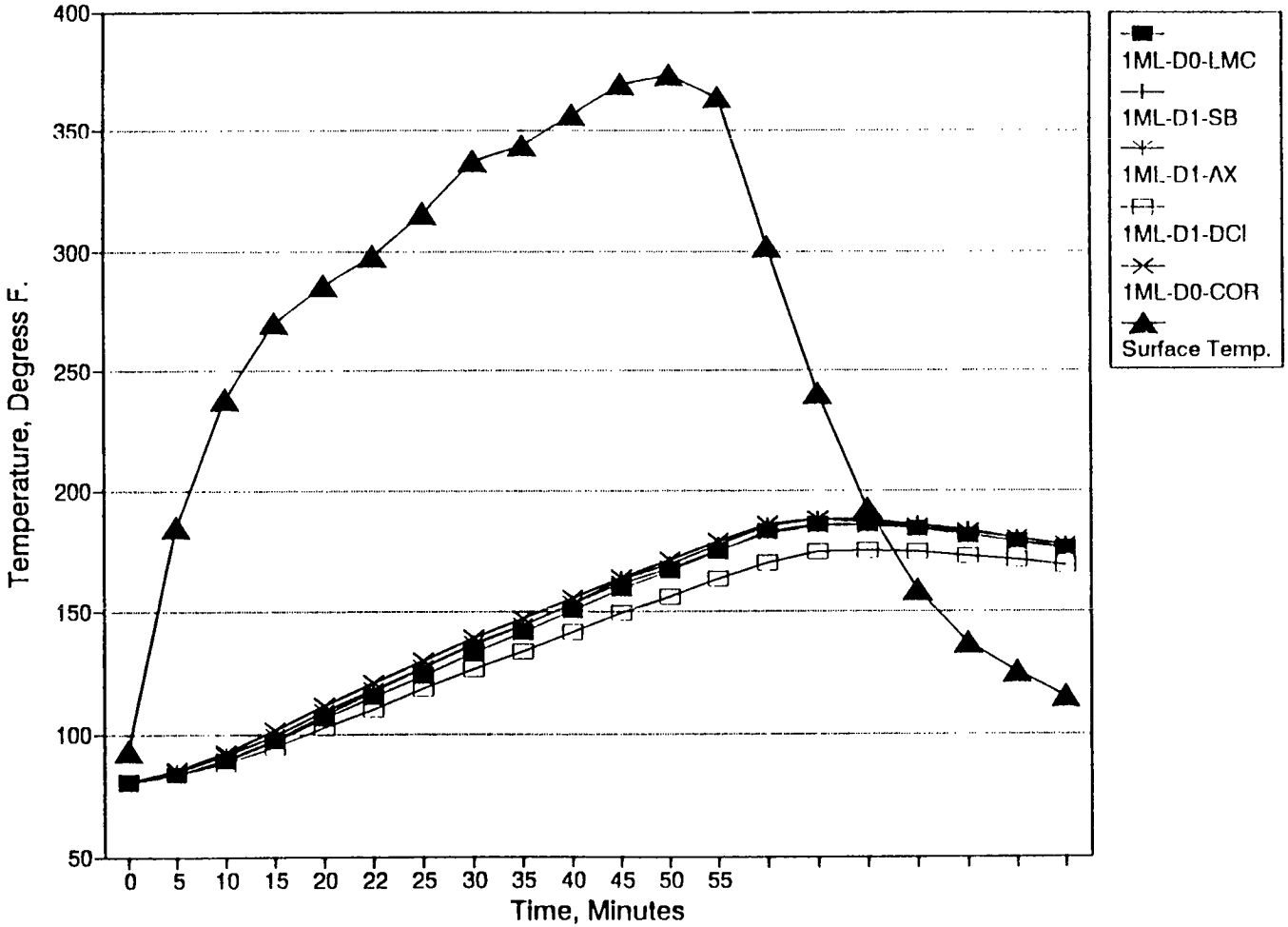

Fig. C-2 Drying Temperatures Effect On ML Initial Corrosion Rate Specimens

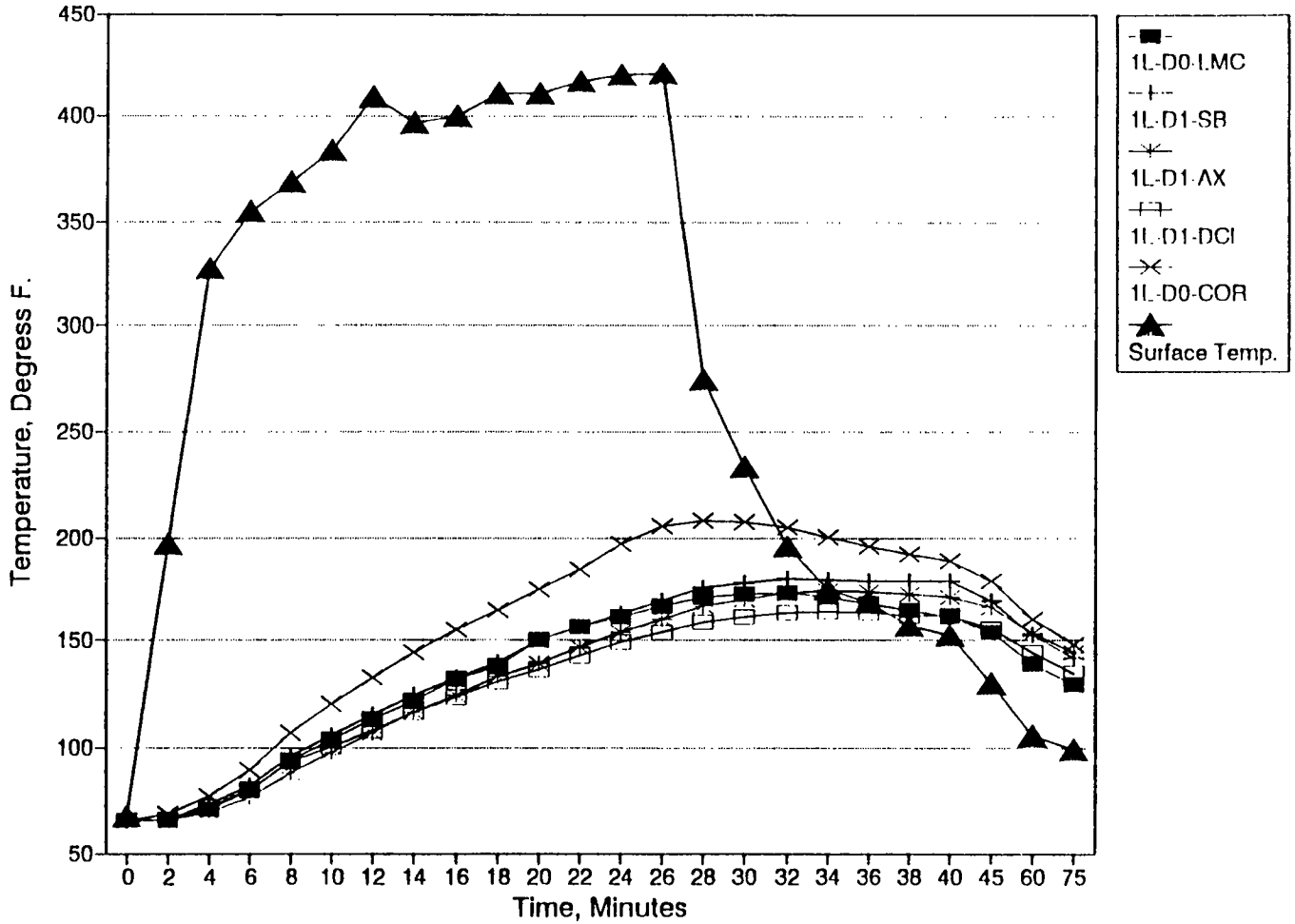

Fig. C-3 Drying Temperatures Effect On Low Initial Corrosion Rate Specimens

Table C-16 ASTM C666 Standard Test Method for Resistance of Concrete to Rapid Freezing and Thawing

P = Relative Dynamic Modulus of Elasticity

	Initial Reading		4/2/92, 24 cycles			4/6/92, 49 cycles			4/15/92 100 cycles		
Specimen	Flex. (KHz)	Long. (KHz)	Flex. (KHz)	Long. (KHz)	P(24)	Flex. (KHz)	Long. (KHz)	P(49)	Flex. (KHz)	Long. (KHz)	P(100)
DCI-M4-1	2.199	1.745	2.028	1.613	58.1	1.471	1.081	44.7	0.397	1.670	3.3
DCI-M4-2	2.209	1.729	2.148	1.677	94.6	1.770	1.379	64.2	0.866	0.858	15.4
COR-M1-1	2.285	1.820	2.253	1.800	97.2	2.260	1.800	97.8	2.260	1.810	97.8
COR-M1-2	2.275	1.796	2.253	1.778	98.1	2.256	1.780	98.3	2.260	1.790	98.7
COR2-1	2.274	1.787	2.262	1.774	98.9	2.251	1.772	98.0	2.250	1.780	97.9
COR2-2	2.277	1.793	2.252	1.783	97.8	2.250	1.772	97.6	2.250	1.780	97.6
COR-M4-1	2.234	1.763	2.218	1.751	98.6	2.223	1.763	99.0	2.220	1.770	98.8
COR-M4-2	2.267	1.791	2.252	1.782	98.7	2.253	1.782	98.8	2.260	1.800	99.4

	Initial Reading		4/15/92, 51 cycles			5/4/92, 149 cycles			5/27/92 265 cycles		
Specimen	Flex. (KHz)	Long. (KHz)	Flex. (KHz)	Long. (KHz)	P(24)	Flex. (KHz)	Long. (KHz)	P(49)	Flex. (KHz)	Long. (KHz)	P(49)
Normal-1	2.322	1.819	2.310	1.800	99.0	2.310	1.820	99.0	2.340	1.820	101.6
Normal-1	2.268	1.780	2.230	1.780	96.7	2.280	1.790	101.1	2.290	1.790	101.9

	Initial Reading		5/4/92, 100 cycles			5/27/92, 225 cycles		
Specimen	Flex. (KHz)	Long. (KHz)	Flex. (KHz)	Long. (KHz)	P(24)	Flex. (KHz)	Long. (KHz)	P(49)
LMC-1	2.120	1.710	2.190	1.730	106.7	2.200	1.750	107.7

Table C-16 ASTM C666 Standard Test Method for Resistance of Concrete to Rapid Freezing & Thawing - Cont'd

P = Relative Dynamic Modulus of Elasticity

	5/4/92 200 cycles			5/27/92 315 cycles		
Specimens	Flex. (KHz)	Long. (KHz)	P(100)	Flex. (KHz)	Long. (KHz)	P(100)
DCI-M4-1	NA	NA	NA	NA	NA	NA
DCI-M4-2	NA	NA	NA	NA	NA	NA
COR-M1-1	2.280	1.830	99.6	2.310	1.830	102.2
COR-M1-2	2.270	1.800	99.6	2.280	1.800	100.4
COR2-1	2.280	1.780	100.5	2.290	1.800	101.4
COR2-2	2.290	1.790	101.1	2.290	1.800	101.1
COR-M4-1	2.260	1.790	102.3	2.260	1.800	102.3
COR-M4-2	2.280	1.820	101.2	2.310	1.820	103.8

Table C-17 ASTM C666 Resistance of Concrete to Rapid Freezing and Thawing Elastic Modulus Determination March 28, 1992

Specimen	Length (mm)	Height (mm)	Width (mm)	Mass (kg)	Density (g/cm^3)	Poison's EF,G	Ratio EL,G
DCI-M4-1	401.0	104.0	77.0	7.08	2.205	0.28	0.03
DCI-MR-2	401.0	105.0	76.5	7.06	2.192	0.27	0.03
COR-M1-1	401.0	103.0	77.0	7.17	2.254	0.26	0.03
COR-M1-2	401.0	103.0	76.0	7.16	2.281	0.29	0.03
COR2-1	401.0	103.0	76.0	7.10	2.262	0.28	0.03
COR2-2	401.0	103.0	76.0	7.10	2.262	0.26	0.03
COR-M4-1	401.0	103.0	75.0	6.99	2.256	0.23	0.03
COR-M4-2	401.0	103.0	77.0	7.11	2.236	0.27	0.03

Specimen	Flex. (KHz)	Long. (KHz)	Tors. (KHz)	Flex. (msi)	Long. (ksi)	Tors. (msi)
DCI-M4-1	2.199	1.745	2.728	5.06	633	1.98
DCI-MR-2	2.209	1.729	2.713	5.00	618	1.96
COR-M1-1	2.285	1.820	2.786	5.65	704	2.24
COR-M1-2	2.275	1.796	2.831	5.68	693	2.21
COR2-1	2.274	1.787	2.839	5.62	681	2.20
COR2-2	2.277	1.793	2.862	5.62	685	2.24
COR-M4-1	2.234	1.763	2.818	5.38	661	2.18
COR-M4-2	2.267	1.791	2.851	5.51	676	2.18

References

1. ENR Washington Observer. *Engineering News Record* 277, No. 2 (July 15, 1991): 7.

2. Portland Cement Association, U.S. Bureau of Public Roads & Ten State Highway Agencies *Durability of Concrete Bridge Decks*, Report 5. Washington, D.C.: 1969, 46.

3. Portland Cement Association U.S. Bureau of Public Roads & Ten State Highway Agencies, *Durability of Concrete Bridge Decks*, Final Report. Washington, D.C.: 1970, 35.

4. Browne, R. D. "Design Prediction of the Life for Reinforced Concrete in Marine and Other Chloride Environments." *Durability of Building Materials* 1, (1982): 113-125.

5. Funashi, M. "Predicting Corrosion-Free Service Life of a Concrete Structure in a Chloride Environment." *American Concrete Institute Materials Journal* 87, No. 6 (November - December 1990): 581-587.

6. Cady, P. D. and R. E. Weyers. "Predicting Service Life of Concrete Bridge Decks Subject to Reinforcement Corrosion." *Corrosion Forms and Control for Infrastructure*, American Society for Testing and Materials STP 1137. Philadelphia: American Society for Testing and Materials, 1992.

7. Cady, P. D. and R. E. Weyers. "Deterioration Rates of Concrete Bridge Decks." *Journal of Transportation Engineering*, ASCE, 110, No. 1 (January, 1984): 34-44.

8. AASHTO, FHWA, Transportation Research Board, NCHRP, Strategic Highway Research Program. *Research Plans*, Final Report, Technical Research Area 43 (May, 1986): pp. TRA 4-1 through TRA 4-60.

9. "Durability of Concrete Bridge Decks." *NCHRP Synthesis of Highway Practice No. 57.* Transportation Research Council. Washington, D.C., May, 1979.

10. Babei, K. and N. M. Hawkins. "Evaluation of Bridge Deck Protective Strategies." *National Cooperative Highway Research Program Report*, No. 297. Washington, D. C.: Transportation Research Board, September 1987, 35.

11. Tvarusko, A. "Cathodic Protection of Rebars in Old and New Concrete Structures." *Evaluation and Rehabilitation of Concrete Structures and Innovations in Design*, SP-128, American Concrete Institute, vol. 1. Detroit: American Concrete Institute 1991, 359-372.

12. Slater, J. E. et al. "Electrochemical Removal of Chlorides From Concrete Bridge Decks." *Transportation Research Record*, No. 604. Washington, D. C.: Transportation Research Board, 1976, 6-15.

13. Dillard, J. G., J. O. Glanville, W. D. Collins, I. L. Al-Qadi, and R. E. Weyers. *Concrete Bridge Protection and Rehabilitation: Chemical and Physical Techniques*, Strategic Highway Research Program, SHRP-S-XXX, National Research Council, Washington, D.C., 1993, 168.

14. Weyers, R. E., and P. D. Cady. "Development: Deep Grooving - A method for Impregnating Concrete Bridge Decks." *Transportation Research Record 962*. 1984: 14-18.

15. Weyers, R. E., and P. D. Cady. "Application: Deep Grooving - A method for Impregnating Concrete Bridge Decks." *Transportation Research Record 962*. 1984: 19-21.

16. Weyers, R. E., and P. D. Cady. "Deep Impregnation of Concrete Bridge Decks." *Transportation Research Record 1184*. 1988: 41-49.

17. Manning, David G. "Detecting Defects and Deterioration in Highway Structures." *National Cooperative Highway Research Program, Synthesis of Highway Practice 118*. Washington, D. C.: Transportation Research Board, National Research Council, July 1985.

18. Vassie, P. R. *A Survey of Site Tests for the Assessment of Corrosion in Reinforced Concrete*, LR 953: England, U.K., Transport and Road Research Laboratory, 1980.

19. Mason, J. A. et al. "Use of Polymers in Highway Concrete." *NCHRP Report 190*. Washington, D. C.: Transportation Research Board (1978): 77.

20. Cady, P. D., and R. E. Weyers. "Field Performance of Deep Polymer Impregnations" *Journal of Transportation Engineering*, American Society of Civil Engineers 113, No. 1 (January 1987), 1-15.

21. Dutta, T. "Evaluation of the Effectiveness of Deep Polymer Impregnation as a Corrosion Abate Technique for Overlaid Bridge Decks." Blacksburg, VA: Virginia Polytechnic Institute and State University, April 1991: 111-124.

22. Clear, K. C. "Measuring Rate of Corrosion of Steel in Field Concrete Structures." *Transportation Research Record No. 1264* (1990): 12-17.

23. Carrasquillo, R. L. *Evaluation of a Posttreatment Procedure of an Existing Reinforced Concrete Bridge Structure*, Final Report Prepared for W. R. Grace & Co., Austin, TX. January, 1986.

24. *American Society for Testing and Materials C876-87: Standard Test Method for Half-Cell Potentials of Uncoated Reinforcing Steel in Concrete*. Philadelphia: American Society for Testing and Materials, 1987.

25. Berke, N. S., and M. C. Hicks. "Electrochemical Methods of Determining the Corrosivity of Steel in Concrete." *Silver Anniversary Symposium on Corrosion Testing and Evaluation American Society for Testing and Materials STP 1000*. Eds. R. Baboian and S. W. Dean. Philadephia: American Society for Testing and Materials, 1990, 425.

26. Berke, N. S., D. F. Shen, and K. M. Sundberg. "Comparison of Current Interruption and Electrochemical Impedance Techniques in the Determination of Corrosion Rates of Steel in Concrete." *The Measurement and Correction of Electrolyte Resistance in Electrochemical Tests, American Society for Testing and Materials STP 1056*. Eds. L. L. Scribner and S. R. Taylor. Philadelphia: American Society for Testing and Materials, 1990, 191-201.

27. Berke, N. S., and A. Rosenberg. "Technical Review of Calcium Nitrite Corrosion Inhibitor in Concrete." *Transportation Research Record No. 1211.* Washington, D. C.: Transportation Research Board, National Research Council, 1989, 18-27.

28. Manson, J. A. et al. "Use of Polymers in Highway Concrete." *National Cooperative Highway Research Program 190.* Washington, D. C.: Transportation Research Board, 1978.

29. Clear, K. C. *3LP Package - Test Procedure, Data Analysis, Procedure and General Information* June, 1988.

30. James Instruments, Inc. *CL Test Model 500 Instruction Manual.* Chicago: James Instruments, Inc., 1988, 11.

31. Herald, H. E. et al. *Condition Evaluation of Concrete Bridges Relative to Reinforced Corrosion, Volume 6: Method for Field Determination of Total Chloride Content*, Report No. SHRP-S-328, Washington, D. C.: Strategic Highway Research Program, National Research Council, 1992, 155.

32. Clear, K. C. "Reinforcing Bar Corrosion in Concrete: Effect of Special Treatments." SP-49, *American Concrete Institute*, Detroit: 1975, 71-82.

33. Clear, K. C. *Time to Corrosion of Reinforcing Steel In Concrete Slab*, Report No. FHWA RD-76-70. Washington, D. C.: Federal Highway Administration, April 1976.

34. Tremper, B., J. L. Beaton, and R. F. Stratfull, "Causes and Repair of Deterioration to a California Bridge Due to Corrosion of Reinforcing Steel in a Marine Environment Part II: Fundamental Factors Causing Corrosion." *Highway Research Bulletin 182.* Washington, D. C.: Transportation Research Board, National Research Council, 1958, 18-41.

35. Browne, R. D.. "Mechanisms of Corrosion of Steel in Concrete in Relation to Design, Inspection and Repair of Offshore and Coastal Structures." *Performance of Concrete in a Marine Environment, SP-65, American Concrete Institute*, 169-204.

36. Griffin, D. F., "Corrosion Inhibitors for Reinforced Concrete." *Corrosion of Metals in Concrete*, SP 49-8, American Concrete Institute, Detroit: 1975, 95-102.

37. Dean, S. W., Jr. et al. "Inhibitor Types." *Materials Performance.* 20, Vol. 1, No. 11, National Association of Corrosion Engineers (November, 1981): 47-51.

38. Wrangl'n, G. *An Introduction to Corrosion and Protection of Metals.* New York: Chapman and Hall, 1985, 165-173.

39. Miksic, B. A. "Use of Vapor Phase Inhibitors for Corrosion Protection of Metal Products." *Corrosion 83.* No. 308. Houston: National Association of Civil Engineers, 1983.

40. Dillard, J. G. et al. "Surface Characterization of Reinforcing Steel and the Interaction of Steel with Inhibitors in Pore Solution." *Transportation Research Record* 30, Washington, D. C.: Transportation Research Board National Research Council, 1991 in press.

41. Berke, N. S., and A. Rosenberg, "Technical Review of Calcium Nitrite Corrosion Inhibitor in concrete." *Transportation Research Record No. 1211.* (1991): 18-27.

42. Dillard, J. G. et al. "Migration of Inhibitors in Aqueous Solution Through Concrete." *Transportation Research Record No. 30*, Washington, D. C.: Transportation Research Board National Research Council, 1991, in press.

43. "Field Test for Surface Soundness and Adhesion." *American Concrete Institute Manual of Concrete Practice* Part 5, American Concrete Institute, Detroit: 1991, Appendix 30-32.

44. Webster, L. A. et al. "Electrochemical Studies of Rebar Corrosion and Inhibition in simulated Pore Solution." *Transportation Research Record No. 30*, Washington, D. C.: Transportation Research Board National Research Council, 1991, in press.

45. Kosmatka, S. H. and W. C. Panarese. *Design and Control of Concrete Mixtures*, Skokie: Portland Cement Association, 1990, 6.

46. Dressman, S. et al. "A Screening Test for Rebar Corrosion Inhibitors." *Transportation Research Record 30*, Washington, D. C.: Transportation Research Board National Research Council, 1991, in press.

47. Ahlrich, R. C., and G. L. Anderton. *Construction and Evaluation of Resin Modified Concrete Pavement*, Final Report No GL-91-13, Waterways Experiment Station, Vicksburg: U. S. Army Corps of Engineers, July 1991, 86.

48. Mamlouk, M. S., and R. T. Sarofim. "Modulus of Asphalt Mixtures -- an Unresolved Dilemma." *Transportation Research Record No. 1171*. Washington, D.C.: 1988, 193-198.

49. Lottman, R. P. "Predicting Moisture-Induced Damage to Asphaltic Concrete: Ten Year Field Evaluation." *Final Report, NCHRP Project 4-8(4)*. Washington, D. C.: Transportation Research Board, National Research Council, 1986.

50. Tunnicliff, D. G. and R. E. Root. "Testing Asphalt Concrete for Effectiveness of Antistripping Additives." *Proceedings*, Association of Asphalt Paving Technologists 52 (1983): 535-560.

51. Kennedy, T. W., F. L. Roberts, and K. W. Lee. "Evaluation of Mixture Susceptibility of Asphalt Mixtures Using the Texas Freeze-Thaw Pedestal Test." *Proceedings, Association of Asphalt Paving Technologists* 51. Kansas City: 1982, 327-341.

52. Al-Swailmi, S. and R. L. Terrel. "Evaluation of Water Damage of Asphalt Concrete Mixtures Using the Environmental Conditioning system (ECS)." Presented at the Annual Meeting of Association of Asphalt Paving Technologists, Charleston, SC, 1991.

53. Parker, F., Jr., and F. A. Gharaybeh. "Evaluation of Tests to Assess Stripping Potential of Asphalt Concrete Mixtures." *Transportation Research Record No. 1171*. Washington, D. C.: 1988, 18-26.

54. Detwiler, R. J., B. J. Dalgleish, and R. B. Williamson. "Assessing the Durability of Concrete in Freezing and Thawing." *American Concrete Institute Materials Journal*, American Concrete Institute (Jan-Feb 1989): 29-35.

55. Herald, S. E., et al. *Condition Evaluation of Concrete Bridges Relative to Reinforced Corrosion, Volume 6: Method for Field Determination of Total Chloride Content*, Report No. SHRP-S-328. Washington, D. C.: National Research Council, July 1992, 155.

Concrete and Structures Advisory Committee

Chairman
James J. Murphy
New York Department of Transportation (retired)

Vice Chairman
Howard H. Newlon, Jr.
Virginia Transportation Research Council (retired)

Members

Charles J. Arnold
Michigan Department of Transportation

Donald E. Beuerlein
Koss Construction Co.

Bernard C. Brown
Iowa Department of Transportation

Richard D. Gaynor
National Aggregates Association/National Ready Mixed Concrete Association

Robert J. Girard
Missouri Highway and Transportation Department

David L. Gress
University of New Hampshire

Gary Lee Hoffman
Pennsylvania Department of Transportation

Brian B. Hope
Queens University

Carl E. Locke, Jr.
University of Kansas

Clellon L. Loveall
Tennessee Department of Transportation

David G. Manning
Ontario Ministry of Transportation

Robert G. Packard
Portland Cement Association

James E. Roberts
California Department of Transportation

John M. Scanlon, Jr.
Wiss Janney Elstner Associates

Charles F. Scholer
Purdue University

Lawrence L. Smith
Florida Department of Transportation

John R. Strada
Washington Department of Transportation (retired)

Liaisons

Theodore R. Ferragut
Federal Highway Administration

Crawford F. Jencks
Transportation Research Board

Bryant Mather
USAE Waterways Experiment Station

Thomas J. Pasko, Jr.
Federal Highway Administration

John L. Rice
Federal Aviation Administration

Suneel Vanikar
Federal Highway Administration

11/19/92

Expert Task Group

Charles J. Arnold
Michigan Department of Transportation

Jack J. Fontana
Consultant

Ronald I. Frascoia
State of Vermont Agency of Transportation

Andrew D. Halverson
Minnesota Department of Transportation

Gary Hoffman
Pennsylvania Department of Transportation

Crawford Jencks
Transportation Research Board

Paul D. Krauss
Wiss Janney Elstner Associates

Louis Kuhlmann
Larkin Laboratory--Dow Chemicals USA

Alberto Sagues
University of South Florida

Frederick Szczepanek
New York Department of Transportation

Paul Virmani
Federal Highway Administration

Consultant to the Expert Task Group
John Broomfield